Multiple Corrosion-Protection Systems for Reinforced Concrete Bridge Components

U.S. Department of Transportation
Federal Highway Administration

FOREWORD

Eleven systems combining epoxy-coated reinforcement (ECR) with another corrosion-protection system were evaluated using rapid macrocell, southern exposure, cracked beam, linear polarization resistance, and field tests. The systems included bars that were pretreated with zinc chromate to improve the adhesion between the epoxy and the reinforcing steel, two epoxies with improved adhesion to the reinforcing steel, one inorganic corrosion inhibitor (calcium nitrite), two organic corrosion inhibitors, an epoxy-coated bar with a primer containing microencapsulated calcium nitrite, three epoxy-coated bars with improved adhesion combined with the corrosion inhibitor calcium nitrite, and multiple-coated (MC) bars with an initial 50-µm (2-mil) coating of 98 percent zinc and 2 percent aluminum followed by a conventional epoxy coating. The systems were compared with conventional uncoated reinforcement and conventional ECR.

The results presented in this report indicate that the coated bars provided superior corrosion protection to the reinforcing steel. In addition, bars with damaged coatings initiated corrosion at several times the chloride contents within concrete and typically corroded at rates two orders of magnitude less than conventional reinforcement. Limited additional protection was achieved using bars with primer coating, MC bars, and concrete containing calcium nitrite and one of the organic corrosion inhibitors, although the latter resulted in reduced compressive strength and reduced resistance to surface scaling.

Jorge E. Pagán-Ortiz
Director, Office of Infrastructure
Research and Development

TECHNICAL REPORT DOCUMENTATION PAGE

1. Report No. FHWA-HRT-11-060	2. Government Accession No.	3. Recipient's Catalog No.
4. Title and Subtitle Multiple Corrosion-Protection Systems for Reinforced Concrete Bridge Components		5. Report Date November 2011
		6. Performing Organization Code
7. Author(s) David Darwin, JoAnn Browning, Matthew O'Reilly, Carl E. Locke Jr., and Y. Paul Virmani		8. Performing Organization Report No. SM Report No. 101
9. Performing Organization Name and Address University of Kansas Center for Research, Inc. 2385 Irving Hill Road Lawrence, KS 66045-7563		10. Work Unit No.
		11. Contract or Grant No. DTFH61-03-C-00131
12. Sponsoring Agency Name and Address Office of Infrastructure Research and Development Federal Highway Administration 6300 Georgetown Pike McLean, VA 22101-2296		13. Type of Report and Period Covered Final Report September 2003–February 2011
		14. Sponsoring Agency Code
15. Supplementary Notes The Contracting Officer's Technical Representative (COTR) was Y.P. Virmani, HRDI-60.		

16. Abstract

Eleven systems containing epoxy-coated reinforcement (ECR) in combination with another corrosion-protection system are evaluated using the rapid macrocell, southern exposure, cracked beam, linear polarization resistance, and field tests. The systems include bars pretreated with zinc chromate to improve the adhesion between the epoxy and the reinforcing steel, two epoxies with improved adhesion to the reinforcing steel, one inorganic corrosion inhibitor (calcium nitrite), two organic corrosion inhibitors (Rheocrete® 222$^+$ and Hycrete™), an epoxy-coated bar with a primer containing microencapsulated calcium nitrite, three epoxy-coated bars with improved adhesion combined with the corrosion inhibitor calcium nitrite, and multiple-coated (MC) bars with an initial 50-μm (2-mil) coating of 98 percent zinc and 2 percent aluminum followed by a conventional epoxy coating. The systems are compared with conventional uncoated reinforcement and conventional ECR. The coatings on all bars are penetrated to simulate the effects of damage during fabrication and placement in the field.

The results presented in this report indicate that the coated bars provide superior corrosion protection to the reinforcing steel and that bars with damaged coatings initiate corrosion at chloride contents within concrete that are several times greater and corrode at rates that are typically two orders of magnitude below those exhibited by conventional reinforcement. Limited additional protection is achieved using bars with the primer coating, MC bars, and concrete containing the corrosion inhibitors calcium nitrite and one of the organic corrosion inhibitors, although the latter resulted in reduced compressive strength and reduced resistance to surface scaling. The differences in costs over a 75-year design life are relatively small for coated bars. Cracks in concrete directly over and parallel to the reinforcement, such as found in bridge decks, result in earlier corrosion initiation and higher corrosion rates than obtained with intact concrete for all systems. Epoxies that provide initially high adhesion to the underlying steel provide no advantage over conventional epoxy coatings. All coated bars that were evaluated exhibited corrosion losses at openings through the coating. A reduction in adhesion between an epoxy coating and the reinforcing steel occurs after a period of exposure to corrosive conditions. This reduction increases with increasing chloride content in the concrete and in the presence of cracks and decreases with the use of corrosion inhibitors, with the use of MC reinforcement, and with electrical isolation of the epoxy-coated bars from each other. Corrosion products form under the coating where adhesion has been reduced. For periods up to five years under exposure conditions representative of those in bridge decks, the reduction in adhesion between an epoxy coating and the reinforcing steel did not affect the rate at which coated bars corrode.

17. Key Words Adhesion, Chlorides, Concrete, Corrosion, Corrosion inhibitor, Durability, Epoxy-coated steel, Zinc-coated steel	18. Distribution Statement No restrictions. This document is available to the public through the National Technical Information Service, Springfield, VA 22161.		
19. Security Classif. (of this report) Unclassified	20. Security Classif. (of this page) Unclassified	21. No of Pages 255	22. Price

Form DOT F 1700.7 (8-72)   Reproduction of completed pages authorized

SI* (MODERN METRIC) CONVERSION FACTORS

APPROXIMATE CONVERSIONS TO SI UNITS

Symbol	When You Know	Multiply By	To Find	Symbol
LENGTH				
in	inches	25.4	millimeters	mm
ft	feet	0.305	meters	m
yd	yards	0.914	meters	m
mi	miles	1.61	kilometers	km
AREA				
in^2	square inches	645.2	square millimeters	mm^2
ft^2	square feet	0.093	square meters	m^2
yd^2	square yard	0.836	square meters	m^2
ac	acres	0.405	hectares	ha
mi^2	square miles	2.59	square kilometers	km^2
VOLUME				
fl oz	fluid ounces	29.57	milliliters	mL
gal	gallons	3.785	liters	L
ft^3	cubic feet	0.028	cubic meters	m^3
yd^3	cubic yards	0.765	cubic meters	m^3
NOTE: volumes greater than 1000 L shall be shown in m^3				
MASS				
oz	ounces	28.35	grams	g
lb	pounds	0.454	kilograms	kg
T	short tons (2000 lb)	0.907	megagrams (or "metric ton")	Mg (or "t")
TEMPERATURE (exact degrees)				
^oF	Fahrenheit	5 (F-32)/9 or (F-32)/1.8	Celsius	^oC
ILLUMINATION				
fc	foot-candles	10.76	lux	lx
fl	foot-Lamberts	3.426	candela/m^2	cd/m^2
FORCE and PRESSURE or STRESS				
lbf	poundforce	4.45	newtons	N
lbf/in^2	poundforce per square inch	6.89	kilopascals	kPa

APPROXIMATE CONVERSIONS FROM SI UNITS

Symbol	When You Know	Multiply By	To Find	Symbol
LENGTH				
mm	millimeters	0.039	inches	in
m	meters	3.28	feet	ft
m	meters	1.09	yards	yd
km	kilometers	0.621	miles	mi
AREA				
mm^2	square millimeters	0.0016	square inches	in^2
m^2	square meters	10.764	square feet	ft^2
m^2	square meters	1.195	square yards	yd^2
ha	hectares	2.47	acres	ac
km^2	square kilometers	0.386	square miles	mi^2
VOLUME				
mL	milliliters	0.034	fluid ounces	fl oz
L	liters	0.264	gallons	gal
m^3	cubic meters	35.314	cubic feet	ft^3
m^3	cubic meters	1.307	cubic yards	yd^3
MASS				
g	grams	0.035	ounces	oz
kg	kilograms	2.202	pounds	lb
Mg (or "t")	megagrams (or "metric ton")	1.103	short tons (2000 lb)	T
TEMPERATURE (exact degrees)				
^oC	Celsius	1.8C+32	Fahrenheit	^oF
ILLUMINATION				
lx	lux	0.0929	foot-candles	fc
cd/m^2	candela/m^2	0.2919	foot-Lamberts	fl
FORCE and PRESSURE or STRESS				
N	newtons	0.225	poundforce	lbf
kPa	kilopascals	0.145	poundforce per square inch	lbf/in^2

*SI is the symbol for the International System of Units. Appropriate rounding should be made to comply with Section 4 of ASTM E380.
(Revised March 2003)

TABLE OF CONTENTS

LIST OF FIGURES

viii

CHAPTER 1. INTRODUCTION

There are nearly 600,000 bridges in the United States, and more than 6 percent are structurally deficient due to corrosion-related damage.[1,2] The estimated direct annual cost of corrosion is $8.3 billion, and the estimated indirect cost to users due to traffic delays and lost productivity is equal to about 10 times this amount.[2] Bridge decks represent a special problem because cracks directly over and parallel to reinforcing steel provide an avenue for deicing salts to rapidly reach the reinforcement. Chloride analysis from bridge decks indicates that the chloride content in concrete around cracks can exceed the critical chloride corrosion threshold of conventional steel reinforcement within the first year.[3] Thus, the reinforcing steel in these structures must be protected against corrosion at the time of construction.

For more than 35 years, the corrosion-protection system used in most reinforced concrete structures has been epoxy-coated reinforcement (ECR) combined with increased concrete cover. This system has provided significant improvement over uncoated bars in the corrosion performance of reinforcing steel.[4,5] It has, however, not been without its critics.[6–8] Problems include the poor performance of ECR when the concrete remains saturated, such as in bridge piers in salt water, and the observation that the epoxy tends to lose its adhesion to the steel over time. (See references 4, 6, 7, and 9–11.) This reduction in adhesion, or disbondment, while the epoxy coating is still intact on the reinforcement is accelerated when the concrete remains wet.

Despite observations that portions of ECR have rusted, the corrosion of epoxy-coated steel has not resulted in the need for repairs when used in structures such as bridge decks, which allow the concrete to occasionally dry, except in the case of a few well-documented nonstandard applications.[4,5,8] Because ECR is a good, but not perfect, corrosion-protection system, there is strong impetus to develop methods to improve its performance.

The objective of this research was to evaluate a number of techniques for making ECR more corrosion-resistant by using multiple corrosion-protection strategies for ECR in bridge decks as well as in bridge members in marine environments where salt, moisture, and high temperatures (tropical weather) are prevalent.

This report describes the results for systems including chemical pretreatments and epoxy formulations that increase the adhesion of the epoxy coating to the reinforcing steel, conventional uncoated steel and conventional ECR with inorganic and organic corrosion inhibitors added to the concrete, reinforcement with a primer containing a microencapsulated corrosion inhibitor under a conventional epoxy coating, and bars coated with 98 percent zinc and 2 percent aluminum prior to epoxy application.

CHAPTER 2. EXPERIMENTAL WORK

CORROSION-PROTECTION SYSTEMS

This study involved the evaluation of 11 systems in which ECR was combined with another corrosion-protection system. The research included seven bar types: one uncoated and six with a fusion-bonded epoxy coating fabricated from the same heat of steel. Uncoated conventional reinforcing steel and conventional ECR served as the controls. The multiple corrosion-protection systems included conventional ECR in conjunction with one of three corrosion inhibitors; bars that were treated with a primer coating containing microencapsulated calcium nitrite (a corrosion inhibitor) prior to coating with conventional epoxy; bars with improved adhesion between the epoxy and the reinforcing steel, obtained through the use of either a zinc chromate pretreatment or special epoxies with higher adhesion; the combination of bars with an improved adhesion epoxy and the addition of calcium nitrite to the mortar or concrete; and bars with multiple coatings consisting of a 50-μm (2-mil) layer of 98 percent zinc and 2 percent aluminum that was, in turn, coated with a conventional epoxy. In addition, a second heat of conventional reinforcement was used to evaluate the corrosion performance of uncoated steel cast in concrete containing one of the three corrosion inhibitors used in the study. The systems are listed in table 1 along with the shorthand notation used in this report.

Table 1. Systems studied.

System	Abbreviation
Control	
Conventional uncoated reinforcing bars	Conv. and Conv.2
Conventional ECR	ECR
Epoxies with increased adhesion	
Chromate pretreatment	ECR(Chromate)
DuPont™ coating	ECR(DuPont)
Valspar® coating	ECR(Valspar)
Corrosion inhibitors in mortar or concrete	
Uncoated bars with $Ca(NO_2)_2$	Conv.2(DCI)
Uncoated bars with Hycrete	Conv.2(HY)
Uncoated bars with Rheocrete® 222⁺	Conv.2(RH)
ECR with calcium nitrite	ECR(DCI)
ECR with Hycrete™	ECR(HY)
ECR with Rheocrete® 222⁺	ECR(RH)
3M™ primer containing calcium nitrite	ECR(primer/$Ca(NO_2)_2$)
Epoxies with increased adhesion plus calcium nitrite in mortar or concrete	
Chromate pretreatment	ECR(Chromate)-DCI
DuPont™ coating	ECR(DuPont)-DCI
Valspar® coating	ECR(Valspar)-DCI
Bars with multiple coatings	MC

Control Systems

Uncoated Conventional Steel (Conv.)

With the exception of the tests to evaluate uncoated bars in concrete containing corrosion inhibitors, all tests of both uncoated and coated bars involved the use of a single heat of No. 16 (No. 5) Grade 420 (60) ASTM A615 reinforcing steel, identified as "Conv."[12] The uncoated reinforcement used in the corrosion inhibitor tests is identified as "Conv.2." Chemical analysis is shown in table 2.

Table 2. Chemical analysis of steel by percent.

Steel	Bar Size No.	Heat Number	C	Mn	Si	P	S	Cr	Ni	Mo	Cu	B
Conv.	16 (5)	231159	0.43	0.95	0.21	0.014	0.046	0.20	0.17	0.038	0.49	0.0005
Conv.2	16 (5)	N/A	N/A	N/A	N/A	N/A	N/A	N/A	N/A	N/A	N/A	N/A

C = Carbon; Mn = Manganese; Si = Silicon; P = Phosphorus; S = Sulfur; Cr = Chromium; Mo = Molybdenum;
Cu = Copper; N = Nitrogen; B = Boron.
N/A indicates chemical analysis not available.

Conventional ECR

The conventional reinforcement coated with fusion-bonded thermoset epoxy used as the control was coated with Scotchkote™ 413, manufactured by 3M™.

Epoxies with Increased Adhesion

A number of techniques have been used to improve the adhesion of epoxy coatings to steel. Three systems were evaluated in this study. The first involved pretreatment of uncoated steel with zinc chromate prior to the application of the epoxy coating. This procedure is used in Canada for all ECR, but because it involves the use of hexavalent chromate, which presents a significant environmental problem, it is not widely used in the United States. As an alternative, DuPont™ and Valspar® have developed epoxy powders with improved adhesion to reinforcing steel that do not require pretreating the bars. The three systems are identified as ECR(Chromate), ECR(DuPont), and ECR(Valspar).

Corrosion Inhibitors

Three corrosion inhibitors, one inorganic and two organic, were studied. Calcium nitrite is the most widely used inorganic corrosion inhibitor in U.S. practice. Because calcium nitrite acts as a set-accelerator, DCI® S, an admixture produced by Grace Construction Products that contains a retarder, was used in this study. The organic corrosion inhibitors were Rheocrete® 222+, a water-based combination of amines and esters produced by BASF Admixtures, and Hycrete™, a salt of alkenyl-substituted succinic acid produced by Broadview Technologies for this study and now produced by Hycrete, Inc. A fourth system, in which the epoxy coating Scotchkote™ 413 was applied to the bars after the application of a primer coating that contains microencapsulated calcium nitrite, was also evaluated. According to 3M™, the system provides protection by releasing calcium nitrite as the epoxy coating is damaged. The systems are identified, respectively, as ECR(DCI),

ECR(HY), ECR(RH), and ECR(primer/Ca(NO$_2$)$_2$). The three corrosion inhibitors (DCI$^®$ S, Hycrete™, and Rheocrete$^®$) were also studied in conjunction with conventional uncoated reinforcement and are identified as Conv.2(DCI), Conv.2(HY), and Conv.2(RH), respectively.

Epoxies With Increased Adhesion Plus Calcium Nitrite

The three types of ECR with improved adhesion were also evaluated in mortar and concrete containing the corrosion inhibitor calcium nitrite. The systems are identified as ECR(Chromate)-DCI, ECR(DuPont)-DCI, and ECR(Valspar)-DCI.

Multiple Coatings

Western Coating developed a patented process for multiple-coated (MC) bars that involves the application of a layer of 98 percent zinc and 2 percent aluminum to reinforcing steel using a thermal spray coating process prior to the application of the epoxy coating. The zinc layer has a nominal thickness of 50 μm (2 mil). Following application of the zinc, the bars in this study were coated with DuPont™ 8-2739 Flex West Blue, a conventional epoxy.

One applicator applied the epoxy to the conventional ECR and ECR(Valspar) bars. A second applicator handled the MC and ECR(DuPont) bars while two other applicators individually handled the ECR(Chromate) and ECR(primer/Ca(NO$_2$)$_2$) bars.

PRETEST EVALUATION OF EPOXY-COATED BARS

Prior to corrosion testing, the bars used in this study were evaluated for coating thickness and number of holidays. The bars were also evaluated for coating adhesion using the cathodic disbondment test in accordance with ASTM A775-04a and ASTM G8-96 (referred to hereafter as ASTM A775 and ASTM G8, respectively).[13,14]

Evaluation of Coating Thickness and Holidays

The six types of ECR bars used in this study were evaluated for coating thickness and number of holidays. The results are summarized in table 3. All bars met the coating thickness requirements of ASTM A775 except the bars with the calcium nitrite primer coating, which tended to have larger percentages of coating measurements below 175 and 125 μm (6.89 and 4.92 mil) than the maximum allowable values of 10 and 5 percent, respectively.[1][13] Only the bars with the calcium nitrite primer coating exhibited holidays, although the number of holidays was below the maximum allowable of 3 holidays/m (1 holiday/ft) specified in ASTM A775. The other five bar types exhibited no measurable holidays on full-size bars. Additional tests of small bar samples, however, indicated the presence of a small number of holidays on all bar types.

---

[1] The requirements for coating thickness measurements have changed since the initiation of this study, but with the exception of the bars with the calcium nitrite primer coating, it is expected that the bars in this study would meet the current coating thickness criteria (ASTM A775-07b).[15]

Table 3. Coating thickness.

Type of Bar	Number of Measurements[a]	Maximum (μm)	Minimum (μm)	Average (μm)	Coefficient of Variation
ECR	4 bars, 144 locations	307	175	244	0.10
ECR(Chromate)	1 bar, 36 locations	241	175	213	0.07
ECR(DuPont)	1 bar, 36 locations	249	160	213	0.08
ECR(Valspar)	1 bar, 36 locations	262	175	226	0.11
ECR(primer/ Ca(NO$_2$)$_2$)	4 bars, 126 locations	264	102	188	0.16
MC	1 bar, 36 locations	251	213	236	0.04

1 μm = 0.0394 mil
[a] Bars were 6.1 m (20 ft) long; 15 to 18 measurements were evenly spaced along each side of the test bar.

Cathodic Disbondment Tests

Cathodic disbondment tests involve the penetration of the epoxy coating on a test specimen using a 3-mm (0.12-inch)-diameter drill bit. The specimen is then immersed for 168 h in an electrolyte (3 percent sodium chloride) solution at 24 ±2 °C (75 ±3.6 °F) and maintained at a -1.5 V potential difference with an anode, measured with respect to a saturated calomel electrode (SCE). The test setup, as described in ASTM A775, is shown in figure 1.[13]
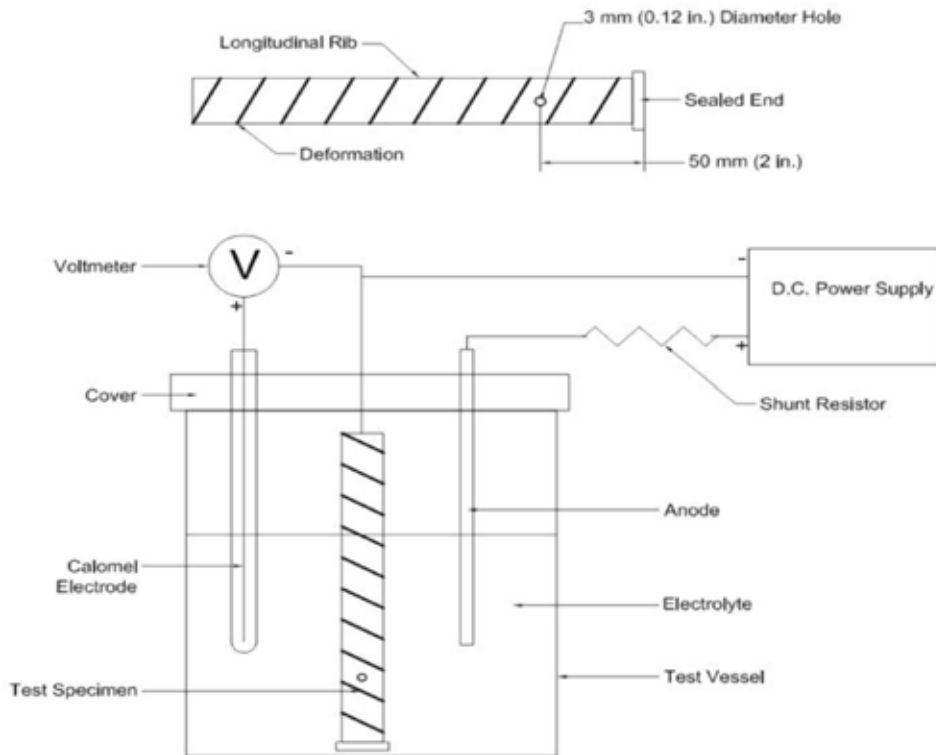
Figure 1. Illustration. Cathodic disbondment test setup (after reference 13).

An examination is performed immediately upon termination of the test. At the end of the test period, the test area is rinsed with warm tap water. The sample is immediately wiped dry, and the entire area of coating is visually examined at the edge of the intentional defect. A new defect, to serve as a reference, is drilled in a portion of the coated area that was not immersed. Two radial cuts at 90 degrees to each other and oriented 45 degrees with respect to the longitudinal axis of the bar are made through the coating, intersecting the center of both intentional defects, using a sharp, thin-bladed knife. An attempt is then made to lift the coating at both the reference defect and the submerged defect with the point of the knife. The bond at the reference defect is then used to judge the quality of the bond at the submerged holiday. Finally, the increase in radial area and total area of the disbonded coating at the submerged defect are measured and recorded.

In this study, three rounds of cathodic disbondment tests were performed, with one specimen per round for each of the six types of ECR. Tests were also performed on conventional epoxy-coated bars that had been used in a previous study. In accordance with ASTM A775, four radial measurements were taken of the disbonded region at 0, 90, 180, and 270 degrees with respect to the longitudinal axis of the bar, and the values were averaged.[13] The cathodic disbondment tests were recorded in terms of both the area of the disbonded coating (in accordance with ASTM G8) and the average coating disbondment radius (four measurements).[14] The results are summarized in table 4. The area of the disbonded coating and the radius do not include the original penetration through the coating. As shown in table 4, the average coating disbondment radius was above 4 mm (0.16 inches), the maximum allowed in annex A1 of ASTM A775, for the conventional ECR and ECR(Valspar) bars, indicating that these bars failed the coating disbondment requirements. The MC reinforcement, ECR(DuPont), ECR(Chromate), and ECR(primer/Na(NO$_2$)$_2$) bars met the coating disbondment requirements. Table 4 also shows that the conventional ECR exhibited the highest area of disbonded coating, with an average value of 178 mm^2 (0.271 in^2). The high-adhesion Valspar® bars had an area of disbonded coating of 151 mm^2 (0.230 in^2), followed by ECR with calcium nitrite primer at 67 mm^2 (0.102 in^2) and the high-adhesion DuPont™ bars at 65 mm^2 (0.099 in^2). The MC and ECR(Chromate) bars had the lowest areas of disbonded coating, with average values of 27 and 20 mm^2 (0.041 and 0.030 in^2), respectively. Like the conventional ECR used in this study, the conventional ECR from the previous study also exhibited an average disbondment radius, 5.5 mm (0.21 inches), that exceeded the 4 mm (0.16 inches) allowed by ASTM A775; the disbonded area equaled 168 mm^2 (0.256 in^2).

Table 4. Cathodic disbondment results.

Type of Bar	Test No.	Thickness (µm)	Coating Disbondment Radius[a] (mm)					Area of Disbonded Coating[b] (mm²)
			0°	90°	180°	270°	Average	
ECR	1	NM	6.5	6.5	6	5.5	6.1	183
	2	NM	6.5	5	3.5	4	4.8	133
	3	249	6.5	6.5	7.5	6.5	6.8	219
	Average						5.9	178
ECR[c]	1	300	5.5	6.5	5.5	5	5.6	170
	2	274	5.5	4.5	4.5	5.5	5.0	161
	3	241	6.5	5.5	5.5	5.5	5.8	174
	Average						5.5	168
ECR(Chromate)	1	NM	0.5	1	0	0	0.4	6
	2	NM	1	0.5	2	2.5	1.5	35
	3	279	1.5	0.5	0.5	1.5	1.0	19
	Average						1.0	20
ECR(DuPont)	1	NM	4	3	3.5	3.5	3.5	93
	2	NM	1.5	1	1.5	1	1.3	19
	3	224	3.5	4	3.5	4	3.8	83
	Average						2.8	65
ECR(Valspar)	1	NM	4.5	4	4.5	4	4.3	133
	2	NM	6	4.5	5.5	4.5	5.1	167
	3	269	6.5	4.5	5.5	4.5	5.3	154
	Average						4.9	151
ECR (primer/Ca(NO₂)₂)	1	NM	1.5	2	2	2	1.9	58
	2	NM	3.5	2.5	4.5	2.5	3.3	77
	3	203	3	2.5	2.5	2.5	2.6	67
	Average						2.6	67
MC	1	NM	2.5	1.5	1	1	1.5	22
	2	NM	2	1.5	1.5	3	2.0	35
	3	284	0.5	2.5	1.5	1.5	1.5	25
	Average						1.7	27

1 µm = 0.0394 mil
1 mm = 0.039 inches
1 mm² = 0.00155 in²
NM = Not measured
[a] Coating disbondment radius measured from edge of 3-mm (0.12-inch)-diameter hole.
[b] Area of disbonded coating is the total area after disbondment minus the original area of a 3-mm (0.12-inch)-diameter hole.
[c] Conventional ECR from previous study.

The criteria in annex A1 of ASTM A775 are qualification requirements for the epoxy coating itself and are not meant to be applied to production bars such as those used in this study. Thus,

although all bars did not all meet the qualification criteria, they are considered to be representative of bars used in practice. Further, as observed in earlier tests by McDonald et al., the performance of the bars in the cathodic disbondment tests did not prove to be a predictor of their performance in the corrosion tests in this study.[16]

CORROSION TEST PROCEDURES

The corrosion-protection systems in this study were evaluated using a combination of laboratory and field tests. The performance of each system was compared to that of conventional ECR and uncoated mild steel reinforcement. The tests included rapid macrocell tests, bench-scale tests, linear polarization resistance, and field tests.

Rapid Macrocell Tests

Summary of Method

The response of the multiple corrosion-protection systems was first evaluated using the rapid macrocell test, originally developed at the University of Kansas under the Strategic Highway Research Program and since updated. (See references 17 through 26). The goal of the test is to obtain a realistic measure of the performance of corrosion-protection systems in a short time period. The basic test specimen consists of either a bare reinforcing bar or a bar clad in mortar (mortar-wrapped), as illustrated in figure 2 through figure 4. The procedures used for bare bars are incorporated in annex A2 of ASTM A955.[27] The contact surface between the mortar and the bar simulates the contact obtained between concrete and reinforcing bars in structures through the use of realistic water-cement and sand-cement ratios.
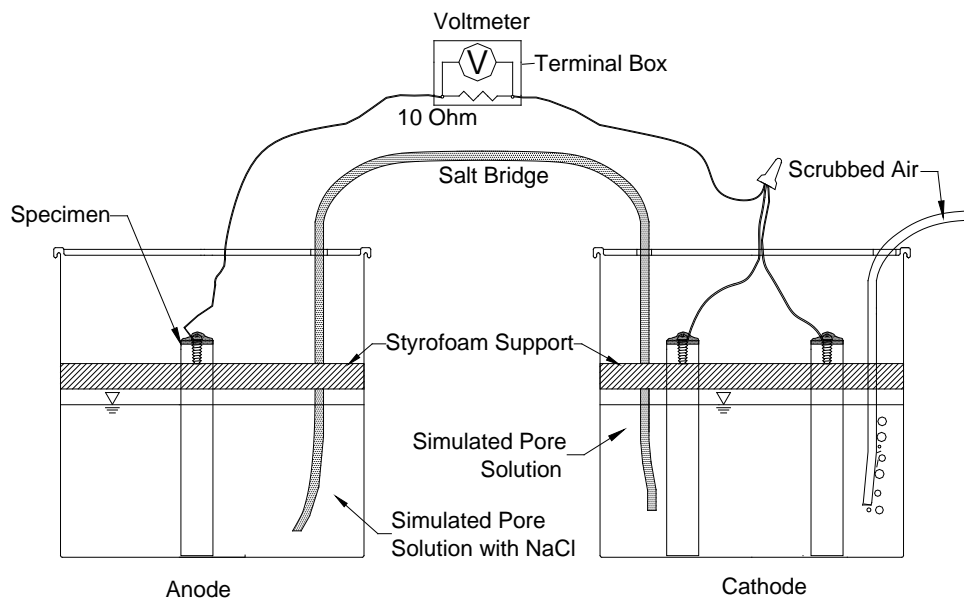
Figure 2. Illustration. Macrocell test with bare bar specimens.

9
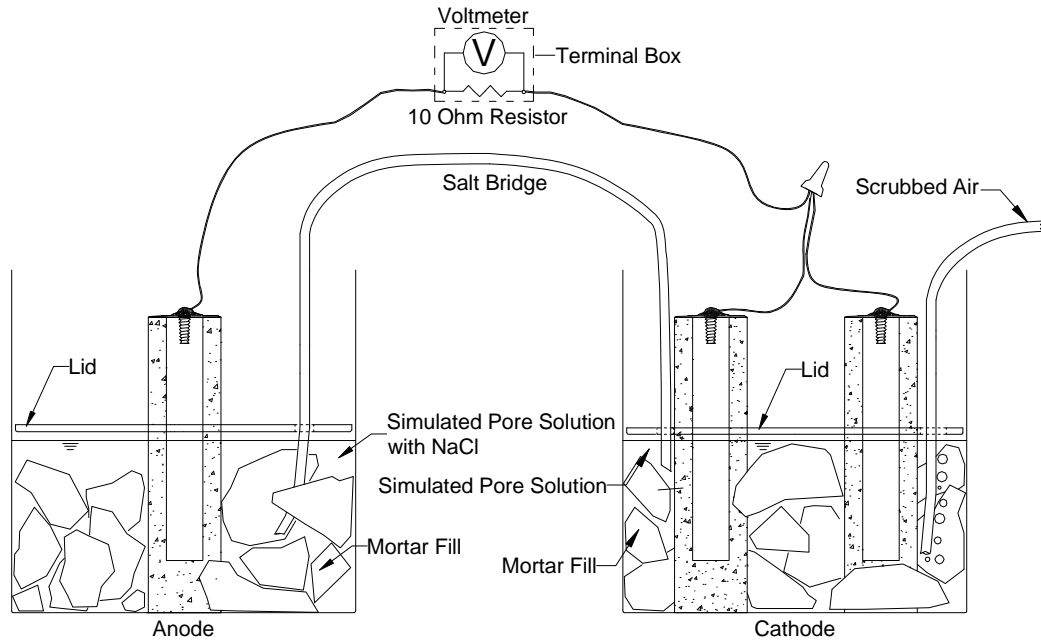
Figure 3. Illustration. Macrocell test with mortar-clad specimens.
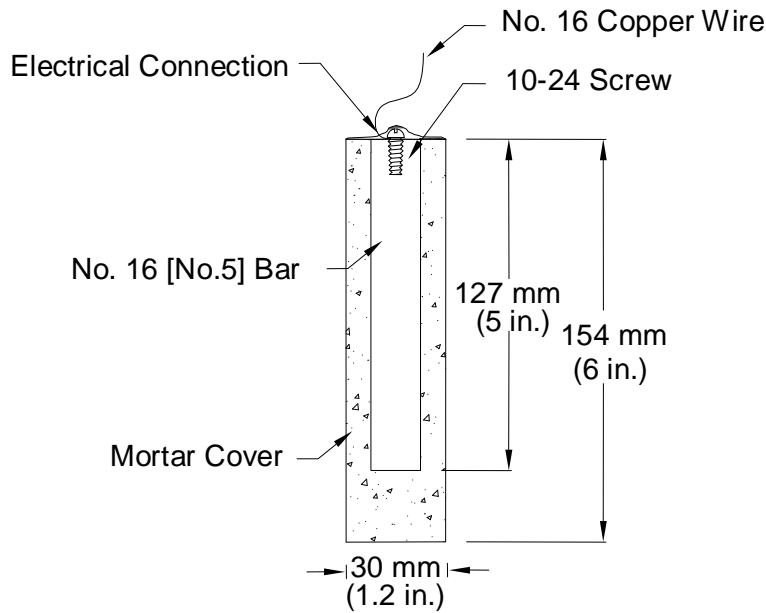
Figure 4. Illustration. Mortar-wrapped specimen containing conventional reinforcing bar.

The macrocell tests shown in figure 2 and figure 3 require two containers. The test specimen, either a bare or mortar-wrapped No. 16 (No. 5) bar, is placed in a 1.5-L (1.6-qt) container along with simulated pore solution containing a preselected concentration of sodium chloride (1.6 or 6.04 moles/kg (0.73 or 2.74 moles/lb) of solvent-ion (4.68 or 15 percent) concentration). Two specimens are placed in a second container and immersed in simulated pore solution with no chlorides added. For mortar-wrapped specimens, crushed mortar fill is added to the containers to more closely simulate the concrete environment. The solution depth exposes 76 mm (3.0 inches) of the bar (including the 13-mm (0.5-inch) plastic cap used to protect the end of epoxy-coated

bars) below the level of the solution. The two containers are connected by a salt bridge, and the test specimen in the pore solution containing sodium chloride (anode) is electrically connected across a single 10-ohm resistor to the two specimens in the simulated pore solution (cathode). The resistors are mounted between binding posts in a terminal box to consolidate the specimen wires. Air (scrubbed to remove carbon dioxide) is bubbled into the liquid surrounding the cathode to ensure an adequate supply of oxygen. Plastic lids are placed just above the surface of the solution to hold the specimens in place and reduce evaporation of the solution. Holes are cut in the lids to introduce the specimens, a salt bridge, and the air supply. The air causes some evaporation, which is countered by adding deionized water to the container to maintain a constant volume of solution. The solutions in both containers are changed once every 5 weeks to further protect against carbonation.[2] The corrosion current and the rate of corrosion are determined by measuring the voltage drop across the resistor. The open circuit corrosion potentials of the cathode and anode are also measured with respect to an SCE after the circuit has been open for 2 h to allow the potentials to stabilize. The simulated pore solution, consisting of sodium hydroxide and potassium hydroxide, matches that obtained in a pore solution analysis.[28,29] Epoxy-coated steel is evaluated using specimens in which the coating is breached by four 3.2-mm (0.13-inch)-diameter holes to simulate defects in the epoxy coating (damaged area equals 1.0 percent of total exposed area in the solution). In the rapid macrocell test, bare conventional bars exhibit corrosion initiation within the first 24 h, and conventional bars cast in mortar exhibit corrosion within the first week. The tests last 15 weeks.

Corrosion Rate and Corrosion Loss

The corrosion rate of reinforcing steel (measured in the bench-scale and field tests as well as in the rapid microcell tests) indicates how fast reinforcing steel is oxidized. It may be expressed as a current density in microamps per square centimeter ($\mu A/cm^2$), which is obtained by measuring the rate of electron flow from anodes to cathodes. Based on Faraday's law, current density can be converted to another expression for corrosion rate, a rate of loss of metal from the surface of the steel in $\mu m/year$.[30] The equation in figure 5 shows this conversion for iron.

$$R = k \frac{ia}{nFr} = 11.6i$$

Figure 5. Equation. Corrosion rate for iron.

Where:

R = Corrosion rate, given as rate of metal loss, $\mu m/year$.

i = Corrosion rate, given as current density, $\mu A /cm^2$.

k = Conversion factor = 31.5×10^4 amp·μm s/μA cm·year.[30]

a = Atomic weight of the metal = 55.8 g/mole for iron.

n = Number of electrons transferred = 2 for iron.

F = Faraday's constant = 96,500 Coulombs/equivalent.

r = Density of the metal, g/cm^3 = 7.87 g/cm^3 for iron.

---

[2] The 5-week interval was satisfactory to maintain the pH of the solutions above 13.3.

For example, calculating corrosion loss for a bare conventional bar, a voltage drop of 0.70 mV across the 10-ohm resistor represents a total current of 70.0 µA. For a No. 16 (No. 5) bar and a solution depth of 76 mm (3.0 inches) (the values used in the test), the total surface area in contact with the solution (based on the nominal diameter of the bar and including the end of the bar) is 4,021 mm² (6.233 in²), giving a current density i of 1.74 µA/cm² (11.2 µA/in²). Applying the equation in figure 5 results in the equation in figure 6.

$$R = 11.6i = 11.6 \times 1.74 = 20.2 \ \mu m/year$$

Figure 6. Equation. Example of corrosion rate for iron.

For zinc, the first coating layer on the MC bars, the equation in figure 5 becomes the equation in figure 7.

$$R = k \frac{ia}{nF\rho} = 15.0i$$

Figure 7. Equation. Corrosion rate for zinc.

Where:

a = Atomic weight of the metal = 65.38 g/mole for zinc.

n = Number of electrons transferred = 2 for zinc.

ρ = Density of the metal, g/cm³ = 7.14 g/cm³ for zinc.

For reinforced concrete bridge decks, the measurement of the macrocell current is generally not possible because the top and bottom mats of reinforcing steel are usually connected by steel wire ties and bar supports in the concrete slab. In laboratory tests that simulate the corrosion of steel in bridge decks, however, ties and bar supports are not used, and the macrocell current can be determined by measuring the voltage drop across a resistor that electrically connects the anode and the cathode through an external circuit, as shown in the equation in figure 8.

$$i = \frac{V}{RA}$$

Figure 8. Equation. Corrosion current density.

Where:

i = Corrosion current density, µA/cm².

V = Voltage drop across the resistor, mV.

R = Resistance of the resistor, kilohms.

A = Area of exposed metal on the anode bar, cm².

The measured macrocell current density and the calculated corrosion rate can be affected significantly by the test methods and the details of the test configuration such as the anode to cathode area ratio and the size of the resistor connecting the anode and the cathode.[31,16] Thus, the corrosion rate calculated from the measured macrocell current should be used only to compare the relative performance of corrosion-protection systems under same test conditions.

Corrosion loss represents cumulative metal loss expressed in micrometers and is calculated by numerically integrating the corrosion rate.

Test Specimens

The specimens in the rapid macrocell test consist of 127-mm (5-inch)-long No. 16 (No. 5) reinforcing bars, either bare or embedded in mortar, as illustrated in figure 9 for epoxy-coated bars.
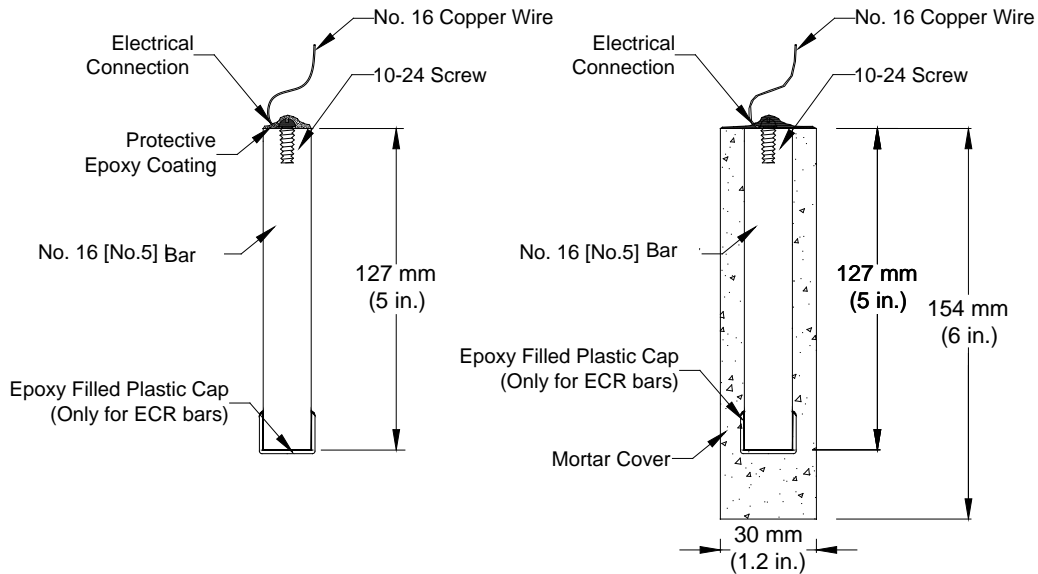
Figure 9. Illustration. Bare bar and mortar-wrapped rapid macrocell specimens with cap to protect the exposed end of epoxy-coated bars.

The following procedure is used to fabricate the specimens:

1. **Preparation of reinforcing bars:** One end of the bar is drilled and tapped 13 mm (0.5 inches) to accommodate a No. 10-24 machine screw. The sharp edges on the bar ends are removed by grinding. Uncoated bars are cleaned with acetone to remove grease and dirt from the surface. ECR bars are cleaned with soap and water. The epoxy coating is penetrated by four 3.2-mm (0.13-inch)-diameter holes to simulate defects in the coating. The holes are made to a depth of 0.5 mm (0.02 inches) using a 3.2-mm (0.13-inch)-diameter four-flute end mill. Two of the holes are placed at the midlength of the bars, and the other two are placed about 32 mm (1.3 inches) from the untapped end, which is submerged in the solution. The submerged end is protected using a plastic cap filled with a repair epoxy. The four holes represent 1 percent damage to the evaluated area of the epoxy-coated bars. When a mortar-wrapped specimen is used, a prepared bare bar is symmetrically embedded in a 154 mm (6-inch)-long mortar cylinder. The cylinder has a 30-mm (1.2-inch) diameter and provides a 7-mm (0.28-inch) mortar cover over the reinforcing bar. Mortar-wrapped bars are cast in a mold consisting of polyvinyl chloride (PVC) pipes and fittings.[24–26]

2. **Casting:** Mortar is placed in a cylindrical PVC mold in four layers. Each layer is rodded 25 times using a 2-mm (0.08-inch) diameter rod, followed by vibration for 30 s on a vibration table with an amplitude of 0.15 mm (0.006 inches) and a frequency of 60 Hz.

3. **Curing:** Specimens are cured in the molds for 1 day at room temperature and then removed from the molds and cured in saturated lime water (pH » 12.4) for 13 days to reach a passive condition. After this period, the specimens are surface-dried with compressed air and then vacuum dried for 1 day.

4. **Wiring and coating:** For both bare and mortar-wrapped bars, a 16-gauge copper electrical wire is attached to the tapped end of each specimen with a 10-24´ 1/2 (13-mm (0.5-inch)-long) screw. The electrical connection is then coated with two layers of Herberts-O'Brien epoxy for bare bars or two layers of Ceilgard 615™ epoxy for mortar-wrapped specimens.

Test Materials

The following materials are used in rapid macrocell tests:

- **Simulated concrete pore solution:** Simulated concrete pore solution is used at the cathode. One liter of the solution contains 974.8 g (34.39 oz) of distilled water, 18.81 g (0.6635 oz) of potassium hydroxide, and 17.87 g (0.6303 oz) of sodium hydroxide, based on pore solution analysis by Farzammehr et al.[28,29]

- **Simulated concrete pore solution with sodium chloride:** The solution was used at the anode and is prepared by adding 45.6 or 172.1 g (1.61 or 6.07 oz) of sodium chloride to 1 L (0.3 gal) of the simulated concrete pore solution to obtain a 1.6 or 6.04 molal ion concentration solution, equal to a 0.8 or 3.02 molal sodium chloride solution.

- **Salt bridges**: A salt bridge provides an ionic path between the cathode and the anode. It consists of a 0.45-m (1.5-ft)-long plastic tube filled with a conductive gel. To prepare a salt bridge, 4.5 g (0.16 oz) of agar, 30 g (1.1 oz) of potassium chloride, and 100 g (3.53 oz) of distilled water are mixed and then heated over a hot plate until the solution starts to thicken. The heated mixture, enough to produce four salt bridges, is poured into plastic tubes using a funnel. The tubes then placed in boiling water for 1 h to firm the gel, keeping the ends of the tubes above the surface of the water. The gel in the salt bridges must be continuous, without interruption by air bubbles.

- **Mortar:** The mortar has a water-cement (w/c) ratio of 0.5 and sand-cement ratio of 2.0 by weight and is made with Type I/II portland cement (ASTM C150), distilled water, and ASTM C778 graded Ottawa sand.[32,33] The mix proportions represent the mortar constituent of concrete. The mortar is mixed in accordance with the procedures outlined in ASTM C305.[34]

- **Mortar fill**: Mortar fill is placed in containers with mortar-wrapped specimens. The fill consists of the same mixture used in the test specimens. The fill is cast in a metal baking sheet to a depth of about 25 mm (1 inch). The mortar in the sheet is air-cured at room temperature for 15 days and broken into 25- to 50-mm (1- to 2-inch) pieces prior to use.

Data Acquisition

A voltmeter with a 0.001 mV resolution is used to measure corrosion potential of the anode and cathode and the voltage drop across the 10-ohm resistor. In a typical test, the voltage drop tends to fluctuate between -0.003 and 0.003 mV when the corrosion current is close to zero. Only voltage drop readings outside of this region are used to evaluate the performance of the corrosion-protection systems. Values between -0.003 and 0.003 mV are treated as zero.

Bench-Scale Tests

During the past two decades, bench-scale tests such as the southern exposure, cracked beam, and ASTM G109 tests have frequently been used to evaluate the corrosion performance of reinforcing steel.[31,35,36] Of these tests, the southern exposure and cracked beam tests have proven to give useful data in a relatively short period. All three test methods were used in this study, but only the results for the first two are reported because they yielded useful data. The ASTM G109 test uses only a 3 percent sodium chloride solution and provides a much milder degree of exposure to the specimens. It yielded no useful information over a 4-year period, twice as long as that used for the southern exposure and cracked beam tests.

Southern Exposure Test

The specimen used in the southern exposure test consists of a small slab containing two mats of reinforcing steel (see figure 10).[37]
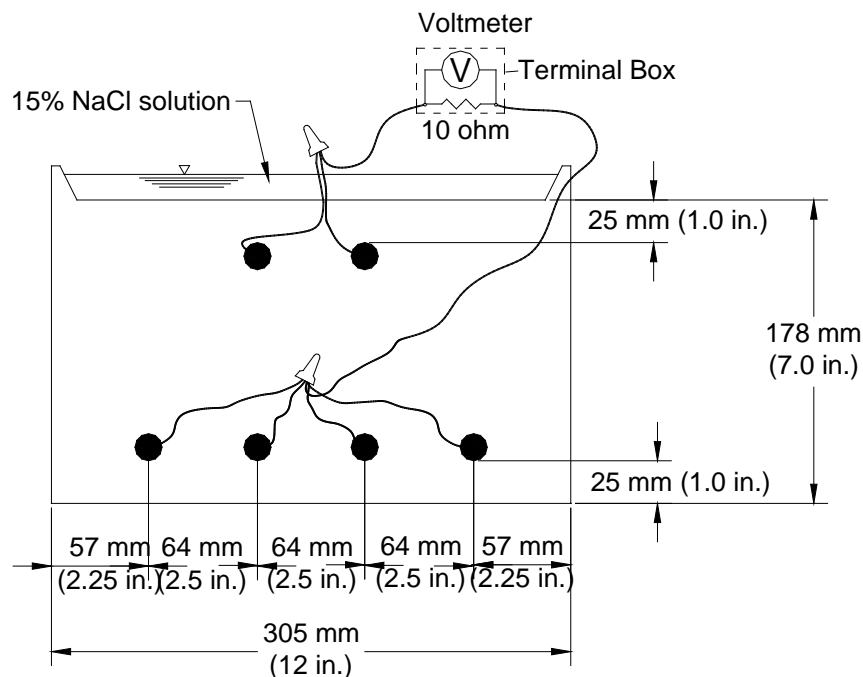
Figure 10. Illustration. Southern exposure test specimen.

The concrete is wet cured for 3 days and then air cured until the test begins at 28 days. The top mat consists of two No. 16 (No. 5) bars, and the bottom mat consists of four No. 16 (No. 5) bars. The mats are connected electrically across a 10-ohm resistor, a dam is placed around the edge of

the top surface (cast integrally with the specimen), and the sides of the concrete are sealed with epoxy. A 15 percent (6.04 molal ion) sodium chloride solution is placed inside the dam, allowing the chlorides to penetrate the concrete. The slabs are subjected to a 7-day alternate ponding and drying regime, with ponding at 23 ±2 °C (73 ±3 °F) for 4 days and drying at 38 °C (100 °F) (thus the name southern exposure) for 3 days. Prior to drying, the solution is removed from the upper surface using an industrial vacuum cleaner. The ponding and drying regime continued for 12 weeks. The specimens were then subjected to continuous ponding for 12 weeks at 23 ±2 °C (73 ±3 °F) after which the alternate ponding and drying regime begins again. The two regimes continued for 96 weeks. Corrosion current and the corresponding corrosion rate are determined by measuring the voltage drop across the resistor. The corrosion potentials of the top and bottom bars are measured.[3] Corrosion performance is also evaluated using monthly linear polarization resistance readings on selected specimens. The test provides a severe corrosion environment that is generally believed to simulate 15–20 years of exposure for marine structures under tropical conditions and 30–40 years of exposure for bridges within a 48-week period.[(38)]

Upon corrosion initiation and at the conclusion of the tests, southern exposure specimens are sampled for chloride content using procedures described in the section on chloride analysis later in this chapter.

Cracked Beam Test

The cracked beam specimen is used to model the corrosion of reinforcing steel in which cracks directly expose the steel to deicing chemicals (see figure 11). The specimen is half the width of the southern exposure specimen, with one bar on top and two bars on the bottom.
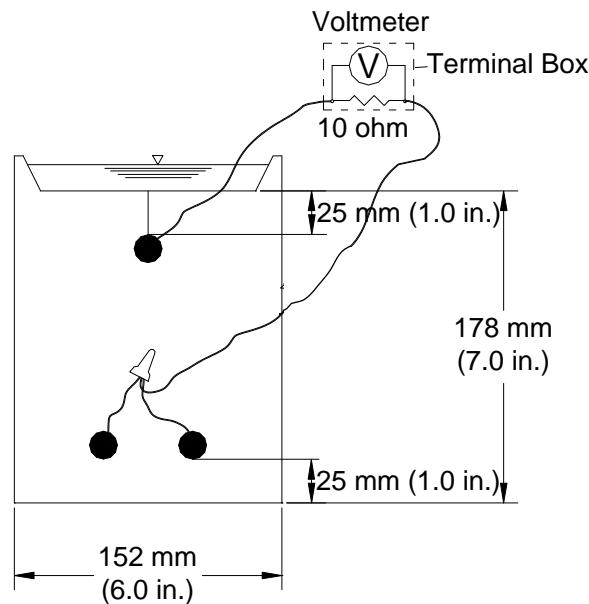
Figure 11. Illustration. Cracked beam test specimen.

---

[3] Corrosion potentials are measured with respect to an SCE on ponded specimens and a copper-copper sulfate (CSE) electrode for dry specimens. Potentials with respect to CSE are approximately 0.075 V more negative than those with respect to SCE.

A crack is simulated parallel to and above the top reinforcing bar through the insertion of a 0.3-mm (12-mil) stainless steel shim when the specimen is fabricated. The shim is removed within 12 h of casting, leaving a direct path for chlorides to the reinforcing steel and simulating the effects of a settlement crack over the bar. An integral dam is used in manner similar to that used for the southern exposure specimen around the upper surface of the specimen. Like the southern exposure specimen, the cracked beam specimen is subjected to cycles of wetting and drying with a 15 percent sodium chloride solution, continuing up to 96 weeks.

Specimen Fabrication

The following process is used to fabricate southern exposure and cracked beam specimens:

1. **Reinforcing bar preparation:** Each reinforcing bar is cut to a length of 305 mm (12 inches). Both ends of the bar are drilled and tapped 13 mm (0.5 inches) to accommodate a No. 10-24 machine screw. The sharp edges on the bar ends are removed with a grinder. Uncoated bars are cleaned with acetone to remove grease and dirt from the surface. ECR bars are cleaned with soap and water. The epoxy coating is then penetrated by four or ten 3.2-mm (0.125-inch)-diameter holes to simulate defects in the coating. The holes are made to a depth of 0.4 mm (16 mil) using a 3.2-mm (0.125-inch)-diameter four-flute end mill. Two or five holes are placed evenly along the length on each side of the bars. On the MC bars, specimens are evaluated with both layers penetrated and with only the epoxy penetrated. The epoxy is penetrated without damaging the zinc using a soldering gun set to a temperature of 205 °C (400 °F), which is above the melting temperature of epoxy but below the melting temperature of zinc. The burned epoxy regions are cleaned with acetone. Four holes represent 0.21 percent damage, and 10 holes represent 0.52 percent damage to the exposed surface of the epoxy-coated bar.

2. **Form assembly:** Formwork is made to cast the specimen in an inverted position. In this study, the forms consist of several pieces of 19-mm (0.75-inch)-thick plywood, including four sides and a bottom. Inside the mold, a smaller beveled wooden piece is bolted to the bottom to create the integral concrete dam after casting. For the cracked beam forms, a 152-mm (6-inch)-long, 0.3-mm (0.012-inch)-wide longitudinal slot is made in the center of the beveled wood to accommodate a 0.3-mm (0.012-inch)-thick stainless steel shim. The shim projects 25 mm (1 inch) from the slot and just touches the test bar. After demolding, the shim is removed from the concrete to form the crack. All parts of the mold are fastened with angles and clamps. The inside corners are sealed with clay. The bars are supported by 10-24×1 (25-mm (1.0-inch)-long) screws through 4.8-mm (0.19-inch)-diameter holes in two side pieces of the form. When epoxy-coated bars are tested, two of the holes in the coating face up and the other two face down.

3. **Casting:** Concrete is mixed in accordance with the requirements of ASTM C192 for mechanical mixing.[39] The concrete mixture proportions are given in table 5. The concretes have a w/c ratio of 0.45 or 0.35 and a nominal air content of 6 percent. The specimens are cast in two layers. Each layer is vibrated for 30 s on a vibrating table with an amplitude of 0.15 mm (0.006 inches) and a frequency of 60 Hz. The concrete surface is finished with a wooden float.

Table 5. Concrete mixtures.

w/c	Cement, kg/m^3	Water, kg/m^3	Fine Aggregate, kg/m^3	Coarse Aggregate, kg/m^3	Air-Entraining Agent, mL/m^3	DCI, L/m^3	Hycrete™, kg/m^3	Rheocrete®, L/m^3	SP, L/m^3
0.45	355	160	851	880	90	–	–	–	–
	355	147.4	851	880	140	15	–	–	–
	355	154.0	851	880	35	–	8.0	–	–
	355	155.7	851	880	300	–	–	5	–
0.35	438	153	764	861	355	–	–	–	2.12
	438	140.4	764	861	740	15	–	–	2.12
	438	145.6	764	861	330	–	9.9	–	2.25
	438	148.7	764	861	1,480	–	–	5	2.25

1 kg/m^3 = 1.69 lb/yd^3
1 mL/m^3 = 0.026 fl oz/yd^3
1 L/m^3 = 0.202 gal/yd^3
SP = Superplasticizer (Rheobuild® 1000 by BASF Admixtures, Inc.)
– Not used.

4. **Curing:** The specimens are cured in the mold for 24 h at room temperature, except the cracked beam specimens, which usually require earlier demolding (8–12 h) to facilitate the removal of the shim. Once removed from the mold, specimens are cured at room temperature in a plastic bag with water until 72 h after casting. The specimens are then removed from the bag and air-cured for 25 days. Testing starts 28 days after casting.

5. **Wiring and coating:** Two days before testing begins, 16-gauge copper electrical wire is attached to one end of each bar embedded in the specimens with a 10-24×1/2 (13-mm (0.5-inch)-long) screw. The other end of the bar is sealed with the same kind of screw. All four sides of the specimens, including the electrical connections, are then coated with two layers of epoxy such as Ceilgard 615™ or ThoRoc® SewerGuard® HBS. The epoxy is mixed and applied according to manufacturer's recommendations.

Test Materials

The properties of the materials were as follows:

- **Cement:** Type I/II portland cement.

- **Coarse aggregate:** Crushed limestone with maximum size = 19 mm (0.75 inches), bulk specific gravity (SSD) = 2.58, absorption (dry) = 2.27 percent, unit weight = 1,536 kg/m^3 (2,589 lb/yd^3).

- **Fine aggregate:** Kansas River sand with bulk specific gravity (SSD) = 2.62, absorption (dry) = 0.78 percent, fineness modulus = 3.18.

- **Air-entraining agent:** Daravair® 1400 by Grace Construction Products.

A 15 percent sodium chloride solution (6.04 molal ion concentration) was used to pond the test specimens: 600 mL (20.3 fl oz) to pond one southern exposure specimen and 300 mL (10.1 fl oz) to pond one cracked beam specimen.

Data Acquisition

The same voltmeter and rules for data conversion described for the rapid macrocell tests were used for the bench-scale tests.

Corrosion Initiation Beam Tests

The corrosion initiation beam test is used to determine the critical chloride corrosion threshold of a corrosion-protection system. While these data are also obtained from southern exposure specimens, corrosion initiation tests are terminated at the onset of corrosion, thus allowing a greater number of samples to be collected. The test was used in this study to evaluate conventional reinforcing steel cast in concrete containing corrosion inhibitors. The specimen is identical to the cracked beam specimen except that no intentional crack is placed above the reinforcement. The corrosion initiation beam specimen is shown in figure 12.
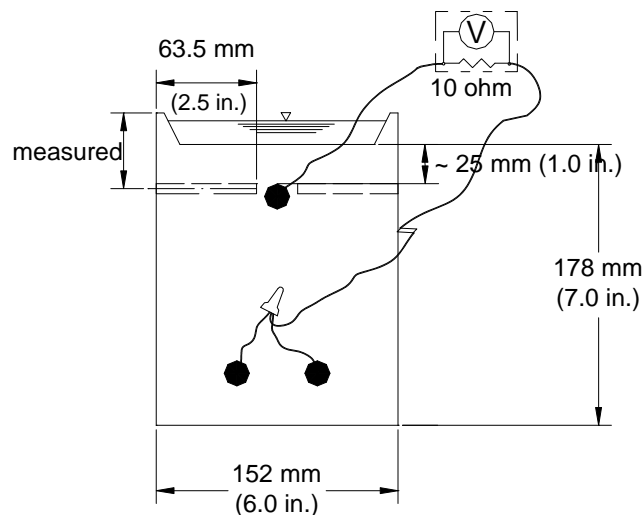
Figure 12. Illustration. Corrosion initiation beam test specimen.

The materials, fabrication, and testing procedures used in the corrosion initiation tests are identical to those used for the southern exposure and cracked beam tests with the exception of test duration. The w/c ratio is 0.45.

For conventional reinforcing steel, corrosion initiation is considered to occur when either the macrocell corrosion rate first reaches a value greater than or equal to 0.3 µm/year (0.01 mil/year) or when the corrosion potential of the top mat of steel first shifts to a value more negative than -0.350 V with respect to a CSE. For zinc-coated steel, corrosion initiation is based on a corrosion rate of 0.3 µm/year (0.01 mil/year) or when a sharp change in corrosion potential is observed, with the former serving as the primary guide.

Once corrosion initiation occurs, testing is halted and concrete samples are taken for chloride analysis. A total of 20 samples are taken from each initiation beam, 10 from each side of the beam starting 40 mm (1.5 inches) from the edge and spaced at 25-mm (1-inch) intervals, as shown in the side view of the specimen in figure 13. For each sample, drilled holes are positioned so that the top of the holes and the top surface of the reinforcing bar are at the same level. To do this, the actual level of the top reinforcing bar in each specimen is measured. Concrete sampling and chloride analysis are preformed as described later in this chapter.
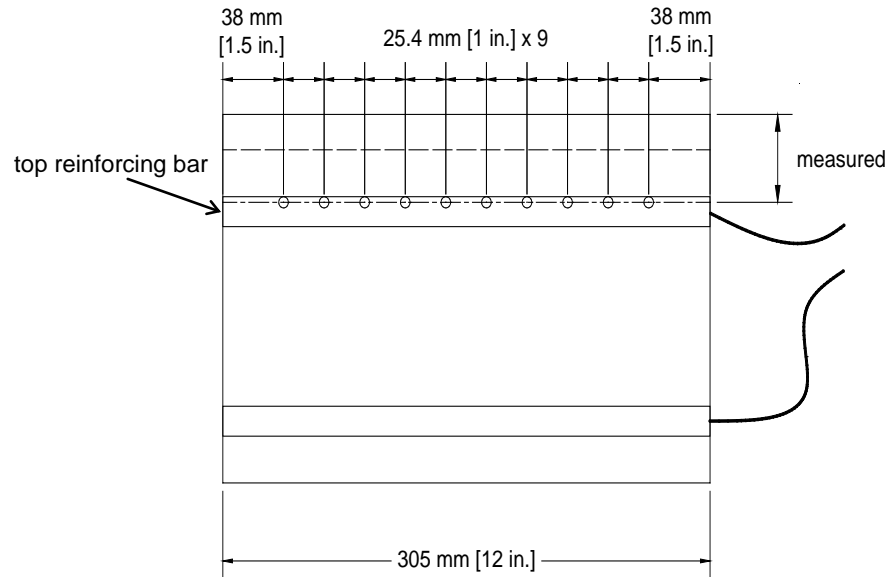
Figure 13. Illustration. Sampling locations for initiation beam tests.

Linear Polarization Resistance Test

A measure of both microcell and macrocell corrosion can be obtained with the polarization resistance test, which uses a noncorroding counter electrode and a reference electrode to establish a polarization curve by imposing a range of potentials on the metal and measuring the corresponding corrosion currents using a potentiostat. Polarization resistance measurements were obtained from selected bench-scale specimens throughout the test period.

Polarization resistance tests were used in this study to obtain the total corrosion rates for bench-scale specimens. In the tests, current readings are taken during a short, slow sweep of bar potential. The sweep typically ranges from -20 to +20 mV relative to the open circuit potential E_{oc}. In this range, the current-versus-voltage curve is roughly linear. The slope of the linear region is proportional to the resistance of the metal. The total corrosion current density is obtained using the relationship shown in figure 14.

$$i = \frac{B}{R_p}$$

Figure 14. Equation. Corrosion current density.

Where:

i = Corrosion current density (A/cm^2).

B = Stern-Geary constant (typically taken as 26 mV for both reinforcing steel and zinc in concrete).

R_p = Slope determined from the polarization curve (kilohms×cm^2).

The total corrosion rate in μm/year is calculated using the equations in figure 5 and figure 7 for iron and zinc, respectively. In this study, the tests are performed using a PC4/750 Potentiostat and DC105 corrosion measurement system from Gamry Instruments.

The tests for bench-scale specimens were performed every 4 weeks to obtain the total corrosion rates for the top mats with the bottom mats disconnected. In the tests, the top mat of reinforcing steel is used as the working electrode, an SCE immersed in salt solution on top of the specimen is used as the reference electrode, and a platinum strip immersed in the salt solution is used as the counter electrode.

The data file from a polarization resistance test is analyzed using the data analysis package provided with the DC105. This analysis software can read the data file and plot a graph based on the data in the file. When a new graph is created in this package, the user picks a range of voltage in the graph and the software automatically uses a linear fit of the data in the selected range to calculate the polarization resistance. The corrosion current density and corrosion rate can then be determined using the polarization resistance.

Field Tests

Using concrete slab test specimens stored outdoors, the field test is designed to obtain a measure of the performance of corrosion-protection systems under realistic exposure conditions. Like the bench-scale specimens, some field test specimens are uncracked and some have simulated cracks directly above and parallel to selected reinforcing bars. A dam made of weatherstripping is attached to the upper concrete surface to hold a salt solution that is ponded on the specimens every 4 weeks. Corrosion rate measurements are obtained for a minimum of 250 weeks.

Field test specimens consisted of a 1,219 × 1,219 × 165-mm (48 × 48 × 6.5-inch) concrete slabs with two mats of No. 16 (No. 5) reinforcing bars (see figure 15 through figure 18). Each mat contains seven bars in both the longitudinal and transverse directions with clear concrete covers 25 mm (1 inch) from the top and bottom and 76 mm (3 inches) from the ends. Selected top and corresponding bottom bars are electrically connected across a 10-ohm resistor to form one test point.
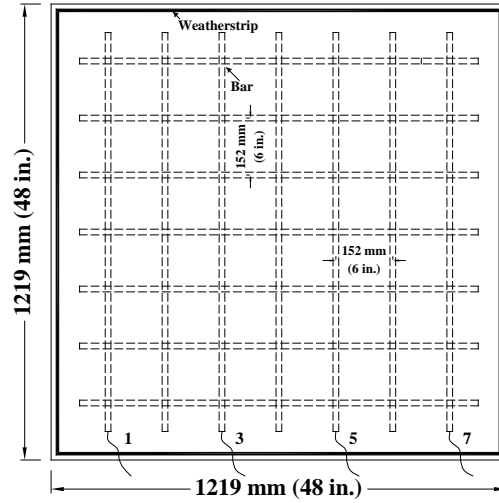
Figure 15. Illustration. Field test specimens, top slab without cracks.
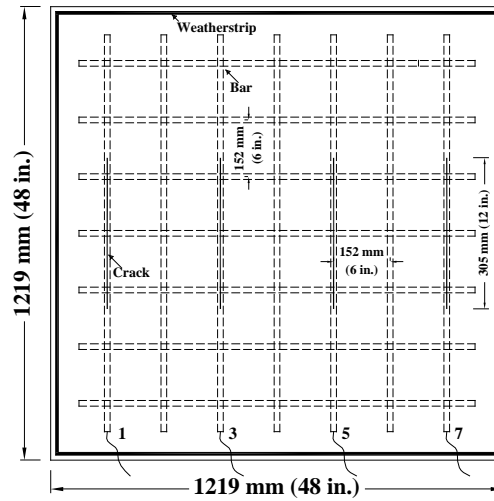
Figure 16. Illustration. Field test specimens, top slab with cracks.
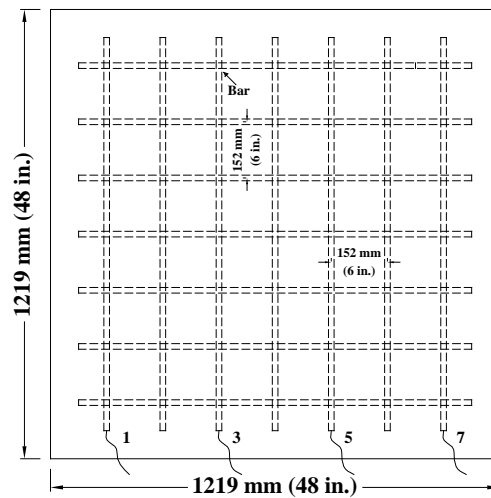
Figure 17. Illustration. Field test specimens, bottom slab.
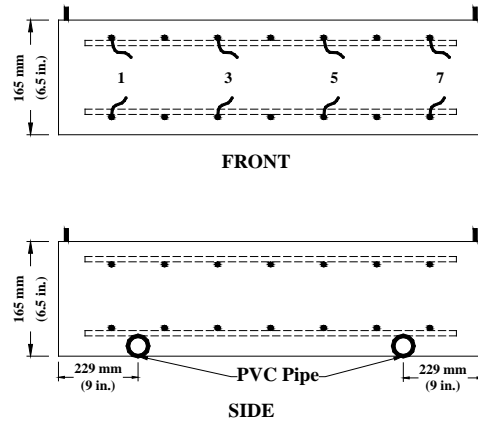
Figure 18. Illustration. Field test specimens, front and side views.

Test specimens are moved to the Adams Campus of the University of Kansas 7 days before testing. The specimens are spaced 0.914 m (3 ft) apart and placed 203 mm (8 inches) above the ground using $203 \times 203 \times 406$-mm ($8 \times 8 \times 16$-inch) concrete blocks.

A 9.5-mm (0.375-inch)-thick dam made of weatherstrip tape is attached to the top concrete surface around the edges and sealed with silicone caulk to prevent leakage. The specimens are ponded with 3.3 L (0.87 gal) of 10 percent rock salt solution, which contains 0.30 kg (0.66 lb) of rock salt, every 4 weeks. Occasionally in winter, rock salt alone is used.

The salt exposure program was based on Kansas salt usage history from 1998 to 2002, as shown in table 6.[40] The average application rate was based on a total length of all driving lanes of 33,742 km (20,967 mi) with an average lane width of 3.7 m (12 ft). The yearly average salt application was 0.66 kg/m^2 (0.13 lb/ft^2).

Table 6. Kansas Department of Transportation (KDOT) salt usage history.[40]

Fiscal Year	Rock Salt Total		Average Application Rate	
	Metric Ton	Ton	kg/m^2	lb/ft^2
1998	86,507	95,374	0.71	0.14
1999	64,254	70,840	0.52	0.11
2000	58,583	64,588	0.48	0.1
2001	124,619	137,392	1.02	0.21
2002	67,673	74,609	0.55	0.11
Average	80,327	88,561	0.66	0.13

The *KDOT Maintenance Manual* provides general guidelines for salt applications in snow season.[41] According to KDOT personnel, bridge decks receive four to five times the amount of salt applied to the adjacent pavement to account for lower temperatures on bridge decks. To match the approximate quantity of salt applied to bridge decks, four times the application rate of salt on pavements in Kansas, which is 2.64 kg/m^2 (0.52 lb/ft^2), is applied to field test specimens. This translates to 3.92 kg (8.32 lb) per specimen per year or 0.30 kg (0.66 lb) of rock salt every 4 weeks, the value used in the tests, as described above.

The 16-gauge copper wires from the top mat bars are connected to red binding posts, and the wires from the bottom mat bars are connected to paired black binding posts. A switch was connected to the red binding post through a 10-ohm resistor. The switches are turned on and off to control the electrical circuits. Binding posts of several specimens are centered together in a terminal box for testing convenience.

The test specimens are ponded with 3.3 L (0.87 gal) of 10 percent rock salt solution on the first day. Two weeks later, the voltage drops across the 10-ohm resistors are measured using a voltmeter. The circuits are then opened and the mat-to-mat resistances are recorded using an ohmmeter. The corrosion potentials are measured about 2 h after opening the circuits. Both anode and cathode corrosion potentials are measured with respect to a CSE. The circuits are closed after all the readings are taken. To achieve consistent measurements, specimens are watered before taking readings, usually about an hour before voltage drops.

Corrosion potential varies with temperature, and temperatures fluctuate in the field.[42] Therefore, a correction factor must be applied to convert potential measurements taken in the field to a value corresponding to 22º C (72º F). For a CSE, the correction is shown in figure 19 and figure 20.

$$E = E_o + 0.9(T\text{-}22)$$

Figure 19. Equation. Temperature correction in Celsius.

$$E = E_o + 0.5(T\text{-}72)$$

Figure 20. Equation. Temperature correction in Fahrenheit.

Where:

T = Temperature, °C or °F.

E_o = Uncorrected corrosion potential reading, mV.

E = Temperature corrected corrosion potential reading, mV.

The test cycle is repeated every 4 weeks. The specimens are ponded at the same time readings are taken. After the specimens reach about 96 weeks, readings are taken every 8 weeks, but the ponding cycle is maintained at 4 weeks.

Corrosion potentials are measured at fixed grid points on the top specimen surface, as shown in 21 through figure 23.
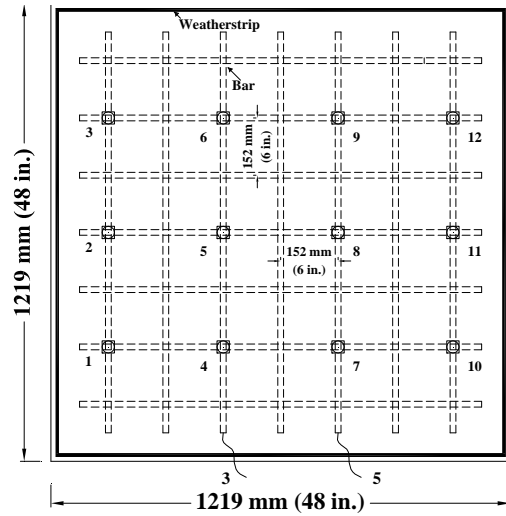
Figure 21. Illustration. Potential test points for conventional steel specimens.
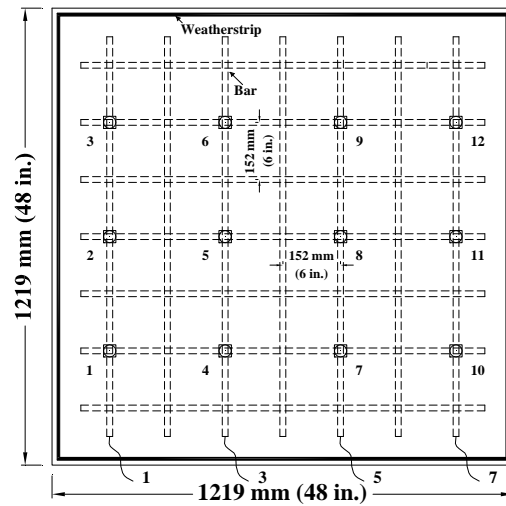
Figure 22. Illustration. Potential test points for epoxy-coated bar specimens with four test bars.
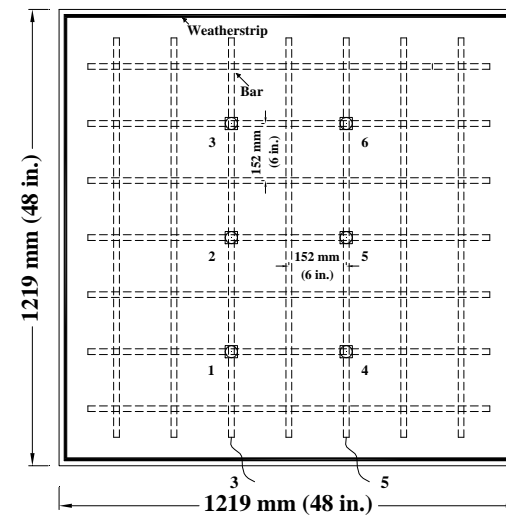
Figure 23. Illustration. Potential test points for epoxy-coated bar specimens with two test bars.

Specimen Fabrication

The following process is used to fabricate field test specimens:

1. **Reinforcing bar preparation:** Reinforcing bars are cut to 1,067 mm (42 inches), and the sharp edges at the ends are smoothed with a grinder. One end of the bar is drilled and tapped to a depth of 13 mm (0.5 inches) to accommodate a 10-24 stainless steel threaded bolt. Conventional bars are cleaned with acetone, and epoxy-coated bars are cleaned with soap and warm water and left to dry in the air. The coatings on the epoxy-coated and MC bars are penetrated with 16 3.2-mm (0.125-inch)-diameter holes. The holes are drilled to a depth of 0.4 mm (16 mil) from the epoxy coating surface using a 3.2-mm (0.125-inch)-diameter four-flute drill bit mounted on a milling machine. Eight holes are evenly distributed on each side of the bar along the length. For MC bars, both the epoxy and zinc layers are penetrated.

   A 914-mm (36-inch)-long 14-gauge electrical copper wire is connected to the tapped end of the test bars with a 10-mm (0.375-inch) 10-24 stainless steel threaded bolt. The connection and all other exposed ends of epoxy-coated and MC bars are coated with 3M™ Rebar Patch epoxy. After the epoxy dried, a 76-mm (3-inch)-long heat-shrinkable tube is used to protect and direct the copper wire out of the specimen. Because 76 mm (3 inches) of the bar is covered by the tube, the holes in the epoxy represent 0.26 percent of the exposed bar surface. The interface between the shrinkable tube and the tapped end is patched with epoxy. As shown in figure 15 through figure 18, bars numbered 1, 3, 5, and 7 are connected across 10-ohm resistors. In some early test specimens, only bars 3 and 5 were connected.

2. **Form assembly:** The forms used for the field test specimens are made of 19-mm (0.75-inch)-thick plywood and held in position with wood screws and clamps. All corners are sealed with modeling clay from the inside to avoid leakage. The inside of the form is coated with mineral oil after cleaning to remove dust. The front and back form pieces are predrilled, and two 25-mm (1-inch)-diameter holes are centered 229 mm (9 inches) away from the specimen sides. Two 1.4-m (4.5-ft)-long PVC pipes are installed through holes perpendicular to the test bars, as shown in figure 18. Two 1.8-m (6-ft)-long No. 16 (No. 5) conventional bars are inserted into the PVC pipes to aid in lifting the specimens.

   Plastic chairs 25-mm (1-inch)-high are used to support bottom mat bars, and 108-mm (4.25-inch)-high plastic chairs are used to support top mat bars to provide 25-mm (1-inch) clear concrete covers. Plastic rather than metal chairs are used to avoid unplanned electrical connections between the top and bottom bars. The steel within each mat is connected using conventional tie wire for conventional steels and plastic-coated tie wire for epoxy-coated steels.

   For specimens with simulated cracks from the top surface, 0.3-mm (12-mil)-thick, 305-mm (12-inch)-long stainless steel shims are placed directly above and parallel to the test bars. The crack thickness is designed based on bridge deck crack surveys.[43] A shim holder is used to position stainless steel shims in place. It is made of plywood and structured as shown in figure 24 through figure 26. The stainless steel shims are attached to the top of the shim holder and the holder is attached into the form using wood screws.
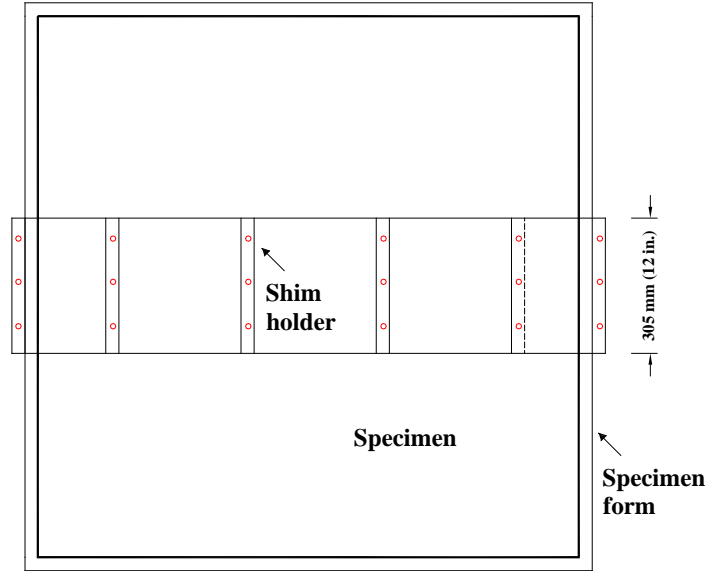
Figure 24. Illustration. Shim holder for field specimens, top view.
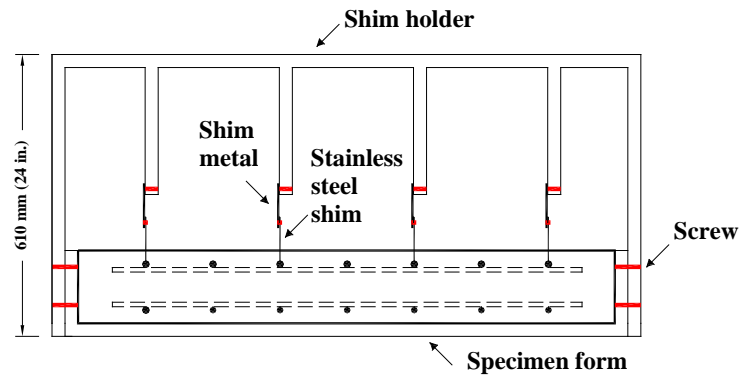
Figure 25. Illustration. Shim holder for field specimens, front view.
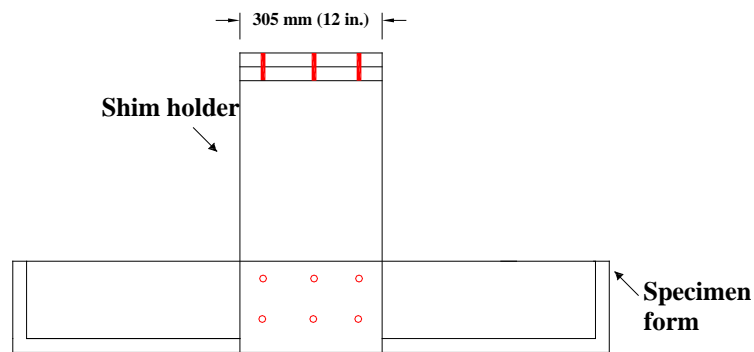
Figure 26. Illustration. Shim holder for field specimens, side view.

3. **Specimen Casting:** Concrete is ordered from a local ready mix plant. The mixture proportions are the same as those shown in table 5 for the bench-scale specimens, with a w/c ratio of 0.45.

Concrete is consolidated during casting using an electric internal vibrator with a 33-mm (1.375-inch)-diameter head. The upper surface is finished with a screed, followed by a

bullfloat. For cracked specimens, a wooden float is used instead of a bullfloat. The stainless steel shims are removed from the concrete about 12 h after casting.

During casting, concrete slump, temperature, unit weight, and air content are measured in accordance with ASTM standards. Test cylinders are made for each batch and stored with the specimens in a curing room and in a curing tank containing lime-saturated water. The cylinders are tested at 28 days to determine compressive strength. Concrete batch information and the properties of the plastic and hardened concrete are summarized in table 7. As shown in the table, the concrete in the specimens containing Rheocrete® and Hycrete™ exhibited reduced compressive strength compared to other specimens independent of w/c ratio. The reduced strengths may be explained in part by analyses of pore solutions in cement pastes by O'Reilly et al., who observed a marked increase in sulfate content at 7 days for pastes containing Rheocrete® and at both 1 and 7 days for cement pastes containing Hycrete™.[44] These increases in sulfate content may also explain differences in the critical chloride corrosion threshold for concretes containing corrosion inhibitors, as discussed in chapter 3.

Table 7. Properties of concrete batches for field tests.

Batch	Steel Designation[a] (No. of Specimens)	w/c	Slump, mm	Concrete Temp., °C	Unit Weight, kg/m³	Air Content, Percent	Average Compressive Strength[b], MPa		
							Curing Tank	Curing Room	With Specimens
1	Conv. (2), ECR (2), ECR(Valspar) (2)	0.39	100	19	2,219	6.25	–	28.4	30.6
2	ECR(DuPont) (2), ECR(Chromate) (2), MC (2)	0.43	100	19	2,319	5.00	–	35.7	37.4
3	ECR(primer/Ca(NO₂)₂) (2), Conv. (2), ECR (2)	0.41	50	28	2,307	4.00	–	34.4	36.9
4	ECR(Valspar) (2), ECR(DuPont) (2), ECR(Chromate) (2)	0.42	125	25	2,296	5.75	–	32.5	32.9
5	MC (2), ECR(primer/Ca(NO₂)₂) (2)	0.44	110	23	2,291	5.25	32.8	32.6	33.2
6	ECR(DCI) (4)	0.48	210	22	2,255	7.25	35.3	30.9	29.6
7	ECR(DCI) (2)	0.40	25[c]	21	–	5.50	36.8	35.9	–
8	ECR(RH) (4)	0.44	165	23	2,295	5.50	29.1	28.5	28.1
9	ECR(HY) (4)	0.41	185	16	2,216	5.65	15.0	13.5	13.1

1 mm = 0.039 inches
°F = 1.8 °C + 32
1 kg/m³ = 1.69 lb/yd³
1 MPa = 145 psi
– Not used.
[a] See table 1 for abbreviation definitions; MC bars have both zinc and epoxy layers penetrated; all epoxy-coated bars are penetrated with 16 surface holes.
[b] Average of three cylinders.
[c] A slump of 150 mm (6 inches) was measured at the ready-mix plant before transporting to the concrete lab.

4. **Curing:** The specimens are covered with saturated burlap and plastic sheeting in the laboratory for 7 days, the curing period required by the *Kansas Standard Specifications for State Road and Bridge Construction* at the time the specimens were fabricated.[45] After 7 days, the specimens are demolded, moved outdoors, and cured in air for 3 months prior to the initiation of the tests.

Chloride Analysis

The sampling and testing procedures to determine chloride ion concentration in bench-scale and corrosion initiation specimens were those adopted by Ji et al.[26] Pulverized concrete samples are obtained by drilling 6.4-mm (0.25-inch)-diameter holes in the side of the specimen using a rotary impact-type drill. Prior to sampling, the drilled concrete surface is cleaned three times, first using soap and water, then using tap water, and finally using deionized water. The surface is then dried using paper towels. Drilling positions are measured and marked. A 152-mm (6-inch)-long, 6.4-mm (0.25-inch)-diameter drill bit is mounted to a heavy-duty drill. The specimen is drilled perpendicular to the reinforcing steel, parallel to the top surface of the specimen. The sample obtained from the first 13-mm (0.5-inch) depth contains epoxy coating from the exterior of the specimen and is discarded. The drilling continues to a depth of 63.5 mm (2.5 inches) to obtain approximately 4 g (0.15 oz) of powder. The pulverized concrete sample from each hole is collected using two pieces of copy paper and transferred to labeled plastic bags. The drill bit is cleaned before and between each sample to avoid contamination. A shop vacuum reserved for drilling is used during the procedure.

Four cores are taken from most field test specimens at end of life using an 89-mm (3.5-inch)-diameter core drill bit and core drill to determine the chloride ion concentration. The cores are taken at the corners of the specimen, 230 mm (9 inches) from the edges. Cores that include reinforcement are not analyzed to avoid measuring the effect of chloride buildup over the bars. After coring, cores are stored at -18° C (0° F) to minimize chloride ion migration prior to sampling. Concrete powder for sampling is obtained from the cores using a milling machine and a 32-mm (1.25-inch)-diamond grit hole saw. The cores are mounted on a rotary table and the hole saw is positioned off center from the core bit so that when the rotary table is rotated the hole saw cuts a 44-mm (2.5-inch)-diameter circle in the core. This path avoids sampling from the edge of the core, where water from the core drill may affect the chloride content. Samples are obtained from different depths so that a depth profile of chloride content can be determined. The powder obtained from the top 4 mm (0.15 inches) of the core is discarded because of possible contamination from the core drill water. Samples are collected from 4–8 mm (0.15–0.30 inches), 8–13 mm (0.3–0.5 inches), 13–19 mm (0.5–0.75 inches), 19–25 mm (0.75–1.0 inches), 25–29 mm (1–1.125 inches), 29–32 mm (1.125–1.25 inches), and 38–41 mm (1.5–1.625 inches) with the aid of a vacuum filter collection system.

Concrete samples are analyzed for water-soluble chloride content using procedure A from AASHTO T 260-94.[46] Samples are boiled in deionized water to free any water-soluble chlorides. The solution is filtered, acidified with nitric acid, and titrated with silver nitrate. The potential of a chloride ion-selective electrode is monitored throughout the titration. The change in potential with respect to the volume of silver nitrate is calculated, with the endpoint indicated by the inflection point of the potential-volume curve—the point at which the greatest change in potential for a given incremental addition of silver nitrate was observed. This procedure gives the chloride ion concentration in terms of percent chloride by weight of concrete. In this study, values are presented in kg/m^3 (lb/yd^3) by multiplying by the unit weight of concrete, taken as 2,246 kg/m^3 (3,786 lb/yd^3).

Average Corrosion Rates Based on Losses After Corrosion Initiation

Corrosion-protection systems are typically compared based on average losses of metal from the surface (expressed as μm) over time for a given test method. These losses are a function of both the time to corrosion initiation and the corrosion rate following initiation. General comparisons do not necessarily require that the time of corrosion initiation be precisely indentified. To develop an estimate of the corrosion performance of a system in a structure such as a bridge deck, however, requires separate estimates for the time to corrosion initiation and the subsequent corrosion rate. Because corrosion rates fluctuate and each specimen is unique, using the combined average losses versus time underestimates both the average time to initiation (losses appear to increase at the earliest initiation time) and the average corrosion rate (losses start slowly because not all specimens are corroding). To rectify this, bench-scale and field test specimens in this study are analyzed individually and the results are combined to determine the average corrosion rate for each system and specimen type.

To illustrate the process, the plots of macrocell corrosion loss versus time for the individual bars in the two field test specimens with conventional steel bars in uncracked concrete containing Rheocrete®, ECR(RH)-U-1 and ECR(RH)-U-2, are shown in figure 27. To determine the average corrosion rate for each bar, the point at which the corrosion loss begins to increase steadily is determined and marked, as shown by red arrows in the figure. The average corrosion rate for the bar is the slope of the line connecting this to the point representing the corrosion loss at the end of the test (see figure 28). The individual averages are combined to obtain the average for the system. Bars that show no increase in corrosion loss, such as ECR(RH)-U-2 (3), are excluded from the average.
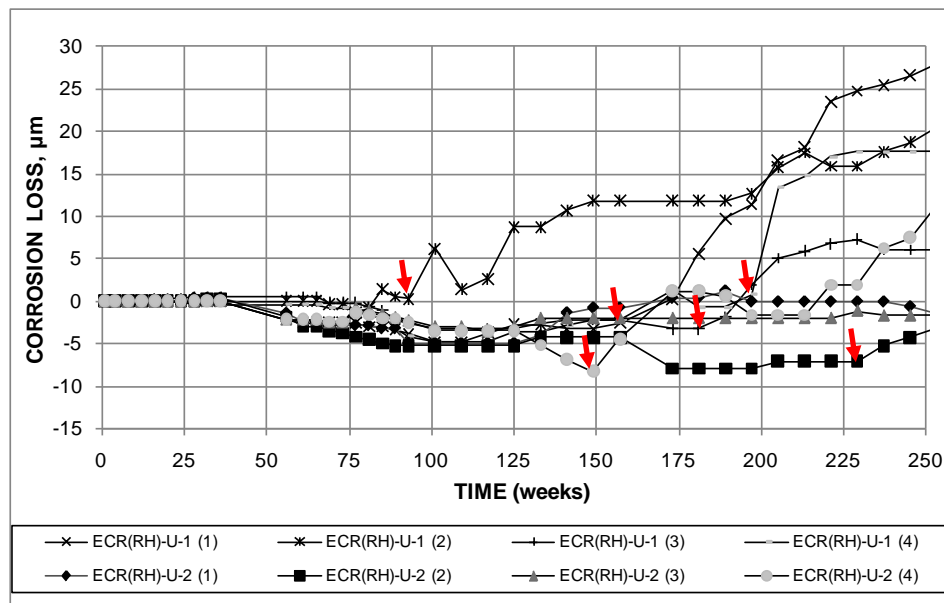
1 μm = 0.0394 mil

Figure 27. Graph. Individual corrosion losses based on total area of the top bars for field test specimens containing Rheocrete® in uncracked concrete, with corrosion initiation marked.
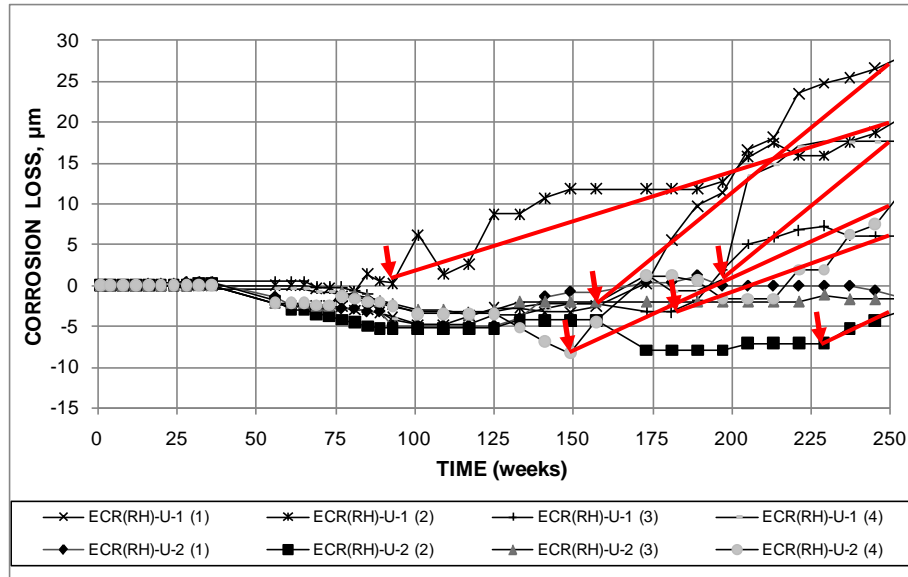
Figure 28. Graph. Individual corrosion losses based on total area of the top bars for field test specimens containing Rheocrete® in uncracked concrete, with lines connecting corrosion loss at initiation to corrosion loss at 250 weeks.

As shown in figure 29 for three southern exposure specimens containing epoxy-coated bars (with four holes through the epoxy) cast in concrete with a w/c ratio of 0.45 containing corrosion inhibitor DCI, some specimens exhibit corrosion loss (the result of short periods of measureable corrosion) and extended periods with no corrosion without having a measureable corrosion rate over time. In figure 29, the corrosion rate after corrosion initiation can be measured for only one of three specimens (ECR-DCI-4h-45-2).
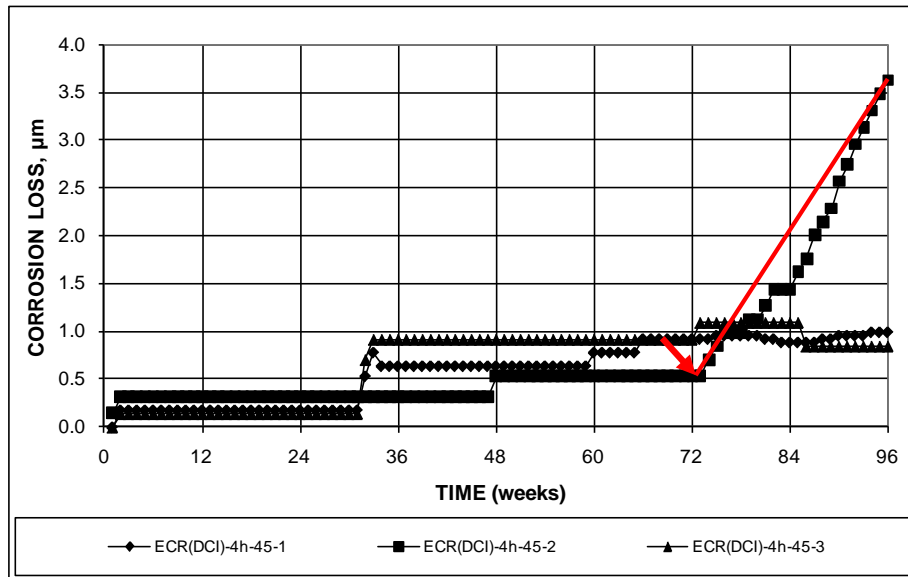
1 µm = 0.0394 mil

Figure 29. Graph. Individual corrosion loss based on exposed area of the top bars for southern exposure specimens containing epoxy-coated bars cast in concrete containing DCI, with lines connecting corrosion loss at initiation to corrosion loss at 96 weeks.

31

TEST PROGRAM

The test program, summarized in table 8, compared the corrosion performance of the 11 multiple corrosion-protection systems with that of conventional reinforcing steel and conventional ECR and compared the effectiveness of corrosion inhibitors when used with conventional reinforcing steel. As shown in the table, rapid macrocell and bench-scale tests were used for all multiple corrosion-protection systems, but all versions of the tests were not used for every system. In all, the work included 126 macrocell tests, 117 southern exposure tests, 93 cracked beam tests, 30 corrosion initiation beams, 42 field tests, and 32 corrosion-loss-to-crack-concrete tests.

Table 8. Number of test specimens in test program.

	Test				
	Macrocell				
System	**Bare**	**Mortar-wrapped[a]**	**SE[b]**	**CB[b]**	**FTS[c]**
Control					
Uncoated bars[d]	6	6	15[e]	9	4[f]
ECR	6	6	18[e,g]	9	4[f]
Epoxies with increased adhesion					
Chromate pretreatment	6	6	6	6	4[f]
DuPont coating	6	6	6	6	4[f]
Valspar coating	6	6	6	6	4[f]
Corrosion inhibitors in mortar or concrete					
Uncoated bars with calcium nitrite[d]	–	–	3	3	–
Uncoated bars with Rheocrete® 222+ [d]	–	–	3	3	–
Uncoated bars with Hycrete™ [d]	–	–	3	3	–
ECR with calcium nitrite	–	6	9[g]	9[g]	6[f]
ECR with Rheocrete® 222+	–	6	9[g]	9[g]	4[f]
ECR with Hycrete™	–	6	9[g]	9[g]	4[f]
3M™ primer containing calcium nitrite	–	6	9[g]	9[g]	4[f]
Epoxies with increased adhesion plus calcium nitrite in mortar or concrete					
Chromate pretreatment	–	6	3[h]	–	–
DuPont™ coating	–	6	3[h]	–	–
Valspar® coating	–	6	3[h]	–	–
Bars with multiple coatings					
Both layers penetrated	6	6	6	6	4[f]
Epoxy only penetrated	6	6	6	6	–

SE = southern exposure; CB = cracked beam; FTS = field test specimen

– No tests.

[a] w/c = 0.5. Specimens with four 3.2-mm (0.125-inch)-diameter holes in coating.

[b] w/c = 0.45. ECR systems tested using 3, 6, or 12 specimens with four 3.2-mm (0.125-inch)-diameter holes in coating and three specimens with 10 3.2-mm (0.125-inch)-diameter holes in coating.

[c] w/c = 0.45. ECR systems tested with 16 3.2-mm (0.125-inch)-diameter holes in coating.

[d] Six or 12 corrosion initiation specimens also tested.

[e] Twelve specimens with w/c = 0.45 and three specimens with w/c = 0.35.

[f] Half without and half with cracks over the test bars.

[g] Includes three additional specimens with w/c = 0.35 and 10 3.2-mm (0.125-inch)-diameter holes in coating.

[h] Three specimens with four 3.2-mm (0.125-inch)-diameter holes in coating.

Rapid Macrocell Test Program

As shown in table 8, the rapid macrocell test with mortar-wrapped specimens was used for all multiple protection systems, while the macrocell test with bare bars was not used to evaluate the effects of corrosion inhibitors. The macrocell tests for the bare and mortar-wrapped specimens for the MC system included bars with penetrations through both layers as well as bars in which only the outer layer of epoxy had been penetrated. The coating on each bar in the rapid macrocell tests was penetrated by four 3.2-mm (0.125-inch)-diameter holes, representing damage to 1.0 percent of the bar area exposed to solutions in these tests. Six specimens were used for each system.

Bench-Scale and Corrosion Initiation Test Programs

Southern exposure, cracked beam, and corrosion initiation tests were used to compare the performance of corrosion-protection systems cast in concrete. A w/c ratio of 0.45 was used in all cases. In addition, concrete with a w/c ratio of 0.35 was used to evaluate the performance of the corrosion inhibitors (as well as the control specimens) because the corrosion protection provided by calcium nitrite relative to that of other corrosion inhibitors has been observed to improve as the w/c ratio and permeability of the concrete decrease.[47] The coatings on bars in the bench-scale tests were penetrated with 4 or 10 holes with a diameters 3.2 mm (0.125 inches), representing damage to 0.21 or 0.52 percent of the bar surface, respectively.

Linear Polarization Resistance Test Program

Linear polarization resistance measurements were performed on a single southern exposure and cracked beam specimen for each configuration and corrosion-protection system in the study (see table 8). The results were used in conjunction with the readings obtained from the macrocell, bench-scale, and field tests to characterize the performance of the corrosion-protection systems.

Field Test Program

Field test specimens were used to compare conventional reinforcing steel and conventional ECR steel to epoxy-coated bars with increased adhesion, epoxy-coated bars with corrosion inhibitors, and MC bars with both layers penetrated. Four specimens were included for each category, except there were six epoxy-coated bar specimens with calcium nitrite. Half of the specimens had simulated cracks above top reinforcing bars. ECR was cast with 16 3.2-mm (0.125-inch)-diameter holes in the coating, representing 0.24 percent of the bar surface.

Following the rapid macrocell, bench-scale, and field tests, specimens were photographed to record cracking and corrosion products visible on the exterior of concrete or mortar and on reinforcing steel and surrounding cementitious materials after the removal of concrete or mortar. Following the bench-scale and field tests, coatings were evaluated for disbondment, and concrete samples were taken to analyze for chloride contents.

CHAPTER 3. TEST RESULTS

The test results presented in this chapter demonstrate that conventional fusion-bonded epoxy coating significantly reduces the corrosion of reinforcing steel. Epoxy-coated bars initiate corrosion at chloride contents that are generally several times greater and corrode at rates that are typically two orders of magnitude below those exhibited by conventional reinforcement. The results show that cracks in concrete directly over and parallel to the reinforcement, such as found in bridge decks, result in earlier corrosion initiation and higher corrosion rates than obtained with intact concrete for all systems tested.

Epoxies that provide initially high adhesion to the underlying steel provide no advantage in terms of improved corrosion performance or improved adhesion when used in concrete. Using concrete with a reduced w/c ratio (and thus, lower permeability) lowers the corrosion rate for both conventional reinforcement and ECR under all conditions in intact concrete but provides only limited corrosion protection, at best, in the presence of cracks, which allow direct access of chlorides to reinforcing bars. Corrosion inhibitors consistently provided improved corrosion protection when used in conjunction with conventional reinforcement and ECR in intact concrete but to a lesser degree in cracked concrete. Corrosion inhibitors had a greater relative effect on uncoated than on coated reinforcement. Bars with an MC system consisting of 98 percent zinc and 2 percent aluminum and conventional epoxy exhibit high corrosion rates in cases when the concrete is often wet but corrosion rates similar to those exhibited by conventional ECR under conditions similar to those in bridge decks; the metallic coating corrodes in preference to the underlying steel, providing some additional protection. All coated bars exhibited corrosion losses at openings through the coating. The reduction in adhesion between an epoxy coating and the reinforcing steel (often referred to as disbondment) that occurs after a period of exposure to corrosive conditions increases with increasing chloride content in the concrete and in the presence of cracks and decreases with the use of corrosion inhibitors, with the use of MC reinforcement, and with electrical isolation of the epoxy-coated bars from each other. Corrosion products form under the disbonded coating. Disbondment does not affect the rate at which coated bars corrode.

RAPID MACROCELL TESTS

All systems were evaluated using rapid macrocell tests. The bare bar test, however, was not used to evaluate corrosion inhibitors. The results presented in this section represent the average of six specimens. The epoxy on all bars was penetrated with four 3.2-mm (0.125-inch)-diameter holes, representing 1.0 percent of the total area in contact with the solution, as previously described.

Corrosion losses (total thickness of metal lost due to corrosion calculated by integrating the corrosion rate) for the individual specimens in the rapid macrocell test are summarized in table 9 and table 10, which express the results based on the total area of the bars in contact with the test solutions and on the area of steel exposed by the four holes through the coating on each epoxy-coated bar.

Table 9. Corrosion loss at 15 weeks (µm) for rapid macrocell specimens based on total area.

Steel Designation[a]	Specimen						Average	Standard Deviation
	1	2	3	4	5	6		
Controls								
Conv.	7.1	5.3	4.7	7.4	6.5	5.2	6.0	1.12
M[b]-Conv.	5.8	6.7	3.5	3.8	3.8	5.4	4.8	1.33
ECR	0.256	0.649	0.215	0.381	0.494	0.018	0.336	0.222
M-ECR	0.000	0.000	0.000	0.000	-0.004	0.000	-0.001	0.001
Epoxies with increased adhesion								
ECR(Chromate)	0.101	0.000	0.000	0.000	0.000	0.055	0.026	0.043
M-ECR(Chromate)	0.000	0.000	0.000	0.000	0.000	0.000	0.000	0.000
ECR(DuPont)	0.000	0.438	0.336	0.361	0.425	0.418	0.330	0.166
M-ECR(DuPont)	0.000	0.000	0.000	0.000	0.000	0.000	0.000	0.000
ECR(Valspar)	0.266	0.389	0.599	0.083	0.056	0.499	0.315	0.221
M-ECR(Valspar)	0.000	-0.003	0.000	0.000	0.000	0.000	0.000	0.001
Corrosion inhibitors in mortar								
M-ECR(DCI)	0.000	-0.003	0.000	0.000	0.000	0.000	0.000	0.001
M-ECR(RH)	0.000	0.000	0.000	0.000	0.000	0.000	0.000	0.000
M-ECR(HY)	0.000	0.000	0.000	0.000	0.000	0.000	0.000	0.000
M-ECR(primer/Ca(NO$_2$)$_2$)	0.000	0.000	0.000	0.000	0.008	0.009	0.003	0.004
Epoxies with increased adhesion plus calcium nitrite in mortar								
M-ECR(Chromate)-DCI	0.000	0.000	0.000	0.000	0.000	0.000	0.000	0.000
M-ECR(DuPont)-DCI	0.000	0.000	0.000	0.000	0.000	0.000	0.000	0.000
M-ECR(Valspar)-DCI	0.000	0.000	0.000	0.000	0.000	0.000	0.000	0.000
Bars with multiple coatings								
MC(both layers penetrated)	0.043	0.041	0.007	0.007	-0.038	0.023	0.014	0.030
M-MC(both layers penetrated)	-0.004	0.001	0.001	0.000	-0.011	0.000	-0.002	0.005
MC(only epoxy penetrated)	0.064	0.022	0.108	0.050	0.039	0.060	0.057	0.029
M-MC(only epoxy penetrated)	0.020	0.030	0.017	0.024	0.006	0.022	0.020	0.008

1 µm = 0.0394 mil
[a] See table 1 for abbreviation definitions.
[b] M prefix indicates mortar-wrapped specimen, otherwise bare bar specimen.

Table 10. Corrosion loss at 15 weeks (μm) for rapid macrocell specimens based on area exposed at holes through coating.

Steel Designation[a]	Specimen						Average	Standard Deviation
	1	2	3	4	5	6		
Controls								
Conv.	–	–	–	–	–	–	–	–
M[b]-Conv.	–	–	–	–	–	–	–	–
ECR	25.6	64.9	21.5	38.1	49.4	1.8	33.6	22.2
M-ECR	0.000	0.000	0.000	0.000	-0.352	0.000	-0.059	0.144
Epoxies with increased adhesion								
ECR(Chromate)	10.14	0.00	0.00	0.00	0.04	5.49	2.61	4.29
M-ECR(Chromate)	0.000	0.000	0.000	0.000	0.000	0.000	0.000	0.000
ECR(DuPont)	0.0	43.8	33.6	36.1	42.5	41.8	33.0	16.6
M-ECR(DuPont)	0.000	0.000	0.000	0.000	0.000	0.000	0.000	0.000
ECR(Valspar)	26.6	38.9	59.9	8.3	5.6	49.9	31.5	22.1
M-ECR(Valspar)	0.000	-0.282	0.000	0.000	0.000	0.000	-0.047	0.115
Corrosion inhibitors in mortar								
M-ECR(DCI)	0.000	-0.282	0.000	0.000	0.000	0.000	-0.047	0.115
M-ECR(RH)	0.000	0.000	0.000	0.000	0.000	0.000	0.000	0.000
M-ECR(HY)	0.000	0.000	0.000	0.000	0.000	0.000	0.000	0.000
M-ECR(primer/Ca(NO$_2$)$_2$)	0.000	0.000	0.000	0.000	0.774	0.925	0.283	0.441
Epoxies with increased adhesion plus calcium nitrite in mortar								
M-ECR(Chromate)-DCI	0.000	0.000	0.000	0.000	0.000	0.000	0.000	0.000
M-ECR(DuPont)-DCI	0.000	0.000	0.000	0.000	0.000	0.000	0.000	0.000
M-ECR(Valspar)-DCI	0.000	0.000	0.000	0.000	0.000	0.000	0.000	0.000
Bars with multiple coatings								
MC(both layers penetrated)	4.26	4.13	0.65	0.66	-3.82	2.27	1.36	2.99
M-MC(both layers penetrated)	-0.35	0.12	0.08	0.00	-1.06	0.00	-0.20	0.45
MC(only epoxy penetrated)	6.35	2.21	10.78	5.00	3.86	6.03	5.70	2.91
M-MC(only epoxy penetrated)	1.96	2.97	1.66	2.37	0.57	2.18	1.95	0.81

1 μm = 0.0394 mil
– No test.
[a] See table 1 for abbreviation definitions.
[b] M prefix indicates mortar-wrapped specimen, otherwise bare bar specimen.

Bare Bar Tests

The average corrosion rates for the systems evaluated using bare bars are shown in figure 30 and figure 31. The two figures differ in the scale of the vertical axis. The corrosion rate represents the average based on the total area exposed to the test solution.
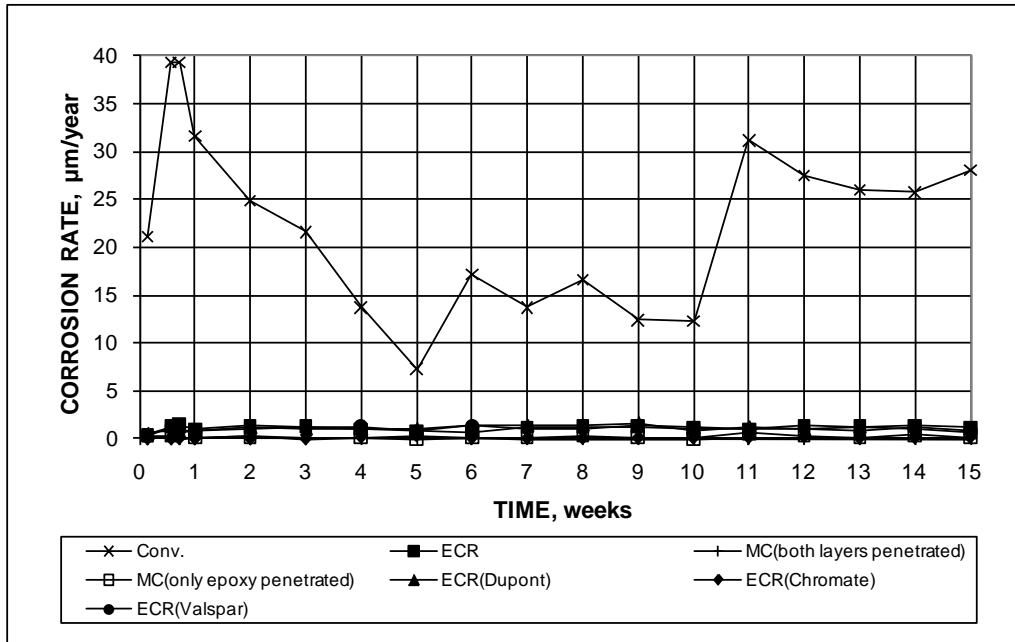
1 µm = 0.0394 mil

Figure 30. Graph. Macrocell test, average corrosion rate for bare conventional, ECR, increased-adhesion ECR, and MC steel in simulated pore solution with 1.6 molal ion concentration of sodium chloride.
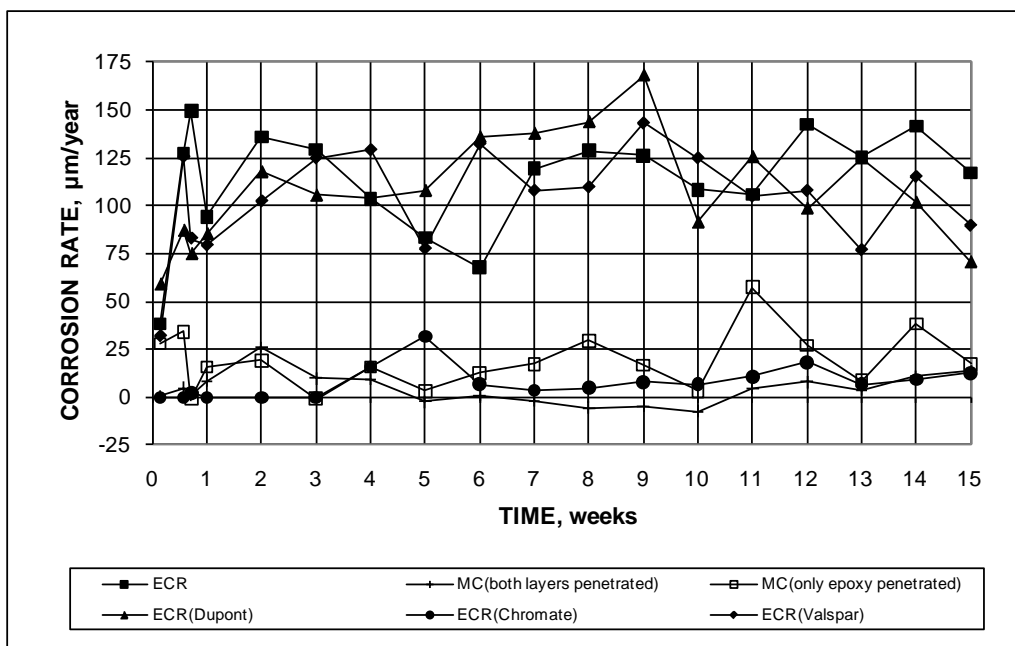
1 µm = 0.0394 mil

Figure 31. Graph. Macrocell test, average corrosion rate for bare ECR, increased-adhesion ECR, and MC steel in simulated pore solution with 1.6 molal ion concentration of sodium chloride (adjusted y-axis).

The results indicate that conventional steel corroded at a much higher rate than any of the epoxy-coated bars in the test, with a rate that ranged between 7 and 40 µm/year (0.3 and 1.6 mil/year)

during the 15-week test. Based on corrosion rate, the epoxy-coated bars fell into two groups, with conventional ECR, ECR(DuPont), and ECR(Valspar) corroding at an average rate between 0.5 and 1.7 µm/year (0.02 and 0.067 mil/year) and ECR(Chromate) and the MC bars (both layers penetrated and only epoxy penetrated) corroding at an average rate between -0.1 and 0.6 µm/year (-0.004 and 0.02 mil/year). The negative corrosion rate, which indicates more oxidation at the cathode than at the anode, may be explained by the amphoteric nature of zinc. As demonstrated in the figures, corrosion rates varied significantly from week to week. Conventional reinforcement exhibited significant increases in corrosion between weeks 5 and 6 and between weeks 10 and 11, when the solutions were changed.

Total corrosion losses, which are calculated by integrating the corrosion rate over the test period, are shown in figure 32 and figure 33 and in table 9 and table 10. Figure 32 expresses the losses based on the total area of the bars in contact with the text solutions, while figure 33 expresses the losses in terms of the area of steel exposed by the holes through the epoxy coating, which for macrocell specimens equals the values based on total bar surface multiplied by a factor of 100. Over the 15-week period, total losses for conventional steel equaled approximately 6 µm (0.2 mil). For conventional ECR, ECR(DuPont), and ECR(Valspar), total losses ranged from 0.31 and 0.34 µm (0.012 and 0.013 mil) based on total area and between 31 and 34 mm (1.2 and 1.3 mil) based on exposed area. For the ECR(Chromate) and MC bars, total losses were below 0.057 µm (0.0022 mil) based on total area and 5.7 µm (0.22 mil) based on exposed area. The low macrocell corrosion rates for the MC bars resulted because the test measures macrocell rather than microcell corrosion and because, as an amphoteric material, zinc is attacked by the alkaline solution at the cathode (with twice that area of the anode) as well as by the combined alkaline and salt solution at the anode, reducing the net macrocell current.
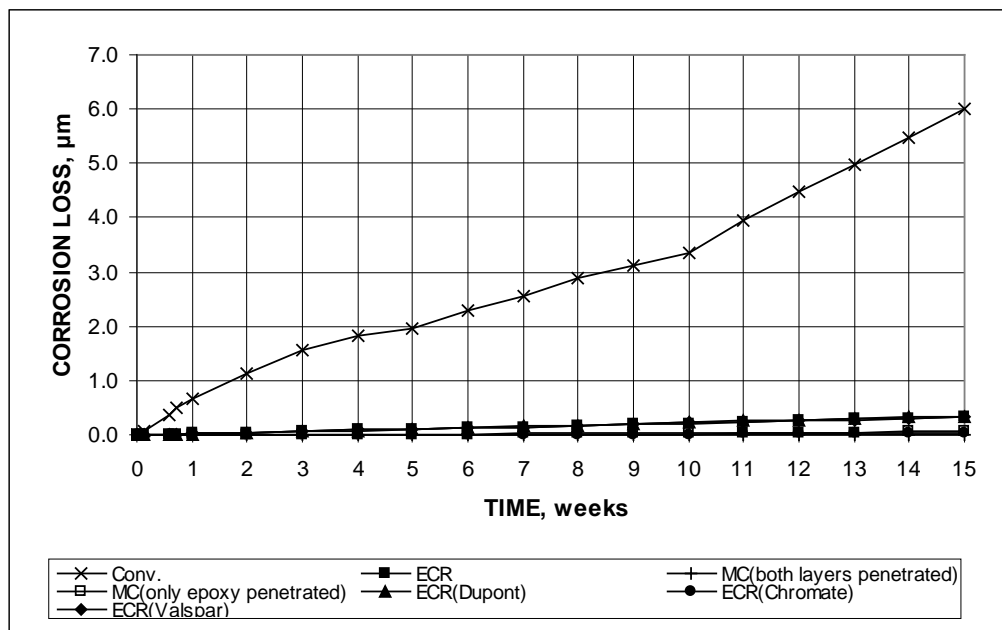
1 µm = 0.0394 mil

Figure 32. Graph. Macrocell test, average corrosion loss based on total area for bare conventional, ECR, increased-adhesion ECR, and MC steel in simulated pore solution with 1.6 molal ion concentration of sodium chloride.

39
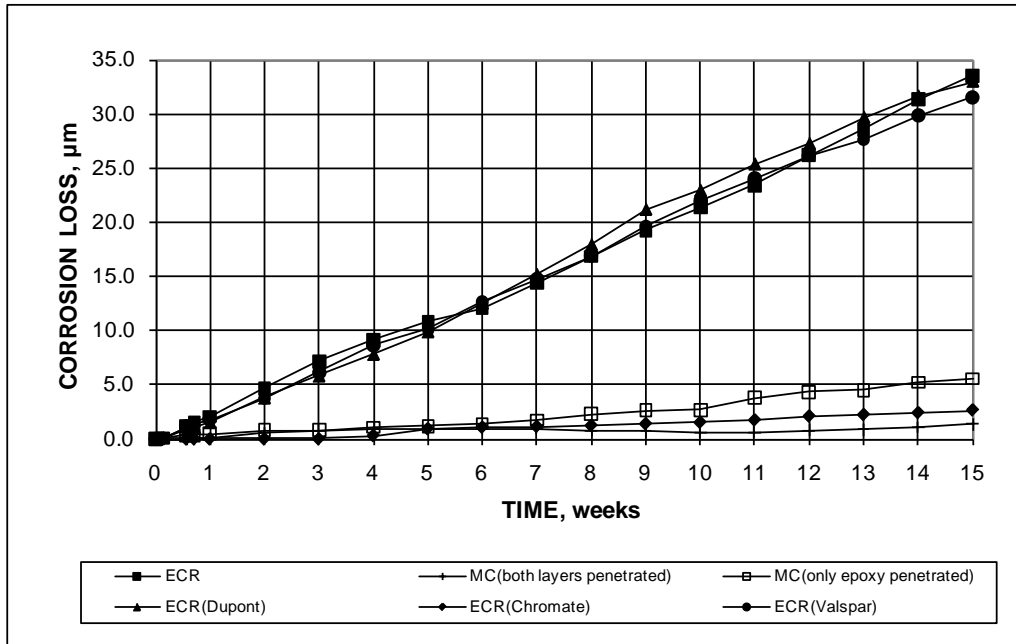
1 µm = 0.0394 mil

Figure 33. Graph. Macrocell test, average corrosion loss based on area exposed at holes through coating for bare conventional, ECR, increased-adhesion ECR, and MC steel in simulated pore solution with 1.6 molal ion concentration of sodium chloride.

The corrosion potentials shown in figure 34 and figure 35 (anode and cathode bars disconnected for 2 h) provide additional information on the behavior of the specimens. With the exception of ECR(Chromate), all specimens exhibited corrosion potentials at the anode more negative than -0.275 V with respect to an SCE (approximately equivalent to -0.350 V for a CSE), indicating that the bars were undergoing active corrosion. In contrast to bars with only steel exposed to the test solutions, the MC bars initially exhibited corrosion potentials of approximately of -1.200 V at both the anode and cathode, indicating active corrosion of the zinc layer. The MC bars with both layers of coating penetrated reached a corrosion potential of about -0.500 V after 3 weeks, indicating that the effect of the zinc surrounding the holes had been largely reduced and that the exposed area of steel was governing the corrosion process. In contrast, the MC bars with only the epoxy penetrated maintained a significantly more negative corrosion potential than the other anode bars, indicating that the zinc was still providing some protection for the underlying steel for a significant portion of the test period. Interestingly, the corrosion potentials of the MC cathode bars are similar to those at the anode throughout the test period. The fact that the MC cathode bars never reached a corrosion potential more positive than -0.275 V, as exhibited by all of the other bars, suggests that the zinc continues to contribute to the performance of the system over time. With the exception of ECR(Chromate), the corrosion potentials exhibited by the other corrosion-protection systems showed a strong similarity to that of uncoated conventional reinforcement, indicating that the differences in observed corrosion rates shown in figure 30 and figure 31 are primarily based on the role of the epoxy coating in limiting the exposed bar surface at both the anode and the cathode. In terms of total metal loss, that effect is significant (see table 9, table 10, figure 32, and figure 33).
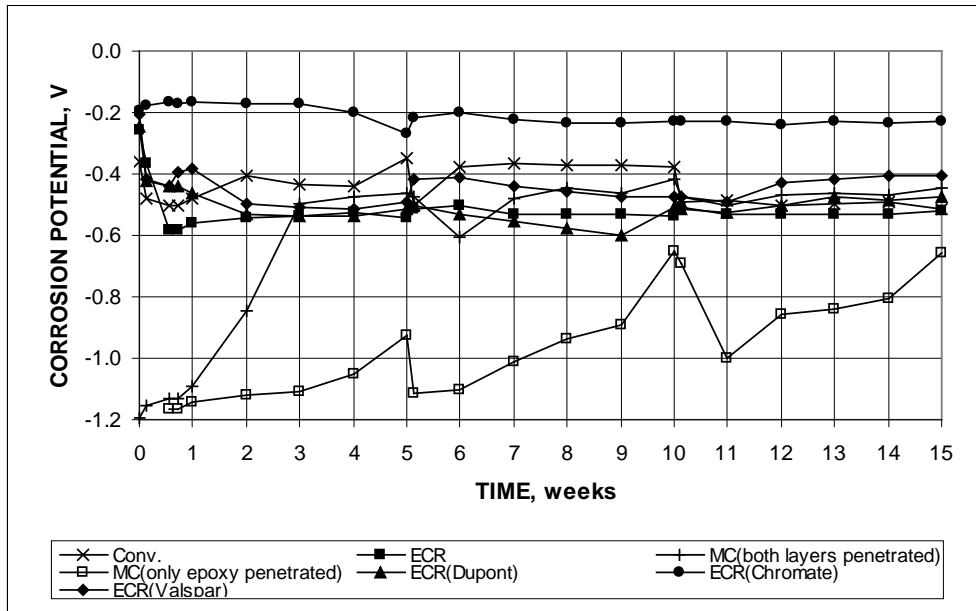
Figure 34. Graph. Macrocell test, average corrosion potential at anode for bare conventional, ECR, increased-adhesion ECR, and MC steel in simulated pore solution with 1.6 molal ion concentration of sodium chloride.
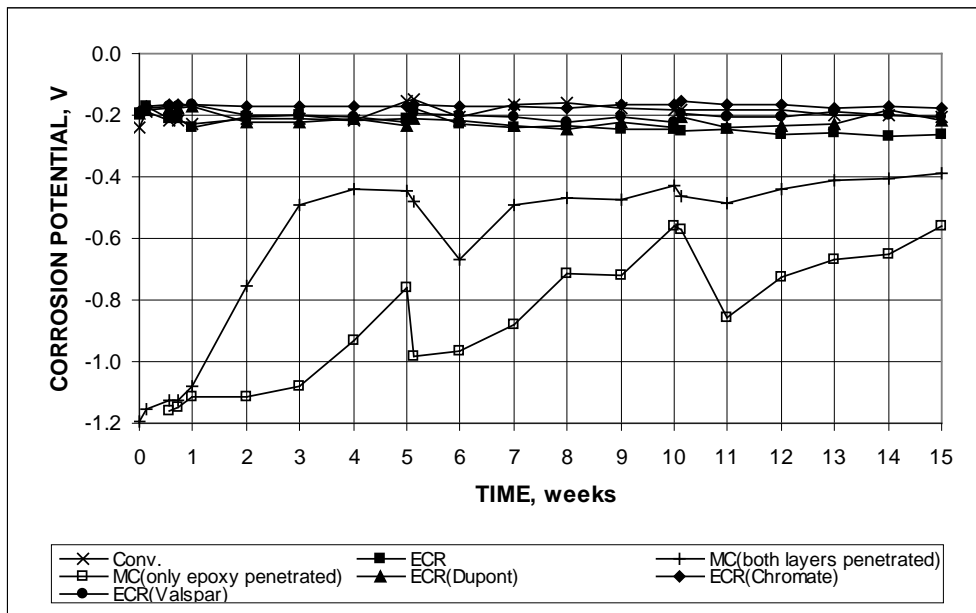
Figure 35. Graph. Macrocell test, average corrosion potential at cathode for bare conventional, ECR, increased-adhesion ECR, and MC steel in simulated pore solution with 1.6 molal ion concentration of sodium chloride.

As a general rule in the bare bar tests, the corrosion rates for ECR based on the area exposed at the holes through the coating were significantly higher than they were for conventional reinforcement based on the total area of the bar (see table 9 and table 10). This behavior, however, does not necessarily mean that corrosion losses on damaged regions of ECR are higher than local metal losses due to corrosion on uncoated conventional reinforcement because the losses recorded for

41

uncoated conventional steel represent values that are averaged over the full contact surface. In practice, corrosion losses on uncoated bars are not uniformly distributed over the bar surface but may be much greater in some areas than in others. In addition, the losses calculated for coated bars may include losses that occur under the coating, instead of just on the exposed regions.

The test specimens were evaluated visually following the tests, and all specimens in the group exhibited significant corrosion, as shown in figure 36, figure 37, and figure 38 for conventional reinforcement, conventional ECR, and MC with only the epoxy layer penetrated, respectively. Figure 38 shows that the zinc was fully consumed on the MC bars in spite of the fact that the total corrosion loss on the exposed area based on the macrocell current (shown in figure 33) amounted to less than 6 µm (0.2 mil) for a coating that was 50 µm (2 mil) thick. This observation demonstrates the impact of microcell corrosion, which was not measured in this test, on the loss of zinc and indicates that macrocell measurements may underestimate total corrosion losses.

Figure 36. Photo. Bare conventional anode bar at 15 weeks showing corrosion products that formed below the surface of the solution.

Figure 37. Photo. Bare ECR anode bar at 15 weeks showing corrosion products that formed at holes through the epoxy.

Figure 38. Photo. Bare MC anode bar with only epoxy penetrated at 15 weeks showing corrosion products that formed at holes through the epoxy.

In addition to the tests described above, bare ECR and MC bars were subjected to extended rapid macrocell tests using 6.04 molal ion sodium chloride solutions for periods of up to 40 weeks with the goal of evaluating the relative disbondment characteristics of conventional ECR and MC bars under the severe exposure conditions produced in the test as a function of corrosion loss and time. The results of that evaluation, reported in detail appendix A, demonstrate that in the rapid macrocell test with a high chloride concentration, the specimens with MC reinforcement show greater corrosion losses than the specimens with conventional ECR but that MC reinforcement shows significantly less disbondment than ECR, both as a function of corrosion loss and as a function of time.

Mortar-Wrapped Bar Tests

The corrosion rates using mortar-wrapped specimens for conventional steel, conventional ECR, ECR(primer/Ca(NO$_2$)$_2$), and MC bars with both layers penetrated and only the epoxy penetrated are shown in figure 39 and Figure 40. In figure 40, the corrosion rate is based on the exposed area at the holes through the coating.
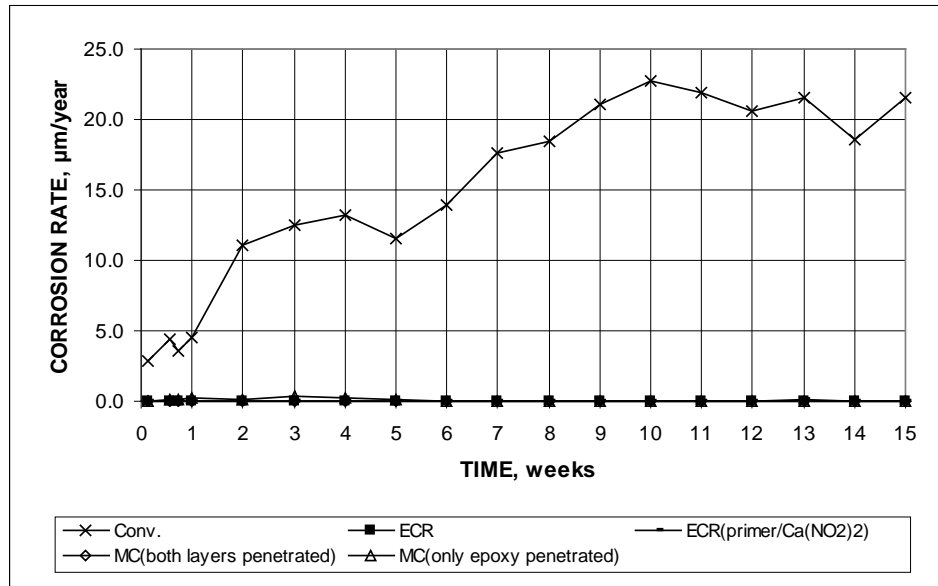
1 μm = 0.0394 mil

Figure 39. Graph. Macrocell test, average corrosion rate based on total area for mortar-wrapped conventional, ECR, ECR with calcium nitrite primer, and MC steel in simulated pore solution with 1.6 molal ion concentration of sodium chloride.
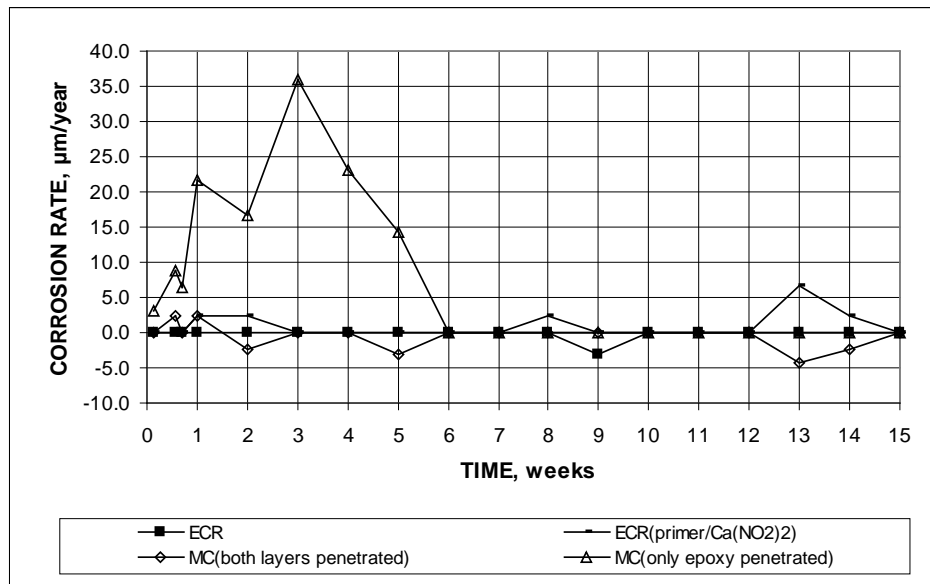
1 μm = 0.0394 mil

Figure 40. Graph. Macrocell test, average corrosion rate based on area exposed at holes through coating for mortar-wrapped conventional ECR, ECR with calcium nitrite primer, and MC steel in simulated pore solution with 1.6 molal ion concentration of sodium chloride.

43

The corrosion rate based on total area for conventional steel started at approximately 2.5 µm/year (0.098 mil/year), increasing to about 21 µm/year (0.83 mil/year) at week 9, and remained between 18 and 23 µm/year (0.71 and 0.91 mil/year) thereafter. As shown in figure 40, conventional ECR exhibited essentially no corrosion during the test, while the corrosion current exhibited by the other test specimens shown in the figure was relatively minor. The MC bars with only the epoxy penetrated exhibited a high corrosion rate between weeks 2 and 5; the rate decreased to zero after week 5. The other systems tested, including ECR with improved adhesion (ECR(Chromate)), ECR(DuPont), ECR(Valspar)), ECR in mortar with a corrosion inhibitor (calcium nitrite, Rheocrete$^®$ 222$^+$ or Hycrete™), and the three epoxies with improved adhesion in mortar with calcium nitrite, exhibited no corrosion in the test.

Corrosion losses based on total and exposed areas for the systems that did exhibit corrosion are shown in figure 41 and figure 42, respectively. Corrosion losses at 15 weeks for all specimens are presented in table 9 and table 10. Total losses for conventional steel amounted to 4.8 µm (0.19 mil) at 15 weeks, compared to values of less than 0.02 µm (0.0008 mil) based on total area for other systems and amounted to less than 2 µm (0.08 mil) for the MC bars with only the epoxy penetrated and less than 0.5 µm (0.02 mil) for the other systems based on exposed area.
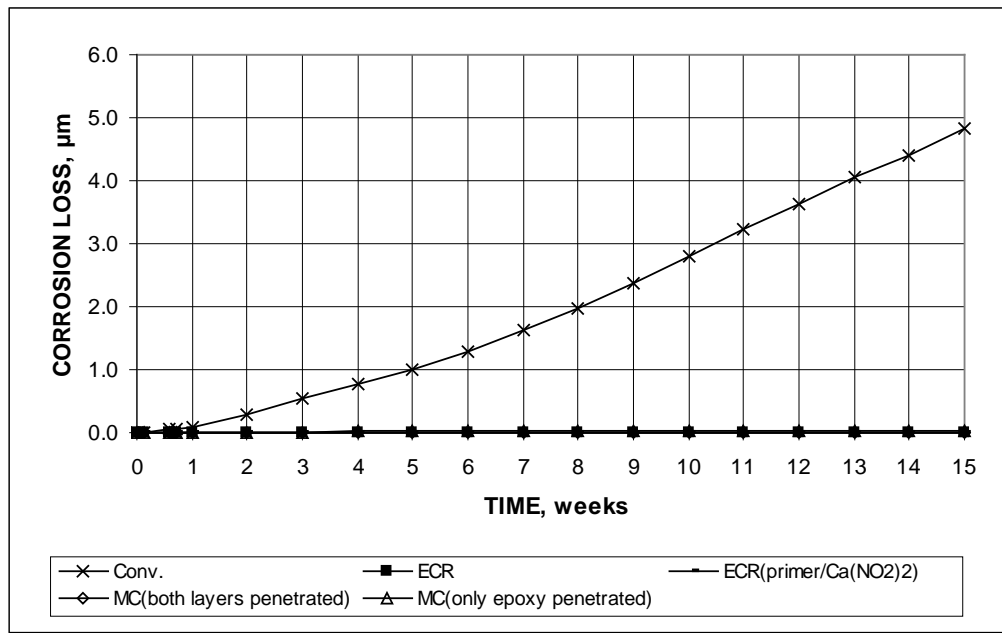
1 µm = 0.0394 mil

Figure 41. Graph. Macrocell test, average corrosion loss based on total area for mortar-wrapped conventional, ECR, ECR with calcium nitrite, and MC steel in simulated pore solution with 1.6 molal ion concentration of sodium chloride.

44
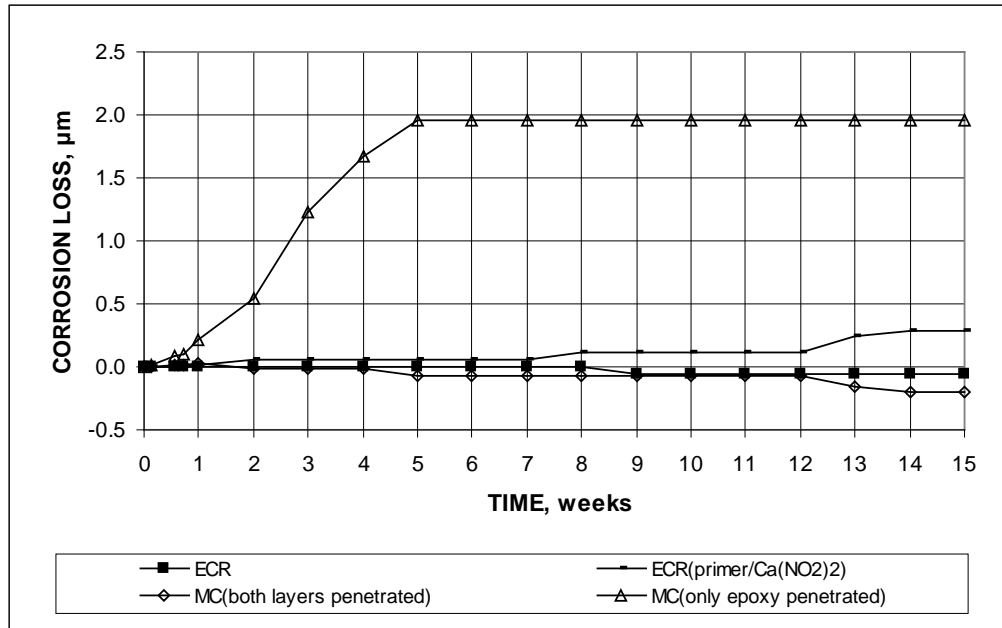
1 µm = 0.0394 mil

Figure 42. Graph. Macrocell test, average corrosion loss based on area exposed at holes through coating for mortar-wrapped conventional, ECR, ECR with calcium nitrite, and MC steel in simulated pore solution with 1.6 molal ion concentration of sodium chloride.

The average corrosion potentials during the tests, shown in figure 43 through figure 46, demonstrate that at the anode, only those steels that exhibited some corrosion loss (see table 9 and table 10) had corrosion potentials more negative than -0.275 V, with the exception of ECR(Chromate) in mortar containing calcium nitrite (ECR(Chromate)-DCI), which dropped below -0.275 V after week 12. The potential of the ECR(primer/Ca(NO$_2$)$_2$) bars, which did exhibit corrosion, dropped to approximately -0.400 V at 7 weeks, maintaining that value thereafter. The MC specimens with both layers penetrated and with only epoxy penetrated, exhibited progressively more negative potentials as the test progressed (see figure 43 and figure 44). For the MC bars with both layers penetrated, the corrosion potential started at approximately -0.400 V, dropping to a value somewhat more negative than -0.700 V at 15 weeks at both the anode and the cathode. The MC bars with only epoxy penetrated started at approximately -0.600 V, ending at a value equal to that for the same bars with both layers penetrated. The corrosion potentials of the cathodes for the MC bar tests started at only slightly more positive values than exhibited by the anodes, dropping to values between -0.600 and -0.800 V at 15 weeks. These results suggest that the MC bars started the tests in a passive condition and became relatively more active as the simulated pore solutions, both with and without sodium chloride, penetrated the mortar. The zinc provided protection during the test for both types of damage to the coating.
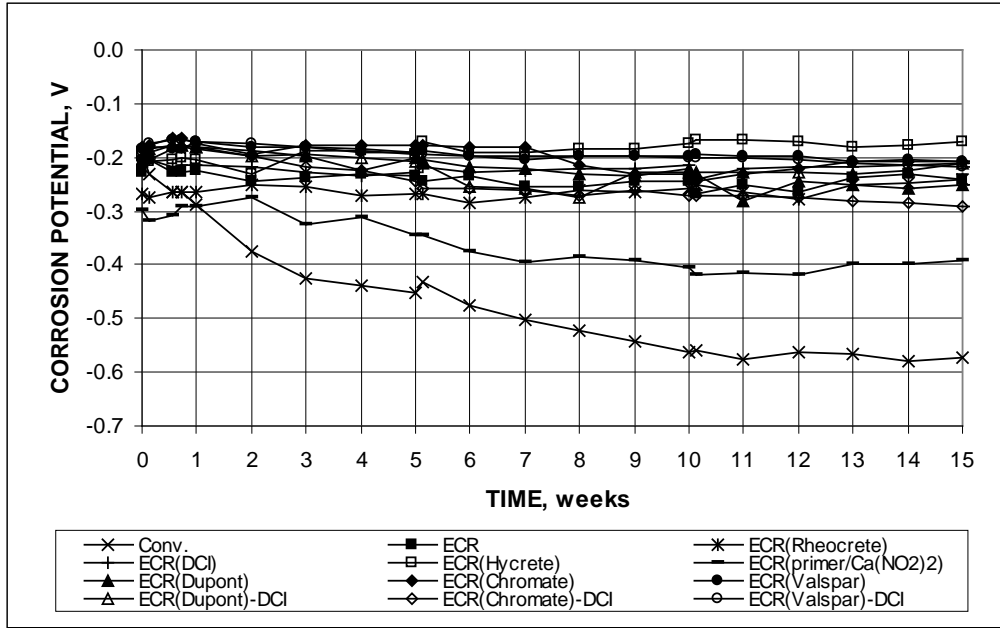
Figure 43. Graph. Macrocell test, average corrosion potential at anode for mortar-wrapped conventional, ECR, ECR with increased adhesion, ECR cast with corrosion inhibitor, and ECR with calcium nitrite in simulated pore solution with 1.6 molal ion concentration of sodium chloride.
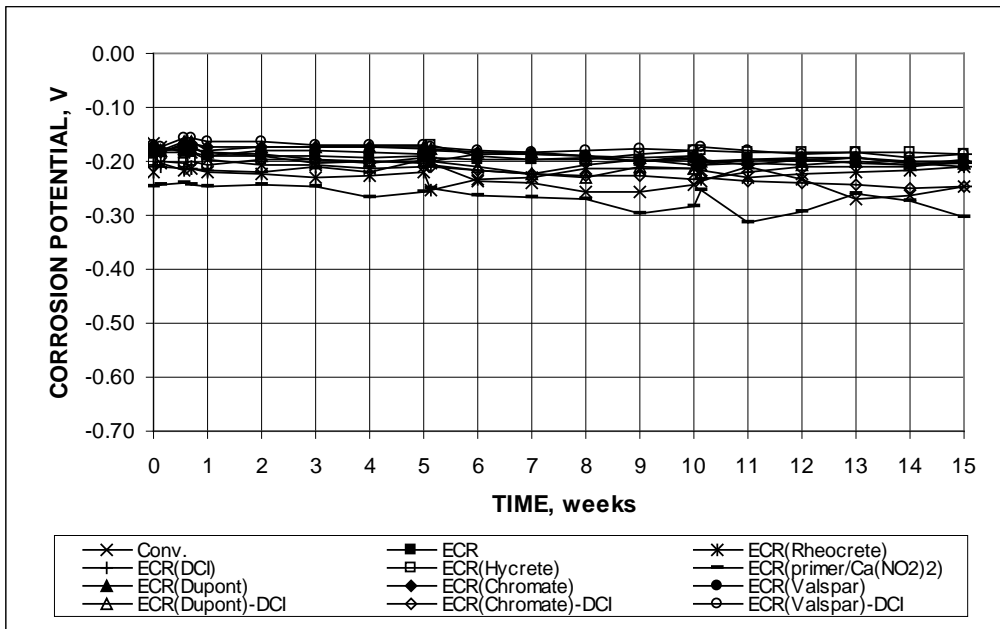
Figure 44. Graph. Macrocell test, average corrosion potential at cathode for mortar-wrapped conventional, ECR, ECR with increased adhesion, ECR cast with corrosion inhibitor, and ECR with calcium nitrite in simulated pore solution with 1.6 molal ion concentration of sodium chloride.
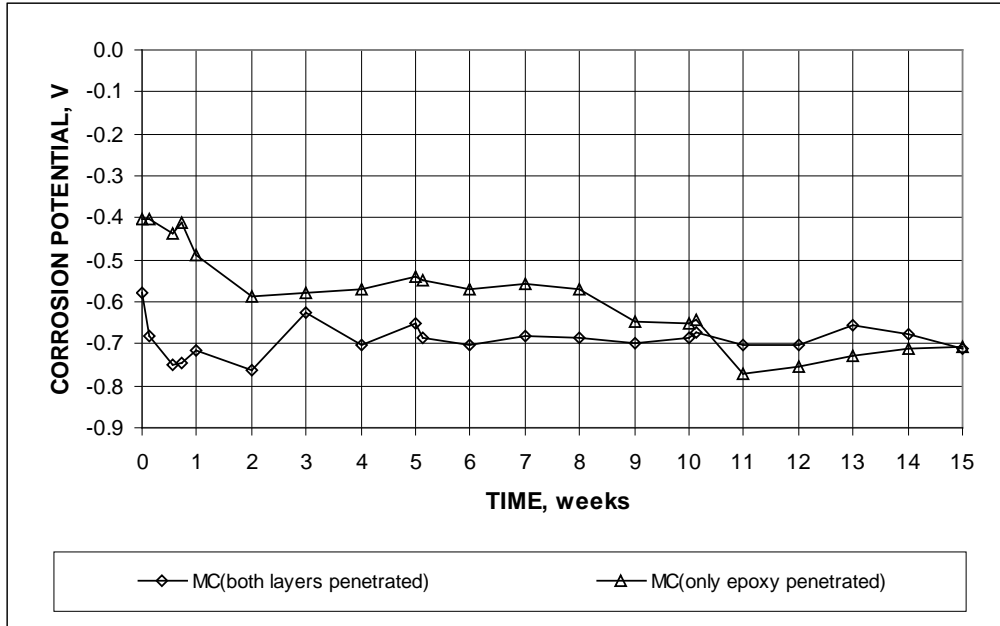
Figure 45. Graph. Macrocell test, average corrosion potential at anode for mortar-wrapped MC steel in simulated pore solution with 1.6 molal ion concentration of sodium chloride.
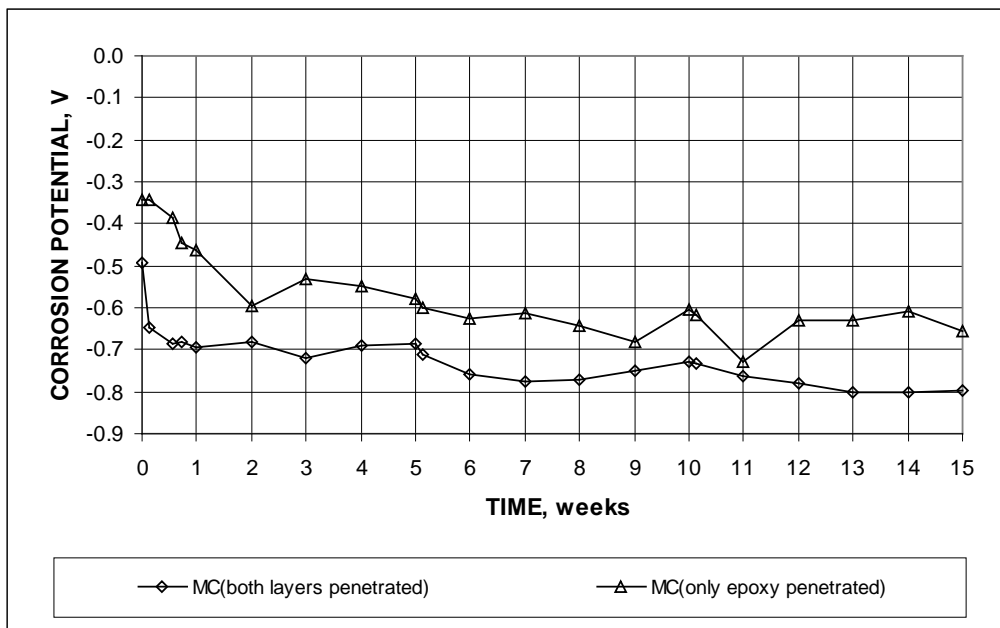
Figure 46. Graph. Macrocell test, average corrosion potential at cathode for mortar-wrapped MC steel in simulated pore solution with 1.6 molal ion concentration of sodium chloride.

At the conclusion of the tests, the mortar was removed and the bars were inspected for evidence of corrosion. The uncoated conventional steel bars exhibited corrosion, as shown in figure 47, while none of the epoxy-coated bars exhibited any corrosion products.

Figure 47. Photo. Conventional anode bar after removal of mortar at 15 weeks.

The results shown in table 9, table 10, and figure 27 through figure 35 indicate several things about the corrosion process for steel with a damaged epoxy coating. As mentioned for the bare bar tests, the epoxy coating significantly reduced total corrosion losses. But more than that, the tests demonstrated that, even with a relatively homogenous material like the mortar used, the chloride concentrations at the surface of the bar are likely to vary, providing concentrations high enough to initiate corrosion at some locations but not high enough at all locations. This is clearly the case for mortar-wrapped conventional steel, as shown in figure 47, where the corrosion products are distributed nonuniformly across the bar surface. The exposed steel at locations where epoxy is damaged should begin to corrode at the same chloride concentration as uncoated conventional steel. When this does not occur, as demonstrated in these tests, it is likely that the chloride concentration at the location of the damaged epoxy has not reached the critical chloride threshold. Thus, even damaged ECR will have an advantage over conventional steel because all locations that are damaged may not be subjected to chloride concentrations high enough to cause corrosion, while under the same conditions for uncoated steel, the chloride concentration would be high enough to initiate corrosion somewhere on the bars.

The test results also suggest that if this test is to be used to evaluate the corrosion protection provided by damaged epoxy coating (as opposed to systems with uncoated bars for which it provides a consistent measure of corrosion resistance), the severity of the exposure conditions should be increased, such as would be provided by an increased number of penetrations in the epoxy or by an increase in the concentration of chloride in the solution at the anode.[31] In the end, the test results for the mortar-wrapped rapid macrocell tests provide a general comparison of the performance of the systems studied.

BENCH-SCALE TESTS

The results of the southern exposure and cracked beam tests provide a detailed picture of the performance of the corrosion-protection systems in this study. The systems, as reported in the following sections, were compared based on average values for a minimum of three specimens for each configuration and corrosion-protection system. Six southern exposure and cracked beam specimens were used for conventional reinforcing steel and conventional ECR with four holes through the epoxy cast in concrete with a w/c ratio of 0.45 (ECR-4h-45).

Southern Exposure Tests

Test results expressed in terms of corrosion loss provide an overall view of system performance. Values based on the total area of the bar in contact with concrete and on the exposed area at holes in the epoxy are presented in table 11 and table 12, respectively. For these tests, the corrosion rates and losses based on the exposed area at the holes for bars with 4 and 10 penetrations through the epoxy on each bar are, respectively, 480 and 192 times the corrosion rate based on total bar area. As noted in the tables, two of the six epoxy-coated bars with four holes through the epoxy cast in concrete with a w/c ratio of 0.45 (ECR-4h-45) and a number of other individual specimens with different types of epoxy are not included in the averages because the corrosion rates remained essentially zero throughout the tests. The low corrosion rate on individual epoxy-coated bars resulted from the highly variable chloride content in the concrete. As observed for the mortar-wrapped rapid macrocell specimens with epoxy-coated bars, if the chloride content adjacent to the damage site on the bar is not high enough, corrosion will not be induced. In contrast, uncoated bars have a much larger exposed area, any part of which is susceptible to a chloride content high enough to induce corrosion. Variations in concrete quality can also play a role, and such variations occurred on this project, as described in the interim report.[48] The original southern exposure specimens containing conventional and conventional ECR had a lower than desired w/c ratio. As a result, those tests were repeated and provided the results in this report. The results through 96 weeks for the original conventional and conventional ECR are reported by Draper et al.[49]

Table 13 and table 14 summarize the average chloride content at a depth of 25 mm (1 inch) in the southern exposure specimens at corrosion initiation and at the conclusion of the 96-week test period. The average values at corrosion initiation are weighted based on the number of samples taken per specimen and are used subsequently in this report to estimate the time to corrosion initiation in bridge decks.

Table 11. Corrosion loss at 96 weeks (μm) for southern exposure specimens based on total area.

Steel Designation[a]	Specimen						Average	Standard Deviation
	1	2	3	4	5	6		
Controls								
Conv.-45	7.23	5.59	6.71	6.06	7.48	9.44	7.083	1.352
Conv.2-45	14.31	13.79	15.23				14.44	0.731
Conv.-35	1.05	4.22	1.10				2.121	1.817
ECR-4h-45	0.038	-0.011[b]	-0.011[b]	0.011	0.011	0.001	0.015	0.016
ECR-10h-45	0.019	0.008	0.023				0.017	0.008
ECR-10h-35	0.011	0.003	0.010				0.008	0.004
Epoxies with increased adhesion								
ECR(Chromate)-4h-45	0.004	0.015	0.035				0.018	0.016
ECR(Chromate)-10h-45	0.011	0.068	0.123				0.067	0.056
ECR(DuPont)-4h-45	0.031	0.017	0.030				0.026	0.008
ECR(DuPont)-10h-45	0.029	0.060	0.050				0.046	0.016
ECR(Valspar)-4h-45	0.039	0.015	0.044				0.032	0.016
ECR(Valspar)-10h-45	0.054	0.044	0.090				0.063	0.024
Corrosion inhibitors in concrete								
Conv.2(DCI)-45	9.63	7.28	8.88				8.60	1.200
Conv.2(RH)-45	3.11	2.29	4.79				3.40	1.276
Conv.2(HY)-45	1.24	1.59	1.82				1.55	0.292
ECR(DCI)-4h-45	0.002	0.008	0.002				0.004	0.003
ECR(DCI)-10h-45	-0.002[b]	0.020	0.016				0.018	0.003
ECR(DCI)-10h-35	0.012	0.001	0.008				0.007	0.006
ECR(RH)-4h-45	0.000	0.030	-0.002[b]				0.015	0.021
ECR(RH)-10h-45	0.001	-0.011[b]	0.003				0.002	0.001
ECR(RH)-10h-35	0.002	0.005	0.003				0.003	0.001
ECR(HY)-4h-45	-0.001[b]	-0.002[b]	-0.002[b]				0.000	–
ECR(HY)-10h-45	0.003	-0.001[b]	0.003				0.003	0.000
ECR(HY)-10h-35	0.006	-0.002[b]	-0.001[b]				0.006	–
ECR(primer/Ca(NO$_2$)$_2$)-4h-45	0.005	0.012	0.026				0.014	0.011
ECR(primer/Ca(NO$_2$)$_2$)-10h-45	0.031	0.137	0.022				0.064	0.064
ECR(primer/Ca(NO$_2$)$_2$)-10h-35	0.003	0.002	0.001				0.002	0.001
Epoxies with increased adhesion plus calcium nitrite in concrete								
ECR(Chromate)-DCI-4h-45	0.002	-0.000[b]	0.018				0.010	0.011
ECR(DuPont)-DCI-4h-45	-0.000[b]	-0.001[b]	0.001				0.001	–
ECR(Valspar)-DCI-4h-45	0.000	0.002	0.033				0.012	0.019
Bars with multiple coatings								
MC(both layers penetrated)-4h-45	0.030	0.013	0.016				0.020	0.009
MC(both layers penetrated)-10h-45	0.055	0.229	0.153				0.146	0.088
MC(only epoxy penetrated)-4h-45	0.012	0.007	-0.001				0.006	0.006
MC(only epoxy penetrated)-10h-45	0.001	0.021	0.026				0.016	0.013

1 μm = 0.0394 mil

– No standard deviation.

Blank cells indicate no specimen tested.

[a] See table 1 for abbreviation definitions. 4h = bar with four holes through epoxy, 10h = bar with 10 holes through epoxy. 35 = concrete with w/c = 0.35, 45 = concrete with w/c = 0.45.

[b] Excluded from average.

Table 12. Corrosion loss at 96 weeks (μm) for southern exposure specimens based on area exposed at holes through coating.

Steel Designation[a]	Specimen 1	2	3	4	5	6	Average	Standard Deviation
Controls								
ECR-4h-45	18.44	-5.26[b]	-5.32[b]	5.07	5.18	0.70	7.35	7.68
ECR-10h-45	3.66	1.58	4.41				3.21	1.47
ECR-10h-35	2.03	0.55	1.83				1.47	0.80
Epoxies with increased adhesion								
ECR(Chromate)-4h-45	2.11	7.28	16.89				8.76	7.50
ECR(Chromate)-10h-45	2.04	12.99	23.66				12.90	10.81
ECR(DuPont)-4h-45	14.71	7.99	14.32				12.34	3.77
ECR(DuPont)-10h-45	5.52	11.50	9.68				8.90	3.07
ECR(Valspar)-4h-45	18.76	7.00	20.97				15.58	7.51
ECR(Valspar)-10h-45	10.33	8.53	17.22				12.03	4.58
Corrosion inhibitors in concrete								
ECR(DCI)-4h-45	0.99	3.62	0.84				1.82	1.57
ECR(DCI)-10h-45	-0.37[b]	3.90	3.17				3.53	0.52
ECR(DCI)-10h-35	2.25	0.11	1.49				1.29	1.08
ECR(RH)-4h-45	0.00	14.46	-0.74[b]				7.23	10.23
ECR(RH)-10h-45	0.27	-2.08[b]	0.63				0.45	0.26
ECR(RH)-10h-35	0.48	0.94	0.52				0.65	0.26
ECR(HY)-4h-45	-0.39[b]	-0.95[b]	-1.13[b]				0.00	–
ECR(HY)-10h-45	0.65	-0.20[b]	0.66				0.65	0.01
ECR(HY)-10h-35	1.17	-0.30[b]	-0.17[b]				1.17	–
ECR(primer/Ca(NO$_2$)$_2$)-4h-45	2.18	5.63	12.35				6.72	5.17
ECR(primer/Ca(NO2)$_2$)-10h-45	6.02	26.41	4.32				12.25	12.29
ECR(primer/Ca(NO$_2$)$_2$)-10h-35	0.61	0.48	0.17				0.42	0.22
Epoxies with increased adhesion plus calcium nitrite in concrete								
ECR(Chromate)-DCI-4h-45	1.06	-0.21[b]	8.59				4.82	5.33
ECR(DuPont)-DCI-4h-45	-0.21[b]	-0.49[b]	0.28				0.28	–
ECR(Valspar)-DCI-4h-45	-0.07[b]	1.16	16.08				8.62	10.55
Bars with multiple coatings								
MC(both layers penetrated)-4h-45	30.47	30.75	21.96				27.73	5.00
MC(both layers penetrated)-10h-45	100.15	136.15	109.50				115.3	18.68
MC(only epoxy penetrated)-4h-45	8.96	25.20	13.51				15.89	8.38
MC(only epoxy penetrated)-10h-45	5.06	34.37	12.70				17.37	15.20

1 μm = 0.0394 mil

– No standard deviation.

Blank cells indicate no specimen tested.

[a] See table 1 for abbreviation definitions. 4h = bar with four holes through epoxy, 10h = bar with 10 holes through epoxy. 35 = concrete with w/c of 0.35, 45 = concrete with w/c of 0.45.

[b] Excluded from average.

Table 13. Chloride content at corrosion initiation (kg/m^3) for southern exposure specimens.

Steel Designation[a]	Samples per Specimen[b]	Specimen 1	2	3	4	5	6	Average	Standard Deviation
Controls									
Conv.-45	6	0.65	1.07	0.38	1.38	0.39	0.66[c]	0.77	0.39
Conv.2-45	6	1.58[c]	0.66[c]	0.48				0.88	0.65
Conv.-35	2	1.93[d]	0.75	1.90				1.69	0.80
ECR-4h-45	6	1.54	0.99	*	3.52	†	2.48	2.13	1.11
ECR-10h-45	2	3.43	9.26[e]	8.36				7.57	2.62
ECR-10h-35	3	†	†	†				†	†
Epoxies with increased adhesion									
ECR(Chromate)-4h-45	2	5.54	8.30[f]	8.47				7.56	2.56
ECR(Chromate)-10h-45	2	2.44	3.73	†				3.08	0.91
ECR(DuPont)-4h-45	2	8.77	7.73	4.24				6.91	2.37
ECR(DuPont)-10h-45	2	1.56	2.17	5.41[d]				3.99	1.96
ECR(Valspar)-4h-45	2	8.17	7.25[f]	7.15				7.48	1.31
ECR(Valspar)-10h-45	2	5.11	2.77	†				3.94	1.65
Corrosion inhibitors in concrete									
Conv.2-DCI-45	6	2.88	3.03	5.26				3.72	1.12
Conv.2-RH-45	6	1.97[c]	2.26	2.24				2.16	0.76
Conv.2-HY-45	6	†	0.82	0.62				1.21	0.24
ECR(DCI)-4h-45	2	4.52	†	5.74[d]				5.44	1.36
ECR(DCI)-10h-45	2	†	5.78	7.29				6.53	1.06
ECR(DCI)-10h-35	2	2.18	2.67	1.41				2.09	0.64
ECR(RH)-4h-45	6	3.44	2.17[f]	3.38				3.16	0.96
ECR(RH)-10h-45	2	†	*	4.01				4.01	–
ECR(RH)-10h-35	2	*	1.52	0.73				1.13	0.56
ECR(HY)-4h-45	6	†	1.19	†				1.19	–
ECR(HY)-10h-45	2	0.79	*	1.03				0.91	0.17
ECR(HY)-10h-35	2	0.60	0.43[d]	0.35[f]				0.44	0.24
ECR(primer/Ca(NO$_2$)$_2$)-4h-45	2	4.47	†	3.51				3.99	0.68
ECR(primer/Ca(NO$_2$)$_2$)-10h-45	2	6.36	13.80	7.47				9.21	4.01
ECR(primer/Ca(NO$_2$)$_2$)-10h-35	6	*	1.48	*				1.48	–
Epoxies with increased adhesion plus calcium nitrite in concrete									
ECR(Chromate)-DCI-4h-45	2	2.26	1.20	4.86				2.77	1.88
ECR(DuPont)-DCI-4h-45	2	3.91	3.50[d]	11.4[f]				5.73	3.65
ECR(Valspar)-DCI-4h-45	2	*	1.56	9.13				5.35	4.13
Bars with multiple coatings									
MC(both layers penetrated)-4h-45	2	†	†	0.71				0.71	–
MC(both layers penetrated)-10h-45	2	†	1.48	0.96				1.22	0.37
MC(only epoxy penetrated)-4h-45	2	0.69	1.75	2.63				1.69	0.97
MC(only epoxy penetrated)-10h-45	2	5.26	2.53	†				3.90	1.92

1 kg/m^3 =1.69 lb/yd^3

* Corrosion initiation not recorded.

† Information not available.

– No standard deviation.

Blank cells indicate no specimen tested.

[a] See table 12 for abbreviation definitions.

[b] Unless otherwise noted.

[c] Five samples analyzed; [d] Six samples analyzed; [e] Four samples analyzed; [f] Three samples analyzed.

Table 14. Chloride content at 96 weeks (kg/m³) for southern exposure specimens.

Steel Designation[a]	Specimen						Average	Standard Deviation
	1	2	3	4	5	6		
Controls								
Conv.-45	10.65	13.16	7.09	8.51	8.08	9.01	9.42	2.18
Conv.2-45	4.53	3.88	6.02				4.81	1.09
Conv.-35	5.96	8.31	5.74				6.67	1.43
ECR-4h-45	6.92	6.83	9.42	8.15	7.79	6.13	7.54	1.17
ECR-10h-45	12.38	13.31	13.34				13.01	0.55
ECR-10h-35	5.96	8.31	5.74				6.67	1.43
Epoxies with increased adhesion								
ECR(Chromate)-4h-45	13.14	15.98	13.74				14.29	1.50
ECR(Chromate)-10h-45	11.34	19.49	9.24				13.35	5.42
ECR(DuPont)-4h-45	12.82	17.49	10.98				13.76	3.36
ECR(DuPont)-10h-45	14.46	15.64	10.74				13.61	2.56
ECR(Valspar)-4h-45	14.34	13.39	23.93				17.22	5.83
ECR(Valspar)-10h-45	17.71	18.79	8.12				14.87	5.88
Corrosion inhibitors in concrete								
Conv.2(DCI)-45	4.73	8.87	8.00				12.11	3.67
Conv.2(RH)-45	4.43	3.97	4.47				7.22	0.47
Conv.2(HY)-45	3.13	2.45	3.23				4.94	0.72
ECR(DCI)-4h-45	†	†	†				–	–
ECR(DCI)-10h-45	†	†	†				–	–
ECR(DCI)-10h-35	7.97	4.53	2.45				4.98	2.79
ECR(RH)-4h-45	3.74	7.76	5.88				5.79	2.01
ECR(RH)-10h-45	7.74	4.99	6.49				6.41	1.38
ECR(RH)-10h-35	1.56	2.94	3.73				2.74	1.10
ECR(HY)-4h-45	2.76	3.04	4.74				3.51	1.07
ECR(HY)-10h-45	1.78	2.89	3.73				2.80	0.98
ECR(HY)-10h-35	0.74	1.61	2.23				1.53	0.75
ECR(primer/Ca(NO₂)₂)-4h-45	9.25	9.93	10.25				9.81	0.51
ECR(primer/Ca(NO₂)₂)-10h-45	9.83	9.19	11.53				10.18	1.21
ECR(primer/Ca(NO₂)₂)-10h-35	1.69	2.81	2.73				2.41	0.62
Epoxies with increased adhesion plus calcium nitrite in concrete								
ECR(Chromate)-DCI-4h-45	7.86	6.42	7.44				7.24	0.74
ECR(DuPont)-DCI-4h-45	7.95	6.06	8.35				7.45	1.23
ECR(Valspar)-DCI-4h-45	8.35	4.93	8.19				7.16	1.93
Bars with multiple coatings								
MC(both layers penetrated)-4h-45	11.13	10.22	11.76				11.04	0.77
MC(both layers penetrated)-10h-45	12.76	12.56	12.79				12.70	0.12
MC(only epoxy penetrated)-4h-45	8.85	15.37	9.84				11.35	3.52
MC(only epoxy penetrated)-10h-45	11.62	13.23	11.21				12.02	1.07

1 kg/m³ =1.69 lb/yd³

† Information not available.

– No standard deviation.

Blank cells indicate no specimen tested.

[a] See table 12 for abbreviation definitions.

The chloride contents at corrosion initiation, 0.77 and 0.88 kg/m^3 (1.30 and 1.48 lb/yd^3), are within the expected range of 0.60 to 1.20 kg/m^3 (1.0 to 2.0 lb/yd^3) for conventional steel cast in concrete with w/c of 0.45 and somewhat higher, 1.69 kg/m^3 (2.85 lb/yd^3), in concrete with w/c of 0.35. With the notable exception of bars cast in concrete containing the corrosion inhibitor Hycrete™ (discussed later in this section), chloride contents at corrosion initiation for epoxy-coated bars and conventional bars cast in concrete containing a corrosion inhibitor are above, and in most cases well above, 1.20 kg/m^3 (2.0 lb/yd^3). The high value for epoxy-coated bars again emphasizes the effects of local variations in chloride content near damaged areas on epoxy-coated bars.

The chloride contents at 96 weeks for concretes without corrosion inhibitors with w/c of 0.45 range from 4.8 to 17.2 kg/m^3 (8.1 to 29.0 lb/yd^3); with just one exception (ECR-4h-45), these values exceed 11 kg/m^3 (18.5 lb/yd^3) only for specimens containing bars coated with epoxies with increased adhesion and bars with multiple coatings. The chloride contents at 96 weeks for concretes with corrosion inhibitors range from 2.4 to 10.1 kg/m^3 (4.1 to 17.1 lb/yd^3). As observed in earlier studies, the chloride values exhibit considerable scatter within individual specimens as well as from specimen to specimen, with the latter demonstrated in the tables.[50]

The variation in chloride contents and corrosion performance observed in these tests provides insight into the variability in corrosion performance observed in the field, where bridge decks reinforced with uncoated bars have provided service lives that range from 4 to 40 years for bridges in the same environment. That variability may be due to differences in concrete quality, both local and global, which can significantly affect the rate of chloride penetration.

Average corrosion rates for the southern exposure specimens, which are based on losses after corrosion has initiated, are summarized in table 15. For bars without coatings, the corrosion rates are expressed in terms of the total bar area, and for bars with coatings, the corrosion rates are expressed in terms of the area exposed at holes through the coating. As noted in chapter 2, there are a number of specimens with epoxy-coated bars for which no corrosion was observed, meaning that the specimens did not exhibit a measureable corrosion rate over time. This may be true even though a net corrosion loss was recorded (see table 11 and table 12).

Table 15. Average corrosion rate (µm/year) based on losses after corrosion initiation for southern exposure specimens.

Bars Without Coatings—Corrosion Rate Based on Total Area								
Steel Designation[a]	Specimen						Average	Standard Deviation
	1	2	3	4	5	6		
Controls								
Conv.-45	5.35	4.41	5.10	6.04	5.82	7.40	5.69	1.01
Conv.2-45	10.7	9.74	10.0				10.1	0.49
Conv.-35	5.99	8.68	1.61				5.43	3.57
Corrosion inhibitors in concrete								
Conv.2(DCI)-45	7.81	5.11	7.09				6.67	1.40
Conv.2(RH)-45	2.57	2.60	3.56				2.91	0.56
Conv.2(HY)-45	0.791	1.03	1.92				1.25	0.60

Bars With Coatings—Corrosion Rate Based on Exposed Area								
Steel Designation	4 holes			10 holes			Average	Standard Deviation
	1	2	3	1	2	3		
Controls								
ECR-45	13.6	b	b	5.98	18.4	12.7	10.43	5.32
	6.74[c]	5.09[c]	bc					
ECR-35				1.49	b	2.35	1.92	0.61
Epoxies with increased adhesion								
ECR(Chromate)	b	13.0	18.1	1.18	11.6	20.5	12.9	7.48
ECR(DuPont)	13.8	24.3	b	4.72	7.79	11.2	12.4	7.51
ECR(Valspar)	15.5	5.91	44.0	12.3	6.52	17.4	16.9	14.0
Corrosion inhibitors in concrete								
ECR(DCI)-45	b	9.36	b	b	11.8	2.33	7.81	4.90
ECR(DCI)-35				2.32	b	1.16	1.74	0.82
ECR(RH)-45	b	b	5.94	b	11.3	b	8.63	3.80
ECR(RH)-35				b	0.558	b	0.558	-
ECR(HY)-45	b	b	b	b	b	0.674	0.674	-
ECR(HY)-35				1.08	b	b	1.080	-
ECR(primer/Ca(NO$_2$)$_2$)-45	b	3.66	22.0	6.56	24.4	6.39	12.6	9.79
ECR(primer/Ca(NO$_2$)$_2$)-35				b	1.41	b	1.41	-
Epoxies with increased adhesion plus calcium nitrite in concrete								
ECR(Chromate)-DCI-45	b	b	10.3				10.3	-
ECR(DuPont)-DCI-45	b	b	b				b	-
ECR(Valspar)-DCI-45	b	b	5.97				5.97	-
MC	5.55[d]	22.7[d]	36.9[d]	6.57[d]	23.1[d]	7.52[d]	31.6	26.2
	19.6[e]	29.2[e]	13.1[e]	65.9[e]	80.7[e]	68.8[e]		

1 µm = 0.0394 mil

– No standard deviation.

Blank cells indicate no specimen tested.

[a] See table 1 for abbreviation definitions. 35 = concrete with w/c of 0.35, 45 = concrete with w/c of 0.45.

[b] No corrosion observed.

[c] Specimens 4, 5, and 6.

[d] Both layers penetrated.

[e] Only epoxy penetrated.

55

In the following sections, a description of the results for the southern exposure tests of the control specimens is followed by those for the multiple corrosion-protection systems. The chapter also covers a study of uncoated conventional reinforcement cast in concrete containing corrosion inhibitors.

Control Specimens

The control specimens for this study consisted of conventional steel cast in concrete with w/c ratios of 0.45 (Conv.-45) and 0.35 (Conv.-35), conventional ECR cast in concrete with w/c of 0.45 with 4 holes (ECR-4h-45) or 10 holes (ECR-10h-45) through the epoxy, and conventional ECR cast in concrete with w/c of 0.35 with 10 holes through the epoxy (ECR-10h-35). The corrosion rates based on total area in contact with the concrete are shown in figure 48. The figure shows that, as seen in the rapid macrocell test, corrosion proceeds at a much higher rate for uncoated than for coated reinforcement, with the latter corroding at well below 1 percent of the rate of the former, a rate that is about equal to the ratio of the area exposed at the holes to the total area of the bars. The lower w/c ratio provides additional protection to conventional steel, with significant corrosion starting at about 48 weeks for the concrete with w/c of 0.35, compared to 24 weeks for the concrete with w/c of 0.45. The corrosion rate for the Conv.-45 specimens reached a maximum of 7.2 µm/year (0.28 mil/year) at 94 weeks, but generally varied between 6 and 7 µm/year (0.24 and 0.28 mil/year) during the final 24 weeks of the test. The corrosion rate of the Conv.-35 specimens reached a maximum of approximately 4.2 µm/year (0.17 mil/year) at 87 weeks while exhibiting a nearly constant rate between 3.9 and 4.2 µm/year (0.15 and 0.17 mil/year) between week 83 and the end of the test.
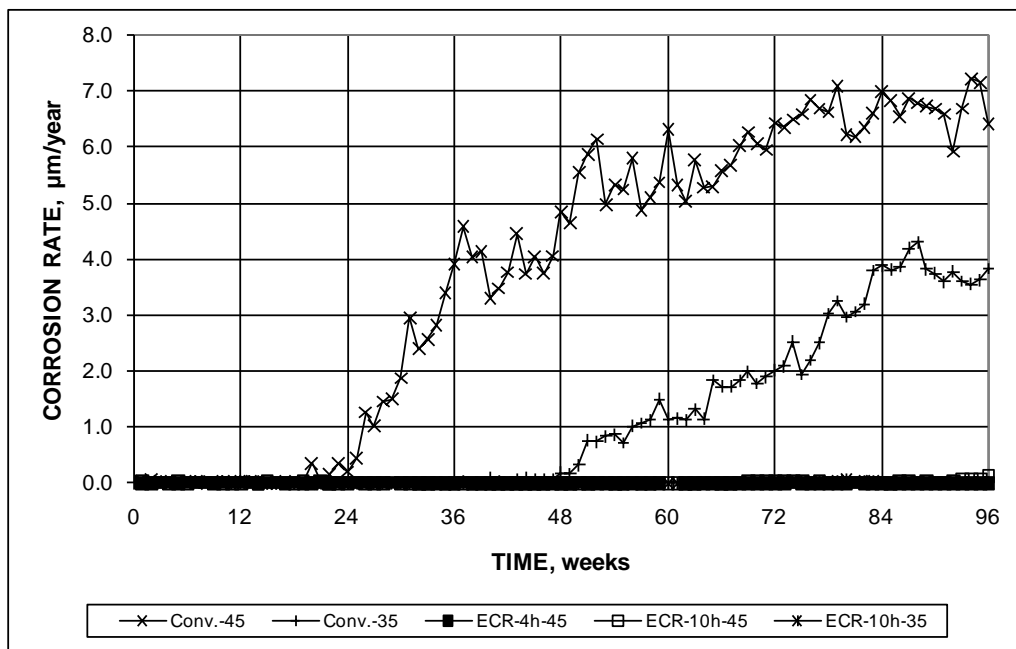
1 µm = 0.0394 mil

Figure 48. Graph. Southern exposure test, average corrosion rates based on total area for conventional reinforcement and ECR.

The average total corrosion losses for the systems are plotted in figure 49 and figure 50, which, like figure 48, show the effect of the lower w/c ratio in delaying corrosion initiation and lowering

corrosion losses. The average losses at the end of the tests equaled 7.1 and 2.1 µm (0.28 and 0.083 mil) for the Conv.-45 and Conv.-35 specimens, respectively.
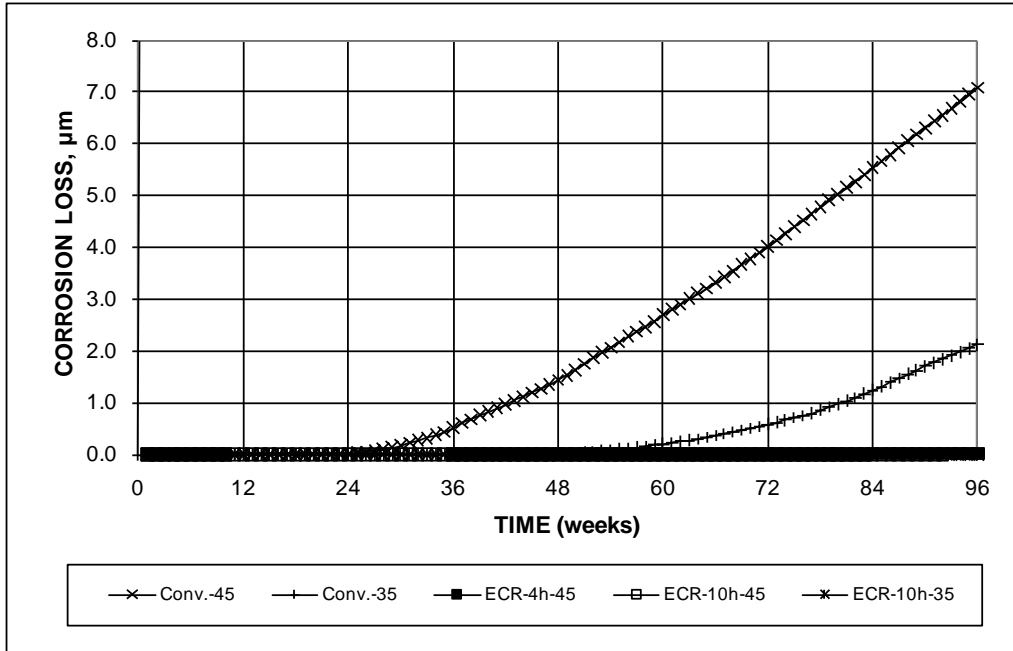
1 µm = 0.0394 mil

Figure 49. Graph. Southern exposure test, average corrosion loss based on total area for conventional reinforcement and ECR.
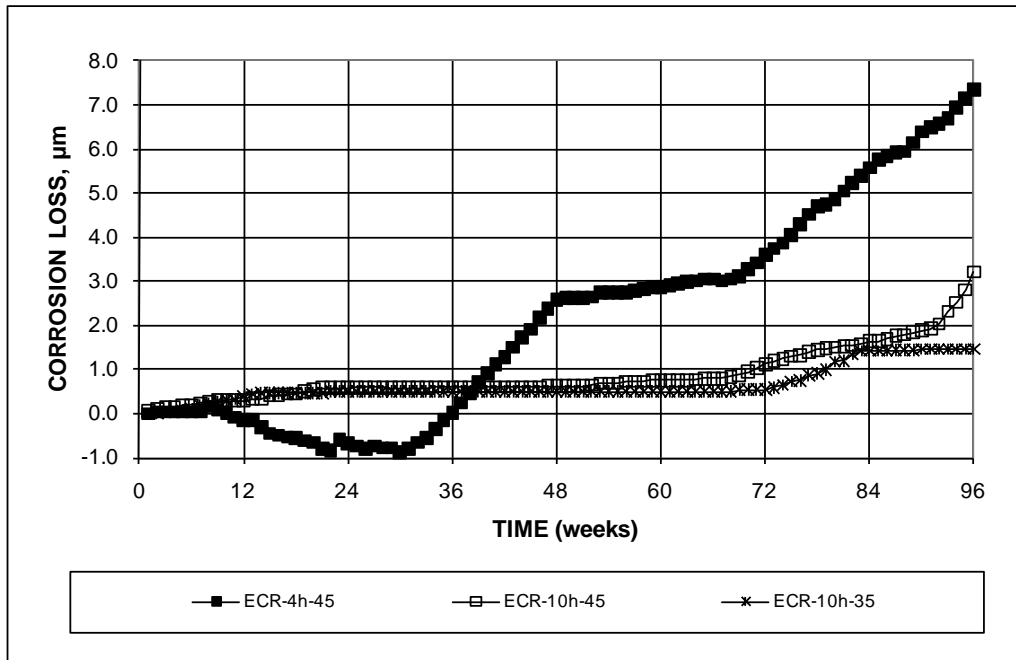
1 µm = 0.0394 mil

Figure 50. Graph. Southern exposure test, average corrosion loss based on area exposed at holes through coating for ECR.

The corrosion losses for the epoxy-coated bars based on the area exposed at the holes through the coating are shown in figure 50. As for the conventional steel, the lower w/c ratio provided additional corrosion protection, with losses at 96 weeks for the ECR-10h-35 specimens equal to about 50 percent of the losses for the ECR-10h-45 specimens. The losses based on exposed area for the ECR-4h-45 specimens are considerably higher (7.2 µm (0.28 mil)), more than twice those based on exposed area for the ECR-10h-45 specimens. The losses based on total area, however, are nearly identical at 0.015 and 0.017 µm (0.00059 and 0.00067 mil) for the specimens with 4 and 10 holes, respectively. As shown in table 11, table 12, and table 15, the scatter for the conventional ECR specimens is quite high, as it is for a number of other systems. As a result, the difference in corrosion between ECR-4h-45 and ECR-10h-45 is not statistically significant. The difference is statistically significant between ECR-10h-45 and ECR-10h-35. The negative corrosion exhibited between weeks 12 and 36 for the ECR-4h-45 specimens is the result of measurements of very low currents caused by low levels of oxidation on the exposed regions of the four bottom bars before corrosion initiates on the two top bars, resulting in current flow that makes the bottom bars appear to be anodes. Once chloride reaches the top bars, the nature of the corrosion reverses, which occurs at about week 30 based on the average corrosion loss versus time relationship shown in figure 50. The flat regions on the corrosion loss curves may be the result of corrosion products temporarily blocking the small exposed areas on the bars.

The corrosion potentials for the top and bottom mats of steel are shown in figure 51 and figure 52, respectively. For the top mat, the average corrosion potential for the ECR-10h-35 bars remained more positive than -0.350 V with respect to a CSE throughout the test, indicating a low probability of corrosion. The corrosion potentials dropped below -0.350 V at weeks 26, 51, 49, and 52 for Conv.-45, Conv.-35, ECR-4h-45, and ECR-10h-45, respectively.
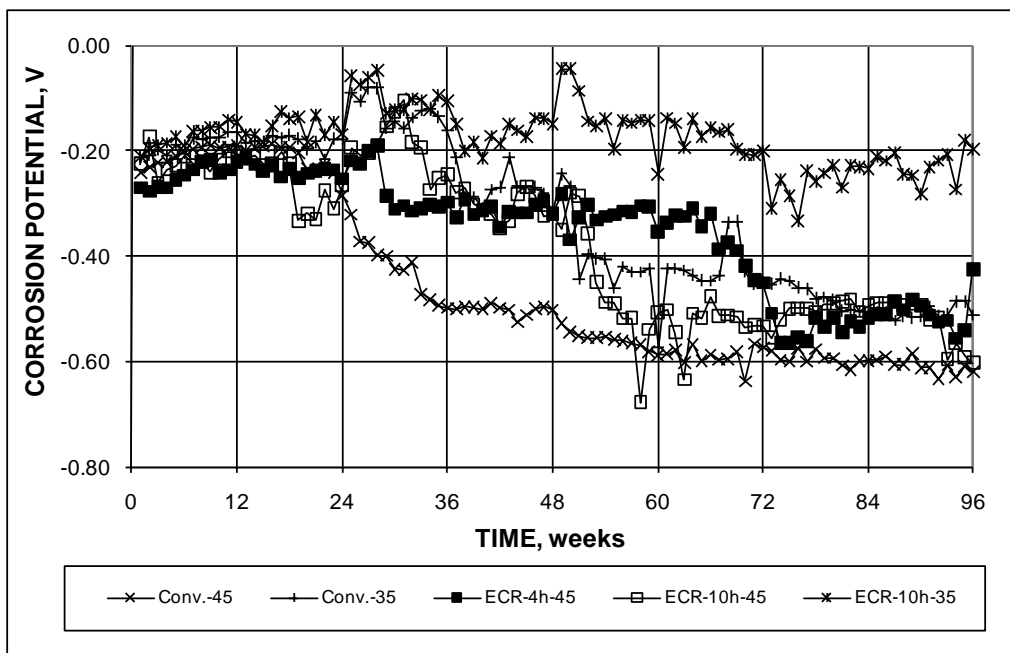
Figure 51. Graph. Southern exposure test, corrosion potential of top mat for conventional reinforcement and ECR.
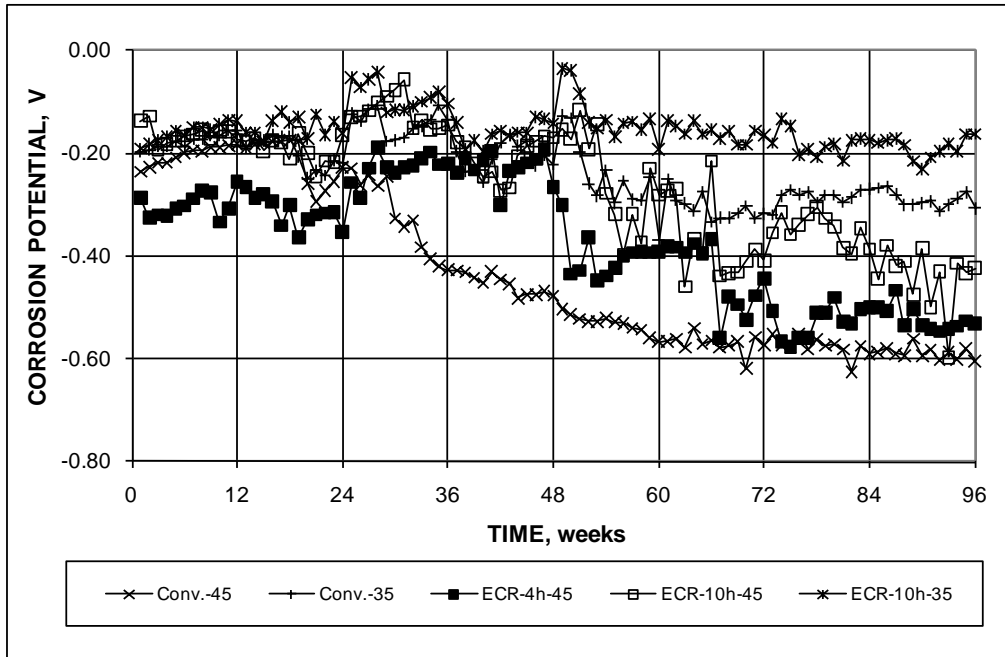
Figure 52. Graph. Southern exposure test, corrosion potential of bottom mat for conventional reinforcement and ECR.

The corrosion potentials for the bottom mat of reinforcement remained more positive than -0.350 V with respect to a CSE throughout the test for Conv.-35 and ECR-10h-35. The potential dropped below -0.350 V at weeks 33, 50, and 56 for Conv.-45, ECR-4h-45 and ECR-10h-45, respectively, indicating that chlorides penetrated to the level of the bottom mat for those specimens.

The values of mat-to-mat resistance for the five systems are shown in figure 53, which illustrates a key difference between systems with coated and uncoated bars. The resistance between the top and bottom steel bars was similar for Conv.-45 and Conv.-35 throughout the 96-week test period, ranging from low values of 126 and 166 ohms, respectively, at week 1 to high values of 588 ohms at week 85 for Conv.-45 and 586 ohms at week 72 for Conv.-35, with values rising for about the first 60 weeks and then leveling off. The values for the epoxy-coated bars also rose early in the test, leveling off somewhat earlier—between 42 and 50 weeks. The major difference from the uncoated bars, however, is the much higher resistance provided by the epoxy coating, with initial readings of 2,099, 742, and 924 ohms for ECR-4h-45, ECR-10h-45, and ECR-10h-35, respectively. The respective high resistance values were 13,247 ohms at week 36, 6,710 ohms at week 51, and 5,989 ohms at week 82. As observed for the uncoated bars, w/c ratio had little effect on the mat-to-mat resistance and the number of openings in the coating had a major effect, with the bars with 4 holes in the coating exhibiting more than twice the mat-to-mat resistance as those with 10 holes. A high mat-to-mat resistance represents a high resistance to ionic current and represents a major advantage to coated reinforcement.
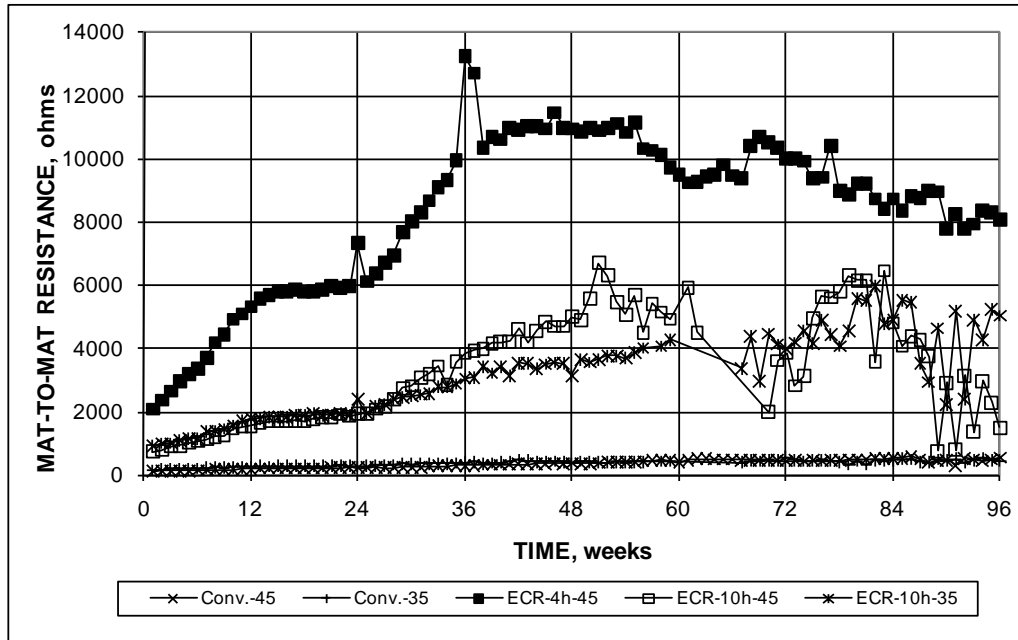
Figure 53. Graph. Southern exposure test, mat-to-mat resistance for conventional reinforcement and ECR.

Epoxies with Improved Adhesion

Comparisons of the corrosion losses for conventional ECR-4h-45 and ECR-10h-45 and the corresponding specimens of ECR(Chromate), ECR(DuPont), and ECR(Valspar) based on total and exposed area are shown in figure 54 and figure 55, respectively. The figures demonstrate that increased adhesion between the epoxy and reinforcing steel provides no benefits under the exposure conditions provided by these tests. In fact, by the end of tests, all of the bars with the higher adhesion epoxies exhibited greater average corrosion losses on the exposed area than the conventional ECR specimens. At 96 weeks, the average chloride contents of the specimens containing bars with the higher adhesion epoxies ranged from 13.6 to 17.2 kg/m^3 (22.9 to 29.0 lb/yd^3) compared with about 7.5 kg/m^3 (12.7 lb/yd^3) for the specimens containing conventional epoxy-coated steel with 4 holes through the epoxy and for the specimens containing conventional epoxy-coated reinforcement with 10 holes through the coating. The variation in corrosion losses exhibited in both figures, however, is likely due to variations in the chloride content along the surface of the individual bars. As shown in table 11 and table 12, the variability in test results can often be explained by a very high reading on a single specimen. This is true for ECR(Chromate)-4h-45, ECR(Chromate)-10h-45, ECR(Valspar)-4h-45, and ECR(Valspar)-10h-45. As shown in figure 56, a plot of corrosion potential for the top mats, the systems exhibited average corrosion potential below -0.350 V by 45 weeks with the exception of conventional ECR (ECR-4h-45), which remained above this value until week 50.

60
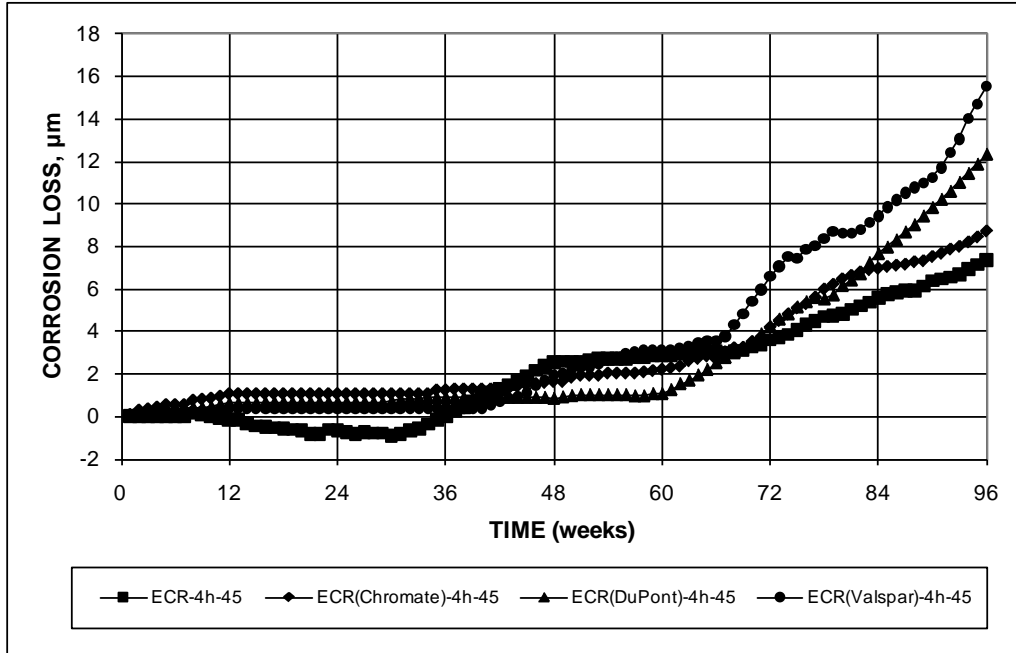
1 µm = 0.0394 mil

Figure 54. Graph. Southern exposure test, corrosion losses based on total area for conventional ECR and increased-adhesion ECR.
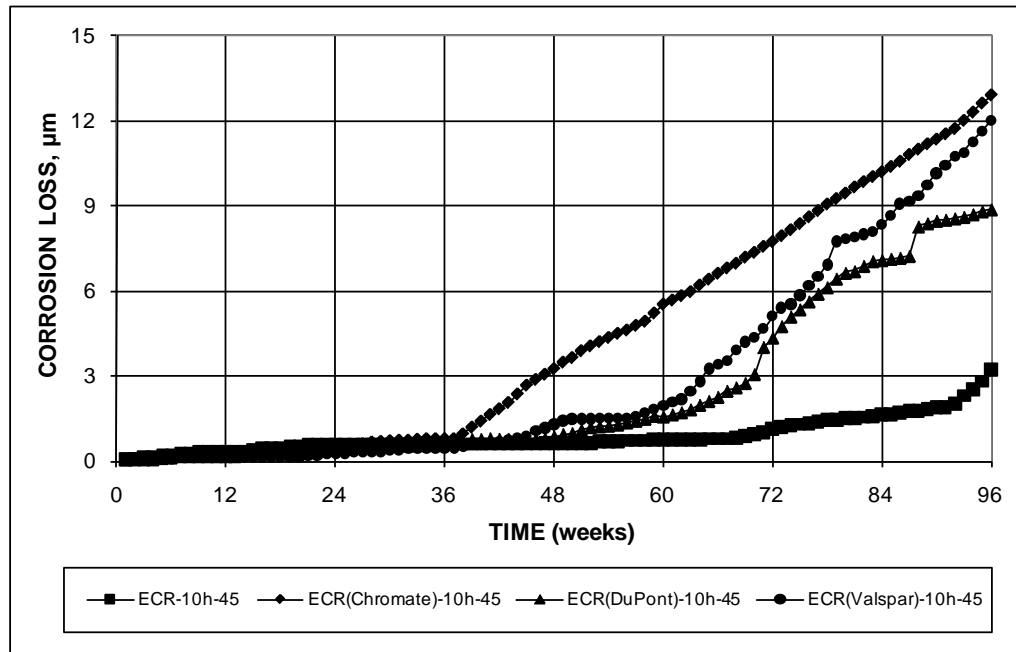
1 µm = 0.0394 mil

Figure 55. Graph. Southern exposure test, corrosion losses based on area exposed at holes through coating for conventional ECR and increased-adhesion ECR.

61
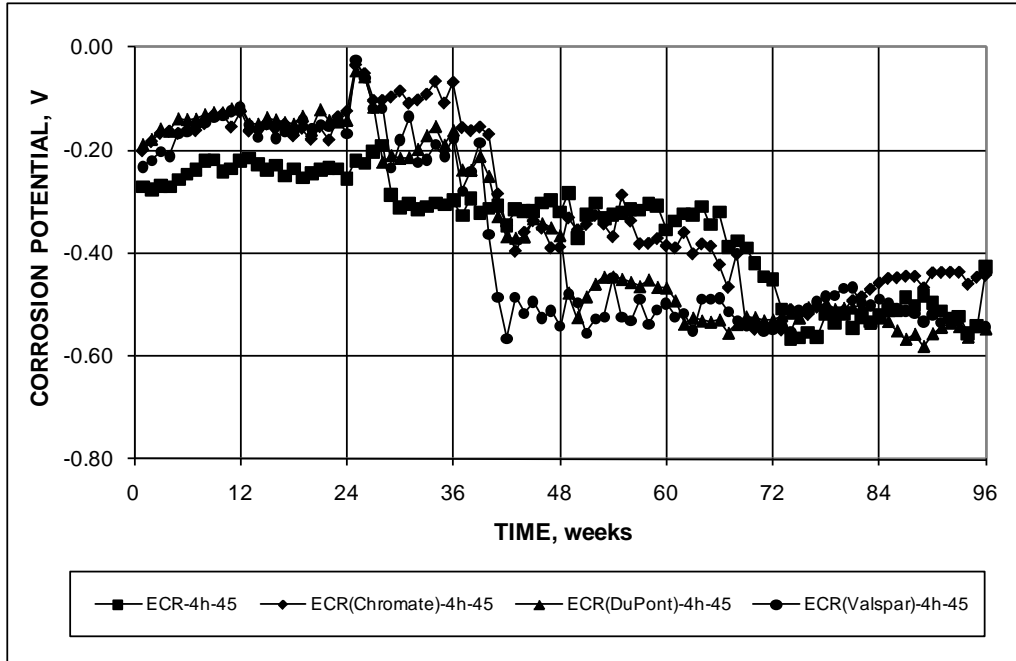
Figure 56. Graph. Southern exposure test, corrosion potential of top mat for conventional ECR and increased-adhesion ECR.

ECR Used in Conjunction with Corrosion Inhibitors

Corrosion losses based on exposed area for conventional ECR cast in concrete without a corrosion inhibitor and cast in concrete with calcium nitrite, Rheocrete$^{®}$ 222^{+}, and Hycrete™ are shown in figure 57, figure 58, and figure 59 for bars with 4 holes in the epoxy and concrete with w/c of 0.45, bars with 10 holes through the epoxy in concrete with w/c of 0.45, and bars with 10 holes cast in concrete with w/c of 0.35, respectively. The figures also include the results for conventional ECR with a primer containing microencapsulated calcium nitrite.
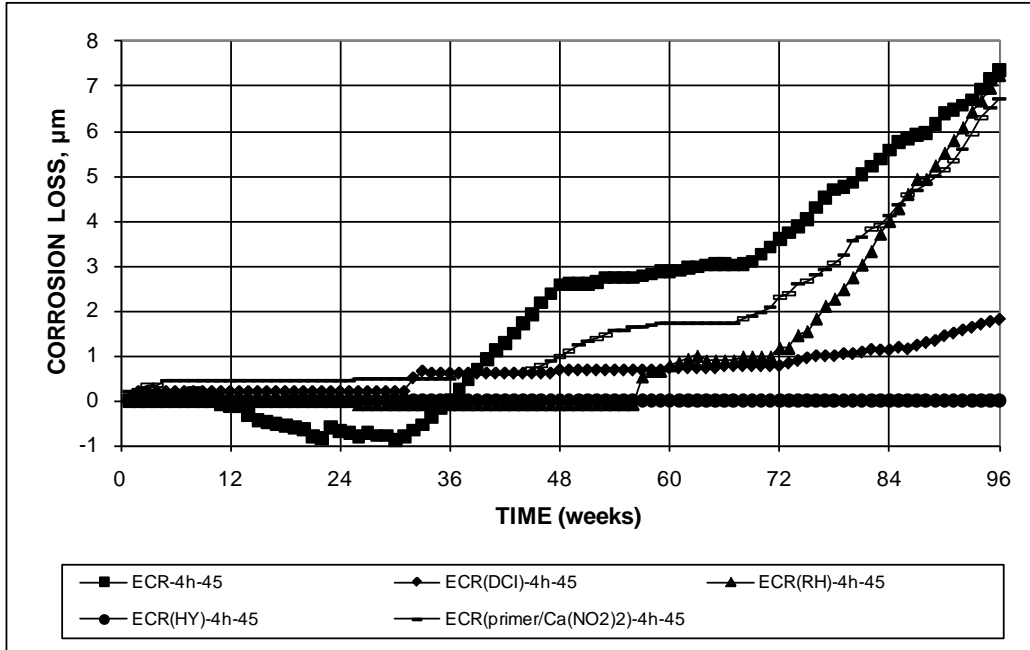
1 µm = 0.0394 mil

Figure 57. Graph. Southern exposure test, corrosion losses based on area exposed at holes through coating for conventional ECR and ECR with inhibitors with bars containing four holes and concrete with w/c = 0.45.
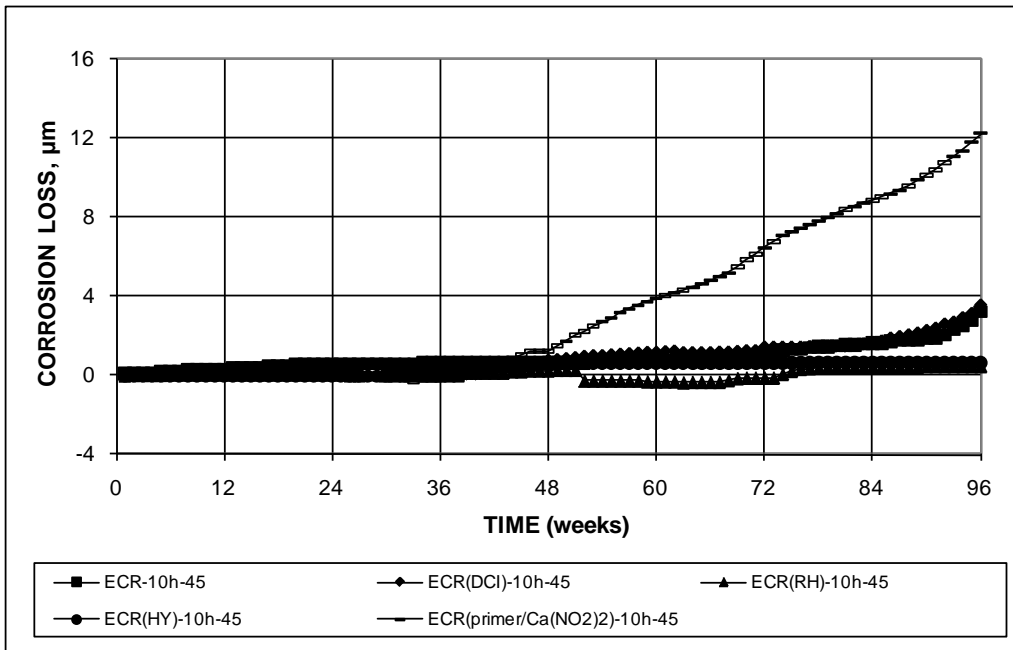
1 µm = 0.0394 mil

Figure 58. Graph. Southern exposure test, corrosion losses based on area exposed at holes through coating for conventional ECR and ECR with inhibitors with bars containing 10 holes and concrete with w/c = 0.45.

1 μm = 0.0394 mil
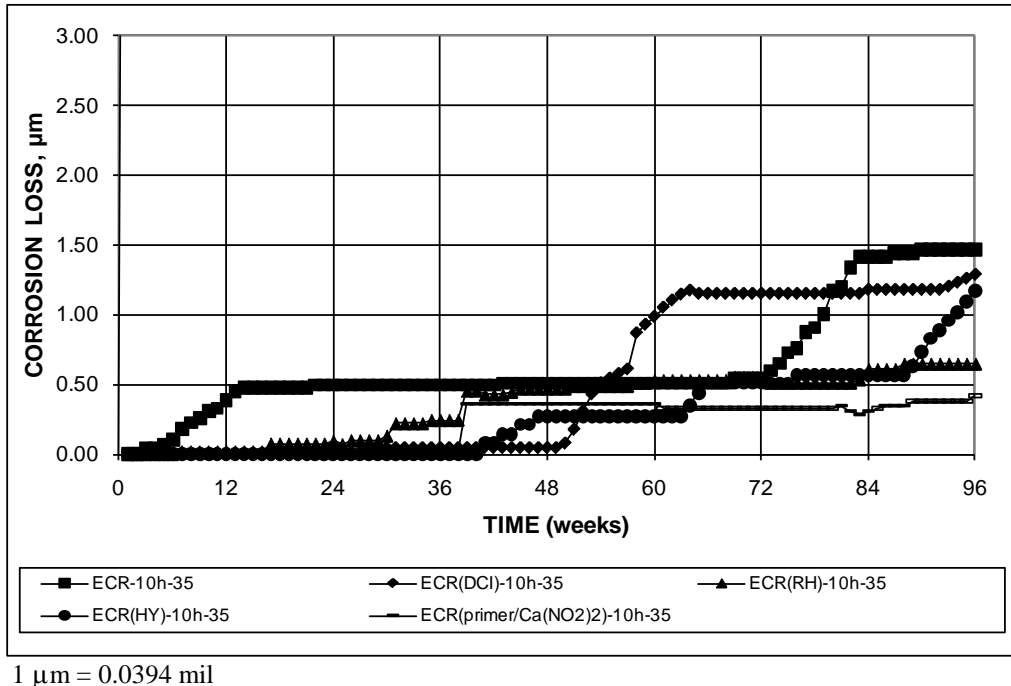
Figure 59. Graph. Southern exposure test, corrosion losses based on area exposed at holes through coating for conventional ECR and ECR with inhibitors with bars containing 10 holes and concrete with w/c = 0.35.

Figure 57 through figure 59 and table 11 through table 15 show that corrosion inhibitors improve the corrosion performance of ECR in uncracked concrete. They also show that a lower w/c ratio, which results in a lower chloride level in the concrete due to reduced permeability, enhances the performance of the corrosion inhibitors. This observation is especially apparent for ECR(primer/Ca(NO$_2$)$_2$). The large differences observed in this case are likely due to the limited quantity of nitrite, which is available only from the exposed primer where the epoxy is penetrated. This limited quantity of nitrite is consumed in a shorter period of time in concrete with a w/c ratio of 0.45 than in concrete with a w/c of 0.35 due to the higher chloride concentration at the bar surface for the higher w/c ratio concrete. In contrast, the quantity of nitrite available was considerably higher for all ECR(DCI) specimens because the calcium nitrite was added to the concrete. Overall, specimens containing a corrosion inhibitor exhibited the same or less corrosion than exhibited by the conventional ECR specimens with the single exception of the ECR(primer/Ca(NO$_2$)$_2$)-10h-45 specimens.

The corrosion potentials exhibited by the top mats for the test specimens are shown in figure 60 through figure 62. The figures indicate that most of the specimens containing a corrosion inhibitor experienced corrosion potentials more negative than -0.350 V with respect to a CSE during the course of the test. The exceptions were ECR(HY)-4h-45, ER(HY)-10h-45, and ECR(primer/Ca(NO$_2$)$_2$)-10h-35.

64
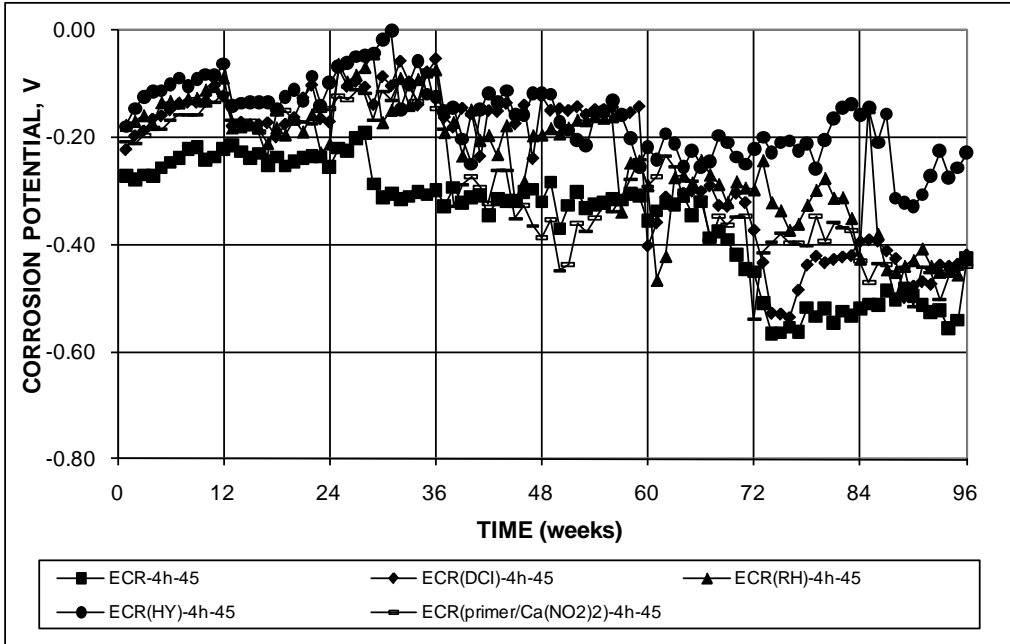
Figure 60. Graph. Southern exposure test, corrosion potential of top mat for conventional ECR with and without corrosion inhibitor with bars containing four holes and concrete with w/c = 0.45.
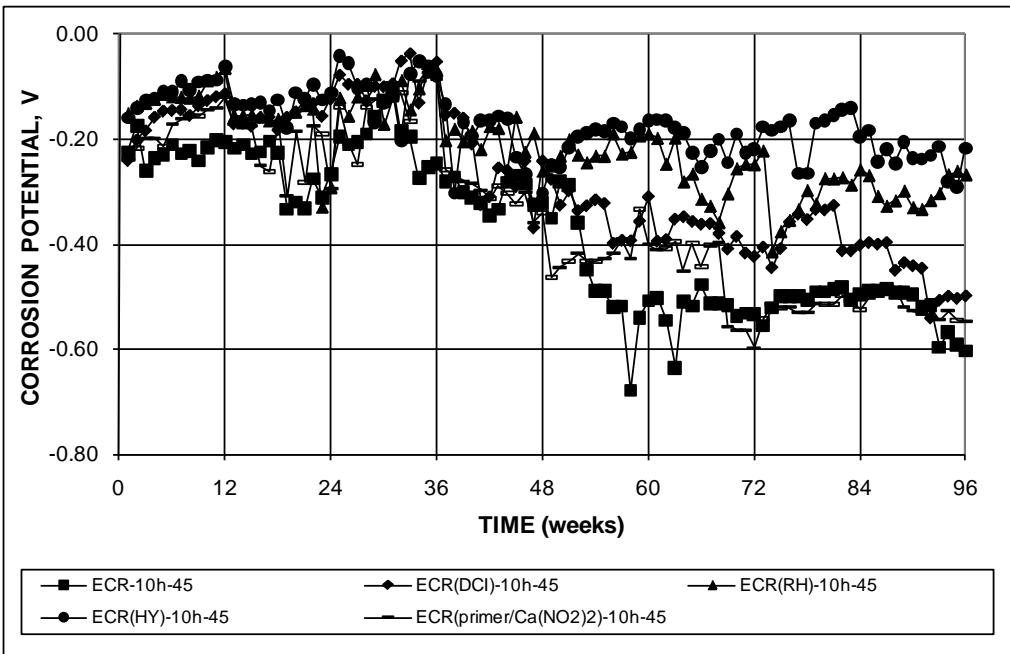
Figure 61. Graph. Southern exposure test, corrosion potential of top mat for conventional ECR with and without corrosion inhibitor with bars containing 10 holes and concrete with w/c = 0.45.
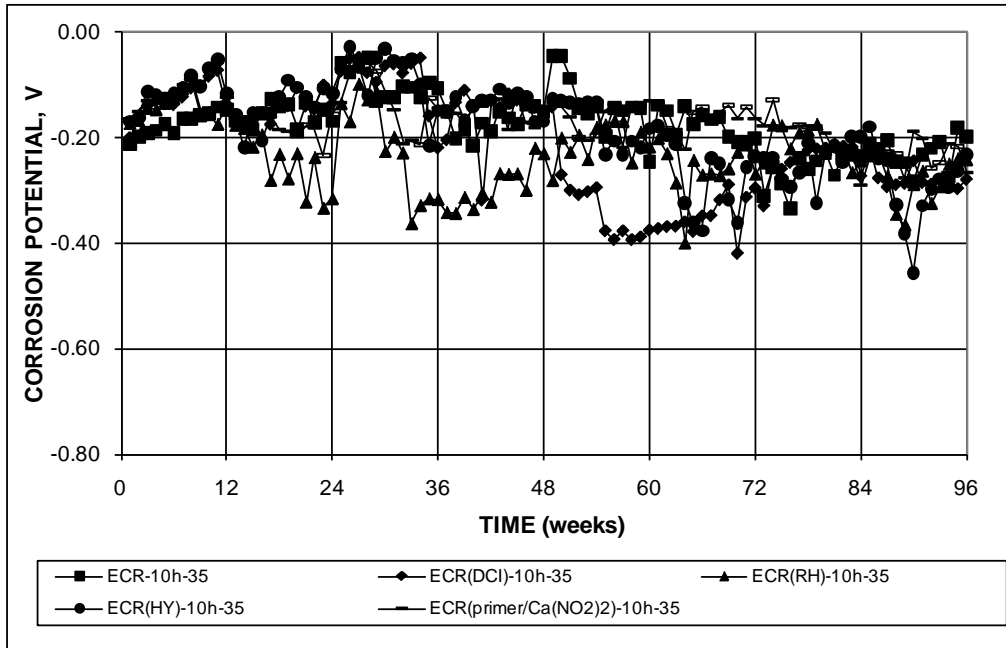
Figure 62. Graph. Southern exposure test, corrosion potential of top mat for conventional ECR with and without corrosion inhibitor with bars containing 10 holes and concrete with w/c = 0.35.

Epoxy Coating with Improved Adhesion Cast in Concrete Containing Calcium Nitrite

A limited number of specimens (four holes in the epoxy with w/c of 0.45) were tested for each of the three epoxies with improved adhesion cast in concrete containing calcium nitrite. As observed in the other tests with concrete containing corrosion inhibitors, the bars with improved adhesion exhibited improved corrosion resistance in the presence of calcium nitrite, as shown in figure 63, and exhibited improved corrosion performance compared to conventional ECR in concrete with calcium nitrite with the exception of ECR(Valspar) after 60 weeks. At the conclusion of the tests, losses based on the area exposed at the holes through the epoxy ranged from 0.28 µm (0.011 mil) for ECR(DuPont)-DCI-4h-45 to 8.62 µm (0.339 mil) for ECR(Valspar)-DCI-4h-45. The scatter in the data shown in table 12 indicates that these values did not differ in a statistically meaningful way from each other. The corrosion potentials for the top mats in these tests are shown in figure 64. The average corrosion potential dropped below -0.350 V by the end of the test in all cases with the exception of ECR(Valspar)-DCI-4h-45, which exhibited the highest corrosion losses in spite of its relatively more positive corrosion potential.

66
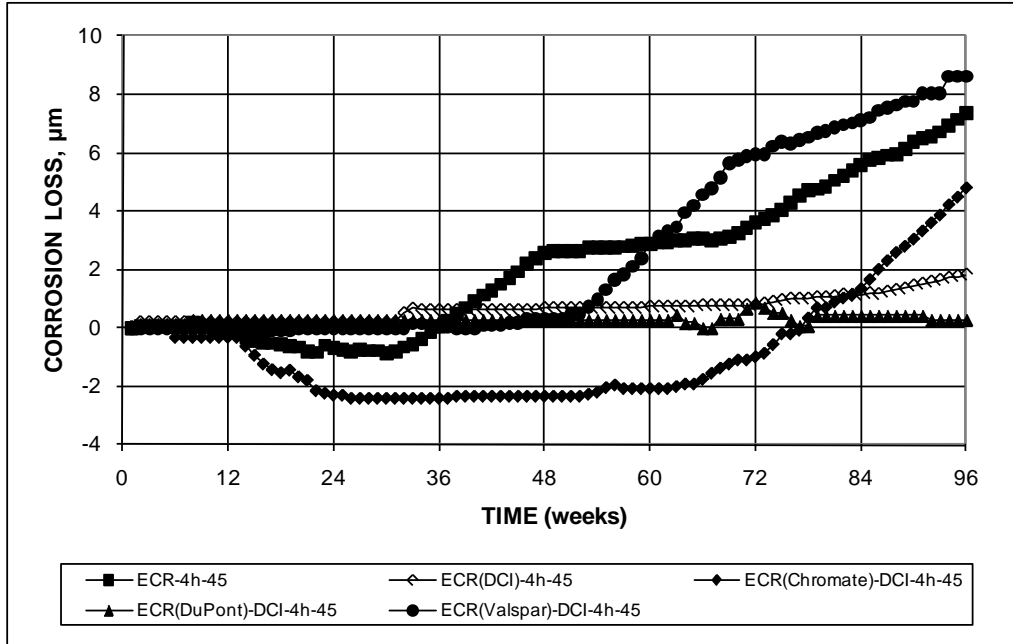
1 µm = 0.0394 mil

Figure 63. Graph. Southern exposure test, average corrosion losses based on area exposed at holes through coating for conventional ECR and ECR with and without increased adhesion and corrosion inhibitor.
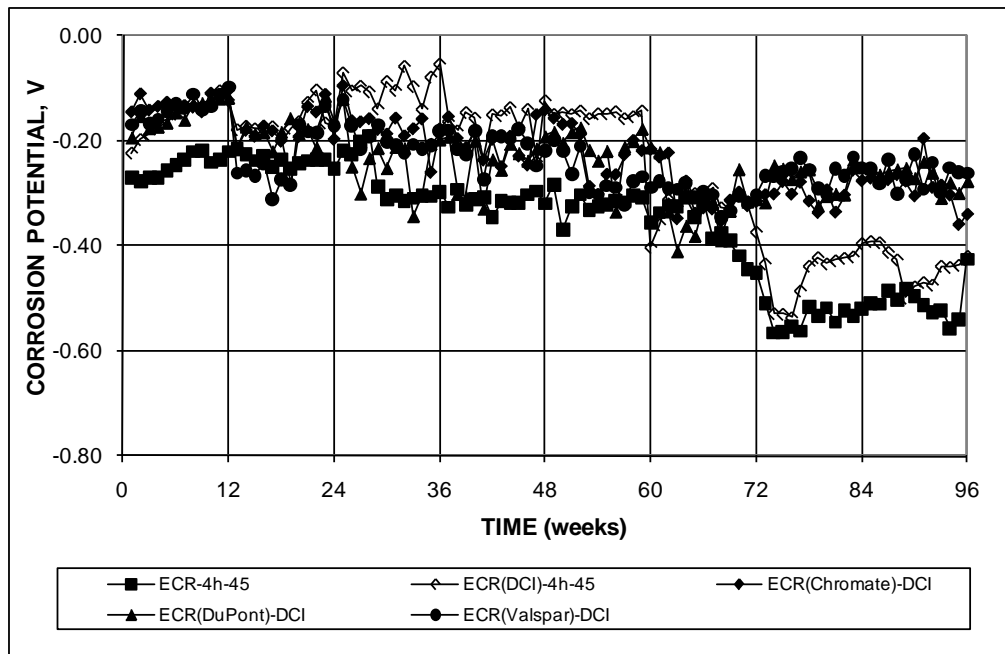
Figure 64. Graph. Southern exposure test, corrosion potential of top mat for conventional ECR with and without corrosion inhibitor and increased-adhesion ECR with corrosion inhibitor.

Bars with Multiple Coatings

The corrosion losses for MC bars are compared with those for conventional ECR in figure 65 and figure 66 for bars with 4 and 10 holes, respectively. The specimens with MC bars consistently exhibited greater corrosion losses than those with conventional ECR. The MC bars with both layers penetrated exhibited average corrosion losses on the exposed area of 27.7 μm (1.09 mil) (for 4 holes) and 115 μm (4.53 mil) (for 10 holes) at the conclusion of the tests compared to values of 7.4 and 3.2 μm (0.29 and 0.13 mil) for conventional ECR. The respective values with only the epoxy penetrated were 15.9 and 17.4 μm (0.626 and 0.685 mil), as shown in figure 65, figure 66, and table 12.
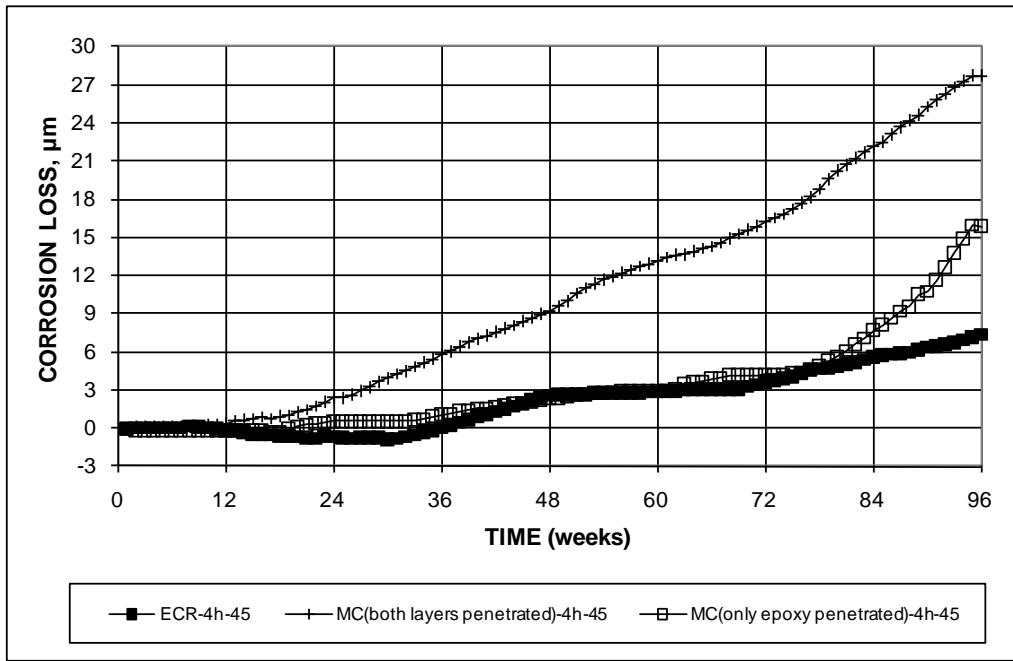
1 μm = 0.0394 mil

Figure 65. Graph. Southern exposure test, corrosion loss based on area exposed at holes through coating for conventional ECR and MC reinforcement with bars containing four holes.

1 μm = 0.0394 mil

Figure 66. Graph. Southern exposure test, corrosion loss based on area exposed at holes through coating for conventional ECR and MC reinforcement with bars containing 10 holes.

The average corrosion potentials for the top and bottom mat are shown in figure 67 and figure 68 for bars with 4 holes and in figure 69 and figure 70 for bars with 10 holes through the epoxy. The top mat corrosion potentials were similar for the cases in which both layers were penetrated and in which only the epoxy was penetrated, differing most widely during the first 10–20 weeks of the tests. For the top mats, the values were more negative than those for conventional ECR until the final 24 weeks of the tests for bars with 4 holes and the final 36 weeks for bars with 10 holes through the epoxy coating. The values for the MC bars ranged between -0.200 and -0.500 V between the beginning of the tests and week 10, stabilizing between -0.500 and -0.600 V after week 20. The autopsy results (described later) show that both the zinc coating and the underlying conventional reinforcement participated in corrosion by the end of the tests.

69
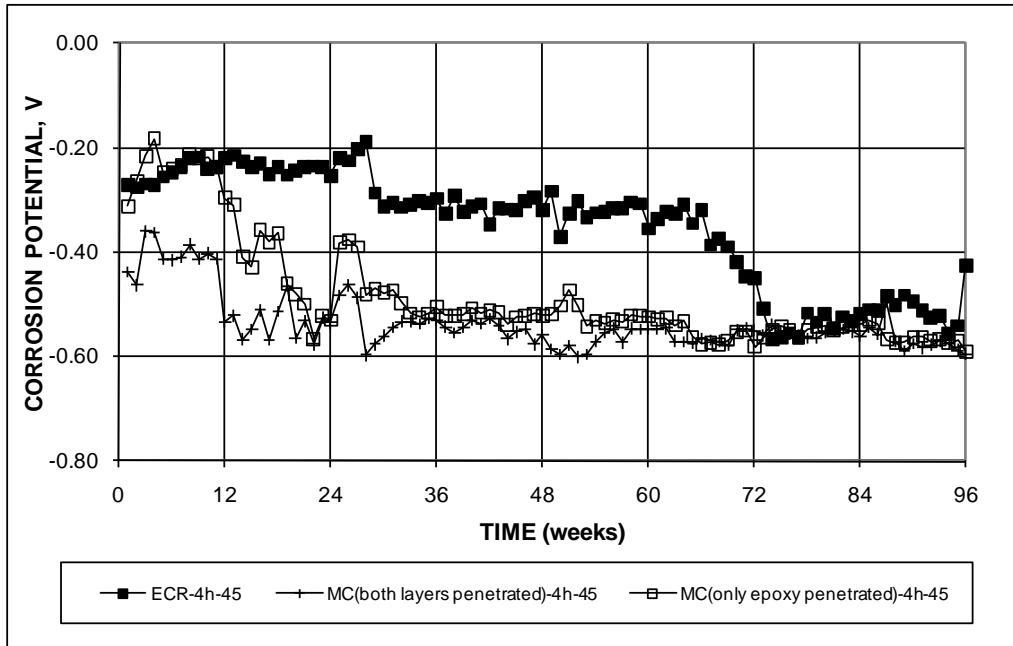
Figure 67. Graph. Southern exposure test, corrosion potential of top mat for conventional ECR and MC reinforcement with bars containing four holes.
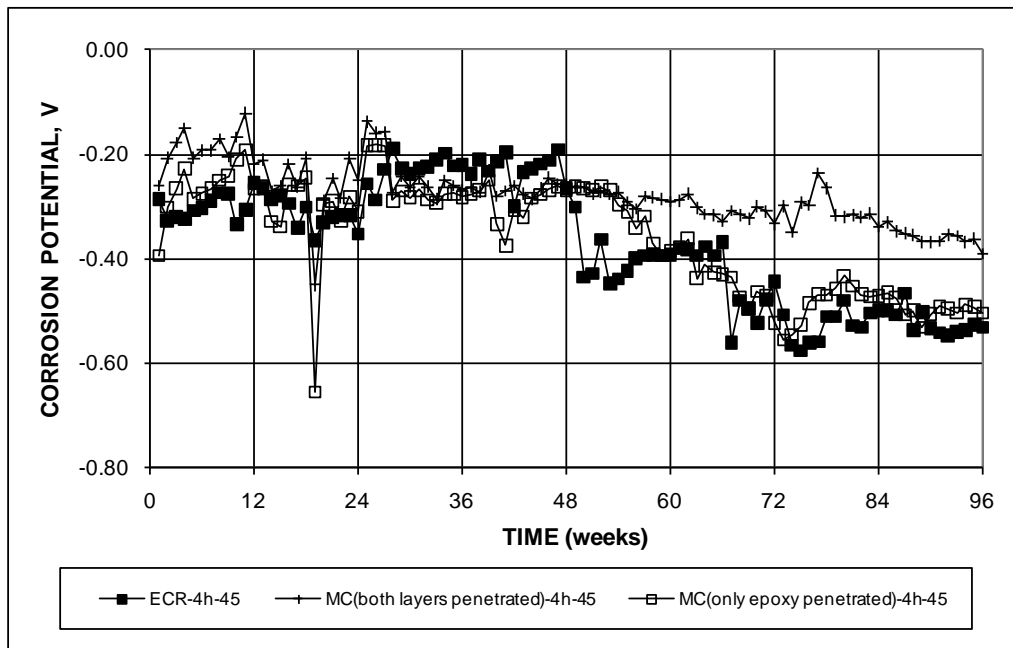
Figure 68. Graph. Southern exposure test, corrosion potential of bottom mat for conventional ECR and MC reinforcement with bars containing four holes.

70
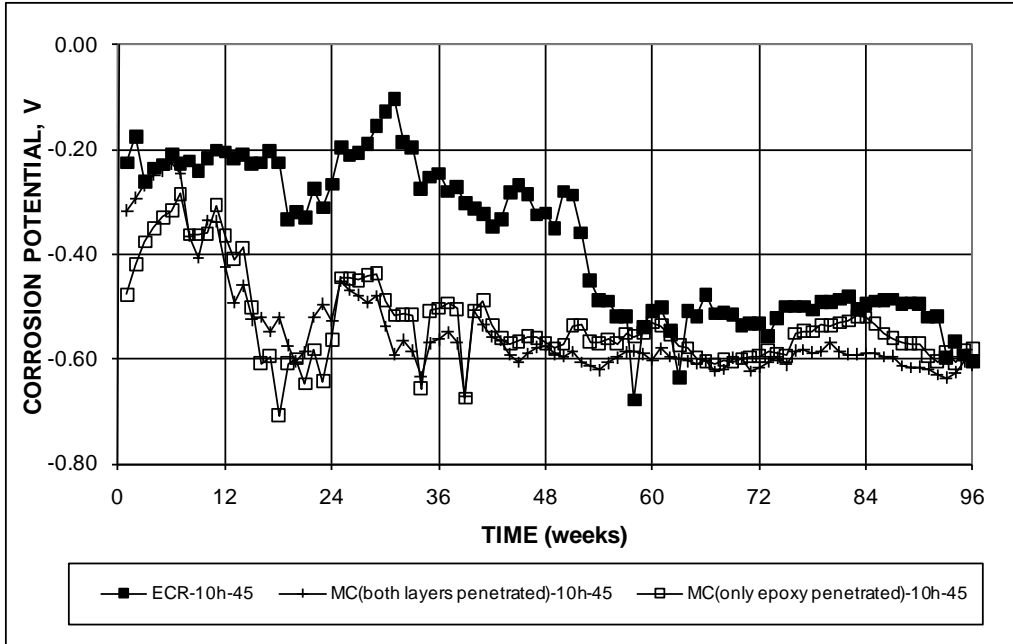
Figure 69. Graph. Southern exposure test, corrosion potential of top mat for conventional ECR and MC reinforcement with bars containing 10 holes.
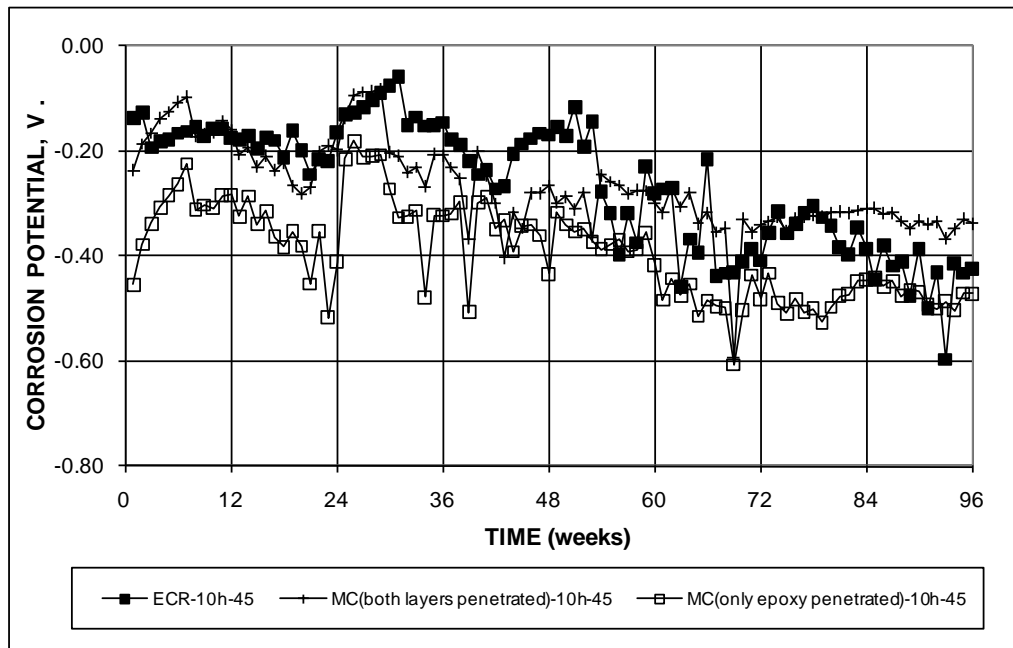
Figure 70. Graph. Southern exposure test, corrosion potential of bottom mat for conventional ECR and MC reinforcement with bars containing 10 holes.

Conventional Steel with Corrosion Inhibitors

Although the corrosion inhibitors used in this study have been evaluated previously, it became clear as the study proceeded that the high level of corrosion protection provided by even damaged epoxy coatings made it difficult to distinguish between the performance of the three inhibitors.[51–56]

71

With that in mind, the inhibitors were evaluated using southern exposure, cracked beam, and corrosion initiation tests containing uncoated conventional reinforcement to gain an improved understanding of their performance using the same test procedures as used to evaluate the multiple corrosion-protection systems in the this study. The properties of the concrete and the results of the southern exposure and corrosion initiation tests are reported here, and the results of the cracked beam tests are reported with the results of the other cracked beam tests.

The properties of the concrete in the corrosion initiation beam specimens are summarized in table 16. The somewhat lower strength exhibited by the concrete containing Rheocrete® 222+, 30.4 MPa (4,410 psi), and the greatly reduced strength of the concrete containing Hycrete™, 14.2 MPa (2,060 psi), compared to the strengths of concrete without a corrosion inhibitor and concrete containing calcium nitrite, 35.8 and 40.0 MPa (5,190 and 5,810 psi), respectively, were also observed in the field test specimens (see table 7).

Table 16. Concrete properties for southern exposure and cracked beam specimens with uncoated bars and corrosion inhibitor in the concrete.

Specimen Designation	Slump, mm	Air Content, percent	Compressive Strength[a], MPa	Standard Deviation, MPa	Coefficient of Variation
Conv.2	55	5.25	35.8	2.35	0.07
Conv.2(DCI)	95	5	40.0	3.65	0.09
Conv.2(RH)	50	4	30.4	4.45	0.15
Conv.2(HY)	90	5.25	14.2	1.93	0.14

1 mm = 0.039 inches
1 MPa = 145 psi
[a] Average of eight cylinders cured in saturated limewater.

The southern exposure tests were performed using the second heat of conventional steel cast in concrete with a w/c ratio of 0.45. Figure 71 compares the corrosion rates of the specimens without a corrosion inhibitor with those with concrete containing Rheocrete® 222+, calcium nitrite, and Hycrete™, designated as specimens Conv.2-45, Conv.2(RH)-45, Conv.2(DCI)-45, and Conv.2(HY)-45, respectively. The specimens without a corrosion inhibitor exhibited the earliest corrosion initiation and highest corrosion rate, which ranged between 8 and 15 µm/year (0.3 and 0.59 mil/year) from week 26 through the end of the test; the only exception occurred at week 34, where the Conv.2(DCI)-45 specimens exhibited a higher corrosion rate. The Conv.2(DCI)-45 specimens exhibited corrosion rates between 3.5 and 9.5 µm/year (0.14 and 0.37 mil/year) after week 33, while the Conv.2(RH)-45 and Conv.2(HY)-45 specimens exhibited respective corrosion rates of 2 to 4 and 0.5 to 2 µm/year (0.08–0.2 and 0.02–0.08 mil/year) between week 33 and the conclusion of the test. The corrosion losses for the specimens are shown in figure 72. At 96 weeks, losses of 14.4, 8.4, 3.4, and 1.4 µm (0.567, 0.33, 0.13, and 0.055 mil) were observed for the Conv.2-45, Conv.2(RH)-45, Conv.2(DCI)-45, and Conv.2(HY)-45 specimens, respectively.
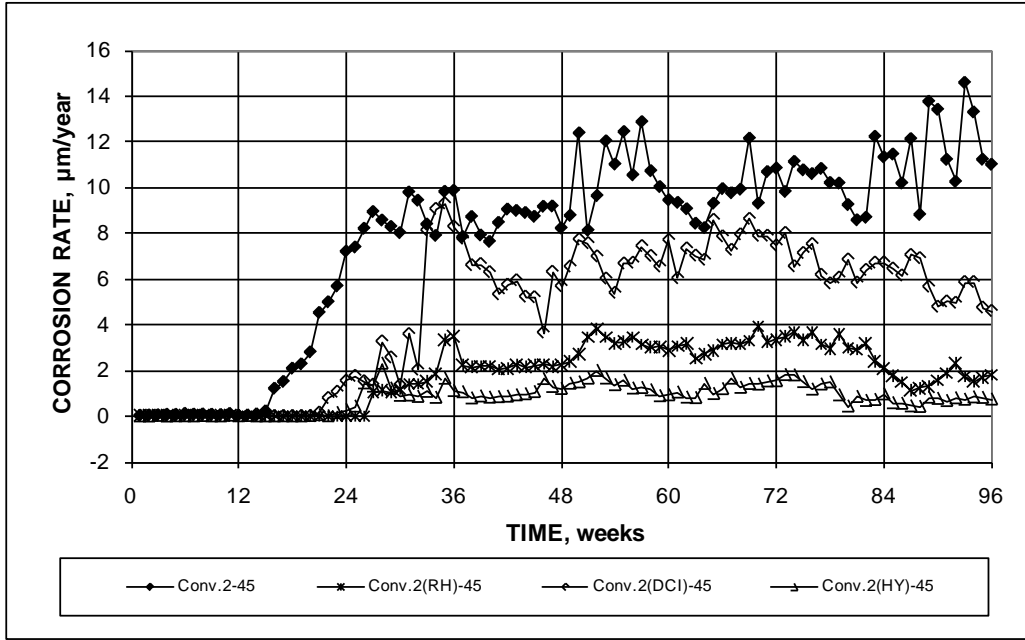
1 µm = 0.0394 mil

Figure 71. Graph. Southern exposure test, average corrosion rates based on total area for conventional reinforcement in specimens without and with corrosion inhibitors.
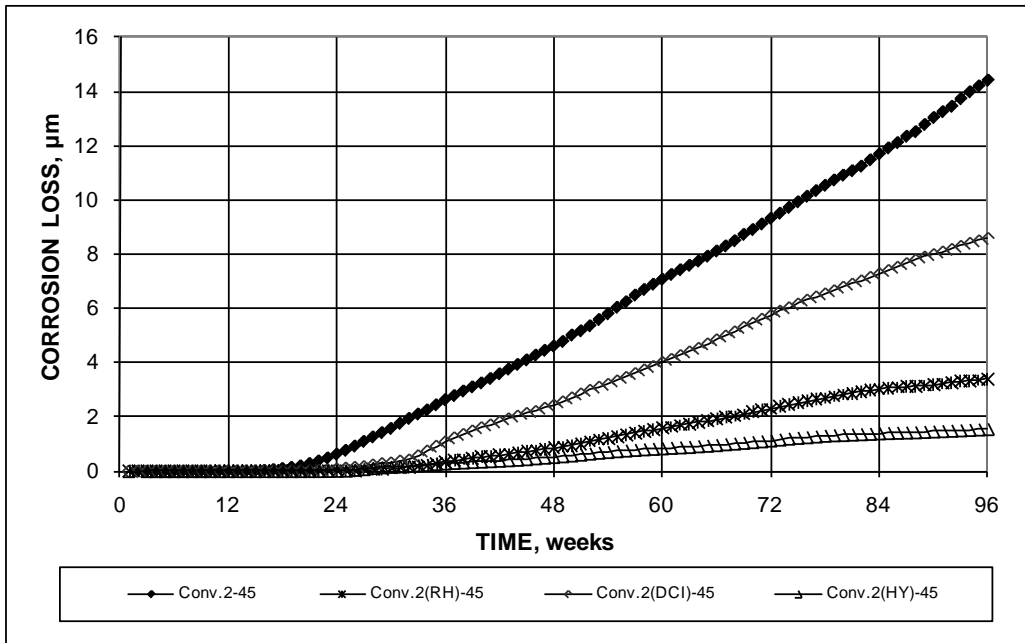
1 µm = 0.0394 mil

Figure 72. Graph. Southern exposure test, average corrosion losses based on total area for conventional reinforcement in specimens without and with corrosion inhibitors.

The average corrosion potentials of the top bars with respect to CSE are shown in figure 73. The initially rising corrosion potentials of the top bars for all four systems indicate increasing passivity through week 14, at which point the specimens without a corrosion inhibitor and those containing calcium nitrite began to exhibit progressively more negative potentials, dropping below a value

of -0.350 V at week 24. The Conv.2(RH)-45 and Conv.2(HY)-45 specimens continued to exhibit increasing passivity until weeks 23 and 26, respectively. The specimens with Rheocrete® and Hycrete™ in the concrete exhibited a negative spike in corrosion potential at week 34, which may be an aberration in the data. The specimens containing Rheocrete® dropped below a corrosion potential of -0.350 V at week 48 and remained there for the balance of the tests. Specimens containing Hycrete™ dropped below a corrosion potential of -0.350 V in week 48, exhibiting corrosion potentials between -0.299 and -0.388 V for the balance of test.
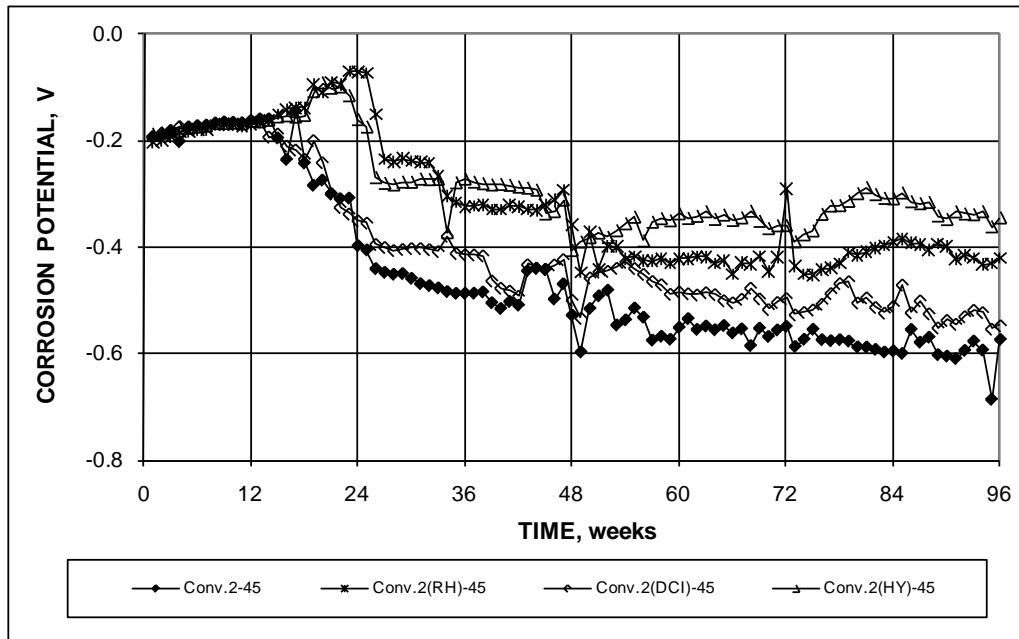
Figure 73. Graph. Southern exposure test, corrosion potential of top mat for conventional reinforcement in specimens without and with corrosion inhibitors.

The resistance between the top and bottom mats of steel, or mat-to-mat resistance, was measured on a weekly basis for all test specimens in this study. For most specimens, mat-to-mat resistance is not included in this report but is presented by Draper et al.[49] It is presented for this group of specimens because it represents a measure of the ion conductivity of the concrete and provides insight into how the inhibitors function.

The mat-to-mat resistance for the southern exposure specimens is presented in figure 74. It is noteworthy that the value of the resistance is nearly identical for the Conv.2-45, Conv.2(RH)-45, and Conv.2(DCI)-45 specimens throughout the test period, beginning at approximately 100 ohms, increasing through week 84 to a peak of approximately 600 ohms (860 ohms for the DCI specimens), and then dropping toward values between 300 and 600 ohms by week 96. In contrast, the specimens containing Hycrete™ exhibited progressively higher resistance throughout the test period, reaching a maximum value of 2,700 ohms at week 90, with values in excess of 1,175 ohms between weeks 78 and 96. The increase in resistivity from the reduction in concrete permeability provided by Hycrete™ played a key role in minimizing the macrocell corrosion measured in this test.

74
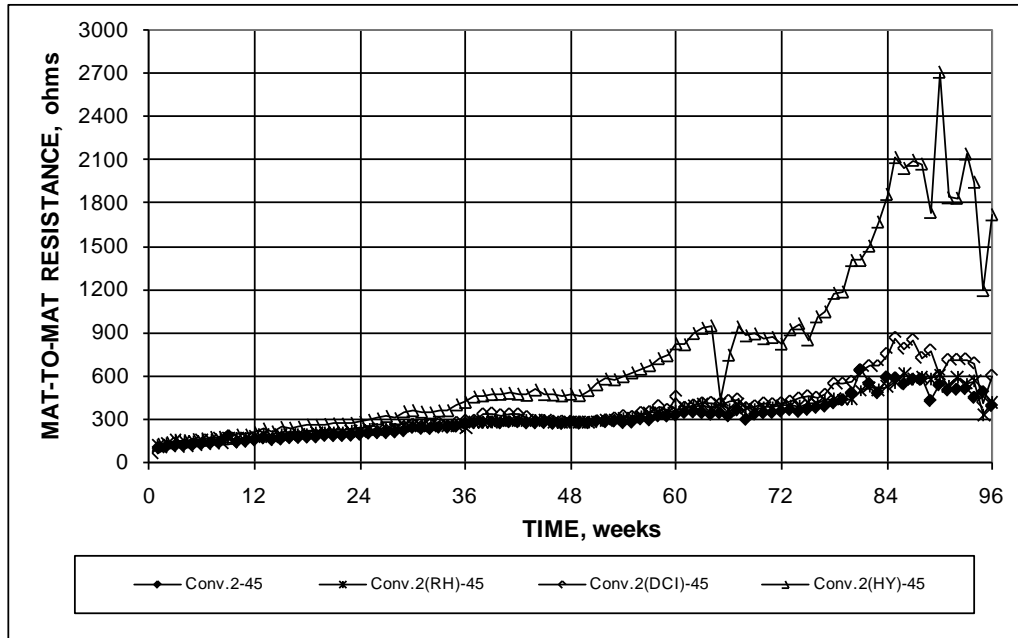
Figure 74. Graph. Southern exposure test, mat-to-mat resistance for conventional reinforcement in specimens without and with corrosion inhibitors.

Corrosion initiation tests are used to obtain a measure of the critical chloride corrosion threshold for corrosion-protection systems. The results of the tests for bare bars cast in concrete containing corrosion inhibitors are summarized in table 17. The initial tests were performed with the first heat of conventional steel (Conv.) in specimens containing Rheocrete®, DCI® S, and Hycrete™. Over the course of those tests, the values for the critical chloride threshold for the specimens containing Hycrete™ were observed to be exceptionally low, averaging 0.43 kg/m^3 (0.72 lb/yd^3), a value below that observed for conventional steel, which typically ranged from 0.60 to 1.20 kg/m^3 (1 to 2 lb/yd^3). To follow up, a second series of specimens was evaluated using Conv.2 steel cast in concrete without and with Hycrete™. The critical chloride corrosion threshold observed in the second series for Hycrete™ (Conv.2(HY)), 0.51 kg/m^3 (0.86 lb/yd^3), closely matches the value in the initial series. In addition to corrosion thresholds, table 17 shows the individual and average values of time to initiation and the corrosion rate and corrosion potential during the week in which corrosion was initially observed, along with the standard deviations for corrosion threshold. The values of standard deviation and coefficient of variation for each specimen represent the variation observed for individual samples within the specimen. The values of standard deviation and coefficient of variation for each group of specimens were calculated based on the individual specimen averages. This is why the coefficient of variation is consistently greater for the individual samples than for each group of samples.

Table 17. Corrosion initiation results for bare bars in concrete without and with corrosion inhibitors (values at time of initiation).

Specimen[a]	Time to Initiation, weeks	Rate, µm/year	Potential[a], V	Average[b], kg/m³	Standard Deviation, kg/m³
Conv.2-1	16	1.50	-0.383	1.23	1.09
Conv.2-2	16	0.404	-0.339	0.88	0.67
Conv.2-3	28	0.922	-0.300	0.42	0.80
Conv.2-4	16	0.869	-0.309	1.45	1.44
Conv.2-5	–	–	–	–	–
Conv.2-6	23	0.389	-0.229	0.54	0.41
Average	**19.8**			**0.90**	**0.44**
Conv.(DCI)-1	43	0.945	-0.337	2.05	0.56
Conv.(DCI)-2	31	0.297	-0.293	1.59	0.40
Conv.(DCI)-3	20	1.166	-0.344	1.39	0.65
Conv.(DCI)-4	23	0.815	-0.331	1.63	0.33
Conv.(DCI)-5	25	0.511	-0.362	2.10	0.66
Conv.(DCI)-6	17	1.684	-0.376	1.19	0.38
Average	**26.5**			**1.66**	**0.36**
Conv.(RH)-1	16	0.320	-0.301	1.27	0.65
Conv.(RH)-2	14	2.614	-0.421	0.57	0.39
Conv.(RH)-3	20	0.853	-0.357	0.94	0.41
Conv.(RH)-4	21	0.800	-0.397	1.23	0.54
Conv.(RH)-5	26	0.953	-0.404	2.13	1.04
Conv.(RH)-6	20	0.979	-0.457	1.77	0.79
Average	**19.5**			**1.32**	**0.56**
Conv.(HY)-1	16	0.549	-0.320	0.33	0.26
Conv.(HY)-2	26	1.349	-0.391	0.24	0.08
Conv.(HY)-3	48	0.343	-0.314	0.54	0.74
Conv.(HY)-4	12	0.549	-0.348	0.41	0.30
Conv.(HY)-5	52	1.158	-0.344	0.71	0.50
Conv.(HY)-6	17	0.457	-0.299	0.37	0.32
Average	**28.5**			**0.43**	**0.17**
Conv.2(HY)-1	58	0.137	-0.218	0.67	0.43
Conv.2(HY)-2	–	–	–	–	–
Conv.2(HY)-3	68	0.899	-0.21	0.47	0.35
Conv.2(HY)-4	24	0.823	-0.294	0.34	0.25
Conv.2(HY)-5	42	2.87	-0.222	0.25	0.21
Conv.2(HY)-6	50	3.76	-0.362	0.69	0.33
Average	**48.4**			**0.51**	**0.31**

1 µm = 0.0394 mil
1 kg/m³ =1.69 lb/yd³
– Initiation was missed.
[a] With respect to an SCE.
[b] Individual specimen averages and standard deviations based on 20 samples per specimen. Overall averages and standard deviations based on specimen averages.

The specimens containing Hycrete™ exhibited the longest time to initiation, 28.5 and 48.4 weeks for the Conv.(HY) and Conv.2(HY) specimens, respectively, followed by the Conv.(DCI), Conv.(RH), and Conv.2 specimens at 26.5, 19.5, and 19.8 weeks, respectively. The conventional steel specimens exhibited an average critical chloride corrosion threshold of 0.90 kg/m^3 (1.52 lb/yd^3), matching earlier results at the University of Kansas using similar specimens but different heats of conventional steel.[50] The specimens containing Rheocrete® and DCI® S exhibited critical corrosion thresholds of 1.32 and 1.66 kg/m^3 (2.22 and 2.80 lb/yd^3), respectively.

To explain the very low corrosion threshold for the conventional steel in concrete containing Hycrete™, O'Reilly et al. used a pore press to extract pore solution from cement paste specimens without inhibitors and with each of the inhibitors used in this study.[44] As described in chapter 2, they observed a marked increase in sulfate content at both 1 and 7 days for cement pastes containing Hycrete™ and at 7 days for pastes containing Rheocrete®. Along with chlorides, sulfates can reduce the passivity of reinforcing steel and may explain the very low critical chloride corrosion threshold for Hycrete™ and the observation that Rheocrete® produces a corrosion threshold below that provided by calcium nitrite.[57]

Cracked Beam Tests

The performance of the corrosion-protection systems in the cracked beam tests is presented in this section. The losses at 96 weeks based on total and exposed area on the ECR bars are summarized in table 18 and table 19. The average corrosion rates after corrosion initiation are summarized in table 20. Unlike the corrosion rates for the southern exposure specimens shown in table 15, corrosion was observed for all but one specimen, specimen 1 for ECR(HY)-45 with 10 holes through the epoxy.

Table 18. Corrosion loss at 96 weeks (μm) for cracked beam specimens based on total area.

Steel Designation[a]	Specimen						Average	Standard Deviation
	1	2	3	4	5	6		
Controls								
Conv.-45	17.56	8.53	7.29	15.40	15.16	14.46	13.06	4.15
Conv.2-45	44.39	22.74	22.62				29.92	12.54
Conv.-35	11.48	6.02	7.51				8.34	2.82
ECR-4h-45	0.04	0.07	0.02	0.07	0.04	0.01	0.04	0.02
ECR-10h-45	0.026	0.083	0.032				0.047	0.031
ECR-10h-35	0.132	0.124	0.162				0.139	0.020
Epoxies with increased adhesion								
ECR(Chromate)-4h-45	0.066	0.058	0.099				0.074	0.022
ECR(Chromate)-10h-45	0.026	0.140	0.480				0.216	0.236
ECR(DuPont)-4h-45	0.124	0.137	0.054				0.105	0.045
ECR(DuPont)-10h-45	0.128	0.127	0.297				0.184	0.098
ECR(Valspar)-4h-45	0.172	0.071	0.009				0.084	0.082
ECR(Valspar)-10h-45	0.081	0.039	0.254				0.125	0.114
Corrosion inhibitors in concrete								
Conv.2(DCI)-45	32.09	26.39	21.56				26.68	5.273
Conv.2(RH)-45	24.58	18.26	22.63				21.82	3.236
Conv.2(HY)-45	8.635	6.314	7.845				7.60	1.180
ECR(DCI)-4h-45	0.025	0.048	0.007				0.026	0.021
ECR(DCI)-10h-45	0.044	0.155	0.039				0.079	0.065
ECR(DCI)-10h-35	0.124	0.095	0.449				0.223	0.197
ECR(RH)-4h-45	0.062	0.314	0.047				0.141	0.150
ECR(RH)-10h-45	0.240	0.134	0.138				0.171	0.060
ECR(RH)-10h-35	0.096	0.302	0.136				0.178	0.109
ECR(HY)-4h-45	0.010	0.005	0.092				0.036	0.049
ECR(HY)-10h-45	0.002	0.116	0.062				0.060	0.057
ECR(HY)-10h-35	0.144	0.159	0.278				0.194	0.073
ECR(primer/$Ca(NO_2)_2$)-4h-45	0.016	0.008	0.028				0.017	0.010
ECR(primer/$Ca(NO_2)_2$)-10h-45	0.152	0.059	0.084				0.098	0.048
ECR(primer/$Ca(NO_2)_2$)-10h-35	0.416	0.315	0.589				0.440	0.139
Bars with multiple coatings								
MC(both layers penetrated)-4h-45	0.489	0.262	0.379				0.377	0.114
MC(both layers penetrated)-10h-45	0.214	1.269	0.532				0.672	0.541
MC(only epoxy penetrated)-4h-45	0.141	0.161	0.581				0.294	0.248
MC(only epoxy penetrated)-10h-45	0.159	0.106	0.398				0.221	0.156

1 μm = 0.0394 mil
Blank cells indicate no specimen tested.
[a] See table 1 for abbreviation definitions. 4h = bar with four holes through epoxy, 10h = bar with 10 holes through epoxy. 35 = concrete with w/c = 0.35, 45 = concrete with w/c = 0.45.

Table 19. Corrosion loss at 96 weeks (μm) for cracked beam specimens based on area exposed at holes through coating.

Steel Designation[a]	Specimen						Average	Standard Deviation
	1	2	3	4	5	6		
Controls								
ECR-4h-45	17.0	34.1	8.0	33.1	20.3	7.0	19.9	11.8
ECR-10h-45	5.0	16.0	6.1				9.0	6.0
ECR-10h-35	25.3	23.8	31.1				26.7	3.8
Epoxies with increased adhesion								
ECR(Chromate)-4h-45	31.5	28.0	47.5				35.7	10.4
ECR(Chromate)-10h-45	5.0	26.9	92.3				41.4	45.4
ECR(DuPont)-4h-45	59.4	66.0	26.0				50.4	21.4
ECR(DuPont)-10h-45	24.6	24.4	57.0				35.3	18.8
ECR(Valspar)-4h-45	82.6	34.2	4.3				40.4	39.5
ECR(Valspar)-10h-45	15.6	7.5	48.8				24.0	21.9
Corrosion inhibitors in concrete								
ECR(DCI)-4h-45	12.1	22.9	3.2				12.7	9.9
ECR(DCI)-10h-45	8.4	29.8	7.6				15.3	12.6
ECR(DCI)-10h-35	23.8	18.2	86.3				42.8	37.8
ECR(RH)-4h-45	29.6	150.6	22.5				67.6	72.0
ECR(RH)-10h-45	46.1	25.7	26.6				32.8	11.6
ECR(RH)-10h-35	18.5	58.0	26.2				34.3	20.9
ECR(HY)-4h-45	4.8	2.4	44.0				17.1	23.4
ECR(HY)-10h-45	0.3	22.4	12.0				11.6	11.0
ECR(HY)-10h-35	27.7	30.6	53.4				37.2	14.1
ECR(primer/Ca(NO$_2$)$_2$)-4h-45	7.8	3.8	13.2				8.3	4.7
ECR(primer/Ca(NO$_2$)$_2$)-10h-45	29.2	11.4	16.1				18.9	9.2
ECR(primer/Ca(NO$_2$)$_2$)-10h-35	79.9	60.5	113.2				84.5	26.6
Bars with multiple coatings								
MC(both layers penetrated)-4h-45	234.9	125.8	182.1				181.0	54.6
MC(both layers penetrated)-10h-45	41.1	243.7	102.1				129.0	104.0
MC(only epoxy penetrated)-4h-45	64.9	76.0	278.8				139.9	120.4
MC(only epoxy penetrated)-10h-45	30.5	20.7	76.4				42.5	29.7

1 μm = 0.0394 mil

Blank cells indicate no specimen tested.

[a] See table 1 for abbreviation definitions. 4h = bar with four holes through epoxy, 10h = bar with 10 holes through epoxy. 35 = concrete with w/c = 0.35, 45 = concrete with w/c = 0.45.

Table 20. Average corrosion rate (µm/year) based on losses after corrosion initiation for cracked beam specimens.

Bars Without Coatings—Corrosion Rate Based on Total Area								
Steel Designation[a]	Specimen						Average	Standard Deviation
	1	2	3	4	5	6		
Controls								
Conv.-45	9.42	4.50	3.82	8.32	8.18	7.74	7.00	2.27
Conv.2-45	24.6	12.2	12.1				16.3	7.16
Conv.-35	7.72	5.05	6.34				6.37	1.34
Corrosion inhibitors in concrete								
Conv.2(DCI)-45	17.5	14.4	11.6				14.5	2.96
Conv.2(RH)-45	13.6	9.80	12.4				11.9	1.96
Conv.2(HY)-45	4.91	3.44	4.16				4.17	0.74
Bars With Coatings—Corrosion Rate Based on Exposed Area								
Steel Designation	4 holes			10 holes			Average	Standard Deviation
	1	2	3	1	2	3		
Controls								
ECR-45	8.57	18.3	2.63	2.29	9.20	3.69	8.07	5.86
	13.8[c]	12.2[c]	1.99[c]					
ECR-35	11.8	12.4	16.9				13.7	2.79
Epoxies with increased adhesion								
ECR(Chromate)-45	14.1	11.9	29.1	2.37	14.3	50.4	20.4	17.0
ECR(DuPont)-45	33.5	48.5	14.5	13.2	14.7	31.1	25.9	14.2
ECR(Valspar)-45	41.1	16.9	0.770	8.28	4.62	26.6	16.4	15.3
Corrosion inhibitors in concrete								
ECR(DCI)-45	6.19	18.9	16.6	4.58	16.7	4.10	11.2	6.90
ECR(DCI)-35				13.1	27.6	47.2	29.3	17.1
ECR(RH)-45	12.7	15.3	17.8	27.1	14.2	15.1	17.0	5.21
ECR(RH)-35				10.1	31.7	14.3	18.7	11.45
ECR(HY)-45	1.87	6.98	25.5	[b]	13.3	6.37	10.8	9.18
ECR(HY)-35				15.1	17.7	30.9	21.2	8.47
ECR(primer/Ca(NO$_2$)$_2$)-45	2.38	13.5	5.74	15.6	6.02	9.19	8.73	5.03
ECR(primer/Ca(NO$_2$)$_2$)-35				43.6	32.9	61.6	46.0	14.5
Bars with multiple coatings								
MC	36.8[d]	44.7[d]	169[d]	16.2[d]	10.5[d]	39.7[d]	68.6	51.9
	129[e]	68.7[e]	98.7[e]	21.8[e]	132[e]	55.5[e]		

1 µm = 0.0394 mil

Blank cells indicate no specimen tested.

[a] See table 1 for abbreviation definitions. 35 = concrete with w/c = 0.35, 45 = concrete with w/c = 0.45.

[b] No corrosion observed.

[c] Specimens 4, 5, and 6.

[d] Both layers penetrated.

[e] Only epoxy penetrated.

Control Specimens

The average corrosion rates and corrosion losses based on the total area of the reinforcing bars are shown in figure 75 and figure 76, respectively, for cracked beam specimens with conventional reinforcing steel and conventional ECR steel. The specimens with ECR have 4 or 10 holes through the epoxy for the concrete with a w/c ratio of 0.45 and 10 holes through the epoxy for concrete with a w/c ratio of 0.35. Because the simulated crack provides direct access to the top reinforcing bars for the 15 percent sodium chloride solution, significant corrosion rates, on the order of 10 μm/year (0.4 mil/year), were observed early in the test for specimens containing conventional steel at both w/c ratios. Throughout the test period, the lower w/c ratio appears to have provided some protection, likely the result of lower concrete permeability, which reduces access of oxygen and moisture to the cathode. At both w/c ratios, however, the corrosion rate is significant, with average rates on the order of 6 to 9 μm/year (0.2 to 0.4 mil/year) for specimens with w/c of 0.45 and 2 to 8 μm/year (0.08 to 0.3 mil/year) after week 10 for specimens with w/c of 0.35. The corrosion rates decreased from the high initial values as a result of the accumulation of corrosion products within the crack. The average macrocell corrosion rates shown in table 20 are 7.00 and 6.37 μm/year (0.276 and 0.251 mil/year) for the Conv.-45 and Conv.-35 specimens, respectively.
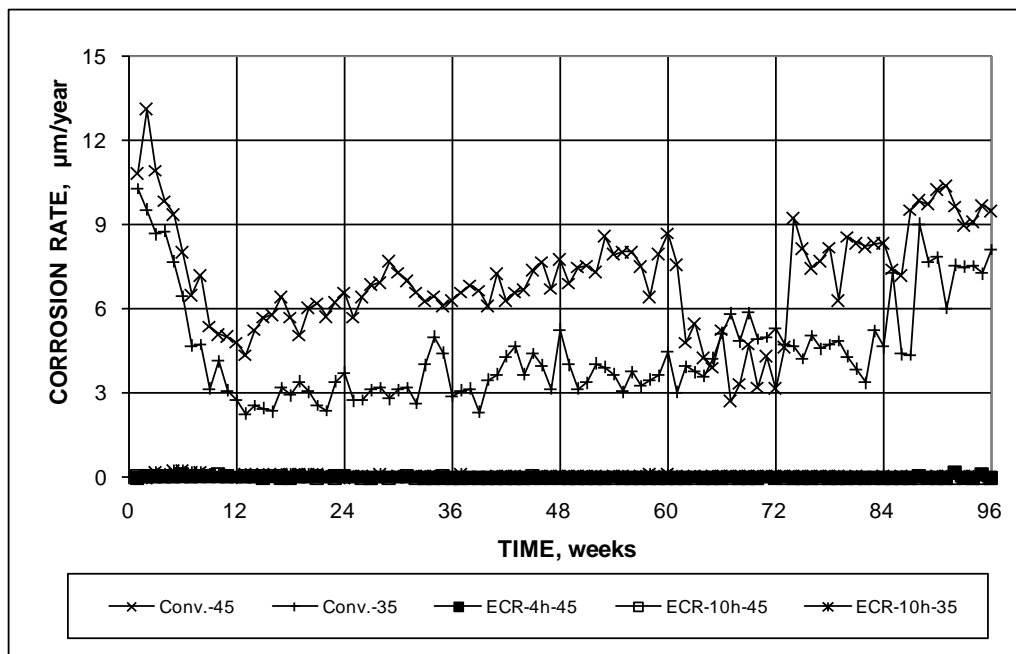
1 μm = 0.0394 mil

Figure 75. Graph. Cracked beam test, average corrosion rates based on total area of control specimens for conventional reinforcement and ECR.
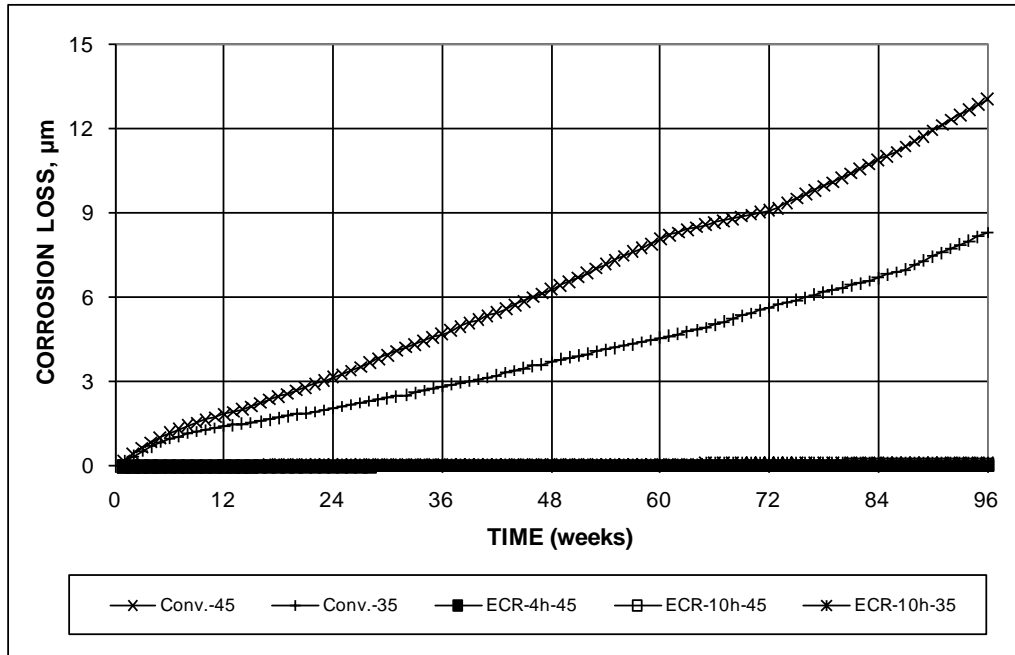
1 µm = 0.0394 mil

Figure 76. Graph. Cracked beam test, average corrosion loss based on total area of control specimens for conventional reinforcement and ECR.

Occasionally, individual specimens exhibited large increases in corrosion rate. This increase was due to the accumulated corrosion products exerting enough stress on the concrete to widen the crack, again providing direct access of the sodium chloride solution to the top reinforcing bar. Corrosion rates increased somewhat during the last 12 weeks of the tests for specimens with both w/c ratios. Figure 76 and table 18 show that the average corrosion losses were 13.1 and 8.3 µm (0.516 and 0.33 mil) at the end of the 96-week test. These values are below the nominal value of 25 µm (0.98 mil) required to crack concrete. However, by the end of the test, a number of specimens produced a high enough quantity of corrosion products to cause severe cracking, as shown in figure 77, which also allowed the sodium chloride solution to reach the lower bars. The observed cracking was likely due to nonuniformity in deposition of the corrosion products, which is evident in the section describing the autopsy of the bench-scale specimens. Overall, figure 75, figure 76, and table 20 indicate a small advantage for a lower w/c ratio for cracked concrete and a significant reduction in corrosion loss provided by epoxy coating.
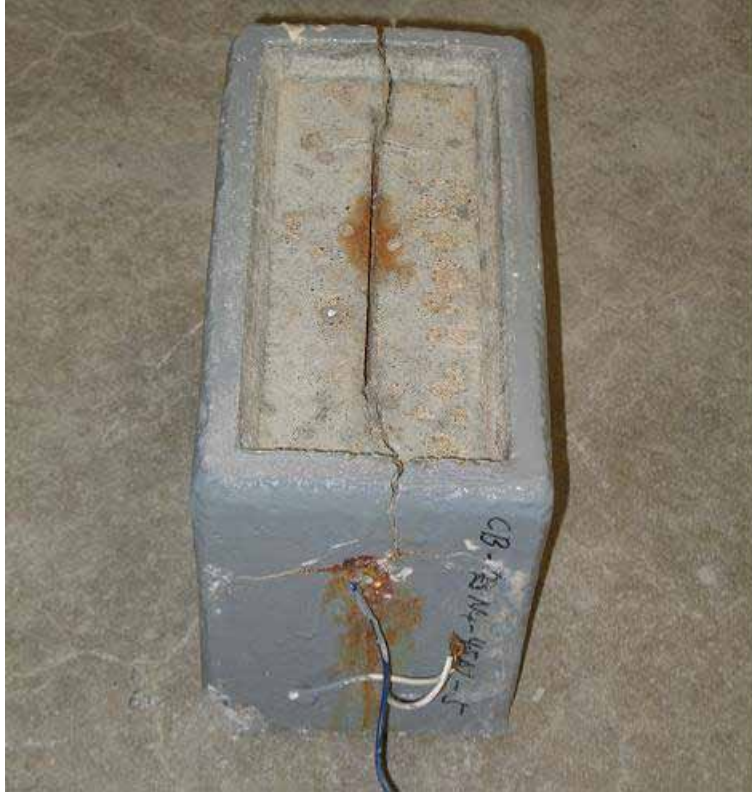
Figure 77. Photo. Cracked beam specimen containing conventional reinforcing steel at end of 96-week test.

Corrosion losses as a function of exposed area are plotted versus time for the ECR specimens in figure 78. The bars with 10 holes through the epoxy cast in concrete with w/c of 0.35 (ECR-10h-35) exhibited two to three times the losses of the same bars cast in concrete with w/c of 0.45 (ECR-10h-45). The bars with four holes through the epoxy in concrete with w/c of 0.45 (ECR-4h-45) exhibited corrosion losses between those for the two other specimen types. The results represent the average of six specimens for ECR-4h-45 and three specimens for the others. For the epoxy-coated bars, there does not appear to be an advantage based on a reduced w/c ratio. The corrosion losses for the ECR bars based on exposed area are 1 to 4 times the average values observed for the uncoated conventional bars.

83
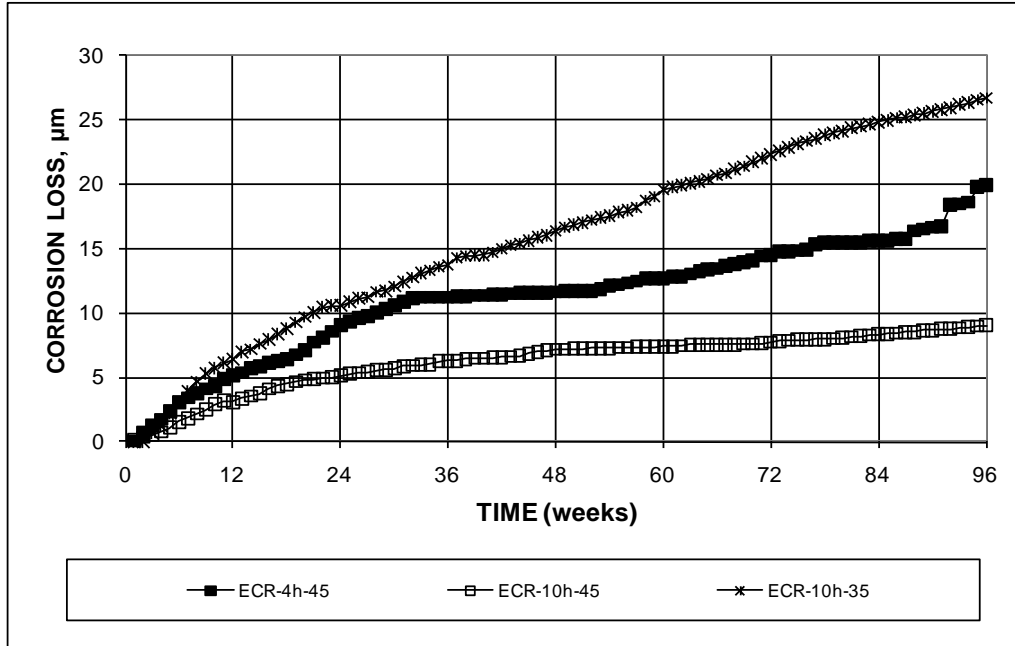
1 μm = 0.0394 mil

**Figure 78. Graph. Cracked beam test, average corrosion loss based on area exposed
at holes through coating for ECR.**

Epoxies with Improved Adhesion

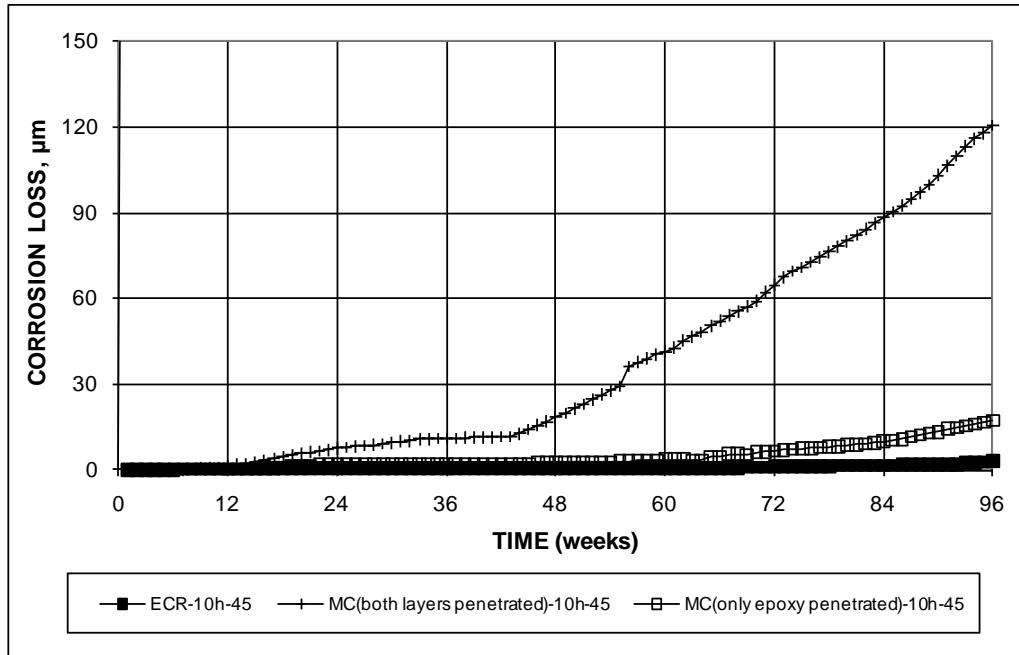The total corrosion losses based on exposed area for the bars coated with the improved adhesion epoxies are compared with losses for conventional ECR in figure 79 and figure 80 for bars with 4 and 10 holes, respectively. As observed in the southern exposure tests, these results indicate that the improved adhesion epoxies provided no advantage with respect to conventional ECR under severe exposure conditions. In fact, the corrosion losses for bars with improved adhesion epoxies were at least 1.7 times those for bars with conventional epoxy for both 4 holes (35.4 to 50.4 μm (1.39 to 1.98 mil) versus 19.9 μm (0.783 mil)) and 10 holes (24.0 to 41.4 μm (0.945 to 1.63 mil) versus 9 μm (0.4 mil)).
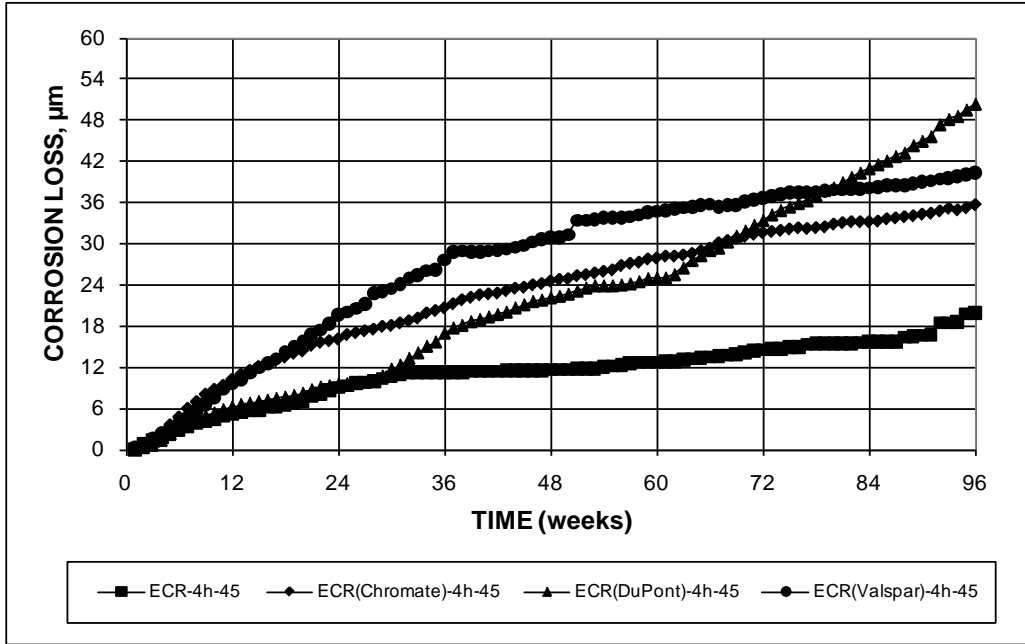
1 µm = 0.0394 mil

Figure 79. Graph. Cracked beam test, average corrosion loss based on area exposed at holes through coating for conventional ECR and increased-adhesion ECR with bars containing four holes.
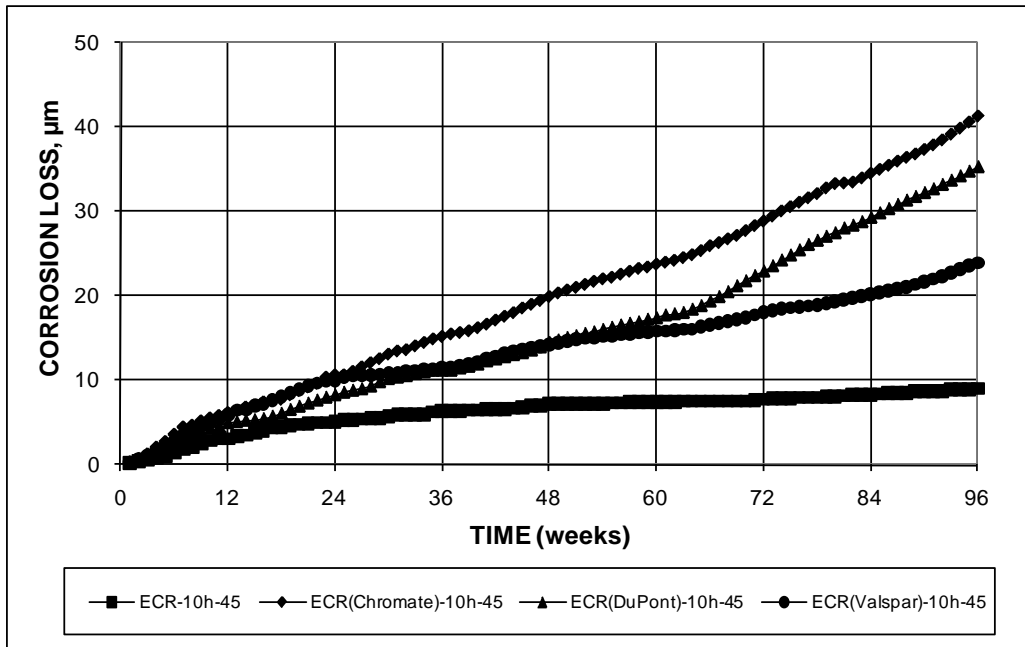

1 µm = 0.0394 mil

Figure 80. Graph. Cracked beam test, average corrosion loss based on area exposed at holes through coating for conventional ECR and increased-adhesion ECR with bars containing 10 holes.

ECR Used in Conjunction with Corrosion Inhibitors

Corrosion losses for cracked beam specimens with conventional ECR cast in concrete with corrosion inhibitors or for ECR bars with primer containing microencapsulated calcium nitrate are shown in figure 81 and figure 82 for specimens with 4 and 10 holes through the epoxy on bars cast in concrete with w/c of 0.45 and in figure 83 for with 10 holes through the epoxy cast in concrete with w/c of 0.35. Unlike the results for intact concrete in the southern exposure test, the presence of a corrosion inhibitor did not provide an advantage in severely cracked concrete as represented by the cracked beam specimen, where chlorides have direct access to the reinforcing steel. Except for ECR (DCI)-4h-45 and ECR (primer/Ca(NO$_2$)$_2$)-4h-45, the corrosion losses are the same or greater for the specimens with a corrosion inhibitor in the concrete or in a primer below the coating than for the conventional ECR specimens.
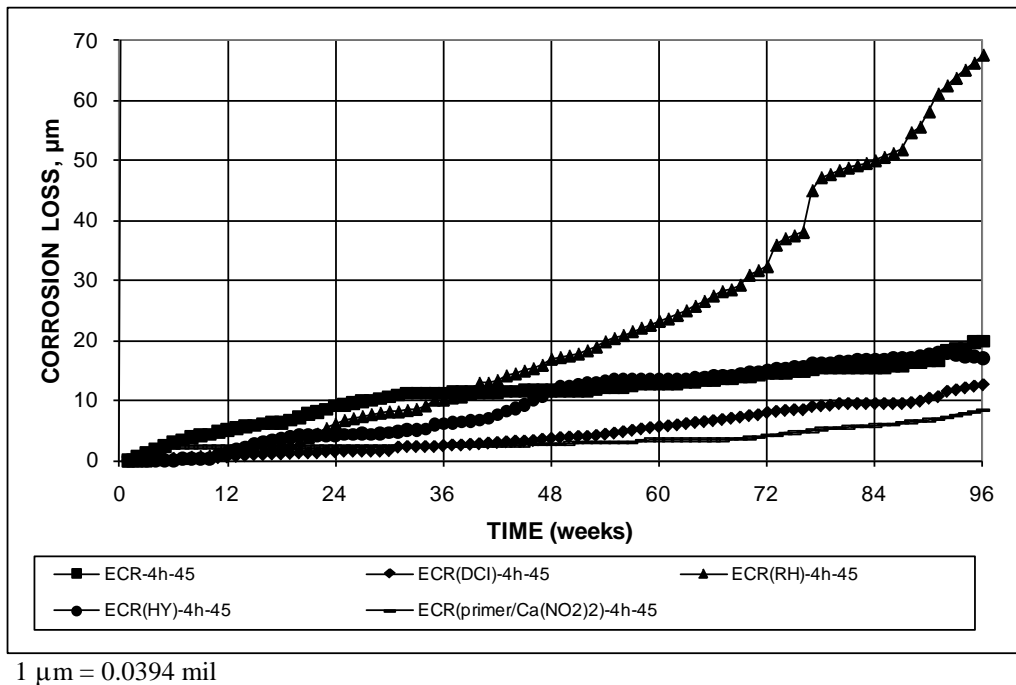
1 μm = 0.0394 mil

Figure 81. Graph. Cracked beam test, average corrosion loss based on area exposed at holes through coating for conventional ECR with and without corrosion inhibitors with bars containing four holes and concrete with w/c = 0.45.
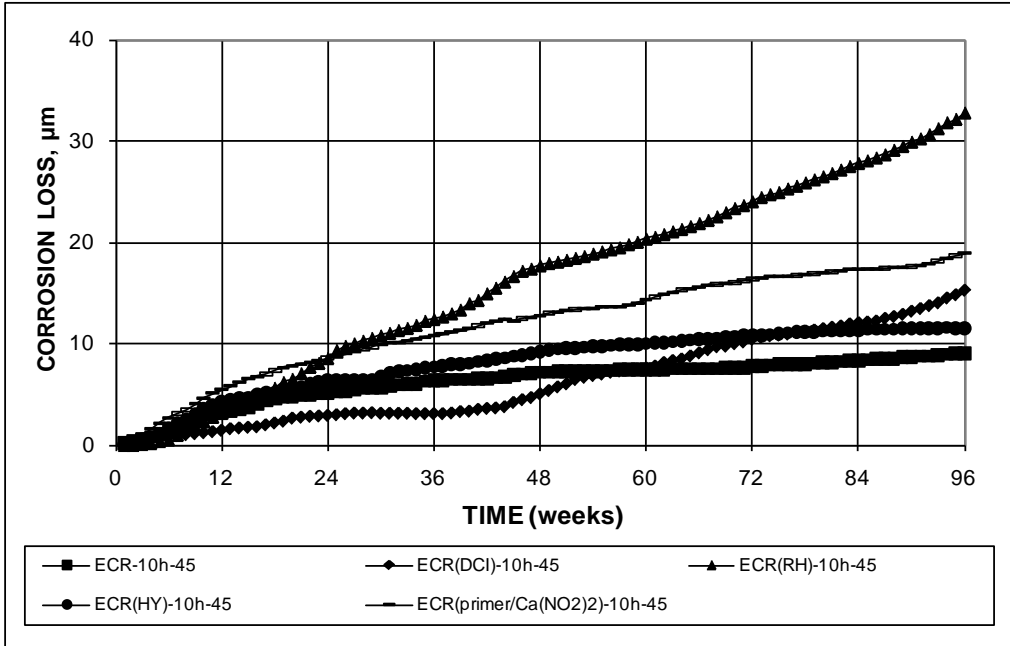
1 µm = 0.0394 mil

Figure 82. Graph. Cracked beam test, average corrosion loss based on area exposed at holes through coating for conventional ECR with and without corrosion inhibitors with bars containing 10 holes and concrete with w/c = 0.45.
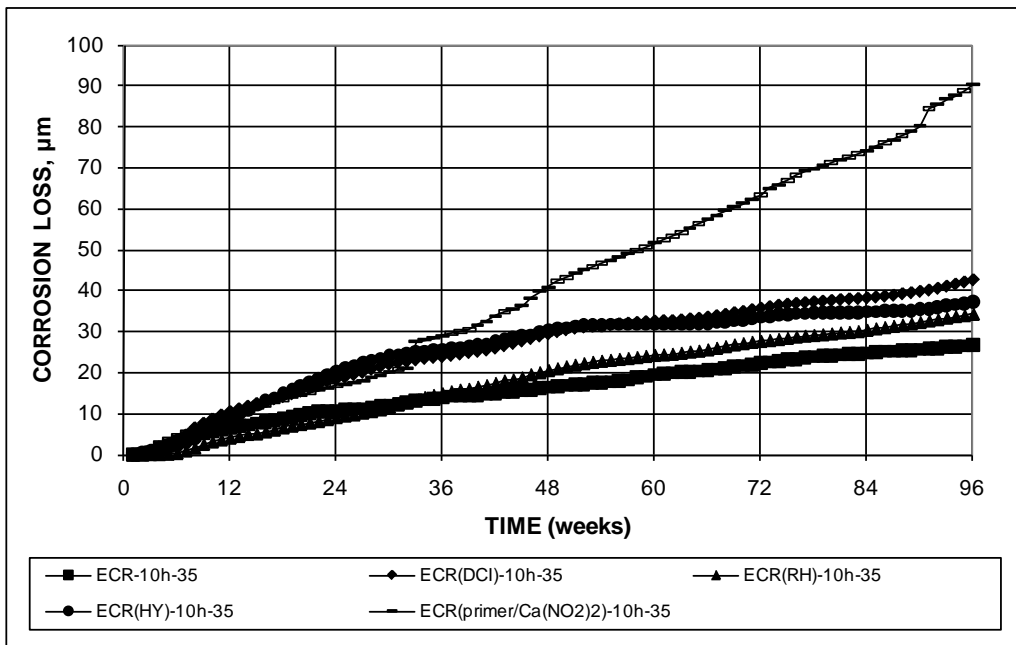
1 µm = 0.0394 mil

Figure 83. Graph. Cracked beam test, average corrosion loss based on area exposed at holes through coating for conventional ECR with and without corrosion inhibitors with bars containing 10 holes and concrete with w/c = 0.35.

87

Bars with Multiple Coatings

The corrosion losses for the bars with multiple coatings are compared with those for conventional ECR in figure 84 and figure 85 for bars with 4 and 10 holes through the coatings, respectively. Both figures show that the highest corrosion losses were attained by the MC bars with both layers penetrated followed by those with only the epoxy layer penetrated and then by conventional ECR. For the specimens with four holes in the epoxy coating, the respective average losses based on exposed area were 181, 140, and 20 μm (7.13, 5.51, and 0.79 mil) at the conclusion of tests. For the specimens with 10 holes, the respective values were 129, 43, and 9 μm (5.08, 1.7, and 0.4 mil) at the conclusion of tests. Corrosion losses less than 50 μm (2 mil), the thickness of the zinc coating, exhibited by the MC(only epoxy penetrated)-10h-45 specimens may indicate that the coating was not penetrated. However, as observed for the rapid macrocell specimens, the values shown do not reflect the effects of microcell corrosion, which increases metal loss. Losses greater than 50 μm (2 mil) indicate that the zinc was penetrated, which was demonstrated when the bars were autopsied, as discussed later in this chapter.
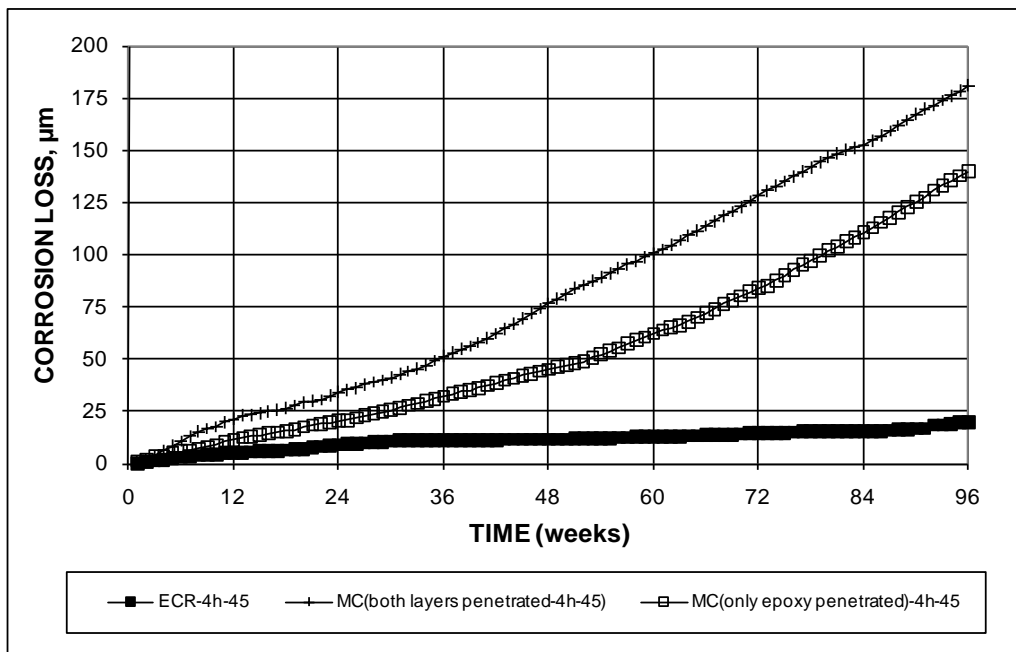
1 μm = 0.0394 mil

Figure 84. Graph. Cracked beam test, average corrosion loss based on area exposed at holes through coating for conventional ECR and MC reinforcement with bars containing four holes.
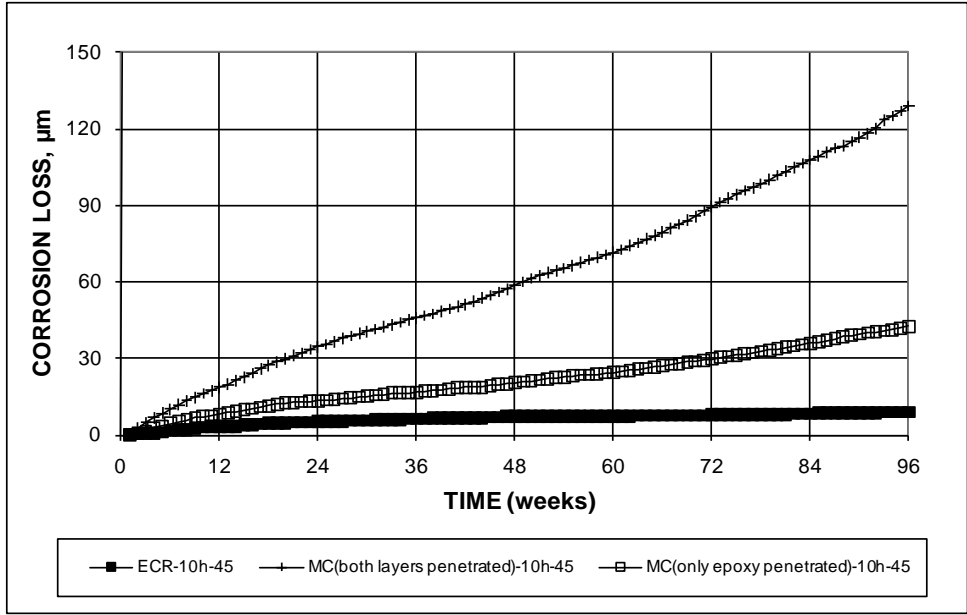
Figure 85. Graph. Cracked beam test, average corrosion loss based on area exposed at holes through coating for conventional ECR and MC reinforcement with bars containing 10 holes.

The corrosion potentials for the specimens are shown in figure 86 and figure 87 for bars with 4 holes and in figure 88 and figure 89 for bars with 10 holes. For both the MC and ECR bars, the top bars reached a potential of about -0.600 V and sustained that value throughout the test period while the corrosion potential of the bottom bars remained between -0.200 and -0.400 V for most of the test for the MC specimens with 4 holes through the epoxy and between -0.200 and -0.450 V for the MC specimens with 10 holes through the epoxy. The corrosion potential of the ECR specimens remain between -200 and -400 V for specimens with both 4 and 10 holes through the epoxy.
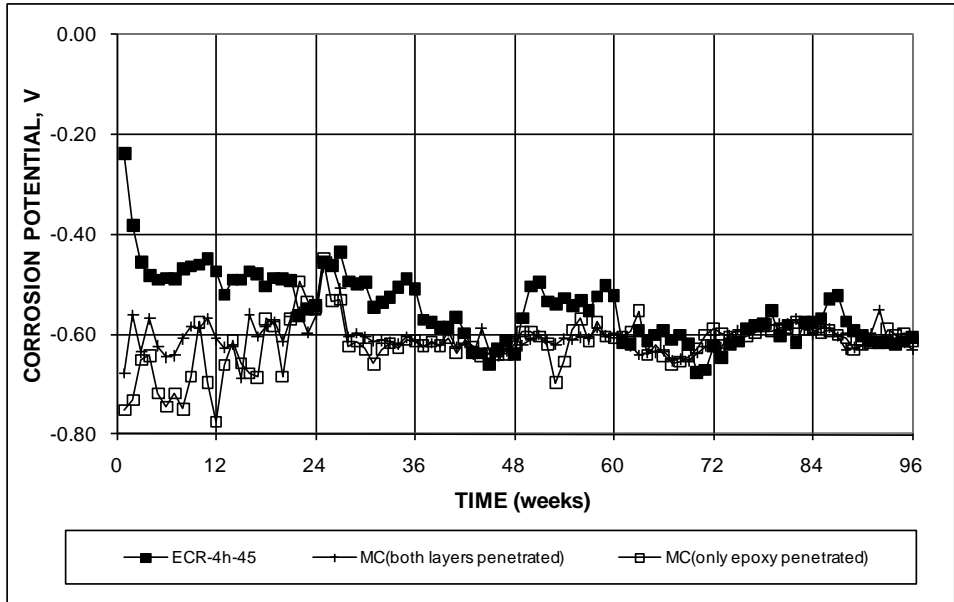
Figure 86. Graph. Cracked beam test, corrosion potential of top mat for conventional ECR and MC reinforcement with bars containing four holes.

89
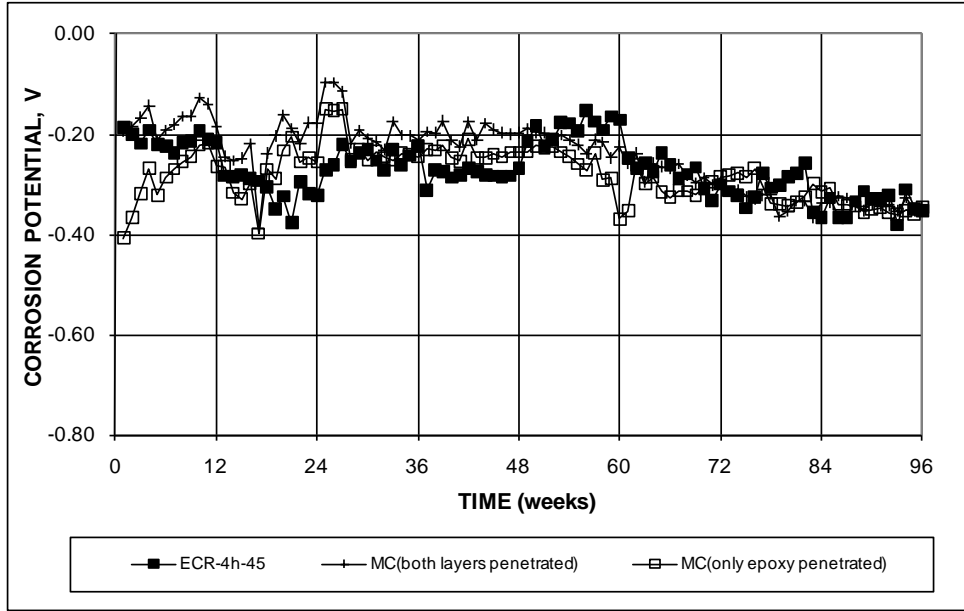
Figure 87. Graph. Cracked beam test, corrosion potential of bottom mat for conventional ECR and MC reinforcement with bars containing four holes.
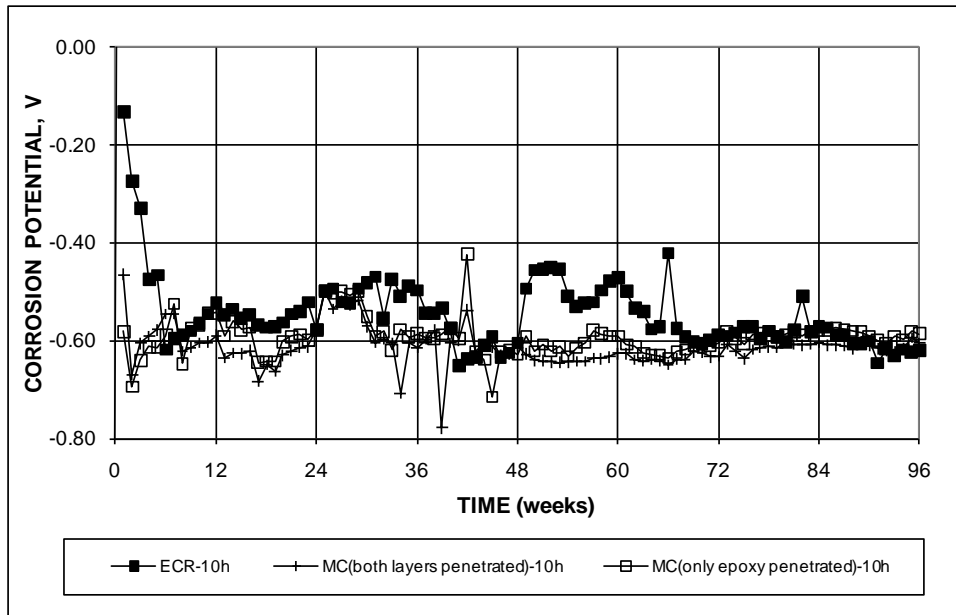
Figure 88. Graph. Cracked beam test, corrosion potential of top mat for conventional ECR and MC reinforcement with bars containing 10 holes.
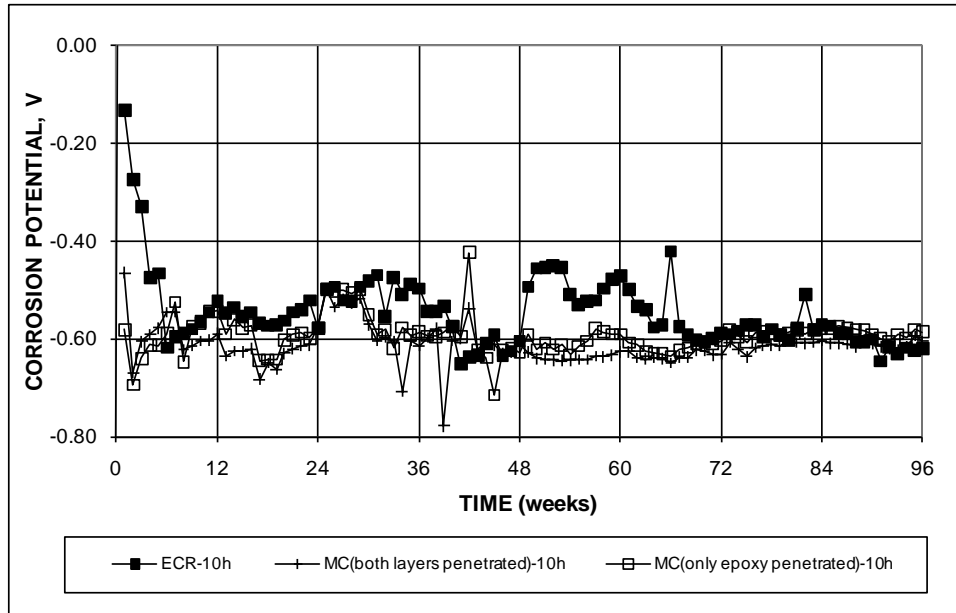
Figure 89. Graph. Cracked beam test, corrosion potential of bottom mat for conventional ECR and MC reinforcement with bars containing 10 holes.

Conventional Steel with Corrosion Inhibitors

The corrosion losses for the cracked beam specimens containing conventional steel cast in concrete with corrosion inhibitors and for the control specimens without a corrosion inhibitor are qualitatively similar to those observed for the matching southern exposure specimens. As shown in table 20 and figure 90, the highest average corrosion losses were exhibited by the specimens without a corrosion inhibitor (Conv.2-45) (29.7 μm (1.17 mil) at 96 weeks), followed by the specimens containing calcium nitrite, Rheocrete® 222+, and Hycrete™ (Conv.2(DCI)-45, Conv.2(RH)-45, and Conv.2(HY)-45), with losses of 26.4, 21.7, and 7.5 μm (1.04, 0.854, and 0.29 mil), respectively. Although qualitatively the same, the average losses for the cracked beam specimens containing Rheocrete® and calcium nitrite were much closer to the average loss for the specimens without a corrosion inhibitor than were the average losses for the specimens containing Hycrete™, indicating that Hycrete™ provided measurably better macrocell corrosion protection to bare bars in cracked concrete than the other two inhibitors. All of the losses were significantly higher than observed in the southern exposure tests. The corrosion potentials for the top mats of steel are shown in figure 91, with all specimens exhibiting an average potential more negative than -0.400 V at week 1 except the specimens containing Hycrete™, which dropped below -0.400 V at week 6. Similar to the southern exposure specimens, the cracked beam specimens containing Hycrete™ exhibited significantly higher mat-to-mat corrosion resistance than the other specimens beginning at about week 24 (see figure 92).
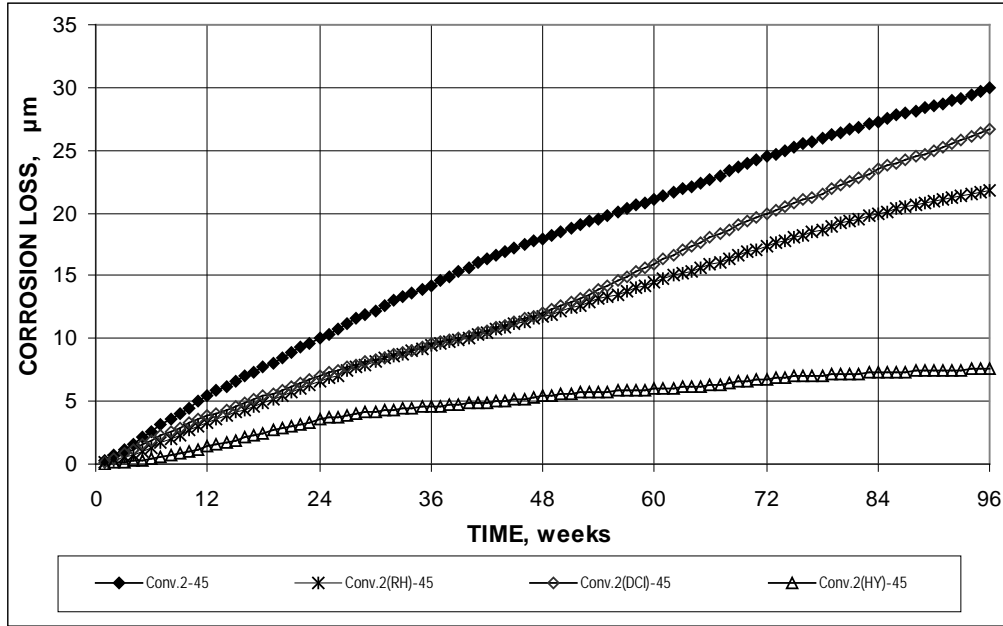
1 μm = 0.0394 mil

Figure 90. Graph. Cracked beam test, average corrosion losses based on the total area for conventional reinforcement in specimens containing corrosion inhibitors.
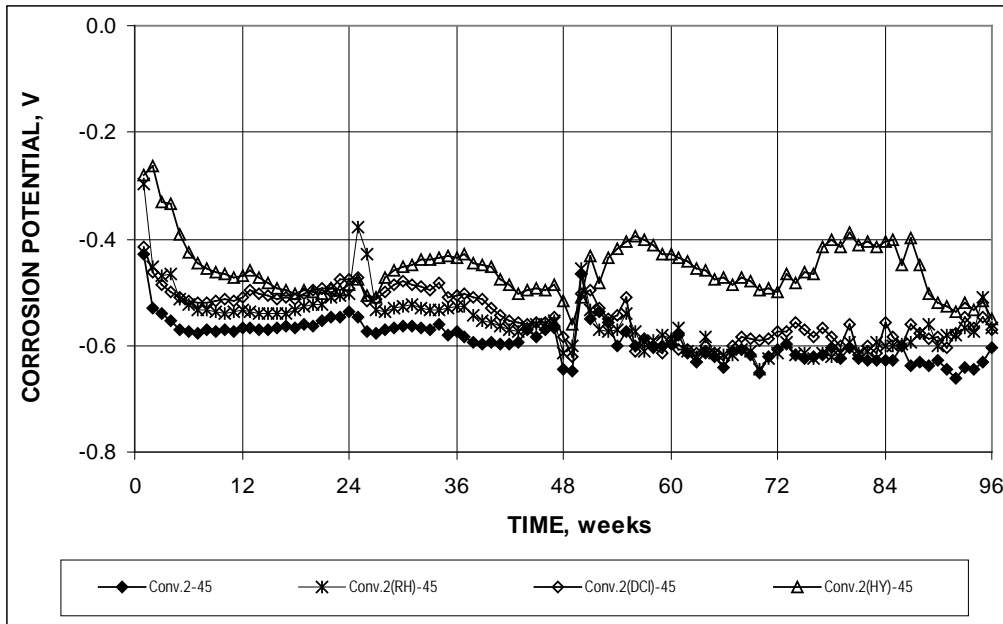
Figure 91. Graph. Cracked beam test, corrosion potential of top mat for conventional reinforcement in specimens containing corrosion inhibitors.
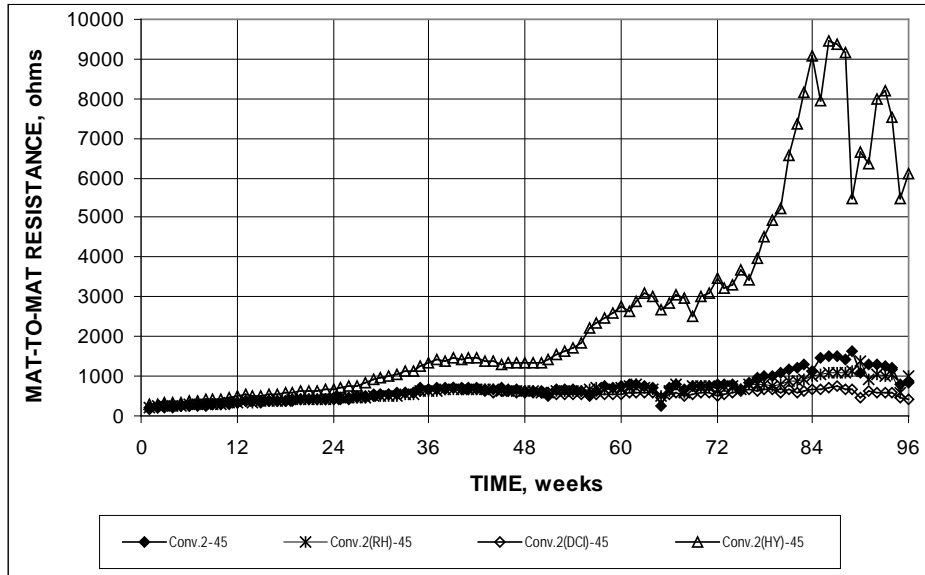
Figure 92. Graph. Cracked beam test, mat-to-mat resistance for conventional reinforcement in specimens containing corrosion inhibitors.

Linear Polarization Resistance Tests

Linear polarization resistance tests provide values of the total corrosion rate (microcell plus macrocell), often expressed as corrosion current density. For ease of comparison with the macrocell results presented in this chapter, the corrosion current densities have been converted to corrosion rates using the equations in figure 5 or figure 7 and integrated to obtain corrosion losses. As an example, the total corrosion losses for conventional steel (Conv.-45 and Conv.-35) and conventional ECR (ECR-4h-45, ECR-10h-45, and ECR-10h-35) in the southern exposure tests based on linear polarization resistance readings are shown in figure 93 and figure 94.
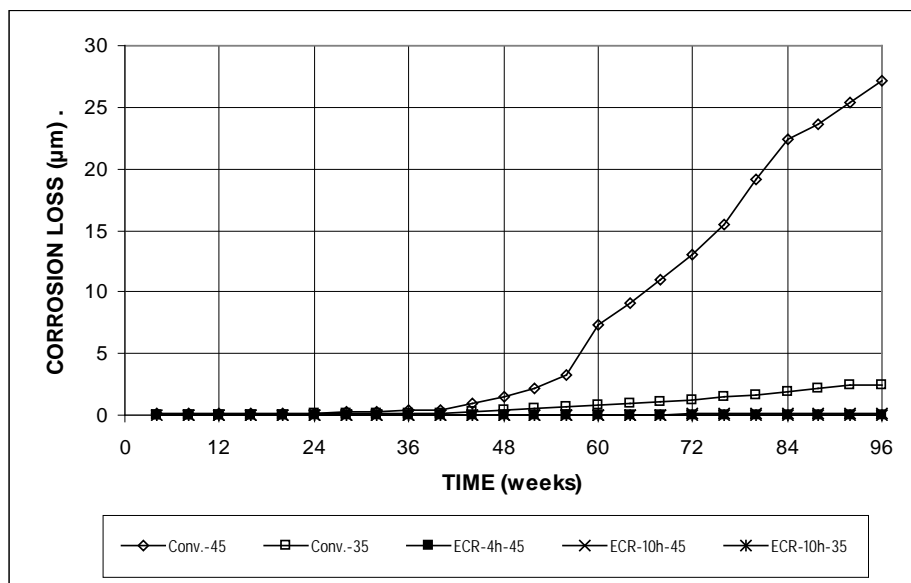
1 μm = 0.0394 mil

Figure 93. Graph. Linear polarization test results for southern exposure specimens, average corrosion loss based on total area for conventional reinforcement and conventional ECR.

93
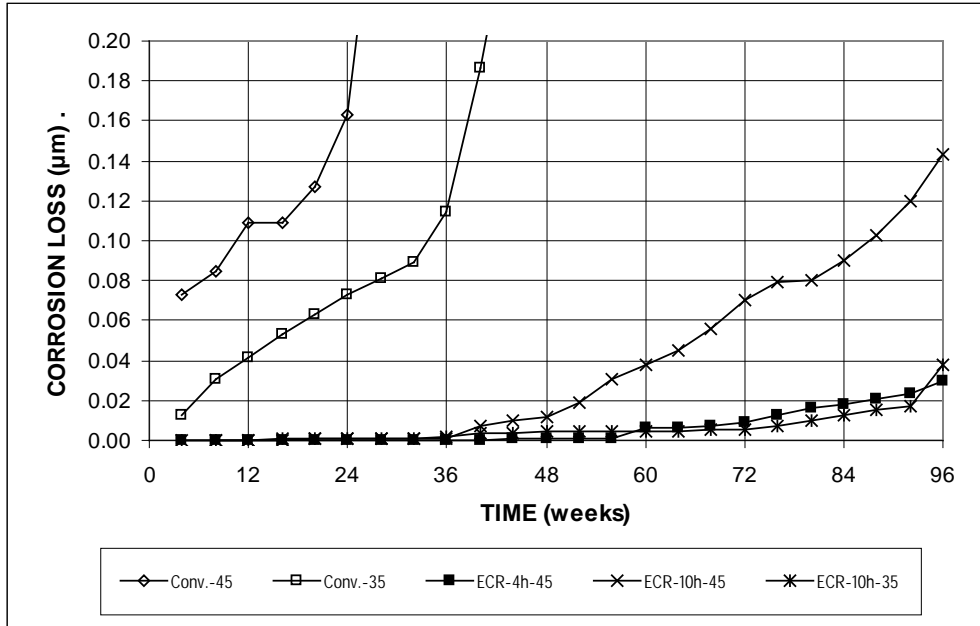
1 μm = 0.0394 mil

Figure 94. Graph. Linear polarization test results for southern exposure specimens, average corrosion loss based on total area for conventional reinforcement and conventional ECR (different scale).

The total losses at 96 weeks for the southern exposure and cracked beam tests are summarized in table 21 based on both total and exposed area (as explained in chapter 2, each of these values represents a single specimen). For comparison, the average macrocell losses at 96 weeks presented in table 11, table 12, and table 20 are shown side-by-side with the total losses. As expected, the losses based on the linear polarization results are, in nearly all cases, higher than those obtained based on macrocell current. This is true in 33 out of 34 cases for the southern exposure tests and in 30 out of 31 cases for the cracked beam test. As observed for macrocell losses, total corrosion losses are noticeably higher for the cracked beam test than for the southern exposure test.

Table 21. Total and macrocell corrosion loss at 96 weeks (μm) for southern exposure and cracked beam specimens expressed in terms of total bar area and area exposed at holes.

Steel Designation[a]	Based on Total Area				Based on Exposed Area			
	Southern Exposure		Cracked Beam		Southern Exposure		Cracked Beam	
	Total	Macrocell	Total	Macrocell	Total	Macrocell	Total	Macrocell
Controls								
Conv.-45	27.1	7.1	166.8	13.1	NA	NA	NA	NA
Conv.2-45	20.5	14.4	49.2	29.9	NA	NA	NA	NA
Conv.-35	2.50	2.121	130.8	8.34	NA	NA	NA	NA
ECR-4h-45	0.030	0.007	0.645	0.041	14.44	3.13	310.0	19.91
ECR-10h-45	0.143	0.017	0.500	0.047	27.44	3.21	96.06	9.04
ECR-10h-35	0.038	0.008	0.842	0.139	7.25	1.47	161.8	26.70
Epoxies with increased adhesion								
ECR(Chromate)-4h-45	0.029	0.018	1.727	0.074	14.13	8.76	829.7	35.66
ECR(Chromate)-10h-45	0.281	0.067	0.550	0.216	54.07	12.90	105.7	41.40
ECR(DuPont)-4h-45	0.106	0.026	0.525	0.105	50.92	12.34	252.1	50.44
ECR(DuPont)-10h-45	0.287	0.046	1.883	0.184	55.22	8.90	361.7	35.30
ECR(Valspar)-4h-45	0.221	0.032	1.912	0.084	105.92	15.58	918.2	40.35
ECR(Valspar)-10h-45	0.450	0.063	1.714	0.125	86.43	12.02	329.2	23.95
Corrosion inhibitors in concrete								
Conv.2(DCI)-45	12.15	8.599	132.8	26.68	NA	NA	NA	NA
Conv.2(RH)-45	4.613	3.398	62.12	21.82	NA	NA	NA	NA
Conv.2(HY)-45	2.611	1.549	27.383	7.598	NA	NA	NA	NA
ECR(DCI)-4h-45	0.056	0.004	0.788	0.026	26.82	1.79	378.6	12.72
ECR(DCI)-10h-45	0.256	0.012	1.288	0.079	49.08	2.23	247.3	15.26
ECR(DCI)-10h-35	0.020	0.007	0.203	0.223	3.83	1.29	38.90	42.75
ECR(RH)-4h-45	0.002	0.010	2.225	0.141	0.96	4.58	1069	67.59
ECR(RH)-10h-45	0.024	-0.002	1.164	0.171	4.55	-0.39	223.5	32.80
ECR(RH)-10h-35	0.018	0.003	0.654	0.178	3.40	0.65	125.6	34.25
ECR(HY)-4h-45	0.005	-0.002	0.357	0.036	2.25	-0.82	171.4	17.06
ECR(HY)-10h-45	0.013	0.002	0.880	0.060	2.52	0.37	169.1	11.55
ECR(HY)-10h-35	0.069	0.001	0.973	0.194	13.21	0.23	186.8	37.22
ECR(primer/Ca(NO$_2$)$_2$)-4h-45	0.033	0.014	0.902	0.017	15.77	6.72	433.0	8.28
ECR(primer/Ca(NO$_2$)$_2$)-10h-45	0.029	0.064	1.030	0.098	5.55	12.25	197.8	18.89
ECR(primer/Ca(NO$_2$)$_2$)-10h-35	0.008	0.002	2.034	0.440	1.54	0.42	390.8	84.50
Epoxies with increased adhesion plus calcium nitrite in concrete								
ECR(Chromate)-DCI-4h-45	0.080	0.007	–	–	15.35	1.26	–	–
ECR(DuPont)-DCI-4h-45	0.010	0.000	–	–	1.95	-0.06	–	–
ECR(Valspar)-DCI-4h-45	0.004	0.012	–	–	0.70	2.29	–	–
Bars with multiple coatings								
MC(both layers penetrated)-4h-45	0.931	0.058	1.436	0.377	447.3	27.70	690.0	181.0
MC(both layers penetrated)-10h-45	1.859	0.628	3.647	0.672	357.0	120.6	700.5	129.0
MC(only epoxy penetrated)-4h-45	0.803	0.033	3.769	0.294	385.9	15.88	1810.5	141.3
MC(only epoxy penetrated)-10h-45	0.681	0.090	1.657	0.221	130.7	17.36	318.2	42.36

1 μm = 0.0394 mil

NA = Not applicable

– No specimen.

[a] See table 1 for abbreviation definitions. 4h = bar with four holes through epoxy, 10h = bar with 10 holes through epoxy. 35 = concrete with w/c of 0.35, 45 = concrete with w/c of 0.45.

The results for total (linear polarization resistance) and macrocell corrosion are shown for the southern exposure tests in figure 95 and figure 96 (w/c = 0.45) and for the cracked beam tests in figure 97 (w/c = 0.45 and 0.35). Losses for conventional steel, including conventional steel cast in concrete with corrosion inhibitors, are based on total area, while losses for ECR are based on the area exposed at holes through the coating and represent the average for specimens with 4 and 10 holes. The figures demonstrate that corrosion losses for conventional reinforcement based on total area are of the same order of magnitude as those for ECR based on exposed area, but, as discussed for the bare-bar rapid macrocell tests, the average corrosion losses based on total area for uncoated bars are generally lower than those based on exposed area for epoxy-coated bars. The figures also demonstrate that, overall, the relative performance of the systems is similar whether based on microcell or macrocell corrosion current.
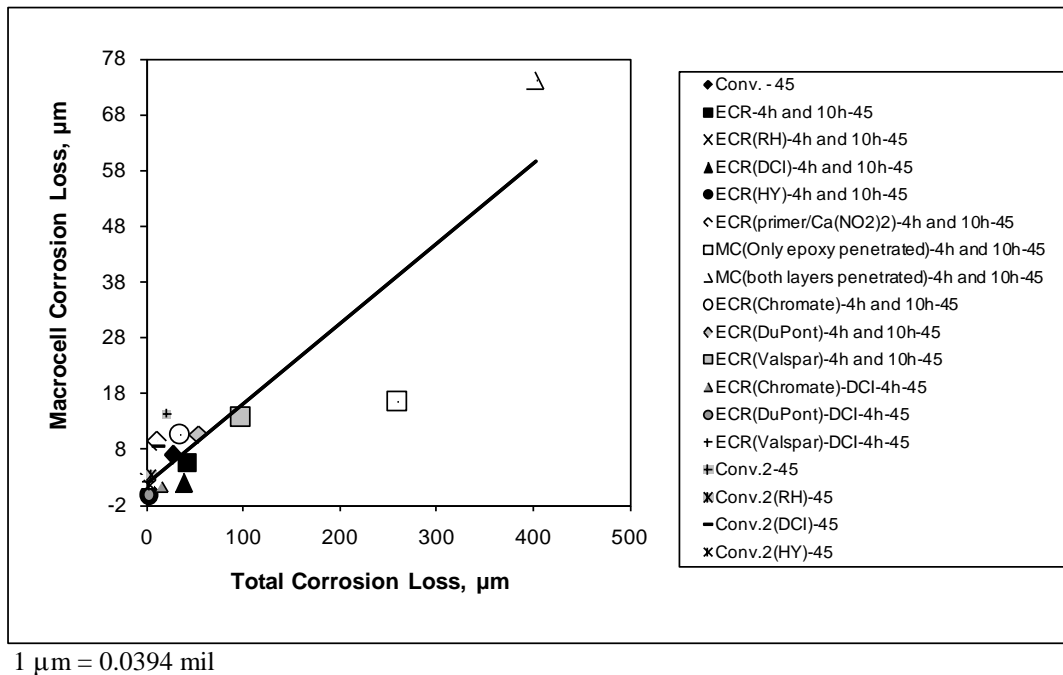
1 µm = 0.0394 mil

Figure 95. Graph. Southern exposure specimens, total versus macrocell corrosion loss based on total area for conventional reinforcement and area exposed at holes through coating for ECR with w/c = 0.45.

96
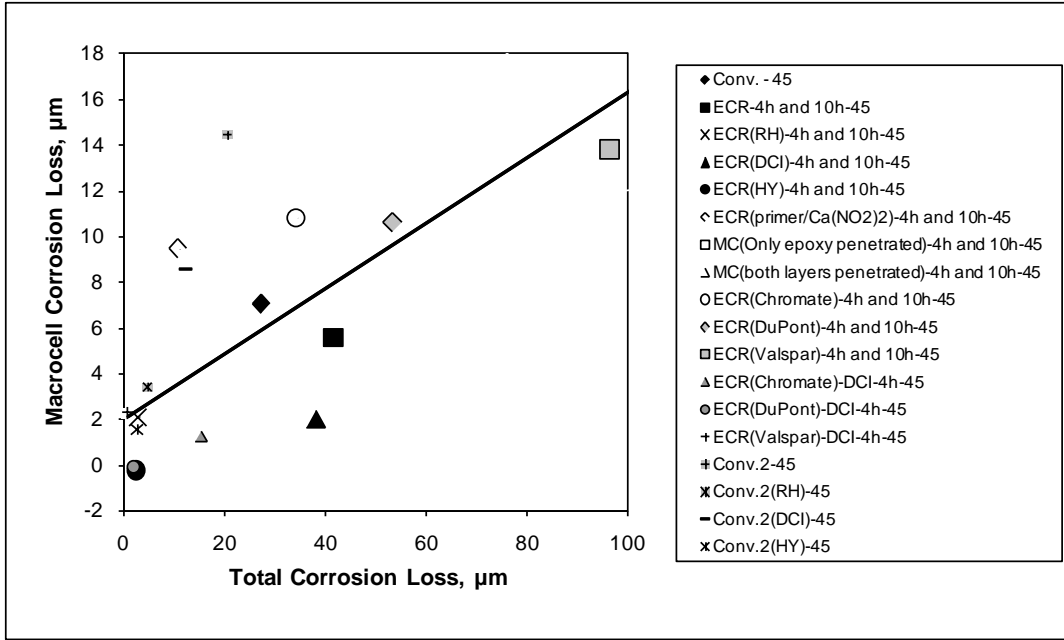
1 μm = 0.0394 mil

Figure 96. Graph. Southern exposure specimens, total versus macrocell corrosion loss based on total area for conventional reinforcement and area exposed at holes through coating for ECR with w/c = 0.45 (different scale).
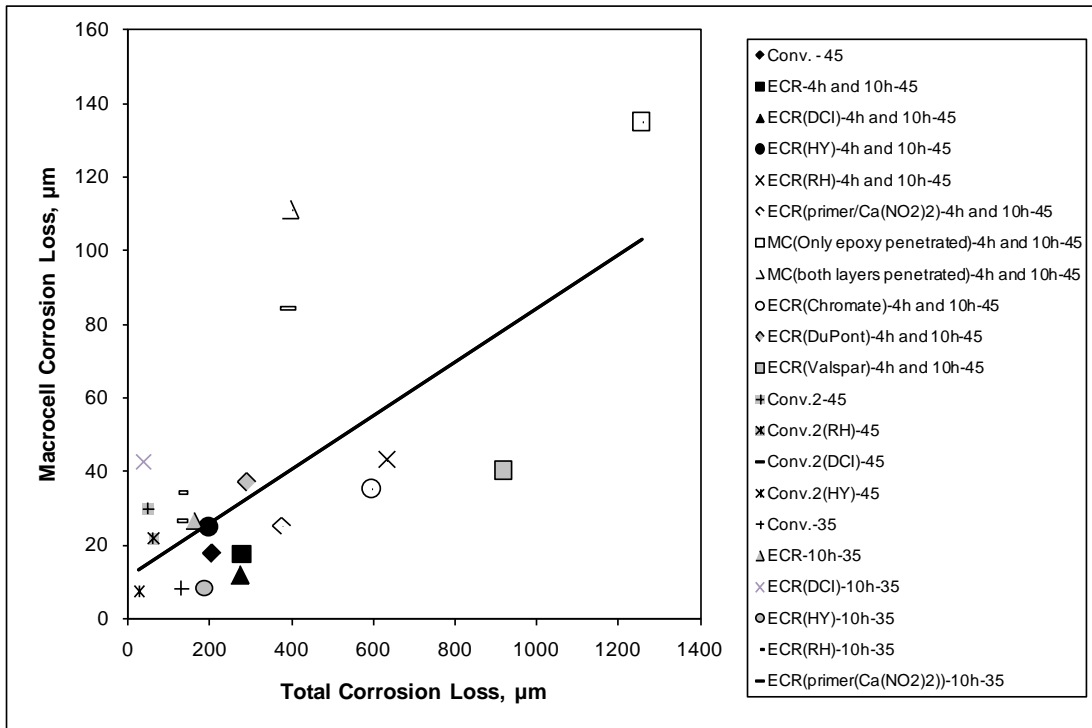
1 μm = 0.0394 mil

Figure 97. Graph. Cracked beam specimens, total versus macrocell corrosion loss based on total area for conventional reinforcement and area exposed at holes through coating for ECR with w/c = 0.45 or 0.35.

97

Total losses were highest for the MC bars and significantly lower for other systems in intact concrete, as shown in figure 95 and figure 96. These figures do not show the results for the southern exposure specimens with concrete with a w/c ratio of 0.35; if plotted, those results would appear in a grouping with macrocell losses between 0.6 and 2.1 μm (0.02 and 0.083 mil) and total losses between 2.5 and 13.2 μm (0.098 and 0.520 mil).

Figure 95 through figure 97 illustrate the relative performance of the systems, with the more effective systems exhibiting data points closer to the origin. Based on corrosion losses in the southern exposure and cracked beam tests as the measure of performance, all of the systems incorporating ECR appear to perform well in intact concrete, with the exception of the MC bars. In cracked concrete, all systems exhibited significantly higher losses and wider scatter in both total and macrocell corrosion, as shown in figure 97. When compared based on total area of steel, the systems involving conventional reinforcement both with and without a corrosion inhibitor did not perform as well as the systems with ECR or MC reinforcement.

Table 22 compares the average corrosion rates based on losses after corrosion initiation calculated using the linear polarization results with those calculated based on macrocell corrosion (see table 15 and table 20). The macrocell corrosion rates represent the individual specimens for which the linear polarization resistance readings were taken. As observed for corrosion losses, the corrosion rates based on the linear polarization results are, in nearly all cases, higher than those obtained based on macrocell current. This is true in 32 out of 34 cases for the southern exposure tests and in all 31 cases for the cracked beam test. Also similar to losses, corrosion rates are much higher for the cracked beam test than for the southern exposure test.

The total and macrocell corrosion rates are compared for the southern exposure tests in figure 98 and figure 99 (w/c = 0.45) and for the cracked beam tests in figure 100 (w/c = 0.45 and 0.35). Following the format used for figure 96 and figure 97, corrosion rates for uncoated bars are based on total area while the rates for coated bars are based on the area exposed at holes through the coating and represent the average for specimens with 4 and 10 holes. Observations based on corrosion rates are similar to those based on losses, with corrosion rates for conventional reinforcement based on total area somewhat lower but of the same order of magnitude as those for ECR based on exposed area. When based on total area, the systems with conventional reinforcement, with and without a corrosion inhibitor, do not perform as well as the systems with ECR or MC reinforcement.

Table 22. Average total and macrocell corrosion rates (µm/year) based on losses after corrosion initiation for southern exposure and cracked beam specimens expressed in terms of total bar area and area exposed at holes.

Steel Designation[a]	Based on Total Area				Based on Exposed Area			
	Southern Exposure		Cracked Beam		Southern Exposure		Cracked Beam	
	Total	Macrocell	Total	Macrocell	Total	Macrocell	Total	Macrocell
Controls								
Conv.-45	20.5	7.40	90.3	7.74	NA	NA	NA	NA
Conv.2-45	17.0	10.7	30.6	24.6	NA	NA	NA	NA
Conv.-35	2.07	1.61	73.03	6.34	NA	NA	NA	NA
ECR-4h-45	0.028	[b]	0.562	0.004	13.2	[b]	269.6	1.99
ECR-10h-45	0.152	0.066	0.358	0.019	29.2	12.7	68.8	3.69
ECR-10h-35	0.030	0.012	1.197	0.088	5.72	2.35	229.9	16.9
Epoxies with increased adhesion								
ECR(Chromate)-4h-45	0.021	[b]	1.008	0.029	10.3	[b]	483.6	14.1
ECR(Chromate)-10h-45	0.199	0.006	0.368	0.012	38.2	1.18	70.6	2.37
ECR(DuPont)-4h-45	0.112	0.029	0.309	0.070	53.9	13.8	148.4	33.5
ECR(DuPont)-10h-45	0.242	0.025	1.261	0.069	46.5	4.72	242.2	13.2
ECR(Valspar)-4h-45	0.193	0.032	1.218	0.086	92.5	15.5	584.6	41.1
ECR(Valspar)-10h-45	0.399	0.064	1.116	0.043	76.7	12.3	214.3	8.28
Corrosion inhibitors in concrete								
Conv.2(DCI)-45	9.79	7.81	106.6	17.5	NA	NA	NA	NA
Conv.2(RH)-45	3.82	2.57	48.34	13.6	NA	NA	NA	NA
Conv.2(HY)-45	1.82	0.791	18.2	4.91	NA	NA	NA	NA
ECR(DCI)-4h-45	0.045	[b]	0.421	0.035	21.7	[b]	202.3	16.6
ECR(DCI)-10h-45	0.227	0.012	0.754	0.021	43.5	2.33	144.7	4.10
ECR(DCI)-10h-35	0.022	0.006	0.239	0.246	4.28	1.16	46.0	47.2
ECR(RH)-4h-45	0.001	0.012	1.25	0.037	0.581	5.94	601.3	17.8
ECR(RH)-10h-45	0.015	[b]	0.658	0.079	2.86	[b]	126.3	15.1
ECR(RH)-10h-35	0.011	[b]	0.920	0.074	2.09	[b]	176.7	14.3
ECR(HY)-4h-45	0.002	[b]	0.215	0.053	1.19	[b]	103.0	25.5
ECR(HY)-10h-45	0.011	0.004	0.468	0.033	2.09	0.674	89.8	6.37
ECR(HY)-10h-35	0.049	[b]	1.37	0.161	9.44	[b]	263.9	30.9
ECR(primer/Ca(NO$_2$)$_2$)-4h-45	0.028	0.046	0.509	0.012	13.3	22	244.3	5.74
ECR(primer/Ca(NO$_2$)$_2$)-10h-45	0.037	0.033	0.608	0.048	7.04	6.39	116.7	9.19
ECR(primer/Ca(NO$_2$)$_2$)-10h-35	0.004	[b]	2.80	0.321	0.741	[b]	537.6	61.6
Epoxies with increased adhesion plus calcium nitrite in concrete								
ECR(Chromate)-DCI-4h-45	0.036	0.021	–	–	17.1	10.3	–	–
ECR(DuPont)-DCI-4h-45	0.004	[b]	–	–	2.12	[b]	–	–
ECR(Valspar)-DCI-4h-45	0.001	[b]	–	–	0.423	[b]	–	–
Bars with multiple coatings								
MC(both layers penetrated)-4h-45	0.572	0.027	0.809	0.206	274.5	13.1	388.1	98.7
MC(both layers penetrated)-10h-45	1.32	0.358	2.04	0.289	254	68.8	391.2	55.5
MC(only epoxy penetrated)-4h-45	0.518	0.077	2.12	0.352	248.8	36.9	1018.8	169
MC(only epoxy penetrated)-10h-45	0.506	0.039	2.33	0.207	97.2	7.52	448.2	39.7

1 µm = 0.0394 mil

NA = Not applicable; – No specimen.

[a] See table 1 for abbreviation definitions. 4h = bar with four holes through epoxy, 10h = bar with 10 holes through epoxy.

35 = concrete with w/c of 0.35, 45 = concrete with w/c of 0.45.

[b] No corrosion observed.
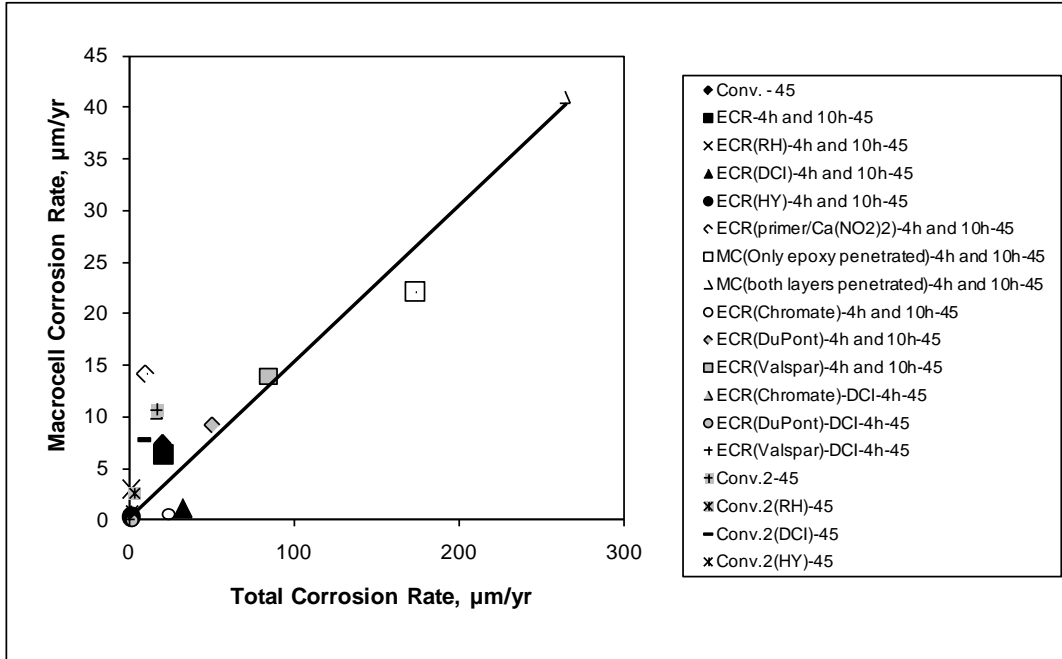
Figure 98. Graph. Southern exposure specimens, average total and macrocell corrosion rates based on losses after corrosion initiation based on total area for conventional reinforcement and area exposed at holes through coating for coated reinforcement, w/c = 0.45.
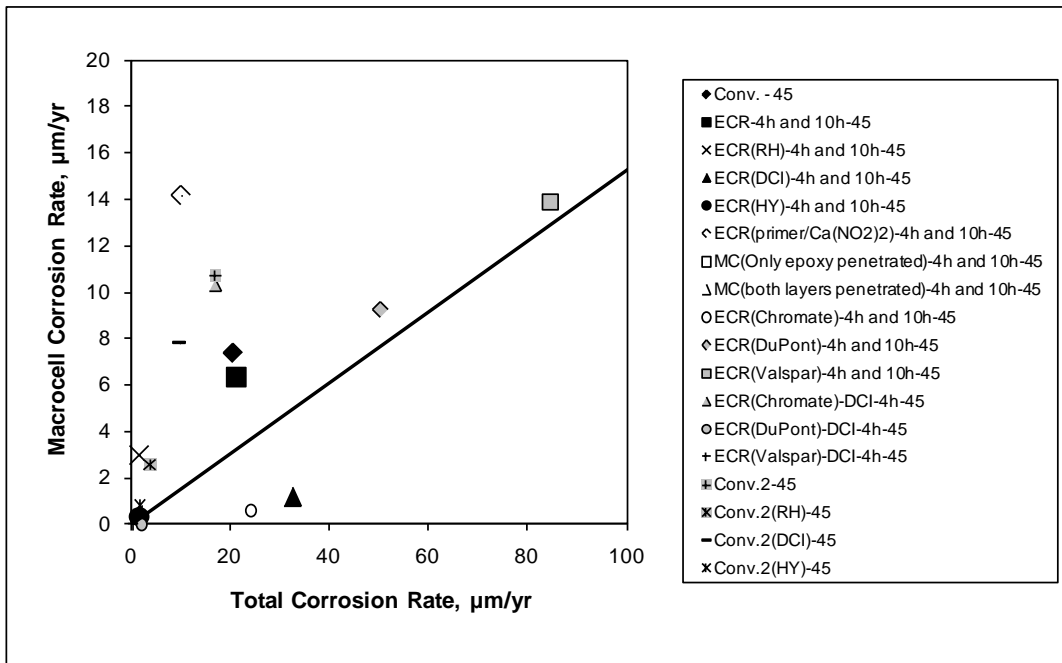
1 µm = 0.0394 mil

Figure 99. Graph. Southern exposure specimens, average total and macrocell corrosion rates based on losses after corrosion initiation based on total area for conventional reinforcement and area exposed at holes through coating for coated reinforcement, w/c = 0.45 (different scale).

1 µm = 0.0394 mil

100
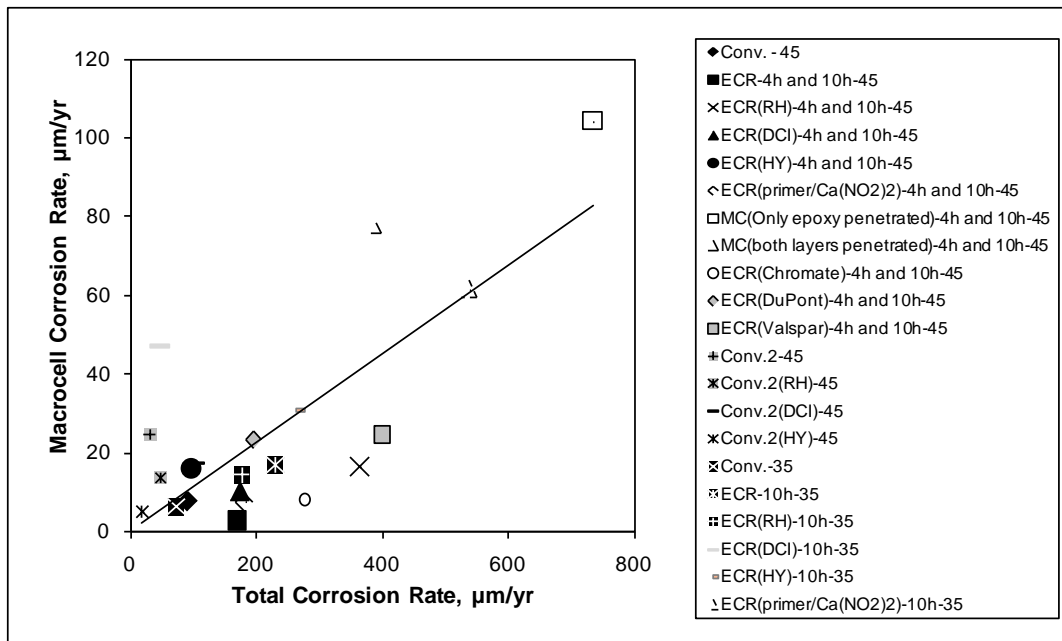
1 μm = 0.0394 mil

Figure 100. Graph. Cracked beam specimens, average total and macrocell corrosion rates based on losses after corrosion initiation based on total area for conventional reinforcement and area exposed at holes through coating for coated reinforcement, w/c = 0.45 or 0.35.

The results in table 22 are used in chapter 4 to estimate total corrosion rates as a function of macrocell corrosion rates for the field tests, for which linear polarization resistance data are not available.

The relative performance of the systems can be judged further based on the autopsies of the specimens, performed after completion of the tests and based on the performance of the field test specimens. As discussed in chapter 4, the tests demonstrated that the coated-bar systems under evaluation would serve well in practice.

Autopsy of Bench-Scale Test Specimens

Following the tests, the specimens were evaluated for staining and cracking and autopsied to observe the degree of corrosion on the reinforcing steel. With the exception of the cracked beam specimens containing conventional steel, little cracking or staining was observed on the surface of the bench-scale test specimens. Upon removal of the concrete, the degree of corrosion damage was observed.

Figure 101 illustrates the extent of corrosion damage at 96 weeks to conventional steel (Conv.) in the southern exposure tests. The two top bars (at the left of the figure) exhibited varying degrees of corrosion along their lengths. The four bottom bars exhibited little if any corrosion damage. In contrast, the cracked beam specimen containing conventional steel, shown previously in figure 77, exhibited stains on the top and sides as well as a crack that extended from the original simulated crack in the center top of the specimen. The cause of the crack extension is shown figure 102, where the top bar shows highly nonuniform but major corrosion with the volume of corrosion products clearly adequate to cause crack extension. The bottom bars exhibited corrosion, as well, especially the center bar in the figure.

101

Figure 101. Photo. Conventional steel bars from southern exposure specimen after 96 weeks.

Figure 102. Photo. Conventional steel bars from cracked beam specimens after 96 weeks.

Upon removal of the concrete from epoxy-coated bars, the epoxy coating was observed to be intact on all specimens, although some specimens exhibited blisters, as shown in figure 103. This figure shows a top bar from a southern exposure specimen containing conventional ECR. Holes placed in the epoxy prior to the test are shown to the center left and right in the figure, while the blister in the epoxy is shown at the center. Corrosion products are apparent at both the left and the right penetrations.
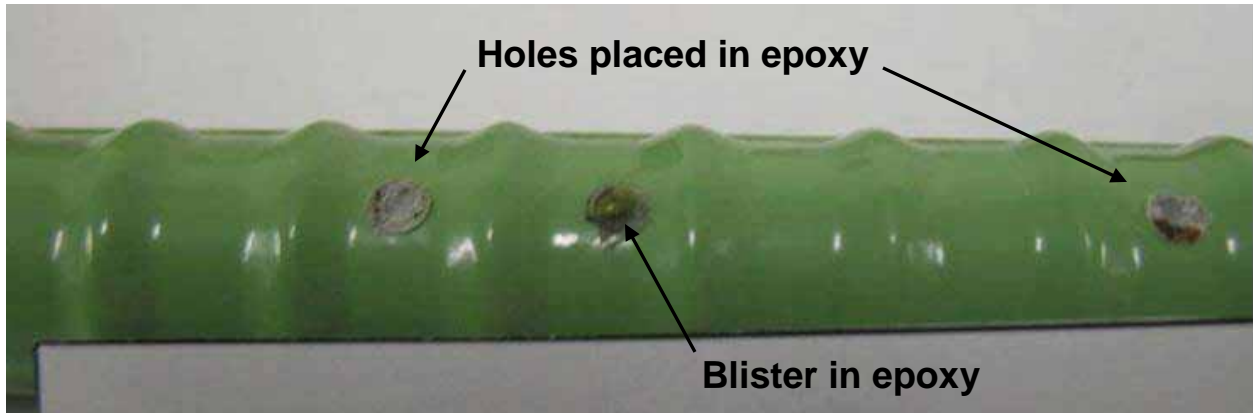
Figure 103. Photo. Conventional epoxy-coated bar from southern exposure specimen after 96 weeks.

To evaluate the bond between the epoxy and the steel, a radial 45-degree cut was made with a knife at the center of selected openings at the intentionally damaged areas. Following the same procedure described in chapter 2 for the cathodic disbondment tests, an attempt was made to lift the coating at these locations. If the bond between the coating and the steel was in good condition, the epoxy could not be removed.

The bar surface was inspected for corrosion products following disbondment. In most cases, the bar surface appeared black or dark brown, suggesting corrosion in the absence of oxygen. Within an hour, the color typically changed to orange or light brown as the corrosion products were exposed to oxygen.

The total area of coating disbondment was used to evaluate the bond between the epoxy coating and the steel. Figure 104 shows the bar from figure 103 shortly after disbondment at one of the penetrations. Figure 105 shows top and bottom bars after disbondment for bars cast in concrete containing calcium nitrite. The greater disbondment exhibited by the top bar compared to the bottom bar is typical. Corrosion products were present at the left penetration and in the disbonded region on the bar. Figure 106 shows a top bar in a southern exposure specimen cast with concrete containing Hycrete™. In this case, corrosion products were apparent at the left penetration, and the epoxy coating exhibited significant disbondment at the penetration near the center of the image but no disbondment at the penetration to the right of the image. Figure 107 illustrates a bar coated with an epoxy (ECR(DuPont)) that initially provided improved adhesion. The upper bar in the image, a top bar in the specimen, underwent complete disbondment while the lower bar in the image, a bottom bar in the specimen, underwent only partial disbondment. For the top bar, all three penetrations in the epoxy exhibited corrosion products, which were also apparent in the disbonded region. MC bars with holes through the epoxy only and with holes penetrating both the epoxy and zinc layers are shown in figure 108 and figure 109, respectively. Corrosion products were present at the points where the epoxy was penetrated. Both bars exhibited varying degrees of disbondment. In all cases, some corrosion products were observable within the disbonded region. For the MC bars, the zinc, the more active metal, was seen to preferentially corrode under the epoxy coating, thus protecting the underlying steel.

Figure 104. Photo. Conventional epoxy-coated bar from figure 103 after disbondment test.

Figure 105. Photo. Conventional epoxy-coated top and bottom bars from southern exposure specimen containing calcium nitrite after 96 weeks.
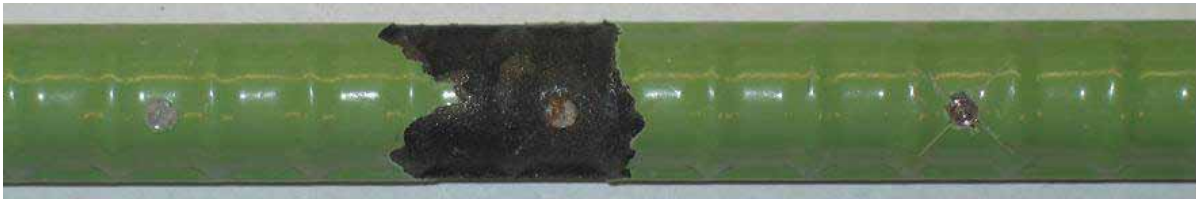
Figure 106. Photo. Conventional epoxy-coated top bar from southern exposure specimen containing Hycrete™ after 96 weeks.

Figure 107. Photo. DuPont™ high-adhesion epoxy-coated top and bottom bars from southern exposure specimen after 96 weeks.

Figure 108. Photo. MC top bar with holes through epoxy only from southern exposure specimen after 96 weeks.

Figure 109. Photo. MC top bar with holes penetrating both epoxy and zinc from southern exposure specimen after 96 weeks.

In addition to visual inspection, the disbonded area on the bars was measured using a grid of 2.5-mm (0.1-inch) squares printed on a transparent plastic sheet superimposed on the disbonded region. For each southern exposure and cracked beam specimen, one bar each from the top and bottom mats was chosen to measure disbondment. Disbondment tests were performed at two locations on the upper surface of each bar. When the disbonded area extended a distance greater than 14.7 mm (0.58 inches) in all directions, the bar was said to exhibit total disbondment. Damage locations that exhibited total disbondment were assigned to disbonded area of 680 mm^2 (1.05 in^2), the approximate area of the circle with a 14.7-mm (0.58-inch) radius.

Figure 110 and figure 111 show the disbonded areas for bars in the southern exposure and cracked beam specimens, respectively, cast with concrete with a w/c ratio of 0.45. In the uncracked concrete, disbondment greater than 515 mm^2 (0.8 in^2) was observed on the top mat of steel for the conventional ECR specimens as well as for all bars with improved adhesion between the epoxy and the steel cast in concrete without an inhibitor, with a maximum values in excess of 680 mm^2 (1.05 in^2) for the ECR(DuPont) bars. Less disbondment was observed for the MC bars and for all bars cast in concrete containing corrosion inhibitors, including those with improved adhesion cast in concrete containing calcium nitrite. The bars in concrete containing Hycrete™ exhibited the least disbondment. Disbondment in the bottom mat was below 130 mm^2 (0.2 in^2) for all bars, with MC bars and epoxy-coated bars cast in concrete containing inhibitors showing less bottom mat disbondment than the control and improved adhesion bars.

In cracked concrete, a disbonded area greater than 515 mm^2 (0.8 in^2) was observed for the top bars in all specimens except MC bars, which exhibited an average disbonded area of approximately 355 mm^2 (0.55 in^2). ECR(Chromate) specimens exhibited total disbondment. All bottom-mat bars in the cracked beam specimens exhibited increased disbondment compared to bars in uncracked concrete with the exception of the MC bars, which exhibited somewhat less.
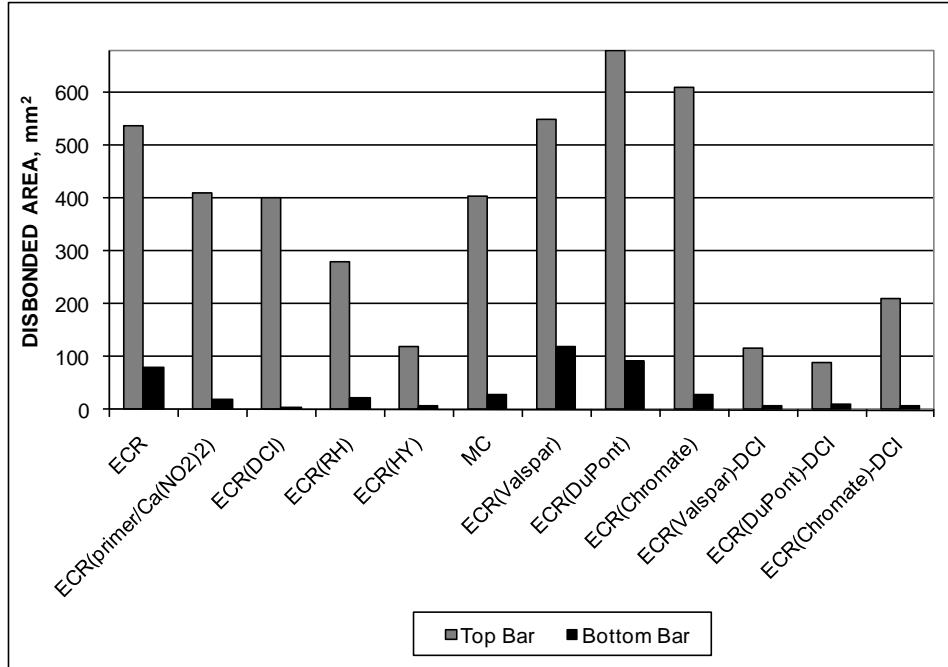
1 mm^2 = 0.00155 in^2

Figure 110. Graph. Disbondment results for southern exposure specimens.
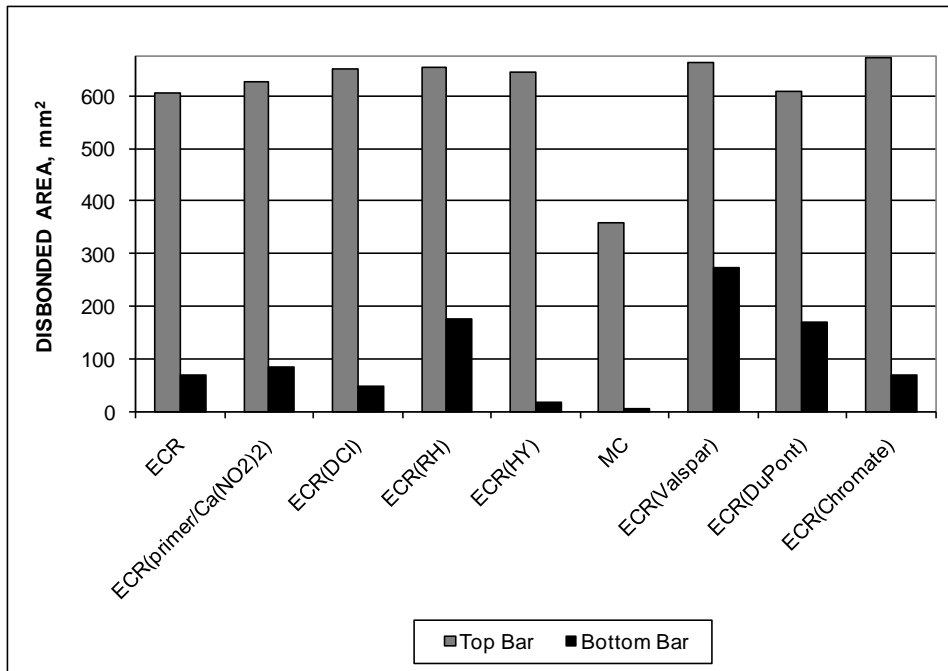
1 mm^2 = 0.00155 in^2

Figure 111. Graph. Disbondment results for cracked beam specimens.

Figure 112 and figure 113 compare the disbondment of bars in southern exposure and cracked beam specimens cast in concrete with a w/c ratio of 0.35 with that for similar specimens cast with a w/c ratio of 0.45. As shown in figure 112, the average disbonded areas for bars in the southern exposure specimens with w/c of 0.35 ranged from 11 percent (ECR(RH)) to 76 percent

106

(ECR(DCI)) of the values for the southern exposure specimens with w/c of 0.45. In contrast, figure 113 shows that little difference was observed for the cracked beam specimens as a function of w/c ratio, emphasizing both the negative impact of cracks on disbondment and the inability of a lower w/c ratio to limit disbondment in the presence of cracks.
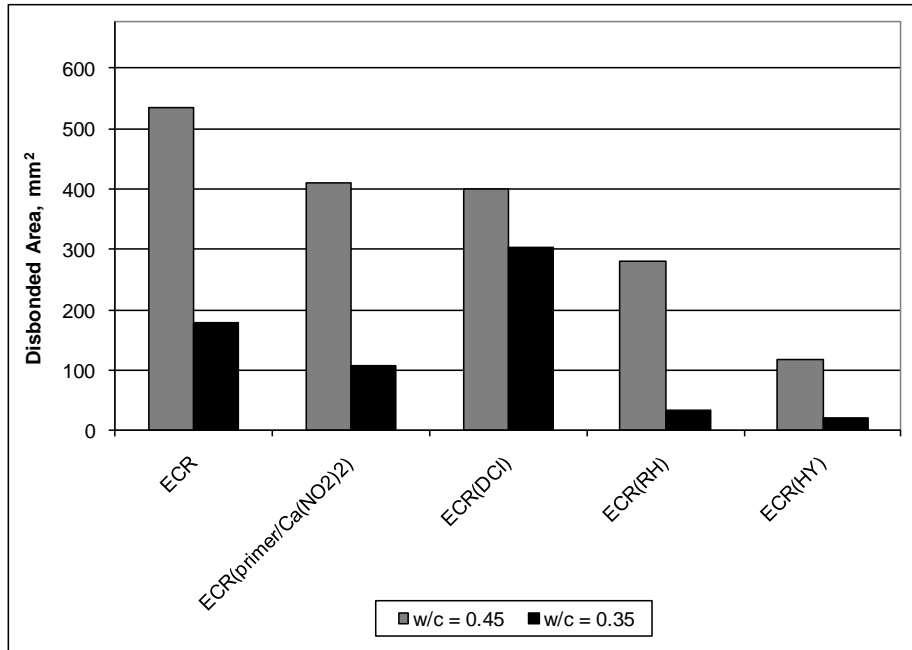
$1\ mm^2 = 0.00155\ in^2$

Figure 112. Graph. Comparison of disbondment of top bars in southern exposure specimens cast in concrete with w/c = 0.35 and 0.45.
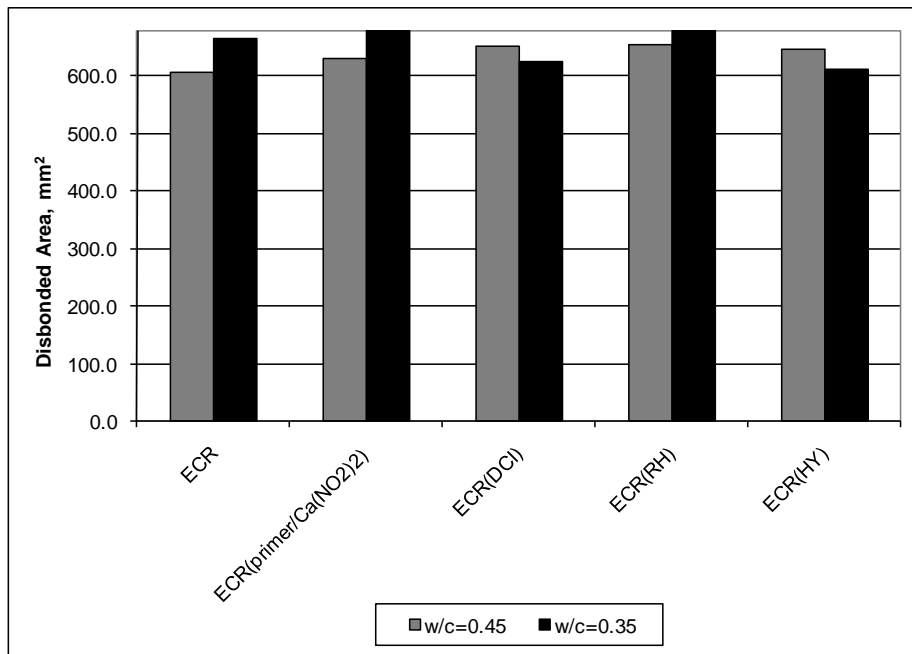
$1\ mm^2 = 0.00155\ in^2$

Figure 113. Graph. Comparison of disbondment of top bars in cracked beam specimens cast in concrete with w/c = 0.35 and 0.45.

FIELD TESTS

The field tests provided a highly realistic evaluation of corrosion-protection systems. The test specimens were designed to match bridge decks. The key difference was the use of a 25-mm (1-inch) top cover, which provides earlier corrosion initiation than obtained with the 150-mm (3-inch) top cover typically used in practice for bridge decks. Four specimens were used to evaluate each corrosion-protection system except those cast with the corrosion inhibitor calcium nitrite, for which six specimens were used.

As shown in table 7 in chapter 2, the field tests specimens were cast in nine batches. Half of the specimens were cast without cracks and half of the specimens contained simulated cracks over four of the seven top reinforcing bars. The coating on epoxy-coated bars was penetrated by 16 3.2-mm (0.125-inch)-diameter holes to simulate defects in the coating. Rock salt in solution or solid form was applied every 4 weeks to provide a salt application rate matching that used on bridge decks in Kansas, as described in chapter 2. At the conclusion of the tests (250 or 254 weeks after initial exposure), chloride samples were obtained from cores taken at the four corners of each specimen in batches 3 through 9. The chloride contents for those specimens at a depth of 25 mm (1 inch) are listed in table 23. The chloride content for the specimens in batch 1 was extrapolated from vacuum drill samples taken at 213 weeks. No data is available for batch 2.

Table 23. Average chloride content (kg/m^3) at a depth of 25 mm (1 inch) at end of field tests.

Batch	Specimen[a]	Uncracked	Cracked
1[b]	Conv.-1, ECR-1, ECR(Valspar)-1	4.40	4.40
2	ECR(Chromate)-1, ECR(DuPont)-1, MC-1	–	–
3	Conv.-2	1.97	3.85
	ECR-2	3.22	2.18
	ECR(primer/Ca(NO$_2$)$_2$)-1	–	–
4	ECR(Chromate)-2	3.53	4.89
	ECR(DuPont)-2	4.78	4.43
	ECR(Valspar)-2	3.03	4.82
5	ECR(primer/Ca(NO$_2$)$_2$)-2	9.86	8.36
	MC-2	8.92	8.78
6	ECR(DCI)-1	8.30	9.67
	ECR(DCI)-2	7.73	9.03
7	ECR(DCI)-3	8.26	5.20
8	ECR(RH)-1	9.34	8.49
	ECR(RH)-2	6.23	7.56
9	ECR(HY)-1	0.55	1.12
	ECR(HY)-2	0.29	1.10

1 kg/m^3 = 1.69 lb/yd^3
– No data.
[a] See table 1 for abbreviation definitions.
[b] Extrapolated from vacuum drill samples taken at 213 weeks.

The chloride content at a depth of 25 mm (1 inch) is plotted versus the w/c ratio in figure 114 for the seven batches for which data are available not including the concrete in batch 9, which

contained Hycrete™. Hycrete™ was excluded because, as observed for the southern exposure tests, the chloride content of the specimens containing Hycrete™ was very low (0.77 kg/m³ (1.30 lb/yd³)). As expected, the figure shows a general trend of increasing chloride content with increasing w/c ratio. The variation in w/c ratio between batches is the result of variations in the quality of the ready-mix concrete delivered for casting the specimens and is typical of the range of properties obtained in the field. Overall, the average chloride contents differed markedly, ranging from 0.77 kg/m³ (1.30 lb/yd³) for the concrete containing Hycrete™ to 2.81 kg/m³ (4.73 lb/yd³) for batch 3 and 8.73 kg/m³ (14.7 lb/yd³) for batch 5 for concretes without a corrosion inhibitor. Extreme values for individual specimens ranged from a low of 0.29 kg/m³ (0.49 lb/yd³) for uncracked Hycrete™ specimen 2 to a high of 9.86 kg/m³ (16.6 lb/yd³) for uncracked ECR(primer/Ca(NO$_2$)$_2$) specimen 2. The chloride contents for the individual specimens are shown graphically in figure 115 and figure 116 for specimens without and with cracks, respectively. Because the chloride samples were taken from the corners of the specimens, the values of chloride content do not reflect the effect of the cracks. They are best used as a measure of the permeability of the concrete.
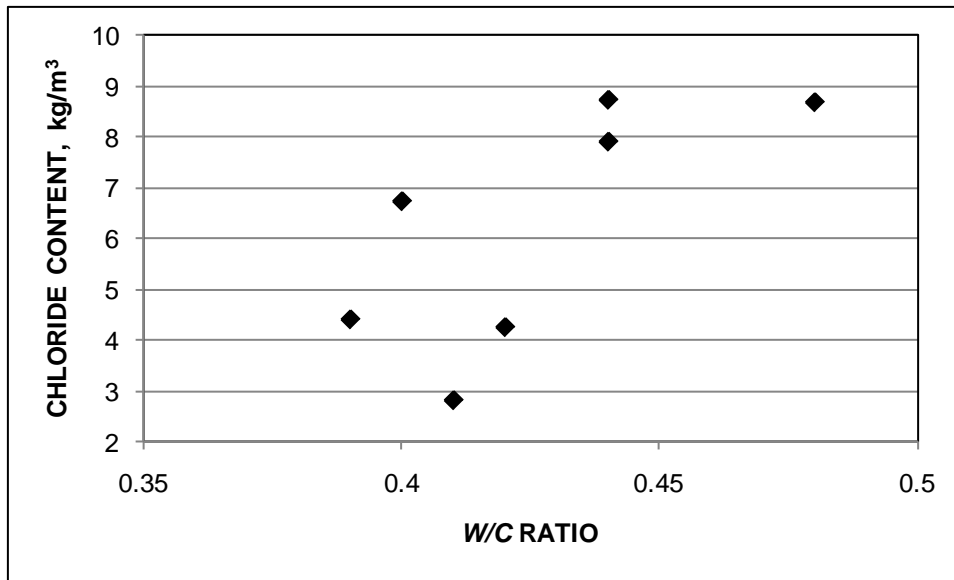
1 kg/m³ = 1.69 lb/yd³

Figure 114. Graph. Average chloride content at a depth of 25 mm (1 inch) versus w/c ratio at end of field tests.
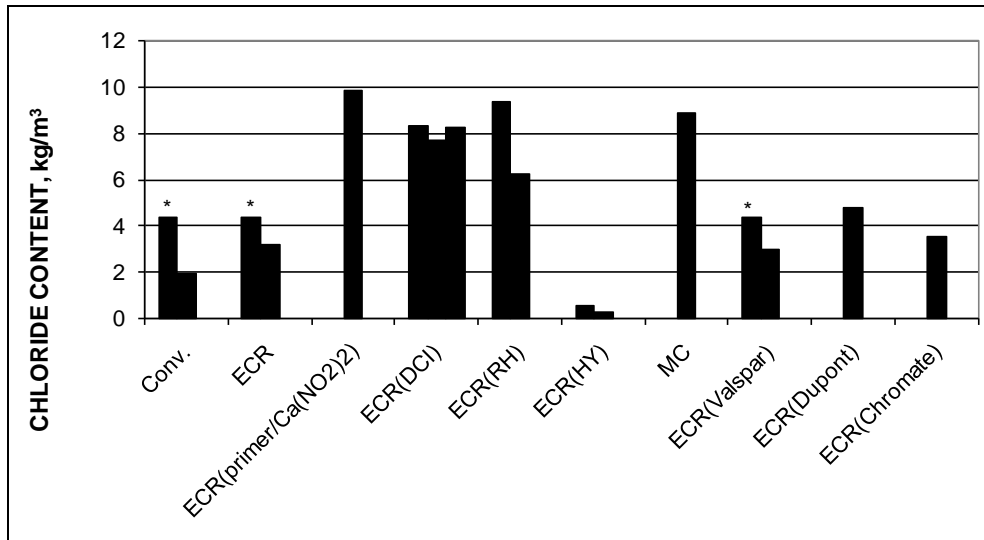
1 kg/m^3 = 1.69 lb/yd^3

* Extrapolated from vacuum drill data taken at 213 weeks.

Figure 115. Graph. Average chloride content at a depth of 25 mm (1 inch) at end of field tests for uncracked field test specimens.
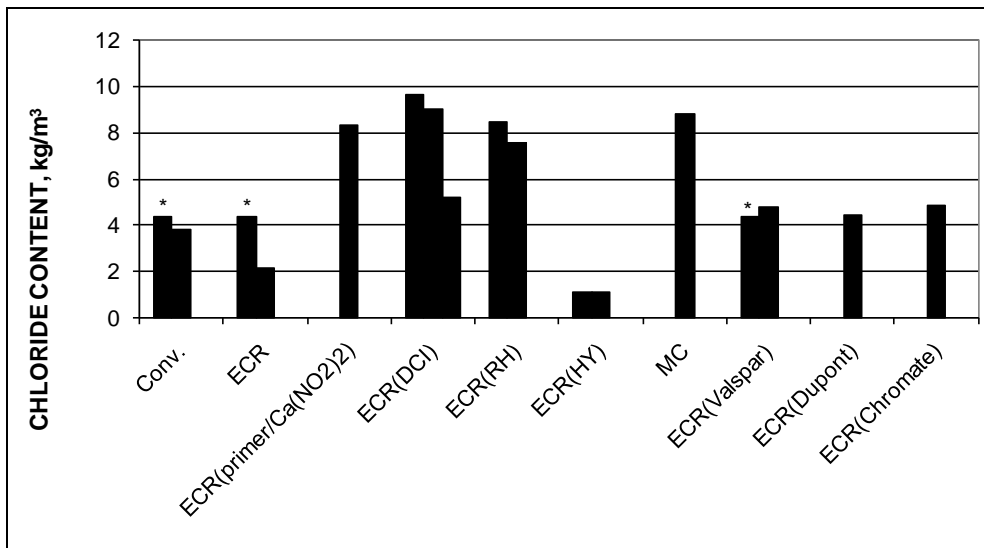
1 kg/m^3 = 1.69 lb/yd^3

* Extrapolated from vacuum drill data taken at 213 weeks.

Figure 116. Graph. Average chloride content at a depth of 25 mm (1 inch) at end of field tests for cracked field test specimens.

Corrosion Losses

The corrosion losses based on the total area of the bar in contact with the concrete and on the exposed area at the holes in the epoxy are presented in table 24 and table 25 for specimens without cracks and in table 26 and table 27 for specimens with cracks. The data represent two or four bars per specimen, as shown in the tables. As noted on the tables, negative values of corrosion loss are excluded from the average values of loss.

110

Table 24. Corrosion loss at end of field tests (µm) based on total area for specimens without simulated cracks.

Steel Designation[a]	Exposure Time (weeks)	Test Bar 1	2	3	4	Average[b]	Standard Deviation
Controls							
Conv. (1)	250	3.67	2.49			3.08	0.833
Conv. (2)	254	0.142	1.17			0.657	0.728
ECR (1)	250	0.024	0.069			0.046	0.032
ECR (2)	254	0.016	0.008	-0.005[c]	0.004	0.009	0.006
Bars with increased adhesion							
ECR(Chromate) (1)	250	0.015	0.013			0.014	0.001
ECR(Chromate) (2)	254	0.047	-0.042[c]	-0.006[c]	0.025	0.036	0.016
ECR(DuPont) (1)	250	0.028	0.014			0.021	0.010
ECR(DuPont) (2)	254	0.016	0.007	0.011	0.037	0.018	0.013
ECR(Valspar) (1)	250	0.009	0.024			0.016	0.010
ECR(Valspar) (2)	254	0.025	-0.009[c]	0.100	0.041	0.055	0.040
Corrosion inhibitors in concrete							
ECR(DCI) (1)	250	0.031	0.038	0.019	0.030	0.030	0.008
ECR(DCI) (2)	254	0.062	0.097	0.045	0.017	0.055	0.033
ECR(DCI) (3)	254	0.035	0.034	0.007	0.023	0.025	0.013
ECR(RH) (1)	250	0.068	0.048	0.016	0.045	0.044	0.022
ECR(RH) (2)	254	-0.003[c]	-0.008[c]	-0.004[c]	0.029	0.029	–
ECR(HY) (1)	250	-0.001[c]	0.003	0.011	0.047	0.020	0.023
ECR(HY) (2)	254	0.022	0.017	0.033	0.025	0.024	0.007
ECR(primer/Ca(NO$_2$)$_2$) (1)	250	0.000	0.020	0.033	0.028	0.027	0.007
ECR(primer/Ca(NO$_2$)$_2$) (2)	254	0.070	0.030	0.024	0.046	0.042	0.020
Bars with multiple coatings							
MC (1)	250	0.024	0.023			0.024	0.001
MC (2)	254	0.047	0.008	0.007	0.049	0.028	0.023

1 µm = 0.0394 mil

– No standard deviation.

Blank cells indicate that the test bar was not present.

[a] See table 1 for abbreviation definitions. All epoxy-coated bars are penetrated with 16 surface holes.

[b] Based on top mat only.

[c] Excluded from average.

Table 25. Corrosion loss at end of field tests (μm) based on area exposed at holes through coating for specimens without simulated cracks.

Steel Designation[a]	Exposure Time (weeks)	Test Bar				Average[b]	Standard Deviation
		1	2	3	4		
Controls							
ECR (1)	250	9.25	27.0			18.1	12.6
ECR (2)	254	6.27	3.29	-2.04[c]	1.62	3.73	2.36
Bars with increased adhesion							
ECR(Chromate) (1)	250	5.72	5.02			5.37	0.498
ECR(Chromate) (2)	254	18.4	-16.5[c]	-2.34[c]	9.93	14.2	5.99
ECR(DuPont) (1)	250	11.1	5.57			8.32	3.90
ECR(DuPont) (2)	254	6.39	2.87	4.47	14.4	7.03	5.10
ECR(Valspar) (1)	250	3.49	9.18			6.33	4.02
ECR(Valspar) (2)	254	9.72	-3.49[c]	38.9	16.0	21.5	15.4
Corrosion inhibitors in concrete							
ECR(DCI) (1)	250	12.2	14.8	7.57	11.9	11.6	3.00
ECR(DCI) (2)	254	24.1	37.7	17.5	6.46	21.4	13.1
ECR(DCI) (3)	254	13.8	13.3	2.59	9.00	9.66	5.18
ECR(RH) (1)	250	26.6	18.7	6.06	17.6	17.3	8.47
ECR(RH) (2)	254	-1.34[c]	-3.12[c]	-1.69[c]	11.2	11.2	–
ECR(HY) (1)	250	-0.458[c]	1.25	4.42	18.3	7.99	9.07
ECR(HY) (2)	254	8.59	6.69	13.1	9.76	9.52	2.67
ECR(primer/Ca(NO$_2$)$_2$) (1)	250	-0.141[c]	7.73	12.9	11.0	10.5	2.62
ECR(primer/Ca(NO$_2$)$_2$) (2)	254	27.1	11.6	9.53	17.9	16.5	7.91
Bars with multiple coatings							
MC (1)	250	9.54	8.81			9.17	0.515
MC (2)	254	18.4	2.94	2.89	18.9	10.8	9.10

1 μm = 0.0394 mil

– No standard deviation.

Blank cells indicate that the test bar was not present.

[a] See table 1 for abbreviation definitions. All epoxy-coated bars are penetrated with 16 surface holes.

[b] Based on top mat only.

[c] Excluded from average.

Table 26. Corrosion loss at end of field tests (µm) based on total area for specimens with simulated cracks.

Steel Designation[a]	Exposure time (weeks)	Test Bar				Average[b]	Standard Deviation
		1	2	3	4		
Controls							
Conv. (1)	250	2.26	6.71			4.49	3.14
Conv. (2)	254	4.01	3.34			3.68	0.475
ECR (1)	250	0.015	0.065			0.040	0.035
ECR (2)	254	0.056	0.171	0.044	0.042	0.078	0.062
Bars with increased adhesion							
ECR(Chromate) (1)	250	0.039	0.030			0.035	0.006
ECR(Chromate) (2)	254	0.099	0.066	0.051	0.061	0.069	0.021
ECR(DuPont) (1)	250	0.026	0.050			0.038	0.017
ECR(DuPont) (2)	254	0.048	0.029	0.066	0.234	0.094	0.095
ECR(Valspar) (1)	250	0.071	0.177			0.124	0.075
ECR(Valspar) (2)	254	0.023	0.064	0.018	0.153	0.064	0.062
Corrosion inhibitors in concrete							
ECR(DCI) (1)	250	0.043	0.065	0.079	0.072	0.065	0.015
ECR(DCI) (2)	254	0.023	0.041	0.074	0.064	0.050	0.023
ECR(DCI) (3)	254	0.105	0.124	0.004	0.020	0.063	0.060
ECR(RH) (1)	250	0.073	0.084	0.038	0.059	0.063	0.020
ECR(RH) (2)	254	0.066	0.057	0.073	0.074	0.068	0.007
ECR(HY) (1)	250	0.044	0.019	0.008	-0.006[c]	0.024	0.018
ECR(HY) (2)	254	0.005	0.020	-0.006[c]	-0.004[c]	0.013	0.011
ECR(primer/Ca(NO$_2$)$_2$) (1)	250	0.006	0.017	0.046	0.009	0.019	0.018
ECR(primer/Ca(NO$_2$)$_2$) (2)	254	0.016	0.043	0.041	0.067	0.042	0.021
Bars with multiple coatings							
MC (1)	250	0.044	0.056			0.050	0.008
MC (2)	254	0.074	0.061	0.074	0.021	0.057	0.025

1 µm = 0.0394 mil

Blank cells indicate that the test bar was not present.

[a] See table 1 for abbreviation definitions. All epoxy-coated bars are penetrated with 16 surface holes.

[b] Based on top mat only.

[c] Excluded from average.

Table 27. Corrosion loss at end of field tests (µm) based on area exposed at holes through coating for specimens with simulated cracks.

Steel Designation[a]	Exposure time (weeks)	Test Bar				Average[b]	Standard Deviation
		1	2	3	4		
Controls							
ECR (1)	250	5.72	25.2			15.5	13.8
ECR (2)	254	21.9	66.8	17.1	16.4	30.6	24.3
Bars with increased adhesion							
ECR(Chromate) (1)	250	15.3	11.7			13.5	2.52
ECR(Chromate) (2)	254	38.7	25.9	19.9	23.7	27.1	8.16
ECR(DuPont) (1)	250	10.2	19.6			14.9	6.64
ECR(DuPont) (2)	254	18.7	11.3	25.6	91.4	36.8	36.9
ECR(Valspar) (1)	250	27.8	69.2			48.5	29.3
ECR(Valspar) (2)	254	8.9	24.9	7.06	59.6	25.1	24.4
Corrosion inhibitors in concrete							
ECR(DCI) (1)	250	16.8	25.3	30.7	28.1	25.2	6.02
ECR(DCI) (2)	254	9.00	15.9	28.9	24.9	19.7	8.96
ECR(DCI) (3)	254	40.9	48.5	1.48	7.96	24.7	23.4
ECR(RH) (1)	250	28.3	32.7	14.8	23.0	24.7	7.70
ECR(RH) (2)	254	25.9	22.4	28.4	28.7	26.4	2.92
ECR(HY) (1)	250	17.2	7.31	3.31	-2.47[c]	9.27	7.15
ECR(HY) (2)	254	1.95	7.85	-2.24[c]	-1.55[c]	4.90	4.17
ECR(primer/Ca(NO$_2$)$_2$) (1)	250	2.27	6.55	18.0	3.59	7.59	7.14
ECR(primer/Ca(NO$_2$)$_2$) (2)	254	6.38	16.8	16.0	26.0	16.3	8.00
Bars with multiple coatings							
MC (1)	250	17.1	21.8			19.5	3.32
MC (2)	254	28.9	23.8	28.7	8.24	22.4	9.75

1 µm = 0.0394 mil

Blank cells indicate that the test bar was not present.

[a] See table 1 for abbreviation definitions. All epoxy-coated bars are penetrated with 16 surface holes.

[b] Based on top mat only.

[c] Excluded from average.

Control Specimens

As with the bench-scale tests, the control specimens for the field tests consisted of conventional reinforcement and conventional ECR cast in concrete without and with cracks. Due to the more realistic, milder exposure conditions obtained in the field, the corrosion rates were about one-fourth those observed in the bench-scale tests. The average corrosion losses based on exposed area for the control specimens without and with simulated cracks over the top bars are shown in figure 117 over a period of 250 weeks. The losses for the conventional ECR specimens are shown in figure 118. Uncracked specimens are denoted with a "U" and cracked specimens are denoted with a "C" in the figures. The graphs show that specimens with cracks began to corrode earlier and at a higher rate than those with intact concrete and that the ECR bars corroded at a much slower rate than conventional reinforcement. Based on total bar area, average losses at 250 weeks ranged from 3.99 µm (0.157 mil) for conventional steel specimens with cracks and 1.86 µm (0.0732 mil) for

conventional steel specimens without cracks to less than 0.055 µm (0.0022 mil) for ECR specimens. Based on exposed area, the ECR specimens exhibited losses of 10.7 and 22.1 µm (0.421 and 0.870 mil) at 250 weeks for specimens without and with simulated cracks, respectively. As shown in figure 118, the specimens without cracks exhibited negative corrosion between weeks 72 and 152, at which point the net losses became positive. Based on the shape of the curve, corrosion appears to have initiated, on average, at week 144. In contrast, the specimens with simulated cracks exhibited corrosion initiation at week 76.
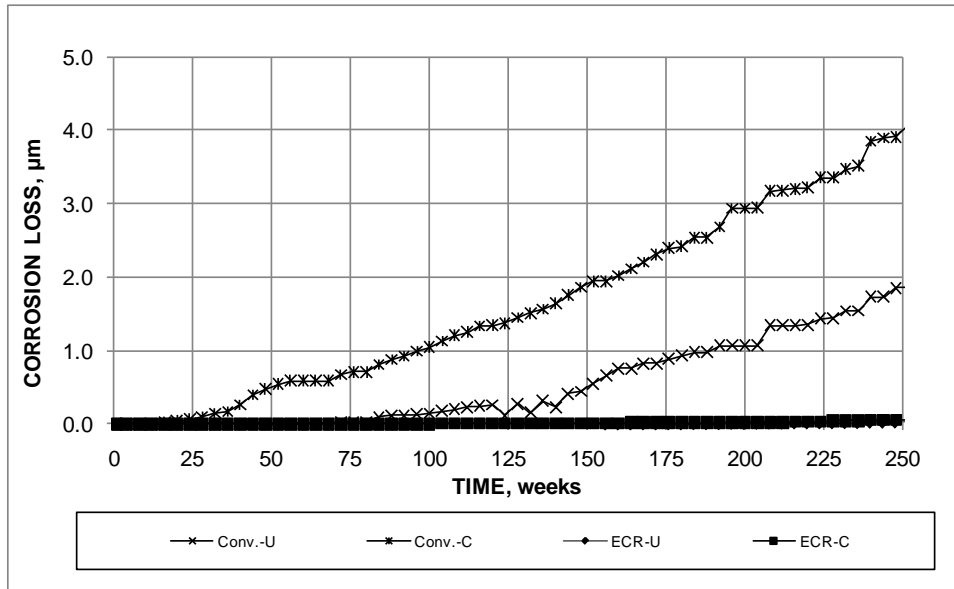
1 µm = 0.0394 mil

Figure 117. Graph. Field test, average corrosion loss based on total area for conventional reinforcement and ECR.
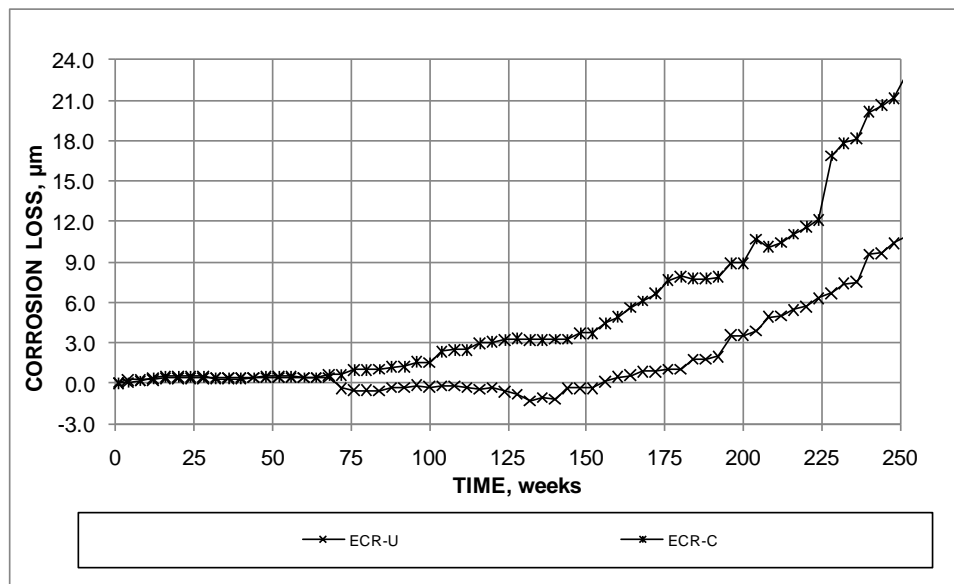
1 µm = 0.0394 mil

Figure 118. Graph. Field test, average corrosion loss based on exposed area for ECR.

115

The average corrosion potentials for the top and bottom bar mats are shown in figure 119 and figure 120, respectively, with the potentials cycling between high and low values as the moisture content and temperature conditions of the specimens varied. The top bars had average corrosion potentials more negative than -0.350 V with respect to a CSE with the exception of the ECR specimens without simulated cracks. As shown in figure 120, the corrosion potentials of the bars in the bottom mats remained above -0.350 V with the exception of the conventional steel specimens with cracks at week 112.
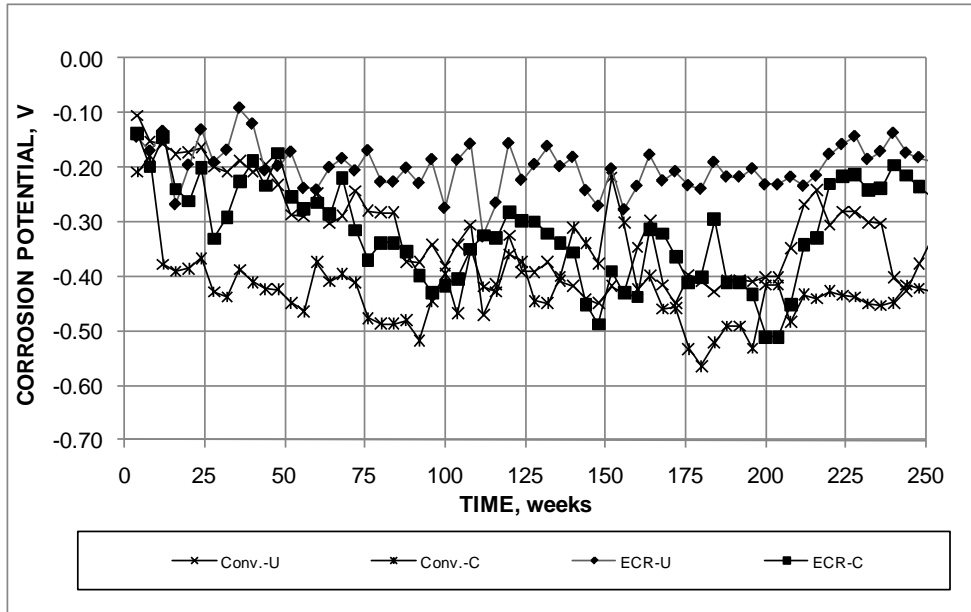
Figure 119. Graph. Field test, corrosion potential of top mat for conventional reinforcement and ECR.
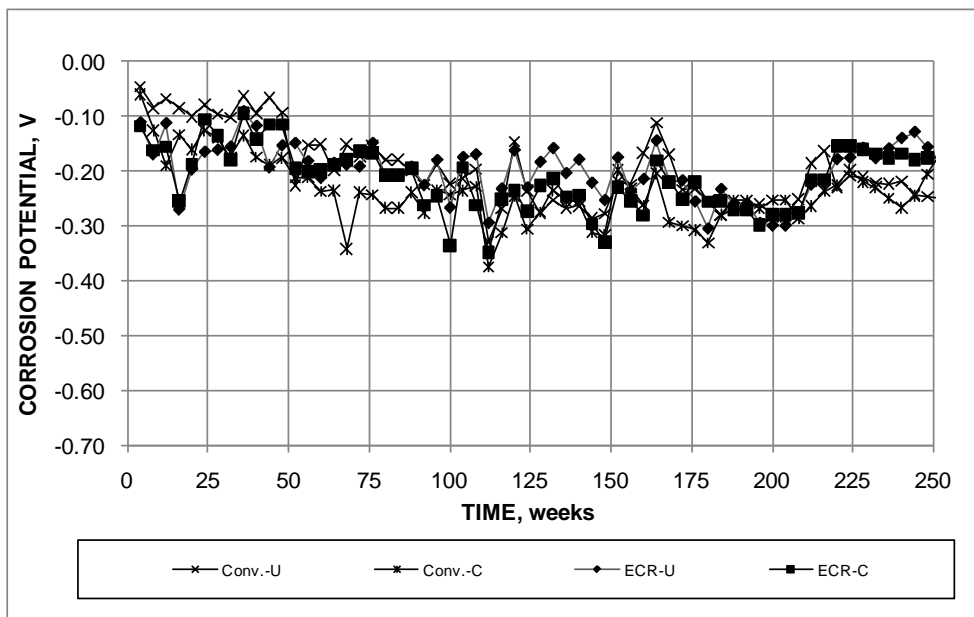
Figure 120. Graph. Field test, corrosion potential of bottom mat for conventional reinforcement and ECR.

116

Epoxies with Improved Adhesion

The corrosion performance of the bars with improved adhesion epoxies, ECR(Valspar), ECR(DuPont), and ECR(Chromate), is compared to that of the conventional ECR in figure 121 and figure 122 based on exposed area for field test specimens without and with simulated cracks, respectively. A comparison of the two figures shows that the corrosion rate of the specimens with simulated cracks was 3 to 5 times the value for specimens without cracks. The results also indicate little difference in the performance of the specimens based on average corrosion loss, although, as shown in table 24 through table 27, significant scatter is evident between results for individual specimens for both uncracked and cracked specimens. At 250 weeks, ECR(Valspar) exhibited the highest average corrosion losses, 12.8 and 36.5 μm (0.504 and 1.44 mil), while ECR(DuPont) exhibited the lowest loss for uncracked specimens, 3.75 μm (0.148 mil) and ECR(Chromate) exhibited the lowest loss for cracked specimens, 20.1 μm (0.791 mil). Considering the very low corrosion losses based on total bar area, however, there is little practical difference in behavior as a function of the degree of adhesion between the epoxy coating and the underlying steel. As observed for the bench-scale specimens and in other studies, the results demonstrate that improved performance in the cathodic disbondment test does not correlate with improved corrosion performance.[16]
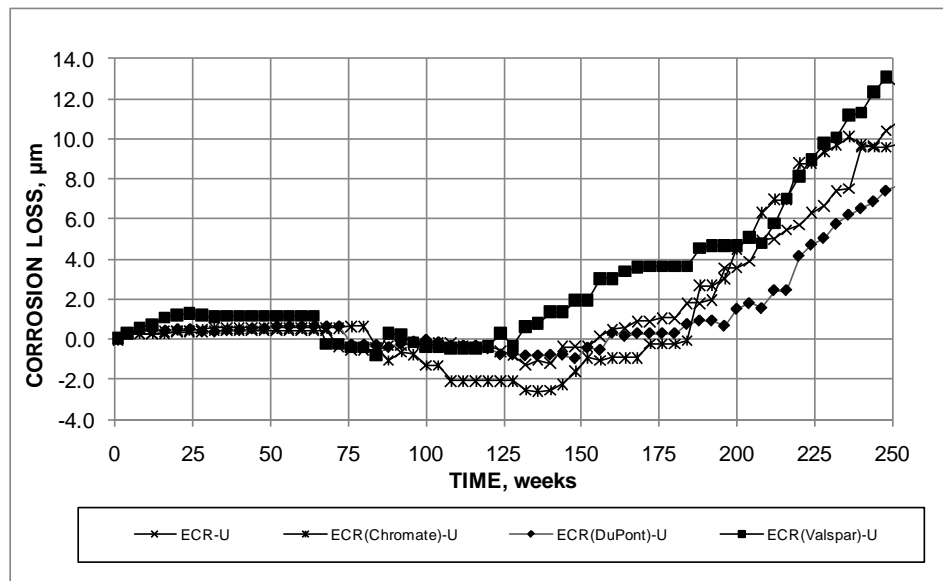
1 μm = 0.0394 mil

Figure 121. Graph. Field test, average corrosion losses based on area exposed at holes through coating for conventional and increased-adhesion ECR without simulated cracks.
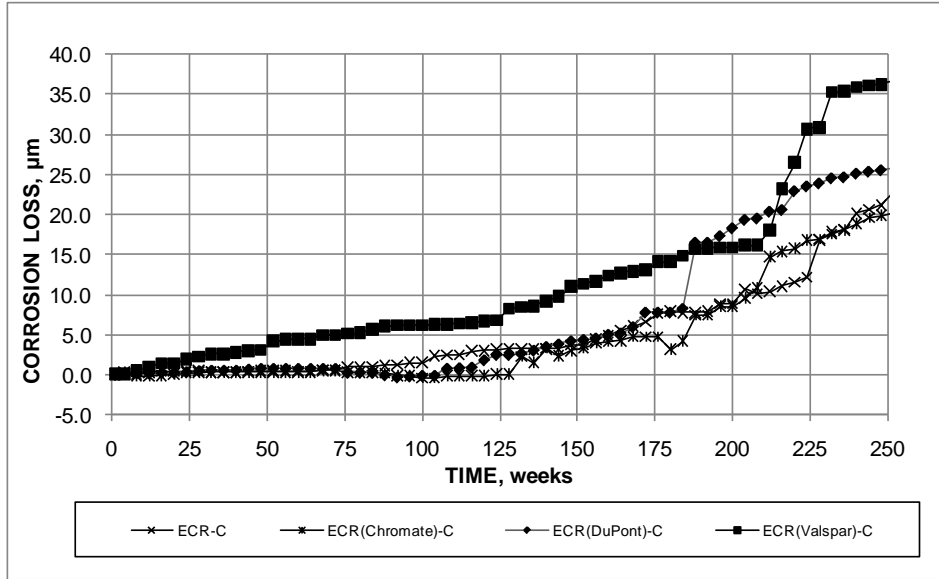
1 µm = 0.0394 mil

Figure 122. Graph. Field test, average corrosion losses based on area exposed at holes through coating for conventional and increased-adhesion ECR with simulated cracks.

The average corrosion potentials for the top and bottom mats of reinforcement in specimens without cracks are shown in figure 123 and figure 124. None of the top bars exhibited a potential more negative than -0.350 V at any time during the test, and only one bottom mat, ECR(Chromate) at week 100, reached an average corrosion potential more negative than -0.350 V. In contrast, figure 125 and figure 126 show that all of the epoxy-coated bars in specimens with simulated cracks reached corrosion potentials more negative than -0.350 V by week 72. The corrosion potentials of the bottom mats of steel for the same specimens were generally more positive than -0.350 V, but at some point during the tests, all bottom mats reached average corrosion potentials below that value.
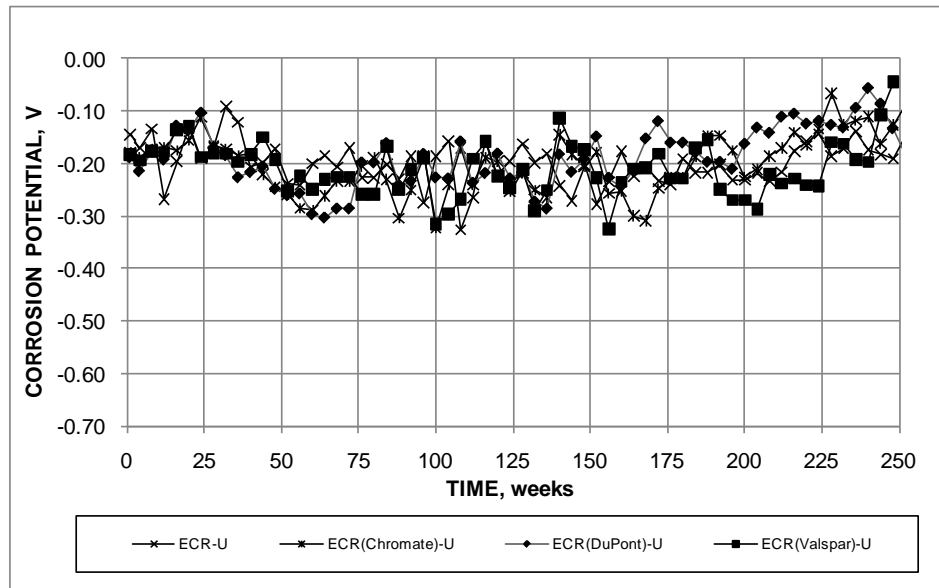
Figure 123. Graph. Field test, corrosion potential of top mat for conventional and increased-adhesion ECR without simulated cracks.

118
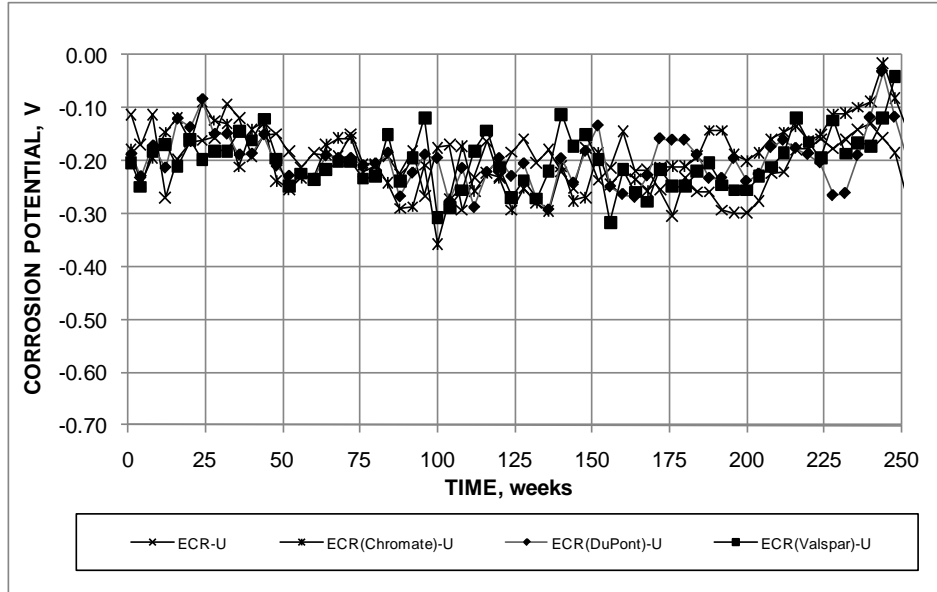
Figure 124. Graph. Field test, corrosion potential of bottom mat for conventional and increased-adhesion ECR without simulated cracks.
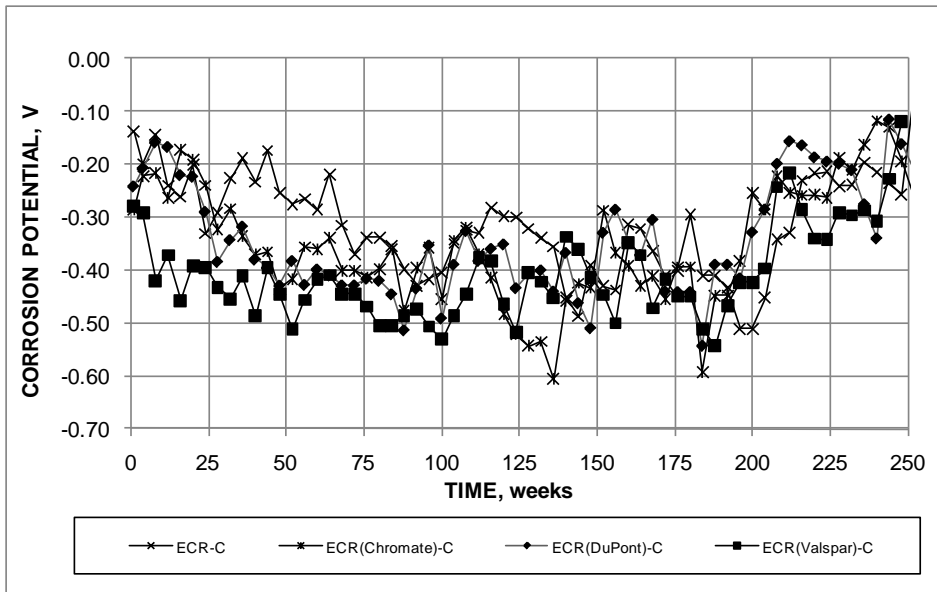
Figure 125. Graph. Field test, corrosion potential of top mat for conventional and increased-adhesion ECR with simulated cracks.

119
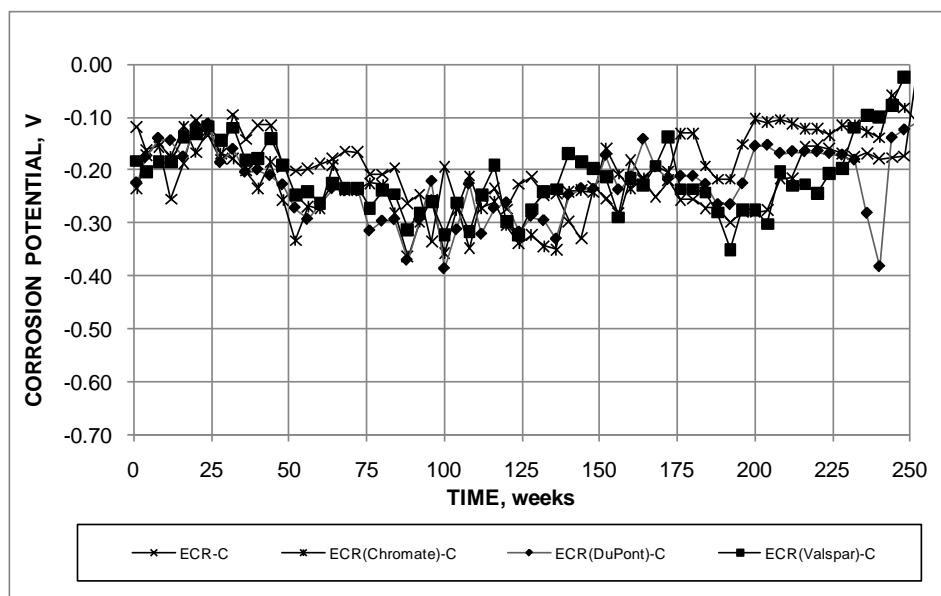
Figure 126. Graph. Field test, corrosion potential of bottom mat for conventional and increased-adhesion ECR with simulated cracks.

Overall, the corrosion potentials of the bottom and top mats of steel became progressively more positive during the last 50 weeks of the test, perhaps because the deposition of corrosion products at some of the penetrations limited access of oxygen and moisture. It is not clear that the changes in potential translated into a change in corrosion rate, although the corrosion rates (based on the slope of the corrosion loss curves) during the last 25 to 50 weeks are, in most cases, below the average rate of corrosion over the final 100 weeks of the test.

ECR Used in Conjunction with Corrosion Inhibitors

Average corrosion losses based on exposed area for conventional ECR cast in concrete without a corrosion inhibitor and cast in concrete with calcium nitrite, Rheocrete® 222+, and Hycrete™, as well as bars with microencapsulated calcium nitrite primer are shown in figure 127 and figure 128.

At 250 weeks for specimens without simulated cracks, the ECR(HY) specimens exhibited the lowest average corrosion loss based on exposed area, 8.2 µm (0.32 mil), while ECR(RH) exhibited the highest loss, 14.2 µm (0.559 mil). Several bars exhibited negative corrosion values, with ECR(RH) exhibiting a negative loss as late as week 172. Based on the slope of the corrosion loss curves, however, it appears that all specimens were undergoing corrosion by week 124. With the exception of specimens containing Hycrete™, the specimens containing corrosion inhibitors exhibited chloride contents 1.5 to 2 times that exhibited by the concrete in the specimens with conventional ECR (see table 23). The difference is likely a function of the higher w/c ratios of the specimens containing a corrosion inhibitor (see table 7).

As shown in figure 128, the specimens with simulated cracks exhibited a wider range in corrosion loss than those without cracks. The ECR(HY) specimens exhibited the lowest average corrosion loss at 250 weeks, 8.04 µm (0.317 mil), based on exposed area, followed by the ECR(primer/Ca(NO$_2$)$_2$) specimens at 11.93 µm (0.4697 mil) (very close to the value observed in the ECR(primer/Ca(NO$_2$)$_2$) specimens without cracks) and then by the ECR, ECR(DCI), and ECR(RH) specimens, with average losses of 22.1, 23.0, and 23.6 µm (0.870, 0.906, and 0.929 mil), respectively.

120
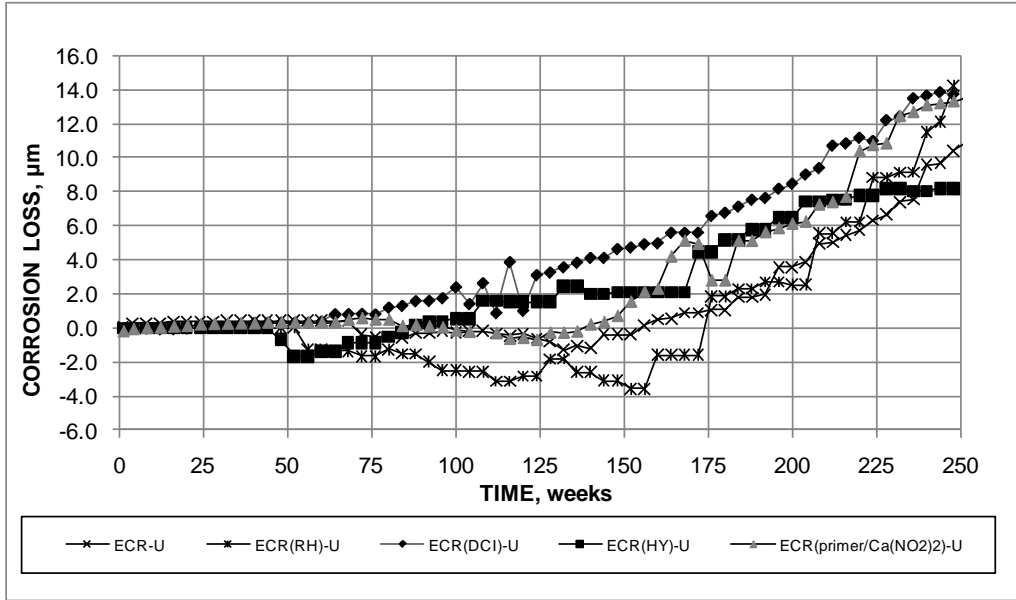
1 µm = 0.0394 mil

Figure 127. Graph. Field test, average corrosion losses based on area exposed at holes through coating for conventional ECR without and with corrosion inhibitors and without simulated cracks.
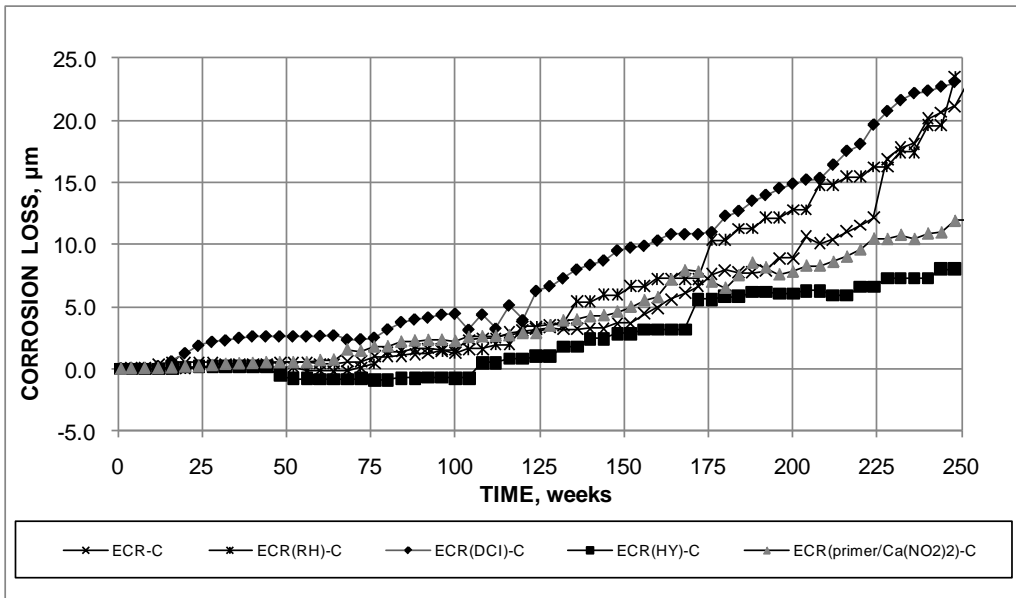
1 µm = 0.0394 mil

Figure 128. Graph. Field test, average corrosion losses based on area exposed at holes through coating for conventional ECR without and with corrosion inhibitors and with simulated cracks.

The corrosion potentials for specimens without simulated cracks are shown in figure 129 and figure 130, and the corrosion potentials for specimens with simulated cracks are shown in figure 131 and figure 132. For the specimens without simulated cracks, the corrosion potentials of the top mats of steel remained more positive than -0.350 V for ECR, ECR(DCI), ECR(HY), and ECR(RH)

throughout the tests while dropping below -0.350 V for ECR(primer/Ca(NO$_2$)$_2$) for two readings during the 250-week test period. The corrosion potential of the bottom mat of reinforcement was more positive than -0.350 V in all cases. Once again, in contrast to uncracked concrete, the corrosion potentials in the top mats for all systems in specimens with simulated cracks were more negative than -0.350 V during the test. For the bottom mat, the corrosion potential was more negative than -0.350 V only for ECR(RH) and only between weeks 160 and 172.
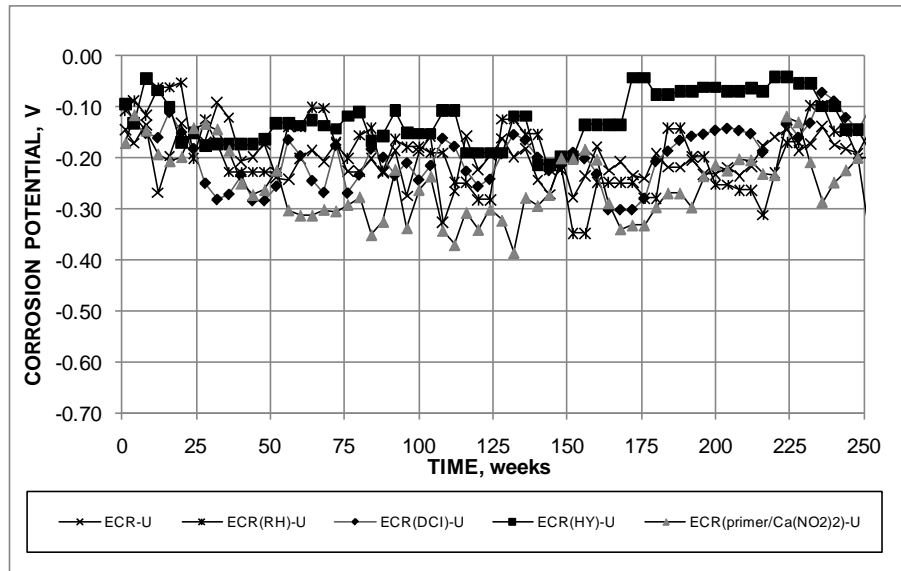
Figure 129. Graph. Field test, corrosion potential of top mat for conventional ECR without and with corrosion inhibitors and without simulated cracks.
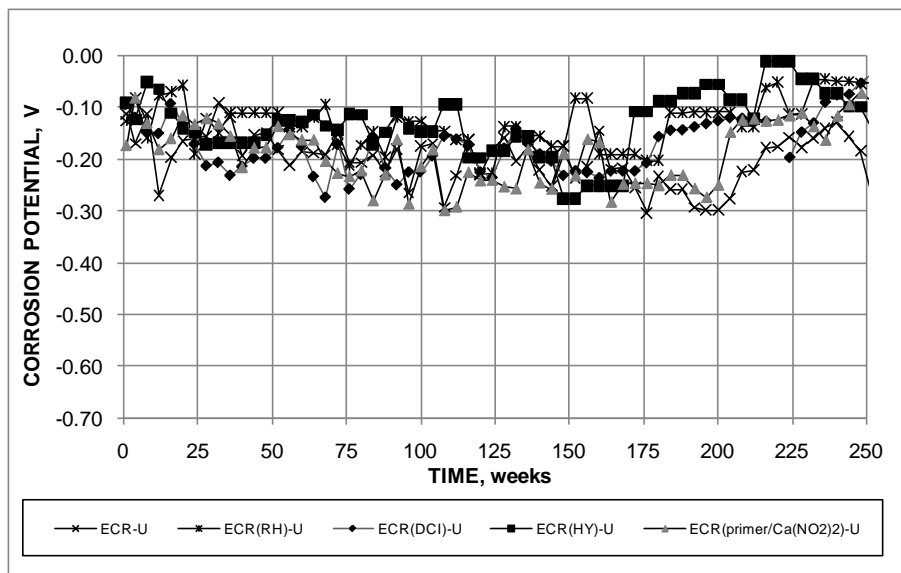
Figure 130. Graph. Field test, corrosion potential of bottom mat for conventional ECR without and with corrosion inhibitors and without simulated cracks.

122
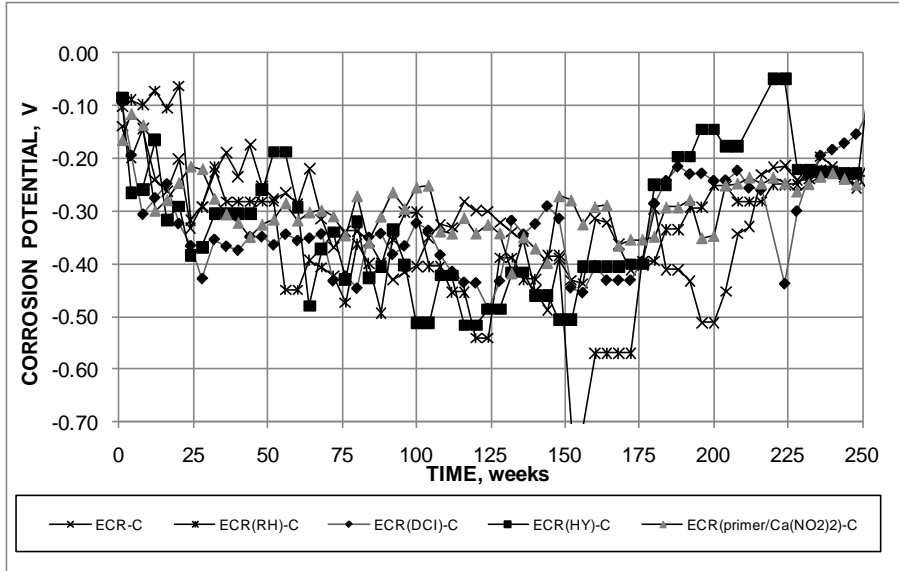
Figure 131. Graph. Field test, corrosion potential of top mat for conventional ECR without and with corrosion inhibitors and with simulated cracks.
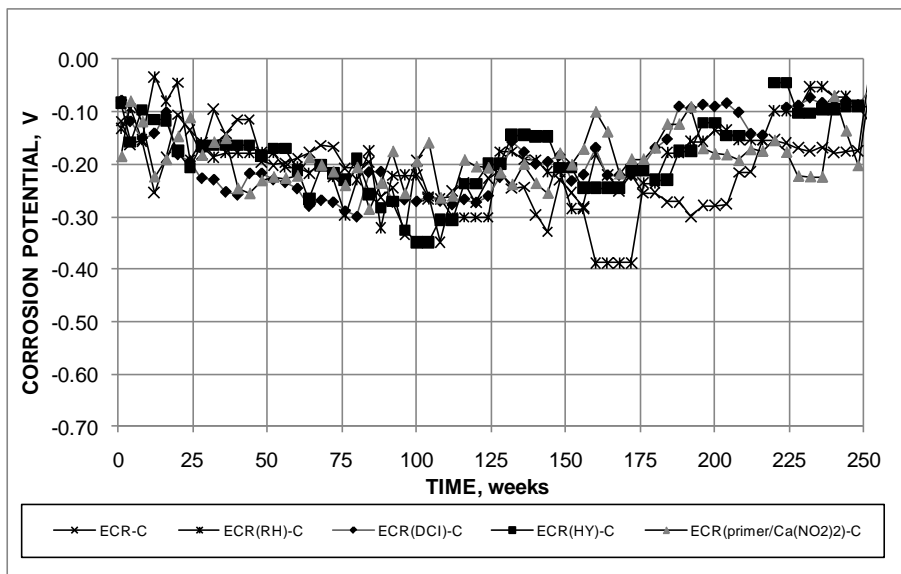
Figure 132. Graph. Field test, corrosion potential of bottom mat for conventional ECR without and with corrosion inhibitors and with simulated cracks.

Bars with Multiple Coatings

The corrosion losses for the bars with multiple coatings are compared with those for conventional ECR in figure 133 and figure 134 for bars without and with simulated cracks over the reinforcement, respectively. The hole through the coatings on the MC bars in the field tests penetrated both the zinc and the epoxy layers. Unlike the results observed for the bench-scale tests, where the MC bars exhibited significantly more corrosion than the conventional ECR bars, the corrosion losses for the MC bars were slightly below those for the ECR bars in the field test, with average corrosion losses at 250 weeks of 10.0 and 10.7 μm (0.394 and 0.421 mil) for MC and ECR bars, respectively, in

123

specimens without cracks and 20.1 and 22.1 μm (0.791 and 0.870 mil), respectively, for MC and ECR bars in specimens with simulated cracks over the bars. The relative behavior of the MC bars in the field and bench-scale tests suggests that MC reinforcement performs much like conventional ECR under exposure conditions similar to those in bridge decks, even providing an advantage since the initial losses represent corrosion of the zinc coating rather than the underlying steel, but will provide no significant advantage in cases where the concrete is often saturated, such as in marine environments.
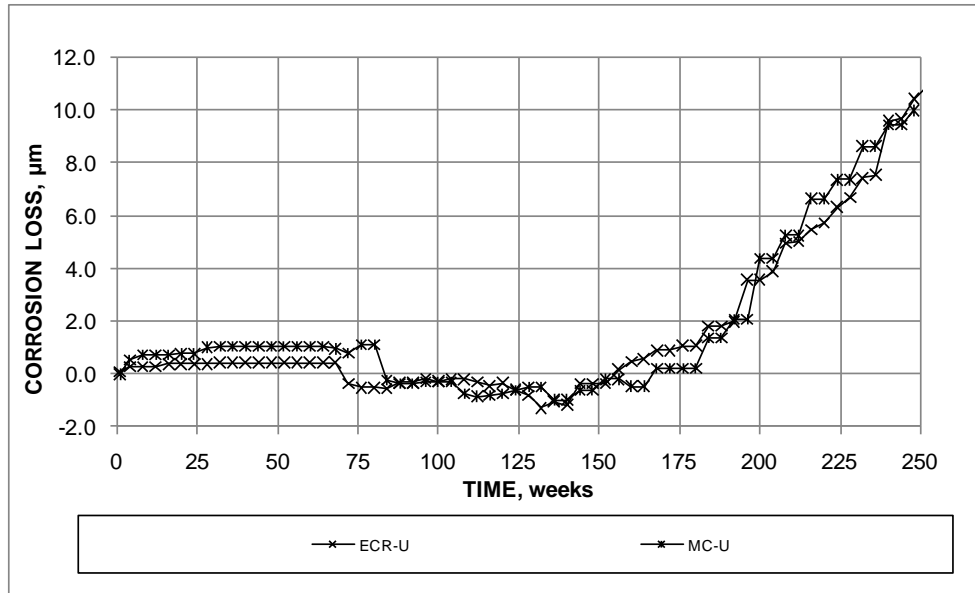
1 μm = 0.0394 mil

Figure 133. Graph. Field test, average corrosion losses based on area exposed at holes through coating for conventional ECR and MC reinforcement without simulated cracks.
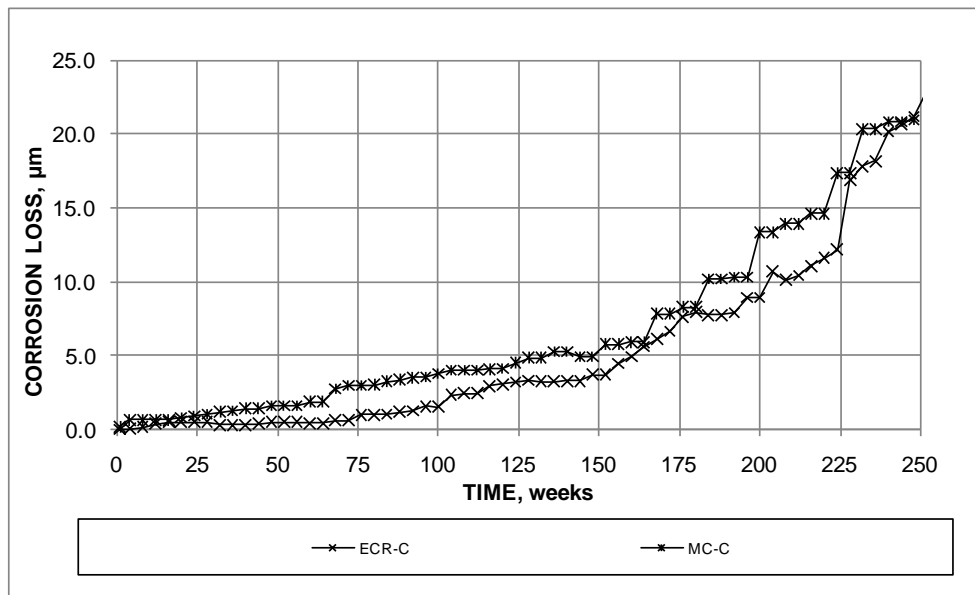
1 μm = 0.0394 mil

Figure 134. Graph. Field test, average corrosion losses based on area exposed at holes through coating for conventional ECR and MC reinforcement with simulated cracks.

124

The corrosion potentials for specimens without and with cracks are shown in figure 135 through figure 138. The corrosion potentials were initially more negative than -0.350 V for the top mats of steel for MC bars in specimens both without and with simulated cracks and somewhat more negative (-0.500 V) for specimens with cracks than those without cracks (-0.400 V).
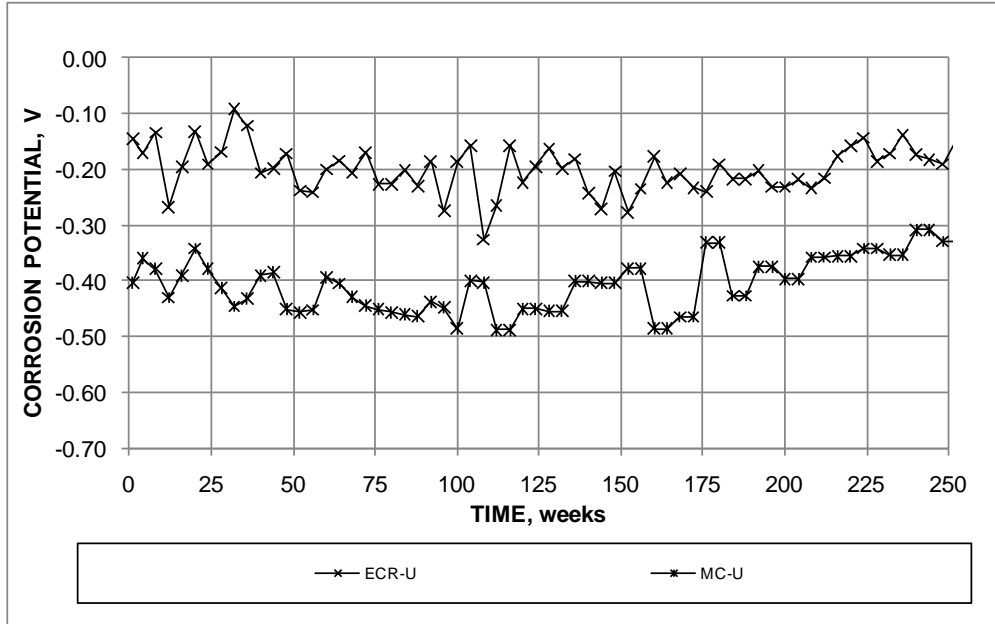
Figure 135. Graph. Field test, corrosion potential of top mat for conventional ECR without and with corrosion inhibitors and without simulated cracks.
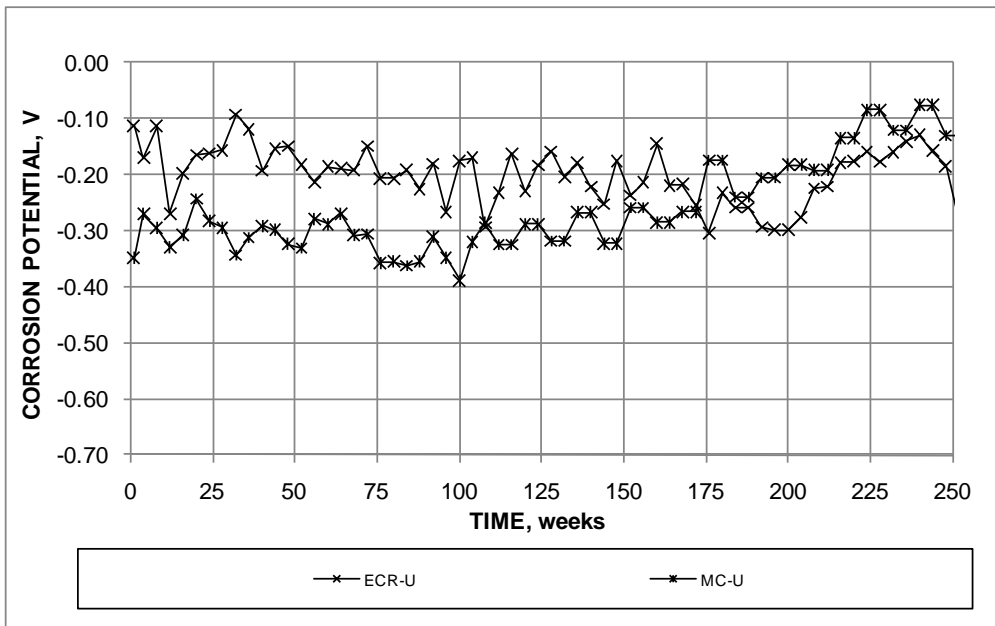
Figure 136. Graph. Field test, corrosion potential of bottom mat for conventional ECR without and with corrosion inhibitors and without simulated cracks.

125
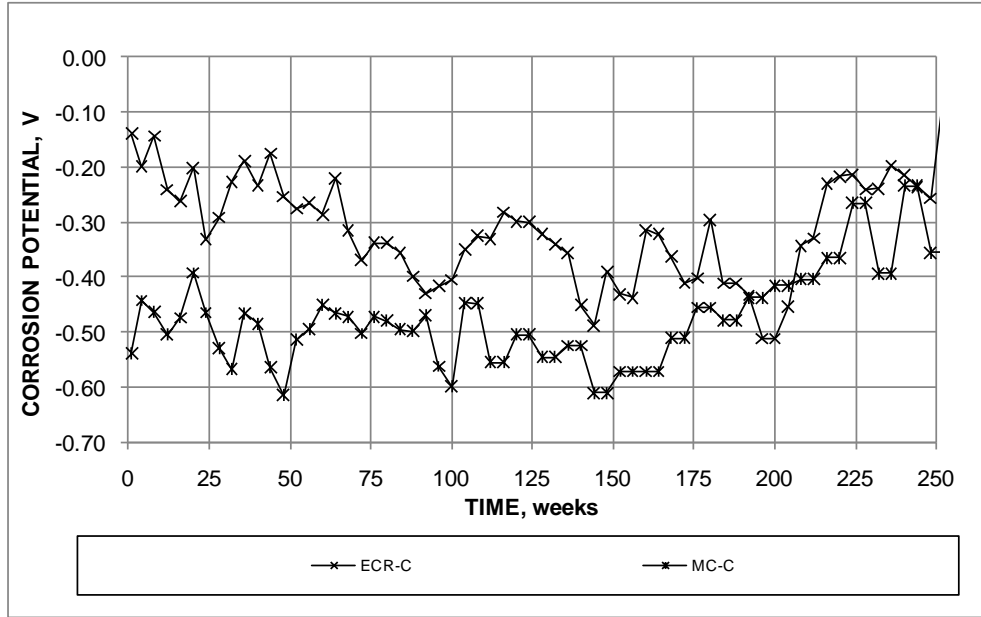
Figure 137. Graph. Field test, corrosion potential of top mat for conventional ECR without and with corrosion inhibitors and with simulated cracks.
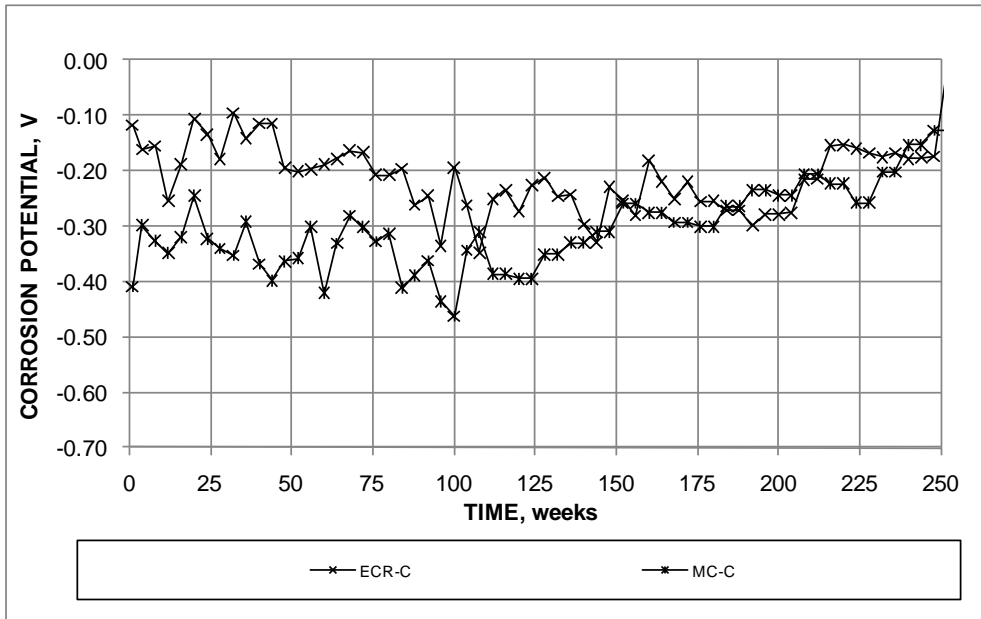
Figure 138. Graph. Field test, corrosion potential of bottom mat for conventional ECR without and with corrosion inhibitors and with simulated cracks.

The top mat corrosion potential for specimens both without and with cracks became more positive toward the end of tests, reaching values in the range of -0.300 to -0.350 V. The corrosion potential of the bottom mats of steel started close to -0.350 V for specimens both without and with simulated cracks, rising to values more positive than -0.150 V by the end of the 250-week test. This behavior suggests that the zinc exposed at the penetrations through the coating dominated the behavior early in the test, but the effect diminished by the end of the test period, with the underlying steel dominating the behavior of the bottom mat.

126

Corrosion Rates Based on Losses After Corrosion Initiation

The average corrosion rates based on losses after corrosion initiation are summarized in table 28 and table 29 for field test specimens without and with simulated cracks, respectively. The rates are expressed in terms of total area for bars without coatings and in terms of exposed area for bars with coatings. The rates shown in the tables provide a good representation of corrosion rates expected in bridge decks because both the exposure conditions and structural design of the specimens closely match those of bridge decks in Kansas.

Table 28. Average corrosion rate (μm/year) based on losses after corrosion initiation for field test specimens without simulated cracks.

Steel Designation[a]	Specimen	Bar 1	Bar 2	Bar 3	Bar 4	Average	Standard Deviation
Bars without coatings—corrosion rate based on total area							
Controls							
Conv.	1	1.55	0.77			0.882	0.62
	2	b	0.322				
Bars with coatings—corrosion rate based on exposed area							
Controls							
ECR	1	9.86	10.1			5.68	4.21
	2	0.587	4.90	b	2.97		
Bars with increased adhesion							
ECR(Chromate)	1	4.86	2.50			4.83	3.35
	2	10.4	b	1.97	4.40		
ECR(DuPont)	1	5.35	2.95			5.14	5.99
	2	0.710	5.35	1.41	17.0		
ECR(Valspar)	1	2.38	9.77			9.11	4.90
	2	15.0	b	12.0	6.39		
Corrosion inhibitors in concrete							
ECR(DCI)	1	3.58	3.69	1.64	2.73	4.26	2.81
	2	6.62	10.3	4.95	1.41		
	3	4.47	7.86	0.904	2.96		
ECR(RH)	1	10.2	5.24	6.49	3.97	5.43	3.68
	2	1.49	0.856	b	9.72		
ECR(HY)	1	1.82	b	1.75	6.09	2.89	1.62
	2	1.52	3.74	3.11	2.18		
ECR(primer/Ca(NO$_2$)$_2$)	1	b	1.89	4.25	2.60	4.49	2.95
	2	10.3	3.78	2.36	6.22		
Bars with multiple coatings							
MC	1	5.54	6.58			6.31	3.39
	2	11.9	6.35	1.29	6.68		

1 μm = 0.0394 mil

Blank cells indicate that the test bar was not present.

[a] See table 1 for abbreviation definitions.

[b] No corrosion observed.

Table 29. Average corrosion rate (µm/year) based on losses after corrosion initiation for field test specimens with simulated cracks.

Steel Designation[a]	Specimen	Bar 1	Bar 2	Bar 3	Bar 4	Average	Standard Deviation
Bars without coatings—corrosion rate based on total area							
Controls							
Conv.	1	0.482	1.65			0.939	0.61
	2	0.897	0.731				
Bars with coatings—corrosion rate based on exposed area							
Controls							
ECR	1	2.91	10.3			8.13	7.82
	2	5.76	22.6	4.58	5.72		
Bars with increased adhesion							
ECR(Chromate)	1	5.06	5.79			8.94	8.65
	2	25.6	6.43	6.31	11.4		
ECR(DuPont)	1	3.79	5.72			6.50	4.05
	2	10.8	2.30	12.8	7.10		
ECR(Valspar)	1	3.76	11.6			7.64	4.93
	2	7.19	16.5	8.46	1.99		
Corrosion inhibitors in concrete							
ECR(DCI)	1	3.20	4.97	8.67	8.22	5.79	3.60
	2	1.62	10.1	7.52	5.51		
	3	0.634	0.500	7.95	10.6		
ECR(RH)	1	9.92	8.34	6.07	7.74	8.38	1.64
	2	11.2	8.38	7.68	7.78		
ECR(HY)	1	6.12	2.06	12.0	[b]	4.32	4.31
	2	2.12	2.28	[b]	1.36		
ECR(primer/Ca(NO₂)₂)	1	9.28	2.22	4.75	[b]	4.65	2.13
	2	1.78	4.25	3.90	6.40		
Bars with multiple coatings							
MC	1	5.64	10.9			8.11	5.29
	2	1.47	5.89	6.40	14.2		

1 µm = 0.0394 mil

Blank cells indicate that the test bar was not present.

[a] See table 1 for abbreviation definitions.

[b] No corrosion observed.

Mat-to-Mat Resistance

The average mat-to-mat resistance results for the field test specimens are shown in figure 139 though figure 145. Uncracked specimens are denoted with a "U" and cracked specimens are denoted with a "C" in the figures. As observed in figure 53 for the southern exposure specimens, the high resistance provided by the epoxy coating was also apparent for the field test specimens, as shown in figure 139, which compares mat-to-mat resistance for conventional reinforcement and conventional ECR in specimens without and with simulated cracks. The highest resistances were exhibited by ECR in concrete containing corrosion inhibitors Rheocrete® and Hycrete™, as shown in figure 142 and figure 143.
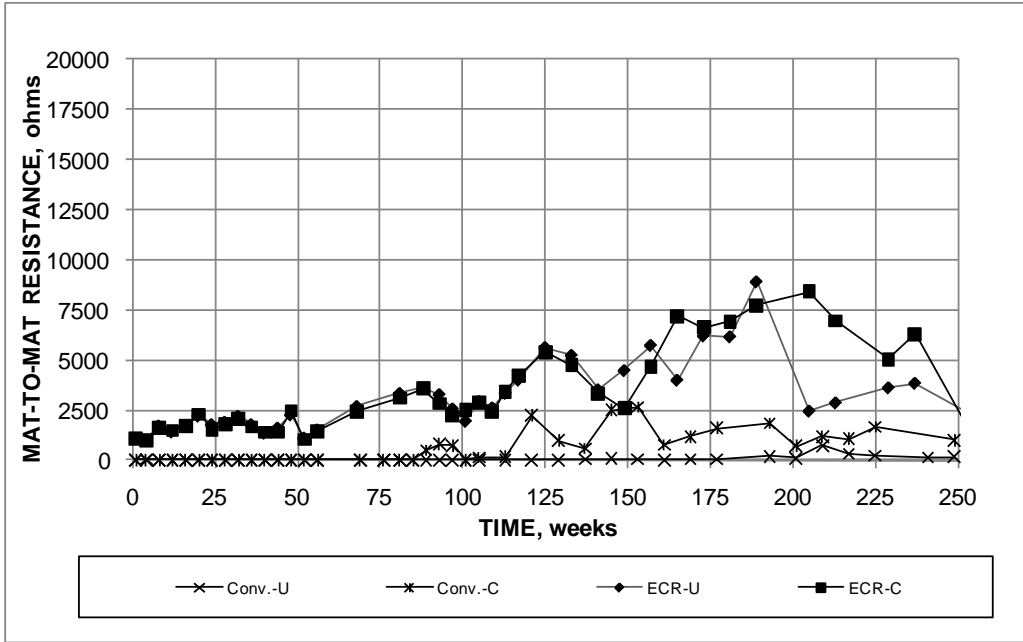
Figure 139. Graph. Field test, mat-to-mat resistance for conventional reinforcement and ECR.
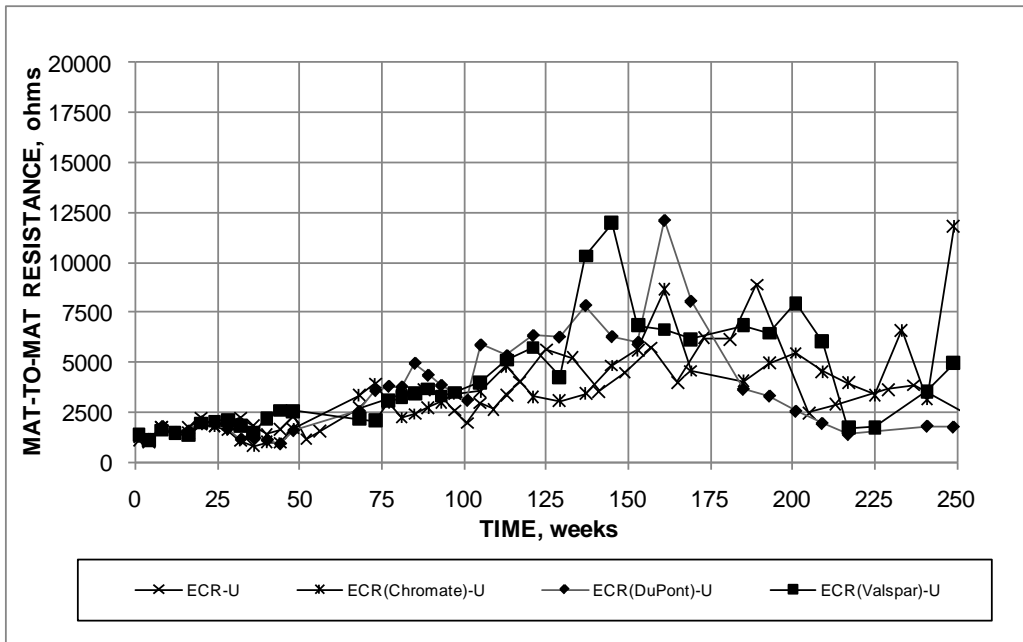
Figure 140. Graph. Field test, mat-to-mat resistance for conventional and increased-adhesion ECR without simulated cracks.
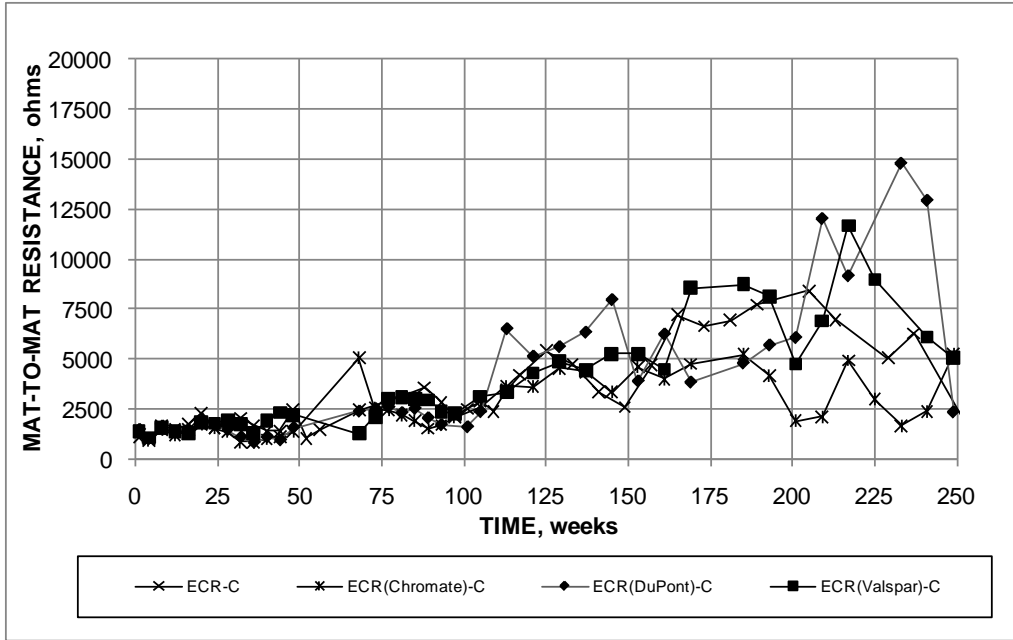
Figure 141. Graph. Field test, mat-to-mat resistance for conventional and increased-adhesion ECR with simulated cracks.
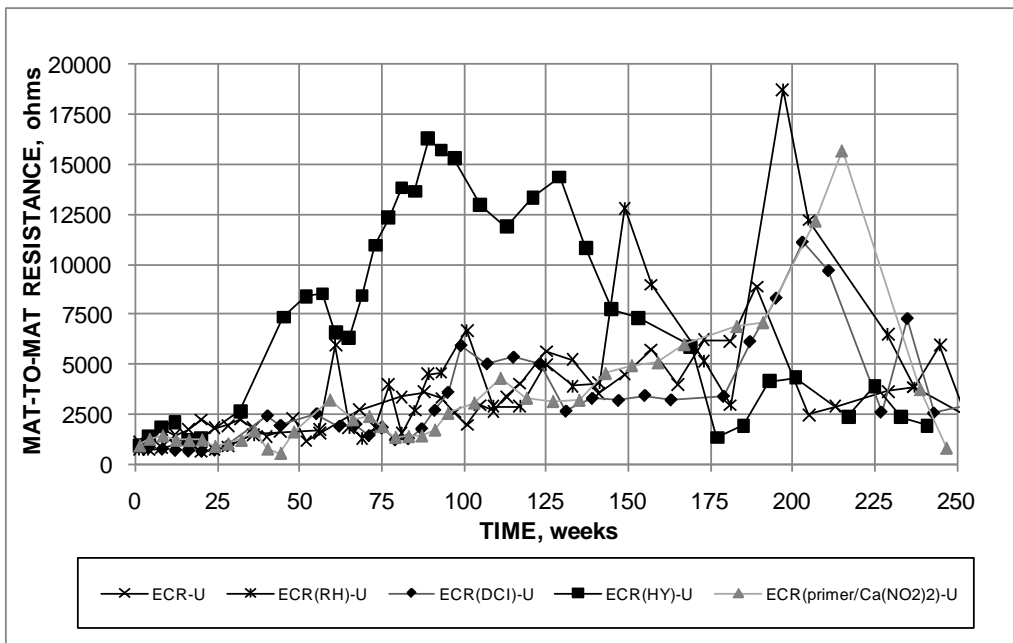
Figure 142. Graph. Field test, mat-to-mat resistance for conventional ECR without and with corrosion inhibitors and without simulated cracks.
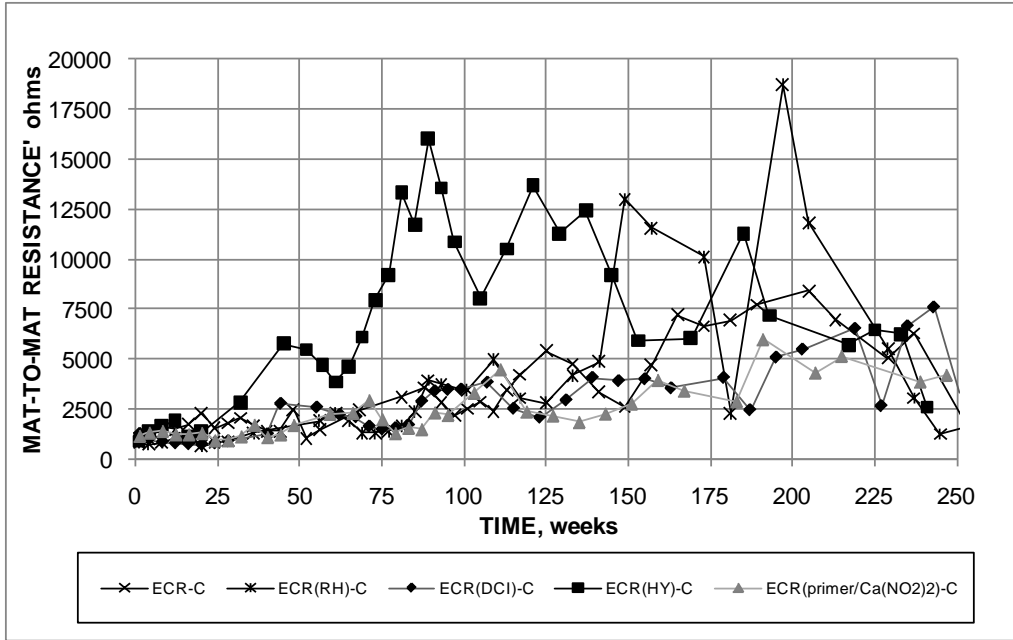
Figure 143. Graph. Field test, mat-to-mat resistance for conventional ECR without and with corrosion inhibitors and with simulated cracks.
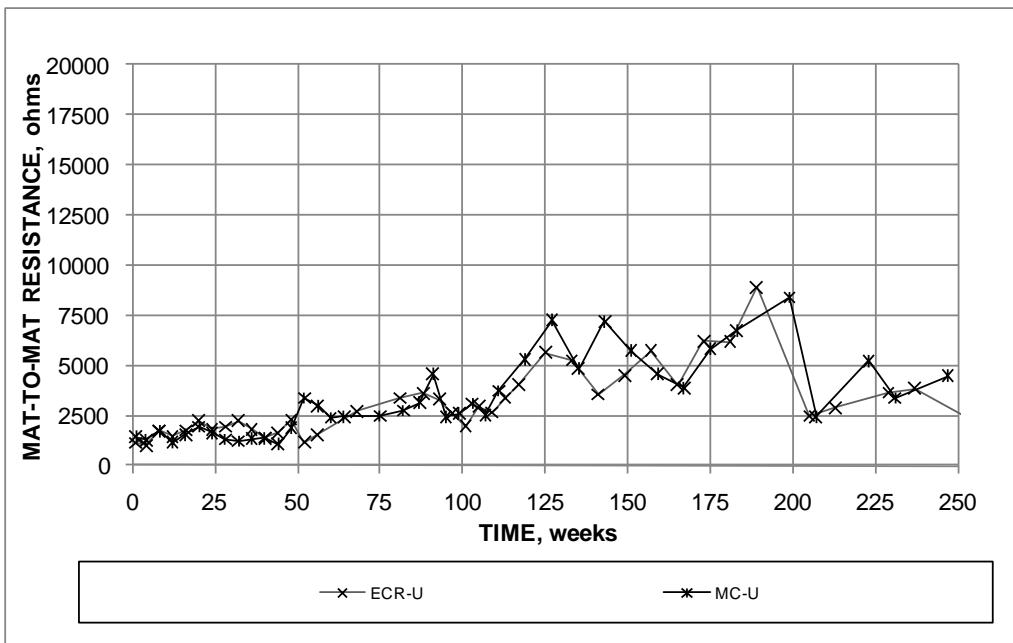
Figure 144. Graph. Field test, mat-to-mat resistance for conventional ECR and MC reinforcement without simulated cracks.
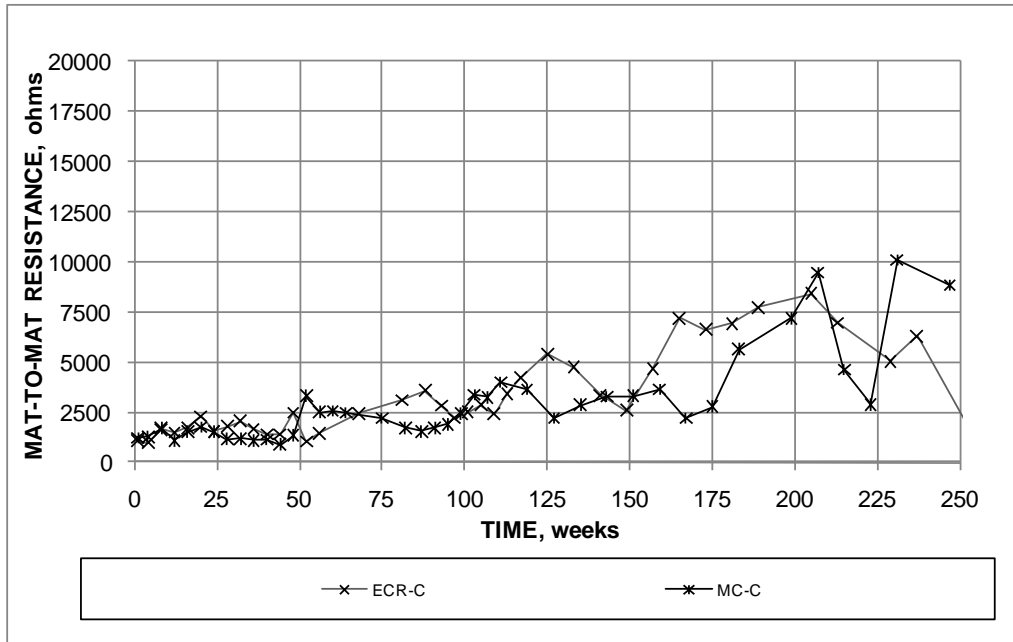
Figure 145. Graph. Field test, mat-to-mat resistance for conventional ECR and MC reinforcement with simulated cracks.

For all bar types, the mat-to-mat resistance rose over time, reached a peak, and then declined or, in a few cases, leveled off. The times at which each bar type reached the peak resistance differ, but a similarity between resistances in specimens without and with cracks for the same bar type is clear. Causes for the decrease in the resistance may include deterioration of concrete, increase in ionic conductivity resulting from the increased chloride content, and for the coated bars systems, disbondment or other damage to the coating. The figures illustrating corrosion loss versus time for the field test specimens indicate little change in the corrosion rates in the latter stages of the tests, suggesting that decreases in mat-to-mat resistance or any damage accompanying the decreases did not result in an increase in corrosion rate for these specimens.

Autopsy of Field Test Specimens

At the conclusion of the field tests at 250 or 254 weeks, specimens were evaluated for staining and cracking and autopsied to evaluate the nature of any corrosion on the reinforcing steel following the same procedures used for the southern exposure and cracked beam specimens. Epoxy-coated bars were evaluated for disbondment. As previously described, specimens in batches 3 through 9 were cored to measure the chloride content at the end of the tests.

The specimens both without and with simulated cracks containing conventional reinforcing steel exhibited staining and cracking of the concrete, as shown in figure 146 through figure 149. The age at crack initiation for each bar instrumented to measure corrosion was estimated from photos of each specimen taken approximately annually beginning at the third year of testing. The age at cracking was assumed to be the average of the specimen age in the last photograph where no cracking was observed above the test bar and the specimen age in the first photograph where cracking was observed. The values for the four field test specimens containing conventional steel are listed in table 30. Also, as shown in the figures, the cracks were primarily parallel to the top

132

reinforcing bars. This cracking occurred in spite of the fact that the average macrocell corrosion loss did not exceed 6.7 µm (0.26 mil) on any individual bar, a value that is below 25 µm (0.98 mil), the corrosion loss typically needed to crack concrete with 25 mm (1 inch) of cover over the reinforcing steel.[44] An explanation is provided for conventional steel specimens without and with simulated cracks in figure 150 and figure 151, which show that some of the top bars had corrosion losses well above 25 µm (0.98 mil) and that the corrosion products were not uniformly distributed over the surface of the bars. In reference to the latter point, a visual inspection of the conventional reinforcement from the field test specimens at the end of testing indicated that corrosion covered only about one-third of the total of bar area in uncracked concrete and about 40 percent of the total bar area in cracked concrete. Thus, although the average corrosion losses based on macrocell corrosion remained well below 25 µm (0.98 mil), enough of the bar surface underwent corrosion adequate to crack the concrete. In addition, the losses given in table 24 and table 26 represent macrocell losses rather than total losses, which, as discussed with the linear polarization resistance results for the bench-scale tests, are several times greater than the macrocell losses. This information is used in chapter 4 to estimate the time to cracking on bridge decks. As illustrated in figure 152 and figure 153, none of the field test specimens containing coated reinforcement exhibited cracking of the concrete.

Figure 146. Photo. Field test specimen without simulated cracks containing conventional reinforcing steel at 250 weeks.

Figure 147. Photo. Field test specimen without simulated cracks containing conventional reinforcing steel at 254 weeks.

Figure 148. Photo. Field test specimen with simulated cracks containing conventional reinforcing steel at 250 weeks.

Figure 149. Photo. Field test specimen with simulated cracks containing conventional reinforcing steel at 254 weeks.

Table 30. Estimated time to cracking for instrumented bars on field test specimens containing conventional steel.

Specimen-Bar[a]	Estimated Time to Cracking (weeks)
Conv. (1)-U-1	227
Conv. (1)-U-2	183
Conv. (2)-U-1[b]	–
Conv. (2)-U-2	222
Conv. (1)-C-1	227
Conv. (1)-C-2[c]	–
Conv. (2)-C-1	171
Conv. (2)-C-2	171

[a] Number in parentheses is specimen number (U = specimen without simulated cracks; C = specimen with simulated cracks; final number is bar number.)
[b] No cracking observed.
[c] Cracking occurred prior to first photo.

Figure 150. Photo. Top bars from field test specimen without simulated cracks containing conventional reinforcing steel at 254 weeks.

Figure 151. Photo. Top bars from field test specimen with simulated cracks containing conventional reinforcing steel at 250 weeks.

Figure 152. Photo. Field test specimen without simulated cracks containing conventional epoxy-coated steel at 254 weeks.

Figure 153. Photo. Field test specimen with simulated cracks containing conventional epoxy-coated steel at 254 weeks.

The only other observation of interest relative to the appearance of the concrete deals with the specimens cast with corrosion inhibitor Hycrete™. Those specimens uniformly exhibited scaling of the upper surface for specimens both without and with simulated cracks, as shown in figure 154 and figure 155. This result suggests that additional work is needed to establish criteria to preclude a loss of durability when Hycrete is used.

Figure 154. Photo. Field test specimen without simulated cracks containing conventional ECR and Hycrete™ corrosion inhibitor at 250 weeks.

Figure 155. Photo. Field test specimen with simulated cracks containing conventional ECR and Hycrete™ corrosion inhibitor at 254 weeks.

All bars were removed from the specimens, and the outermost epoxy-coated bars were evaluated for disbondment, including all top and bottom bars in specimens without cracks and all electrically connected top and bottom bars in specimens with cracks. Disbondment was checked at two points on the upper side of each bar using the procedures described for the bench-scale specimens. In the description that follows, bars that were electrically connected between the top and bottom mats are distinguished from those that were electrically isolated.

Figure 156 and figure 157 show bars following the disbondment tests. Figure 156 shows bars coated with conventional reinforcement cast in concrete containing Rheocrete®, and figure 157 shows bars coated with the high-adhesion DuPont™ coating. The figures are typical of observations made in the field test specimens for all types of ECR and demonstrate that corrosion occurred both at the points where the epoxy was penetrated and under the epoxy coating. Figure 158 shows disbondment results for an MC bar, with a loss of the zinc coating under the epoxy and subsequent corrosion of the steel.

Figure 156. Photo. Conventional epoxy-coated top bars from field test specimen containing Rheocrete® 222+ corrosion inhibitor without simulated cracks after 254 weeks.

Figure 157. Photo. High adhesion DuPont™ epoxy-coated top bars from field test specimen with simulated cracks after 250 weeks.

Figure 158. Photo. MC top bars from field test specimen with simulated cracks after 250 weeks.

The average values of disbondment for the electrically connected top and bottom bars for specimens without and with simulated cracks over the reinforcement are shown in figure 159 and figure 160, respectively. For specimens without cracks, the average values of disbondment for individual specimens with the same corrosion protection systems were quite similar in a number of cases and quite different in others. Specifically, conventional ECR, ECR(HY), ECR(Valspar), ECR(DuPont), and ECR(Chromate) exhibited low values of disbondment for the top bars for both specimens. In contrast, ECR(primer/Ca(NO_2)$_2$), ECR(DCI), ECR(RH), and MC bars exhibited significantly higher disbondment for some but not all of the specimens. The scatter is, in all likelihood, typical of what would be observed in bridge decks. ECR(primer/Ca/NO_2)$_2$ specimens 1 and 2 and ECR specimen 2 exhibited the highest disbondment among bottom bars, at 127, 102, and 110 mm^2 (0.20, 0.16, and 0.17 in^2), respectively, but the bottom bars in most specimens exhibited significantly less disbondment and, in many cases, no disbondment was observed.

1 mm^2 = 0.00155 in^2
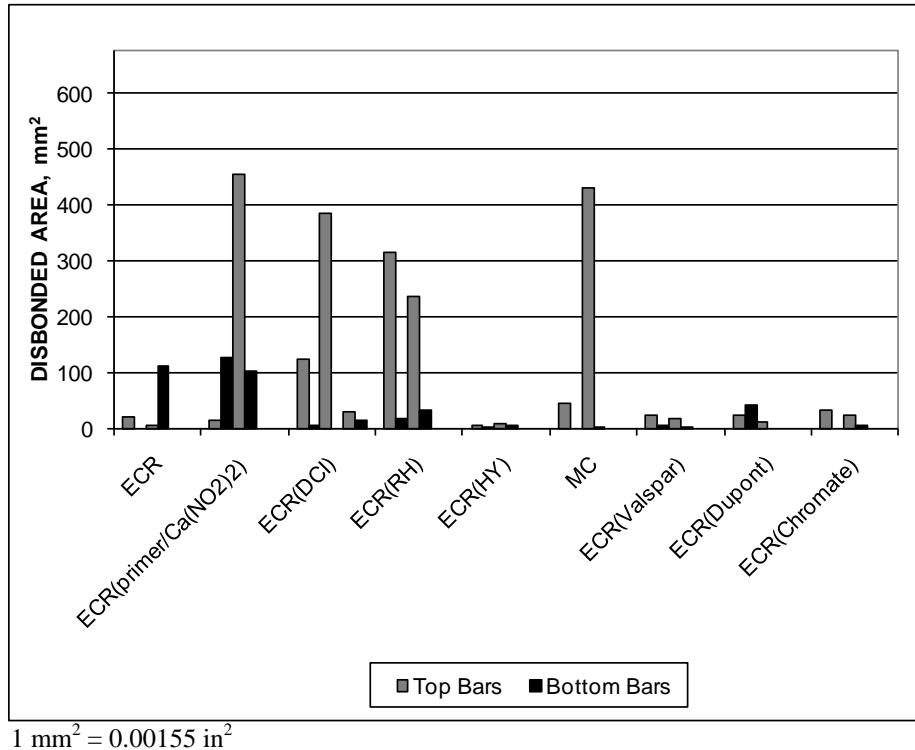
Figure 159. Graph. Disbondment results for electrically connected bars in field test specimens without simulated cracks.

1 mm^2 = 0.00155 in^2
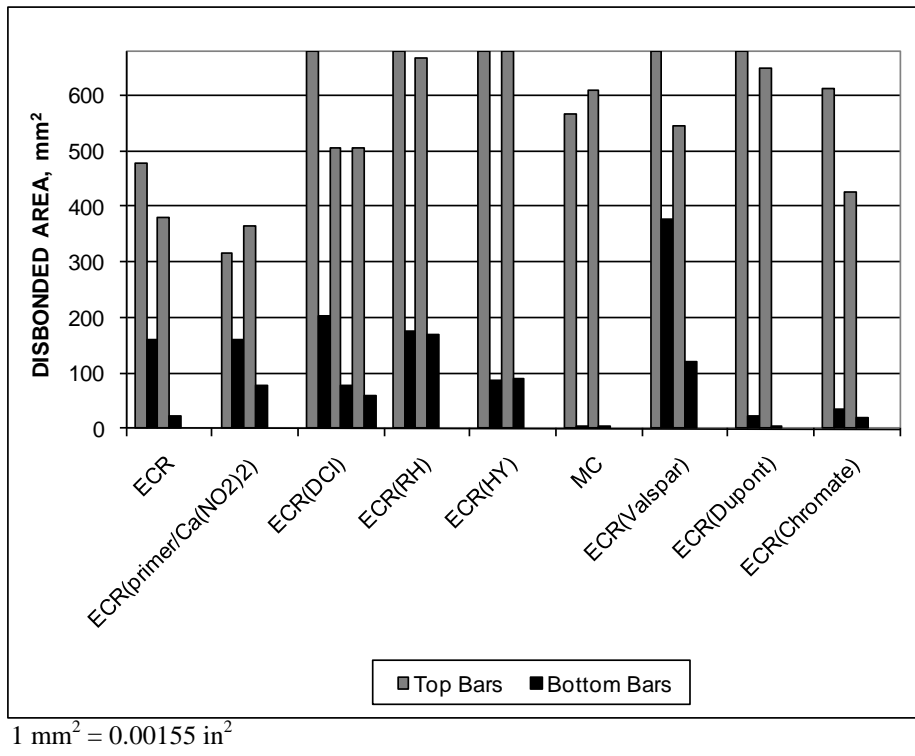
Figure 160. Graph. Disbondment results for electrically connected bars in field test specimens with simulated cracks.

140

Figure 160 shows that, as with the cracked beam specimens, the field test specimens with simulated cracks over the reinforcement exhibited significantly more disbondment than the specimens without simulated cracks. All specimens had average top bar disbondment values in excess of 317 mm^2 (0.49 in^2), and all groups except conventional ECR and ECR(primer/Ca/NO$_2$)$_2$ had at least one specimen with average disbondment in excess of 606 mm^2 (0.94 in^2). One specimen for ECR(DCI), ECR(RH), ECR(Valspar), and ECR(DuPont) and both bars for ECR(HY) exhibited total disbondment of the top bars. As observed in the cracked beam specimens, MC reinforcement exhibited very low disbondment on the bottom mat of steel.

Figure 161 compares the disbondment for top bars in specimens without cracks that are electrically connected with adjacent bars that are electrically isolated. Without exception, the electrically isolated bars exhibited less disbondment and, in most cases, much less disbondment than the bars that were electrically connected. This bodes well for ECR because epoxy-coated bars are electrically isolated in the vast majority of cases in bridge decks.

As observed with respect to the drop in mat-to-mat resistance toward the end of the test period, disbondment does not appear to have affected the corrosion rate of the field test specimens.

1 mm^2 = 0.00155 in^2
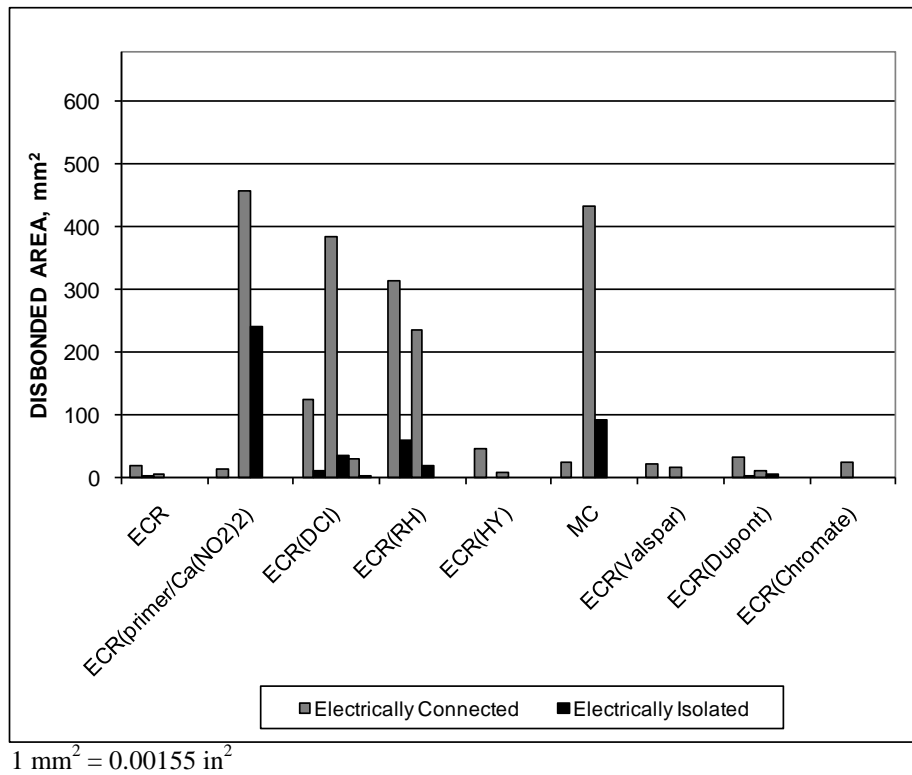
Figure 161. Graph. Comparison of disbondment values for electrically connected and electrically isolated bars in field test specimens without simulated cracks.

CHAPTER 4. EVALUATION

In this chapter, the experimental results presented in chapter 3 are compared and used to develop estimates of the life expectancy and cost effectiveness of the systems.

The comparative performance of the systems is measured based on the chloride content required to initiate corrosion, the average corrosion rate based on corrosion losses after corrosion initiation, and, in the case of coated bars, disbondment of the coating from the surface of the reinforcement.

Estimates of life expectancy and cost effectiveness are determined using a typical monolithic bridge deck with a thickness of 216 mm (8.5 inches) and concrete cover of 76 mm (3 inches) over the top layer of reinforcing steel. Life expectancy depends on the time to first repair. Cost effectiveness is based on the sum of the cost of a new bridge deck and the cost of repairs over a 75-year service life.

The results show that fusion-bonded epoxy coatings significantly improve not only corrosion resistance but also life expectancy and cost effectiveness of reinforcing steel and that additional protection provides only limited additional improvement. Some corrosion inhibitors and the multiple zinc-epoxy coating extend the time to first repair, but differences in the costs over a 75-year design life are relatively small for coated bars.

COMPARATIVE PERFORMANCE

The systems under study are compared based on the chloride content required to initiate corrosion, also known as the critical chloride corrosion threshold (CCCT); the corrosion rate after initiation; and disbondment or separation of the coating from the surface of the reinforcement as it is subjected to a corrosive environment in concrete. The first two criteria can be used to provide an estimate of the life expectancy and, in turn, the cost effectiveness of structures such as bridge decks. Disbondment represents a noteworthy aspect of system performance, although its impact on life expectancy and cost effectiveness remains unclear.

Critical Chloride Corrosion Threshold (CCCT)

Table 31 lists the CCCT for each corrosion-protection system for bars cast in concrete with a w/c ratio of 0.45. The table also lists the number of samples and standard deviations. The standard deviations account for the effect of combining groups of data.

Table 31. Chloride content at corrosion initiation (kg/m³), taken as the CCCT.

Steel Designation[a]	Southern Exposure	Initiation Beam	Total Number of Samples	Weighted Average	Standard Deviation
Bars without coatings					
Controls					
Conv.	0.77	0.94	156	0.90	0.479
Conv.2	0.88	1.00	118	0.98	0.822
Conv. Average			**274**	**0.94**	**0.673**
Corrosion inhibitors in concrete					
Conv.(DCI)	–	1.49	120	1.49	0.604
Conv.2(DCI)	3.72	–	18	3.72	1.69
Conv.(DCI) Average			**138**	**1.78**	**1.02**
Conv.(RH)	–	1.23	120	1.23	0.839
Conv.2(RH)	2.16	–	18	2.16	0.708
Conv.(RH) Average			**138**	**1.35**	**0.769**
Conv.(HY)	–	0.37	120	0.37	0.267
Conv.2(HY)	1.19	0.51	118	0.61	0.317
Conv.(HY) Average			**238**	**0.49**	**0.425**
Bars with coatings					
Control and epoxies with increased adhesion					
ECR	4.31	–	28	4.31	1.14
ECR(Chromate)	5.69	–	11	5.69	2.88
ECR(DuPont)	4.97	–	16	4.97	3.33
ECR(Valspar)	6.08	–	11	6.08	2.90
ECR Average			**66**	**5.00**	**3.17**
Conventional epoxy and epoxies with increased adhesion plus calcium nitrite in concrete					
ECR(DCI)	5.80	–	12	5.80	1.24
ECR(Chromate)-DCI	2.77	–	6	2.77	1.87
ECR(DuPont)-DCI	5.73	–	11	5.73	1.58
ECR(Valspar)-DCI	5.35	–	4	5.35	0.179
ECR(DCI) Average			**33**	**5.17**	**2.71**
Corrosion inhibitors other than calcium nitrite in concrete					
ECR(RH)	4.10	–	17	4.10	1.45
ECR(HY)	1.08	–	10	1.08	0.673
ECR(primer/Ca(NO$_2$)$_2$)	7.11	–	10	7.11	4.04
Bars with multiple coatings					
MC	2.00	–	16	2.00	1.79

1 kg/m³ = 1.69 lb/yd³

– No specimens.

[a] See table 1 for abbreviation definitions.

A w/c ratio of 0.35 was used for five systems: conventional steel, conventional ECR, and conventional ECR cast in concrete with each of the three corrosion inhibitors (calcium nitrite, Rheocrete®, and Hycrete™), but CCCT values for these systems are not used for this comparison. As shown in table 13, no data are available for conventional ECR cast in concrete with a w/c

ratio of 0.35. For each of the systems with a corrosion inhibitor in concrete with a w/c ratio of 0.35, six or fewer samples were taken in total. The corrosion threshold for conventional steel cast in concrete with a w/c ratio of 0.35 is about twice that of conventional steel cast in concrete with a w/c ratio of 0.45, while the corrosion threshold is lower at a w/c ratio of 0.35 than at a w/c ratio of 0.45 for the systems with ECR and a corrosion inhibitor. For these reasons, the effect of w/c ratio on corrosion threshold is considered to be uncertain based on the current test results and will not be addressed further.

In table 31, the values for conventional steel without and with the corrosion inhibitors calcium nitrite, Rheocrete®, and Hycrete™ include values from both southern exposure specimens and initiation beams. The values for coated bars include chloride contents only from southern exposure specimens. The values for bars with 4 and 10 holes through the coating are combined and weighted based on the number of samples collected. As observed in chapter 3, the CCCTs for bars with coatings are consistently several times the CCCTs for bars without coatings. The higher thresholds of the coated bars, all of which have penetrations in the coating, are in all likelihood due to the lack of uniformity of the chloride content in the concrete and the low probability that a region of locally high chloride content will coincide with the point on a bar where the coating is penetrated.

Looking at the individual CCCT values, conventional reinforcement Conv. has an average CCCT of 0.90 kg/m^3 (1.52 lb/yd^3) while conventional reinforcement Conv.2 has an average CCCT of 0.98 kg/m^3 (1.65 lb/yd^3). The two values are combined to obtain a weighted average CCCT for conventional reinforcement of 0.94 kg/m^3 (1.58 lb/yd^3). Similarly, the values for Conv. and Conv.2 reinforcement in concrete containing the corrosion inhibitors calcium nitrite, Rheocrete®, and Hycrete™ are combined to obtain CCCT values of 1.78, 1.35, and 0.49 kg/m^3 (3.00, 2.28, and 0.83 lb/yd^3), respectively. The reason for the low CCCT for Hycrete™ is discussed in chapter 3.

Conventional ECR exhibits an average CCCT of 4.31 kg/m^3 (7.26 lb/yd^3) while the systems with ECR and increased adhesion have CCCT values ranging from 4.97 to 6.08 kg/m^3 (8.38 to 10.3 lb/yd^3). The use of an increased-adhesion epoxy should not affect the chloride threshold of the system, and data for the high-adhesion bars are treated as representing the same population as conventional ECR; therefore, the CCCT values for conventional ECR and ECR with increased adhesion are averaged to produce a single CCCT of 5.00 kg/m^3 (8.43 lb/yd^3).

Among the specimens with ECR and inhibitors, ECR in concrete with calcium nitrite (combining the results for conventional epoxy and the epoxies with increased adhesion) had a CCCT of 5.17 kg/m^3 (8.69 lb/yd^3), just above the CCCT for ECR alone. ECR in concrete with Rheocrete®, however, exhibited a CCCT of 4.10 kg/m^3 (6.93 lb/yd^3), which is lower than the CCCT for ECR in concrete with no inhibitor. ECR in concrete with Hycrete™ has a CCCT of 1.08 kg/m^3 (1.82 lb/yd^3), well below that of ECR in concrete with no inhibitor (5.00 kg/m^3 (8.45 lb/yd^3)). Relatively speaking, this is similar to conventional reinforcement in concrete containing Hycrete™, which exhibits a CCCT of 0.49 kg/m^3 (0.83 lb/yd^3) compared to a CCCT of 0.94 kg/m^3 (1.59 lb/yd^3) for conventional steel in concrete with no inhibitors. With a CCCT of 7.11 kg/m^3 (12.0 lb/yd^3), ECR(primer/Ca(NO$_2$)$_2$) has the highest corrosion threshold of any of the systems tested. The high CCCT value for ECR(primer/Ca(NO$_2$)$_2$) may be due to the fact that the primer places the corrosion inhibitor directly in contact with the steel surface.

In the southern exposure test, MC reinforcement exhibits a CCCT of 2.00 kg/m^3 (3.38 lb/yd^3), which is lower than that of ECR. A study examining the CCCT of galvanized reinforcement, however, found that galvanized steel has an average critical chloride corrosion threshold of 1.52 kg/m^3 (2.57 lb/yd^3), about 50 percent higher than the value for conventional reinforcement, which suggests that a higher value, such as that used for conventional ECR, would be more appropriate for MC bars.[50]

Because the CCCT values given in table 31 are, in some cases, based on a small number of samples, Student's *t*-test can be used to determine if the differences are the statistically significant.

Student's *t*-test compares the means and variances of two data sets to determine the probability a that any differences in the mean values could have arisen by chance; that is, that differences in the mean values μ_1 and μ_2 are due to natural variability, not differences in the systems. For example, $a = 0.05$ indicates a 5 percent chance that the test will incorrectly identify (or a 95 percent chance of correctly identifying) a statistically significant difference in sample means when, in fact, there is no difference. For this analysis, a two-tailed test is performed, meaning that there is a probability of $a/2$ that μ_1 is greater than μ_2 and $a/2$ that μ_1 is less than μ_2 when, in fact, μ_1 and μ_2 are equal. An a value of 0.20 is used as the threshold for statistical significance. If a is greater than 0.20, the systems are considered to be performing in a similar manner. It is worthwhile to note that a threshold a of 0.20 is higher than often selected and values of 0.02, 0.05, and 0.10 are more common. An a value of 0.20 is used here to restrict the number of cases in which systems are treated as similar.

The results of the Student's *t*-test are summarized in table 32 and table 33 for bare and coated bars, respectively. The tables show that all of the differences for bare bars are statistically significant with $a < 0.001$. For the coated bars, all of the differences are statistically significant with $a < 0.162$, with two exceptions: the differences in chloride threshold between conventional ECR and ECR(DCI) (5.00 and 5.17 kg/m^3 (8.45 and 8.69 lb/yd^3)) and between ECR(DCI) and ECR (RH) (5.17 and 4.10 kg/m^3 (8.69 and 6.93 lb/yd^3)). Furthermore, the value of a for the difference between the corrosion thresholds for ECR and ECR(RH) is fairly high at 0.162. Because concrete with Rheocrete® raises the CCCT of conventional reinforcement relative to conventional reinforcement in concrete without an inhibitor and because there is no reason to expect that Rheocrete® would have a negative effect when used with ECR, it would seem appropriate to consider ECR cast in concrete with Rheocrete® as having a CCCT no lower than that of conventional ECR alone. As mentioned earlier in this section, a CCCT of 2.00 kg/m^3 (3.38 lb/yd^3) for MC reinforcement appears to be low because galvanized bars have a higher CCCT than conventional bars. Thus, even though the differences between the CCCT for MC reinforcement and other coated bars are statistically significant, it would also seem appropriate to apply the CCCT of conventional ECR to the MC reinforcement.

Table 32. Student's *t*-test results (α values) for CCCT for bars without coatings cast in concrete with w/c = 0.45.

Steel Designation[a]	CCCT, kg/m^3	Conv.	Conv.(RH)	Conv.(DCI)	Conv.(HY)
CCCT (kg/m^3)		0.94	1.78	1.35	0.49
Conv.	0.94	1	**2.89E-28**	**9.55E-11**	**1.40E-12**
Conv.(DCI)	1.78	**2.89E-28**	1	**6.06E-05**	**2.12E-39**
Conv.(RH)	1.35	**9.55E-11**	**6.06E-05**	1	**5.16E-25**
Conv.(HY)	0.49	**1.40E-12**	**2.12E-39**	**5.16E-25**	1

1 kg/m^3 = 1.69 lb/yd^3
Bold indicates statistical significance.
[a] See table 1 for abbreviation definitions.

Table 33. Student's *t*-test results (α values) for CCCT for bars with coatings cast in concrete with w/c = 0.45.

Steel Designation[a]	CCCT, kg/m^3	ECR	ECR(DCI)	ECR(RH)	ECR(HY)	ECR (primer/ Ca(NO$_2$)$_2$)	MC
CCCT (kg/m^3)		5.00	5.17	4.10	1.08	7.11	2.00
ECR	5.00	1	0.470	**0.162**	**0.001**	**0.029**	**0.044**
ECR(DCI)	5.17	0.470	1	0.344	**4.26E-04**	**0.009**	**0.055**
ECR(RH)	4.10	**0.162**	0.344	1	**6.59E-05**	**0.003**	**0.107**
ECR(HY)	1.08	**0.001**	**4.26E-04**	**6.59E-05**	1	**2.71E-04**	**0.089**
ECR(primer/Ca(NO$_2$)$_2$)	7.11	**0.029**	**0.009**	**0.003**	**2.71E-04**	1	**0.006**
MC	2.00	**0.044**	**0.055**	**0.107**	**0.089**	**0.006**	1.000

1 kg/m^3 = 1.69 lb/yd^3
Bold indicates statistical significance.
[a] See table 1 for abbreviation definitions.

Corrosion Rate

The systems can be compared based on corrosion rate for both bench-scale and field test specimens. As with the chloride threshold comparisons, emphasis is placed on results for concretes with a w/c ratio of 0.45.

The average corrosion rates based on corrosion losses after corrosion initiation for the bench-scale specimens are presented in chapter 3 in table 15 and table 20 for the southern exposure and cracked beam specimens and table 28 and table 29 for field test specimens without and with simulated cracks over the reinforcing steel. The tables include the number of specimens or bars for which the data is obtained as well as the standard deviation, providing a summary for corrosion rate that is equivalent to that presented for chloride content at corrosion initiation in table 31.

To aid in comparisons dealing with conventional reinforcement without and with corrosion inhibitors in the concrete, a modification is made to the data. Table 34 lists bench-scale macrocell corrosion rates for Conv. reinforcement without inhibitors and Conv.2 reinforcement without and with inhibitors. The bench-scale macrocell corrosion rates for Conv.2 reinforcement were 10.1 and

16.3 µm/year (0.398 and 0.642 mil/year) in uncracked and cracked concrete (southern exposure and cracked beam specimens), respectively, about twice the respective a rates for Conv. reinforcement (5.69 and 7.00 µm/year (0.224 and 0.276 mil/year)). All inhibitors reduced the corrosion rate of Conv.2 reinforcement compared to Conv.2 reinforcement with no inhibitor, but in cracked concrete, Conv.2(RH) and Conv.2(DCI) show corrosion rates greater than those observed for Conv. reinforcement. It is assumed that if the inhibitors had been used in conjunction with the earlier tests on Conv. reinforcement, the resulting corrosion rates would have been less than the corrosion rates measured for Conv. reinforcement with no inhibitor. Since all other protection systems (uncoated and coated) used the same heat of steel as Conv. reinforcement and because the mat-to-mat resistance values for the Conv.2 southern exposure and cracked beam specimens are lower than for the corresponding Conv. specimens (which would lead to higher corrosion rates), the only way to achieve a fair comparison between systems is to reduce the corrosion rates for the systems with Conv.2 reinforcement with inhibitors by the ratio of the Conv.2 corrosion rate to the Conv. corrosion rate.[44,58] The designation Conv.* is used when referring to the modified corrosion rate data for conventional reinforcement in concrete with corrosion inhibitors. The modified corrosion rates for these systems are presented in table 34. Based on the modified corrosion rates, the estimated rates for Conv.*(RH) are 1.64 and 5.13 µm/year (0.0646 and 0.202 mil/year) in uncracked and cracked concrete, respectively. Likewise, the estimated rates for Conv.*(DCI) are 3.77 and 6.24 µm/year (0.148 and 0.246 mil/year) and are 0.706 and 1.80 µm/year (0.0278 and 0.0709 mil/year) for Conv.*(HY).

Table 34. Equivalent corrosion rates for conventional reinforcement with inhibitors (µm/year).

Steel Designation	Concrete[a]	Macrocell Corrosion Rate	Ratio of Conv.2 to Conv. Rate	Modified Corrosion Rate (Conv.*)[b]
Corrosion rate (total area)				
Conv.	U	5.69	NA	NA
	C	7.00	NA	NA
Conv.2	U	10.1	1.77	5.69
	C	16.3	2.32	7.00
Conv.2(RH)	U	2.91	1.77	1.64
	C	11.90	2.32	5.13
Conv.2(DCI)	U	6.67	1.77	3.77
	C	14.50	2.32	6.24
Conv.2(HY)	U	1.25	1.77	0.706
	C	4.17	2.32	1.80

1 µm = 0.0394 mil
NA = Not applicable
[a] U = Uncracked concrete (southern exposure), C = cracked concrete (cracked beam).
[b] Estimated corrosion rate in conjunction with Conv. reinforcement.

To determine the statistical significance of the differences in corrosion rates between corrosion-protection systems, the two-tailed Student's *t*-test is again used with a > 0.20 indicating that the observed differences are not statistically significant and that systems can be considered to perform in a similar manner. Bare bars, for which corrosion rates are presented based on total area, are

examined separately from coated bars, for which corrosion rates are based on exposed area. The systems are compared first based on bench-scale results and then based on the field test results.

Table 35 and table 36 list the values of a based on comparisons of corrosion rates for corrosion-protection systems with bare bars in southern exposure and cracked beam specimens, respectively. To prepare the tables, the corrosion rates and standard deviations for conventional reinforcement with inhibitors are scaled by the ratio of Conv.2 corrosion rate to Conv. corrosion rate prior to analysis, as shown in table 34. The comparisons for the southern exposure tests show that, at 5.69 μm/year (0.224 mil/year), the corrosion rate is highest for Conv., followed by Conv.*(DCI), Conv.*(RH), and Conv.*(HY), with values of 3.77, 1.64, and 0.706 μm/year (0.148, 0.0646, and 0.0278 mil/year), respectively. All differences are statistically significant with $a < 0.025$. The comparisons for the cracked beam tests, however, show that while the order of the corrosion rates is the same as for the southern exposure specimens with values of 7.00, 6.24, 5.15 and 1.80 μm/year (0.276, 0.246, 0.203, and 0.0709 mil/year) for Conv., Conv.*(DCI), Conv.*(RH), and Conv.*(HY), respectively, only the rate for Conv.*(HY) differs with statistical significance from the other values.

Table 35. Student's *t*-test results (a values) for average corrosion rates based on corrosion losses after corrosion initiation based on total area for bars without coatings from southern exposure tests.

Steel Designation[a]	Corrosion Rate, μm/year	Conv.	Conv.* (RH)	Conv.* (DCI)	Conv.* (HY)
Corrosion Rate (μm/year)		5.69	1.64	3.77	0.706
Conv.	5.69	1	**9.4E-06**	**0.005**	**1.5E-06**
Conv.*(RH)	1.64	**9.4E-06**	1	**0.012**	**0.025**
Conv.*(DCI)	3.77	**0.005**	**0.012**	1	**0.004**
Conv.*(HY)	0.706	**1.5E-06**	**0.025**	**0.004**	1

1 μm = 0.0394 mil
Bold indicates statistical significance.
[a] See table 1 for abbreviation definitions.

Table 36. Student's *t*-test results (a values) for average corrosion rates based on corrosion losses after corrosion initiation based on total area for bars without coatings from cracked beam tests.

Steel Designation[a]	Corrosion Rate, μm/year	Conv.	Conv.* (RH)	Conv.* (DCI)	Conv.* (HY)
Corrosion Rate (μm/year)		7.00	5.15	6.24	1.80
Conv.	7.00	1	0.22	0.31	**0.004**
Conv.*(RH)	5.15	0.22	1	0.28	**0.003**
Conv.*(DCI)	6.24	0.31	0.28	1	**0.004**
Conv.*(HY)	1.80	**0.004**	**0.003**	**0.004**	1

1 μm = 0.0394 mil
Bold indicates statistical significance.
[a] See table 1 for abbreviation definitions.

Table 37 and table 38 list the values of a for comparisons of corrosion-protection systems with coated bars in the southern exposure and cracked beam tests, respectively. Since only one southern exposure specimen with Hycrete™ initiated corrosion, a statistical analysis cannot be performed for that system.

Table 37. Student's *t*-test results (a values) for average corrosion rates based on corrosion losses after corrosion initiation based on exposed area for bars with coatings from southern exposure tests.

Steel Designation[a]	Corrosion Rate (μm/year)	ECR	ECR (DCI)	ECR (RH)	ECR (HY)	ECR (primer/ Ca(NO$_2$)$_2$)	ECR (Chromate)	ECR (DuPont)	ECR (Valspar)	MC
Corrosion Rate (μm/year)		10.43	7.81	8.63	0.674	12.61	12.86	12.37	16.93	31.63
ECR	10.43	1	0.500	0.274	–	0.649	0.544	0.628	0.313	**0.071**
ECR(DCI)	7.81	0.500	1	0.291	–	0.468	0.344	0.391	0.324	**0.150**
ECR(RH)	8.63	0.274	0.291	1	–	0.613	0.569	0.529	0.977	0.471
ECR(HY)	0.674	–	–	–	–	–	–	–	–	–
ECR(primer/Ca(NO$_2$)$_2$)	12.61	0.621	0.468	0.613	–	1	0.964	0.966	0.577	**0.140**
ECR(Chromate)	12.86	0.544	0.344	0.569	–	0.964	1	0.919	0.576	**0.142**
ECR(DuPont)	12.37	0.628	0.391	0.529	–	0.966	0.919	1	0.532	**0.132**
ECR(Valspar)	16.93	0.313	0.324	0.977	–	0.577	0.576	0.532	1	0.220
MC	31.63	**0.071**	**0.150**	0.471	–	**0.140**	**0.142**	**0.132**	0.220	1

1 μm = 0.0394 mil
Bold indicates statistical significance.
[a] See table 1 for abbreviation definitions.

Table 38. Student's *t*-test results (a values) for average corrosion rates based on corrosion losses after corrosion initiation based on exposed area for bars with coatings from cracked beam tests.

Steel Designation[a]	Corrosion Rate (μm/year)	ECR	ECR (DCI)	ECR (RH)	ECR (HY)	ECR (primer/ Ca(NO$_2$)$_2$)	ECR (Chromate)	ECR (DuPont)	ECR (Valspar)	MC
Corrosion Rate (μm/year)		8.07	11.2	17.0	10.8	8.73	20.4	25.9	16.4	68.6
ECR	8.07	1	0.364	**0.014**	0.506	0.826	**0.064**	**0.005**	**0.158**	**0.005**
ECR(DCI)	11.2	0.364	1	**0.145**	0.938	0.497	0.250	**0.046**	0.465	**0.027**
ECR(RH)	17.0	**0.014**	**0.145**	1	0.211	**0.026**	0.720	0.243	0.893	**0.067**
ECR(HY)	10.8	0.506	0.938	0.211	1	0.645	0.292	**0.072**	0.494	**0.041**
ECR(primer/Ca(NO$_2$)$_2$)	8.73	0.826	0.497	**0.026**	0.645	1	**0.140**	**0.019**	0.270	**0.021**
ECR(Chromate)	20.4	**0.064**	0.250	0.720	0.292	**0.140**	1	0.554	0.680	**0.064**
ECR(DuPont)	25.9	**0.005**	**0.046**	0.243	**0.072**	**0.019**	0.554	1	0.290	**0.097**
ECR(Valspar)	16.4	**0.158**	0.465	0.893	0.494	0.270	0.680	0.290	1	**0.045**
MC	68.6	**0.005**	**0.027**	**0.067**	**0.041**	**0.021**	**0.064**	**0.097**	**0.045**	1

1 μm = 0.0394 mil
Bold indicates statistical significance.
[a] See table 1 for abbreviation definitions.

150

The comparison between rates for the southern exposure test shows that only MC reinforcement, corroding at nearly 3 times the rate of conventional ECR, has a corrosion rate that is significantly different from that of the other systems ($a < 0.20$). ECR(HY) is also assumed to have a statistically significant difference in corrosion rate compared to the other systems because the corrosion rate of ECR(HY), 0.674 µm/year (0.0265 mil/year), is over an order of magnitude lower than any of the other systems.

The results for the cracked beam tests show no statistically significant differences between ECR, ECR(DCI), ECR(HY), and ECR(primer/Ca(NO$_2$)$_2$) ($a > 0.20$), although it is worth noting that the corrosion rate for conventional ECR, 8.07 µm/year (0.318 mil/year), is the lowest rate obtained for any of the systems in the cracked beam tests and that both conventional ECR and ECR(primer/Ca(NO$_2$)$_2$) exhibited lower rates in the cracked beam tests than in the southern exposure tests, highlighting some of the variability inherent in corrosion tests. ECR(RH), ECR(Chromate), ECR(DuPont), and ECR(Valspar) show significant differences in performance relative to ECR, with corrosion rates greater than that for ECR. In practice, however, there is no reason to expect that a corrosion inhibitor or an epoxy with increased adhesion will increase the corrosion rate. The greater corrosion rates observed are likely due to variations in the test or in concrete quality. The corrosion rate of the MC bars, 68.6 µm/year (2.70 mil/year), is significantly different from that of all of the other systems—over 2 times the next closest value, 25.9 µm/year (1.02 mil/year) for ECR(DuPont) and over 8 times greater than that of conventional ECR (8.07 µm/year (0.318 mil/year)).

The results of Student's *t*-test for the field test specimens are shown in table 39 and table 40 for uncracked and cracked concrete, respectively. The analysis does not include bare bar systems because the only bare bar system evaluated using the field test specimens was conventional steel. The comparisons between average macrocell corrosion rates based on losses after corrosion initiation in uncracked concrete show no statistically significant differences in rates for ECR, ECR(RH), ECR(DCI), ECR(primer/Ca(NO$_2$)$_2$), ECR(Chromate), and ECR(DuPont) ($a > 0.20$). Although the rates for ECR(Valspar) and MC are statistically different from other corrosion-protection systems, they are not statistically different from conventional ECR, and these differences are likely due to variations in concrete quality. In addition, the corrosion rate for MC reinforcement (6.31 µm/year (0.248 mil/year)) is only 11 percent higher than that of conventional ECR (5.68 µm/year (0.224 mil/year)), compared to 3 times higher in the southern exposure tests. At 2.89 µm/year (0.114 mil/year), the corrosion rate for ECR(HY) is 68 percent of the next closest corrosion rate and is statistically different from the rates for ECR, ECR(RH), ECR(Valspar), and MC.

Table 39. Student's *t*-test results (a values) for average corrosion rates based on corrosion losses after corrosion initiation based on exposed area for bars with coatings from field test specimens with uncracked concrete.

Steel Designation[a]	Corrosion Rate (µm/year)	ECR	ECR (DCI)	ECR (RH)	ECR (HY)	ECR (primer/ Ca(NO₂)₂)	ECR (Chromate)	ECR (DuPont)	ECR (Valspar)	MC
Corrosion Rate (µm/year)		5.68	4.26	5.43	2.89	4.49	4.83	5.14	9.11	6.31
ECR	5.68	1	0.425	0.915	**0.136**	0.574	0.732	0.949	0.269	0.763
ECR(DCI)	4.26	0.425	1	0.446	0.256	0.871	0.726	0.563	**0.020**	**0.176**
ECR(RH)	5.43	0.915	0.446	1	**0.120**	0.606	0.778	0.989	**0.166**	0.636
ECR(HY)	2.89	**0.136**	0.256	**0.120**	1	0.233	0.209	0.295	**0.010**	**0.033**
ECR(primer/Ca(NO₂)₂)	4.49	0.574	0.871	0.606	0.233	1	0.856	0.708	**0.067**	0.301
ECR(Chromate)	4.83	0.732	0.726	0.778	0.209	0.856	1	0.836	**0.145**	0.463
ECR(DuPont)	5.14	0.949	0.563	0.989	0.295	0.708	0.836	1	0.305	0.750
ECR(Valspar)	9.11	0.269	**0.020**	**0.166**	**0.010**	**0.067**	**0.145**	0.305	1	0.305
MC	6.31	0.763	**0.176**	0.636	**0.033**	0.301	0.463	0.750	0.305	1

1 µm = 0.0394 mil
Bold indicates statistical significance.
[a] See table 1 for abbreviation definitions.

Table 40. Student's *t*-test results (a values) for average corrosion rates based on corrosion losses after corrosion initiation based on exposed area for bars with coatings from field test specimens with cracked concrete.

Steel Designation[a]	Corrosion Rate (µm/year)	ECR	ECR (DCI)	ECR (RH)	ECR (HY)	ECR (primer/ Ca(NO₂)₂)	ECR (Chromate)	ECR (DuPont)	ECR (Valspar)	MC
Corrosion Rate (µm/year)		8.13	5.79	8.38	4.32	4.65	8.94	6.50	7.64	8.11
ECR	8.13	1	0.275	0.923	0.234	**0.200**	0.745	0.656	0.733	0.918
ECR(DCI)	5.79	0.275	1	**0.072**	0.448	0.475	**0.126**	0.501	0.415	0.258
ECR(RH)	8.38	0.923	**0.072**	1	**0.024**	**0.004**	0.554	0.416	0.577	0.947
ECR(HY)	4.32	0.234	0.448	**0.024**	1	0.862	**0.144**	0.269	0.241	**0.181**
ECR(primer/Ca(NO₂)₂)	4.65	**0.200**	0.475	**0.004**	0.862	1	**0.112**	0.216	**0.190**	**0.137**
ECR(Chromate)	8.94	0.745	**0.126**	0.554	0.144	**0.112**	1	0.424	0.486	0.643
ECR(DuPont)	6.50	0.656	0.501	0.416	0.269	0.216	0.424	1	0.893	0.675
ECR(Valspar)	7.64	0.733	0.415	0.577	0.241	**0.190**	0.486	0.893	1	0.774
MC	8.11	0.918	0.258	0.947	**0.181**	**0.137**	0.643	0.675	0.774	1

1 µm = 0.0394 mil
Bold indicates statistical significance.
[a] See table 1 for abbreviation definitions.

The analysis of the cracked field test specimens shows that the corrosion rates for ECR, ECR(DCI), ECR(RH), ECR (HY), ECR(Chromate), ECR(DuPont), ECR(Valspar), and MC are not significantly different (a > 0.20). The rates for two systems combining ECR with inhibitors in the concrete, ECR(DCI) and ECR (HY), and ECR(primer/Ca(NO₂)₂) are lower and significantly different from at least two other systems. The rate for ECR(DCI) is significantly different from the rates for ECR(RH) and ECR(Chromate); the rate for ECR(HY) is significantly different from the rates for

ECR(RH) ECR(Chromate) and MC; and the rate for ECR(primer/Ca(NO$_2$)$_2$) is significantly different from the rates for ECR, ECR(RH), ECR(Chromate), ECR(Valspar), and MC. As observed for the uncracked field test specimens, the specimens containing MC bars had a corrosion rate (8.11 µm/year (0.319 mil/year)) that was close to that of conventional ECR (8.13 µm/year (0.320 mil/year)).

Disbondment

The disbondment results are summarized in figure 110 through figure 112 for the bench-scale specimens and in figure 159 through figure 161 for the field test specimens. In all cases, the top bars exhibited far more disbondment than the bottom bars, indicating that higher chloride content, higher moisture content, or a combination of the two results in increased disbondment. The southern exposure specimens cast with one of the corrosion inhibitors exhibited significantly less disbondment than those cast in concrete without an inhibitor. The same observation does not hold for the cracked beam specimens or for the field test specimens, with or without cracks. The tests uniformly show that when cast in the same quality of concrete, bars with high adhesion epoxies exhibit no reduction in disbondment compared to conventional ECR bars.

Bars in cracked concrete exhibited far more disbondment than those in uncracked specimens in both the bench-scale and field tests. Bottom bars fared better in uncracked concrete than in cracked concrete, presumably because of the higher chloride content lower in the specimens in the presence of a crack.

Bars in southern exposure specimens with a w/c ratio of 0.35 consistently exhibited less disbondment than bars in southern exposure specimens with a w/c ratio of 0.45, in some cases exhibiting no disbondment (see figure 112). The results were mixed for bars in cracked beam specimens. As shown in figure 112, the ECR(primer/Ca(NO$_2$)$_2$) and ECR(DCI) bars cast in concrete with w/c of 0.35 exhibited no disbondment, while ECR, ECR(RH), and ECR(HY) exhibited nearly the same disbondment as those in the specimens with the higher w/c ratio. MC bars exhibited somewhat less disbondment than for the other systems. This trend is especially true for the bottom bars in concrete with cracks (see figure 111 and figure 160). Finally, as shown in figure 153, top bars that were electrically isolated (bars not connected across a 10-ohm resistor to a bottom bar in the same specimen) exhibited far less disbondment than those that were connected, indicating the negative impact of macrocell corrosion and the importance of maintaining electrical isolation between coated bars in reinforced concrete structures.

LIFE EXPECTANCY

The life expectancy of a bridge deck (the structure used to compare life expectancy and cost effectiveness in this study) is based on an estimate of the time to first repair combined with the time between repairs to establish the present cost of a deck over a 75-year design life. In many cases, the time to first repair is based on experience. For example, the South Dakota Department of Transportation (SDDOT) has estimated that the time to first repair for bridge decks containing conventional steel is 10 years under harsh environmental conditions and 25 years in arid conditions.[23] The latter matches the time to first repair estimated by the KDOT.[23,36] In 2001, the time to first repair for bridge decks containing ECR was estimated to be 35 and 40 years by KDOT and SDDOT, respectively. The estimate for decks with ECR was

based on the fact that, as of the 2001, no bridge decks containing ECR had required repair due to corrosion-induced damage since its first use in the late 1970s.[36] Other estimates of time to first repair use models that are based on the time required for chloride to diffuse through uncracked concrete.[59–62] Models of this type usually include a preselected time for the corrosion products to cause the concrete to crack following corrosion initiation. Diffusion-based models have two key drawbacks: (1) they do not account for the role played by cracks in the concrete in allowing rapid penetration of chlorides to the level of the reinforcing steel and (2) a preselected time for the corrosion products to cause the concrete to crack is not based on actual corrosion rates. Because surveys of bridge decks with ages ranging from several months to over 20 years demonstrate that reinforced concrete bridge decks exhibit significant cracking parallel to and directly above the reinforcing bars, estimates of time to first repair are based principally on corrosion in the presence of cracks. (See references 3, 43, and 63–66.)

The procedures used in the current analysis are based on field and laboratory evidence addressing corrosion initiation and propagation in cracked concrete combined with experience with deck repair. Using this approach, the time to first repair depends on: (1) the time required for the chloride content of the concrete to reach the critical chloride initiation threshold for the system, (2) the time required after initiation for corrosion products to cause cracking and spalling of the concrete cover, and (3) the time between first cracking and the time that the repair is made.

Time to Corrosion Initiation

The time to corrosion initiation is estimated based on chloride contents measured at crack locations on bridge decks in Kansas and the CCCT (water-soluble chloride content) for each corrosion-protection system, as previously discussed.[3,43,67]

The chloride contents in bridge decks are based on two studies.[43,67] In those studies, chloride samples were obtained in bridge decks using a vacuum drill. The samples were obtained in increments of 19 mm (0.75 inches) to a depth of 95 mm (3.8 inches) both at and away from cracks in bridge decks primarily in northeast Kansas. Figure 162 shows the relationship between the average chloride content at crack locations interpolated to a depth of 76.2 mm (3 inches) versus age for bridges with an average annual daily traffic (AADT) greater than 7,500 (high traffic bridges).[3] The decks in the survey were cast monolithically and with high-density conventional and silica fume overlays. Figure 162 demonstrates that the chloride content at cracks is independent of the type of deck.
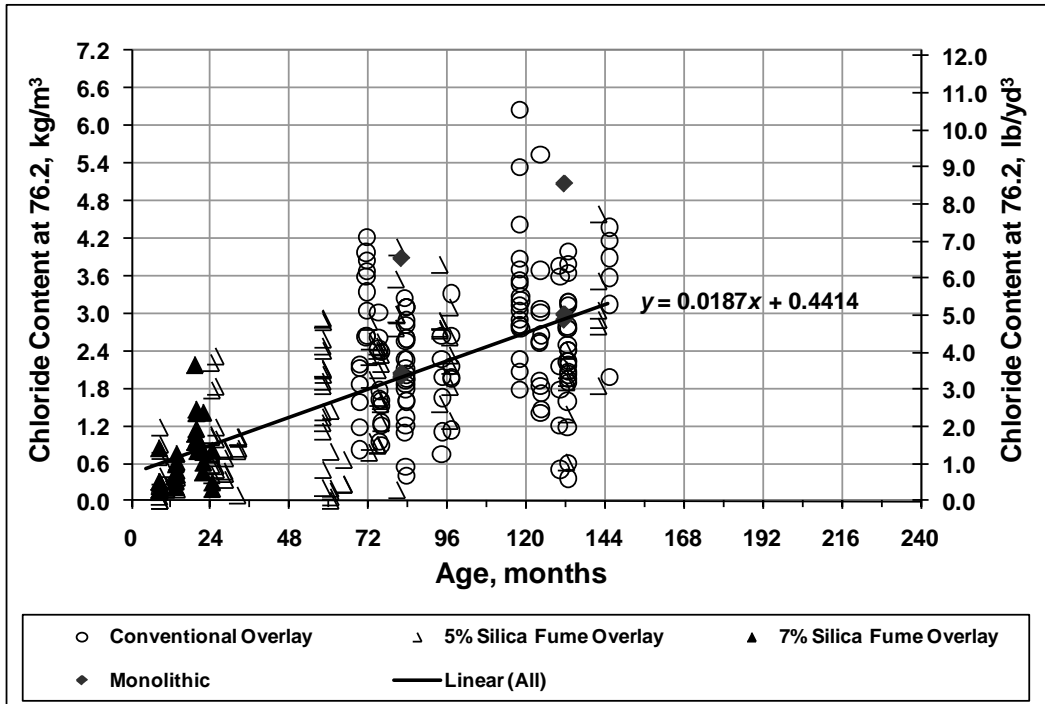
1 kg/m³ = 1.69 lb/yd³

Figure 162. Graph. Chloride content taken at cracks interpolated at a depth of 76.2 mm (3 inches) versus age for bridges with an AADT greater than 7,500.

Based on the data shown in figure 162, the chloride content C (in kg/m³) can be expressed as a function of age at the time of sampling T (in months) by the trendline shown in the equation in figure 163.

$$C = 0.0187\,T + 0.4414$$

Figure 163. Equation. Chloride content trendline.

Using the equation in figure 163, the average time to reach a specific critical chloride threshold T_c can be expressed as a function of the critical chloride threshold C_c, as shown in figure 164.

$$T_c = (C_c - 0.4414) / 0.0187$$

Figure 164. Equation. Average time to critical chloride threshold.

Table 31 lists the chloride contents at corrosion initiation (from table 13 and table 17), taken as the CCCT, for each corrosion-protection system in this study cast in concrete with a w/c ratio of 0.45, a realistic value for bridge decks. The values are combined and weighted based on the number of samples collected.

The CCCT values listed in table 31, with some modifications, are used in conjunction with figure 164 to determine the time to corrosion initiation for each corrosion-protection system. The values, expressed in years, are listed in table 41.

155

Table 41. Estimated time to corrosion initiation for corrosion-protection systems in a bridge deck with 76.2-mm (3-inch) cover on top reinforcing steel.

Steel Designation[a]	Chloride Threshold, kg/m³[b]	Age at Corrosion Initiation in Bridge Decks, years
Bars without coatings		
Control		
Conv.	1.58	2.2
Corrosion inhibitors in concrete		
Conv.(DCI)	3.00	6.0
Conv.(RH)	2.28	4.1
Conv.(HY)	0.83	0.2 (1.0)[c]
Bars with coatings		
Control		
ECR	8.29	20.0
Epoxies with increased adhesion		
ECR(Chromate)	8.29	20.0
ECR(DuPont)	8.29	20.0
ECR(Valspar)	8.29	20.0
Corrosion inhibitors in concrete		
ECR(DCI)	8.29	20.0
ECR(RH)	8.29	20.0
ECR(HY)	1.82	2.8
ECR(primer/Ca(NO$_2$)$_2$)	12.0	29.7
Bars with multiple coatings		
MC	4.92	20.0

1 kg/m³ = 1.69 lb/yd³
[a] See table 1 for abbreviation definitions.
[b] See text for explanation of differences of values from those in table 31.
[c] Rounded up from 0.2 years.

As shown in the table, the system combining uncoated conventional bars with concrete containing Hycrete™ has the lowest calculated time to initiation of corrosion, 0.2 years. Because salt is not applied to bridge decks until the first winter, this value is rounded up to 1 year. Conventional reinforcement with no inhibitor initiates corrosion after 2.2 years. Rheocrete® and calcium nitrite extend the initiation time of conventional reinforcement to 4.1 and 6.1 years, respectively.

Based on the statistical analysis of chloride threshold values presented earlier in this chapter for systems with coated bars, the differences in CCCT value for ECR, the three types of ECR with increased adhesion, and ECR with calcium nitrite or Rheocrete® added to the concrete are not significant. Therefore, the values are averaged (weighted based on the number of samples) to obtain a single CCCT value, 4.92 kg/m³ (8.29 lb/yd³). Because galvanized reinforcement has a higher corrosion threshold than conventional reinforcing steel, the CCCT value obtained in the southern exposure tests for MC bars, 2.00 kg/m³ (3.37 lb/yd³), is considered unrealistic.[50] Thus,

the threshold used for most of the other coated bars, 4.92 kg/m^3 (8.29 lb/yd^3), is used for the MC reinforcement, as well. For this value of CCCT, the time to corrosion initiation is 20.0 years. The use of the calcium nitrite primer under the epoxy significantly increases the time to 29.7 years, the highest of any of the systems in this study. ECR with Hycrete™ initiates corrosion after 2.8 years.

Time to Cracking After Corrosion Initiation

The time required to generate enough corrosion products to crack concrete is a function of the total corrosion rate and the corrosion loss required to cause cracking. The latter is a function of the bar size and the concrete cover. (See references 44 and 68–71.) Total corrosion rates will be covered first. To do this, equivalent field test macrocell corrosion rates must be calculated for conventional reinforcement cast in concrete with corrosion inhibitors because corrosion rates in field test specimens serve as the basis for calculating the time to cracking and because field tests were not performed on conventional reinforcement cast in concrete with corrosion inhibitors.

Equivalent Field Test Corrosion Rates for Conventional Reinforcement Cast in Concrete with Corrosion Inhibitors

As shown in chapter 3, corrosion rates and losses were consistently lower in the field test specimens than in the bench-scale specimens. Because the results for the field test specimens serve as the basis for the life-cycle and cost-effectiveness calculations and because field test specimens were not used for conventional reinforcement cast in concrete with corrosion inhibitors, an estimate of corrosion rates in field test specimens is needed for these systems. This is done using the ratio of the field test to bench-scale macrocell corrosion rates for conventional reinforcement in concrete without and with cracks above the reinforcement. Figure 165 and figure 166 compare the average macrocell corrosion rates after corrosion initiation based on total area for the field test and bench-scale specimens containing conventional reinforcement in uncracked and cracked concrete, respectively. The figures also show the range in the rates for each type of specimen. As shown, the average macrocell corrosion rates in the field test specimens equal 15.5 and 13.4 percent of the rates in the bench-scale specimens in uncracked and cracked concrete, respectively. These values are used to convert the corrosion rates shown in table 34 to equivalent macrocell corrosion rates in field tests shown in table 42.
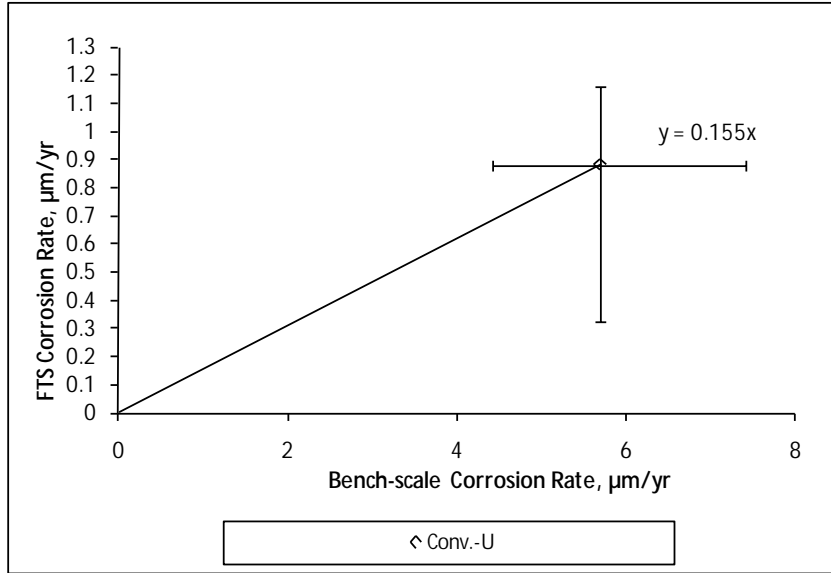
1 μm = 0.0394 mil

Figure 165. Graph. Comparison between average macrocell corrosion rates after corrosion initiation based on total area for bench-scale and field test specimens with conventional reinforcement in uncracked concrete.
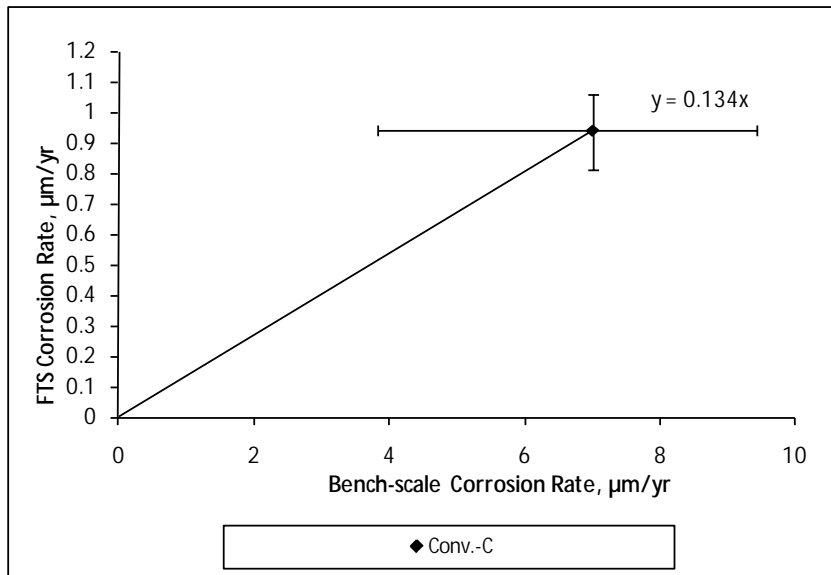
1 μm = 0.0394 mil

Figure 166. Graph. Comparison between average macrocell corrosion rates after corrosion initiation based on total area for bench-scale and field test specimens with conventional reinforcement in cracked concrete.

Table 42. Equivalent field test specimen macrocell corrosion rates (µm/year) for bare bar corrosion-protection systems.

Steel Designation[a]	Concrete[a]	Benchscale Corrosion Rate	Equivalent FTS Corrosion Rate[b]
FTS(Conv.)	U	NA	0.882
	C	NA	0.939
Conv.*(RH)	U	1.64	0.255
	C	6.34	0.939
Conv.*(DCI)	U	3.77	0.584
	C	6.34	0.939
Conv.*(HY)	U	0.706	0.109
	C	1.80	0.241

1 µm = 0.0394 mil
FTS = Field test specimen
NA = Not applicable
[a] See table 1 for abbreviation definitions. U = uncracked concrete, C = cracked concrete.
[b] Estimated using a ratio of FTS to bench-scale rate of 0.155 in uncracked concrete and 0.134 in cracked concrete.

The corrosion rates for bare bar systems assume the entire area of steel is corroding; however, autopsy results from field test specimens indicated corrosion occurs in localized regions on the bars (see figure 150 and figure 151). As discussed in chapter 3, a visual inspection of conventional reinforcement from field test specimens at the end of testing indicated that corrosion covers only about one-third the total area of bars in uncracked concrete and about 40 percent of the total area of bars in cracked concrete. Because corrosion only occurs on limited regions of the bar, the corrosion rates for bare bars in uncracked and cracked concrete are multiplied by 3 and 2.5, respectively, to obtain a macrocell corrosion rate based on effective area for these systems. The results are listed in table 43. As before, conventional reinforcement in concrete with no inhibitor has the greatest corrosion rates based on effective area in both uncracked and cracked concrete, 2.65 and 2.35 µm/year (0.104 and 0.0925 mil/year), respectively. Conv.*(HY) has the lowest corrosion rates based on effective area in uncracked and cracked concrete, 0.328 and 0.602 µm/year (0.0129 and 0.0237 mil/year), respectively. These adjustments appear to be appropriate not only based on the observed area undergoing corrosion but also based on the time to cracking observed for the Conv. field test specimens, as discussed in chapter 3.

Table 43. Equivalent field test specimen macrocell corrosion rates (µm/year) for bare bar corrosion-protection systems based on effective area.

Steel Designation[a]	Concrete[a]	FTS Corrosion Rate (Total Area)[b]	FTS Corrosion Rate (Effective Area)[c]
Conv.	U	0.882	2.65
	C	0.939	2.35
Conv.*(RH)	U	0.255	0.765
	C	0.939	2.35
Conv.*(DCI)	U	0.584	1.75
	C	0.939	2.35
Conv.*(HY)	U	0.109	0.328
	C	0.241	0.602

1 µm = 0.0394 mil
FTS = Field test specimen
[a] See table 1 for abbreviation definitions. U = uncracked concrete, C = cracked concrete.
[b] See table 42.
[c] Estimated using a ratio of 3 in uncracked concrete and 2.5 in cracked concrete.

Total Corrosion Rates

The field test specimens provide realistic models of bridge decks in terms of both configuration and exposure. Because the measurements are based on macrocell corrosion, which represents only a portion of the total corrosion loss, a comparison of the linear polarization resistance and macrocell corrosion results for the southern exposure and cracked beam specimens is used in conjunction with macrocell readings from the field tests to estimate the total corrosion rates in the field tests, and thus, in bridge decks.

To estimate the relationships between the macrocell and total corrosion rates for the different systems and degrees of exposure evaluated in this study, the average corrosion rates based on losses after corrosion initiation for southern exposure (table 15) and cracked beam (table 20) specimens are compared with the average corrosion rates based on total corrosion losses after corrosion initiation as measured using linear polarization resistance (table 22). Because of differences in exposure and corrosion mechanisms, separate comparisons are made for southern exposure and cracked beam specimens for uncoated bars, epoxy-coated bars, and MC bars.

The relationships between total and macrocell corrosion rates are shown in figure 167 and figure 168 for the bench-scale specimens containing uncoated bars, in figure 169 and figure 170 for specimens containing epoxy-coated bars, and in figure 171 and figure 172 for specimens containing MC bars. In each pair of figures, the first represents the results for the southern exposure specimens and the second represents the results for the cracked beam specimens. The figures show trend lines originating at the origin, which give the ratio of total to macrocell corrosion rate. As shown in figure 167 and figure 168 for conventional reinforcement, the total corrosion rates average 1.79 and 3.49 times macrocell corrosion rates for southern exposure and cracked beam specimens, respectively. The multiples are 3.15 and 12.36 for epoxy-coated bars and 4.90 and 5.82 for the MC bars.
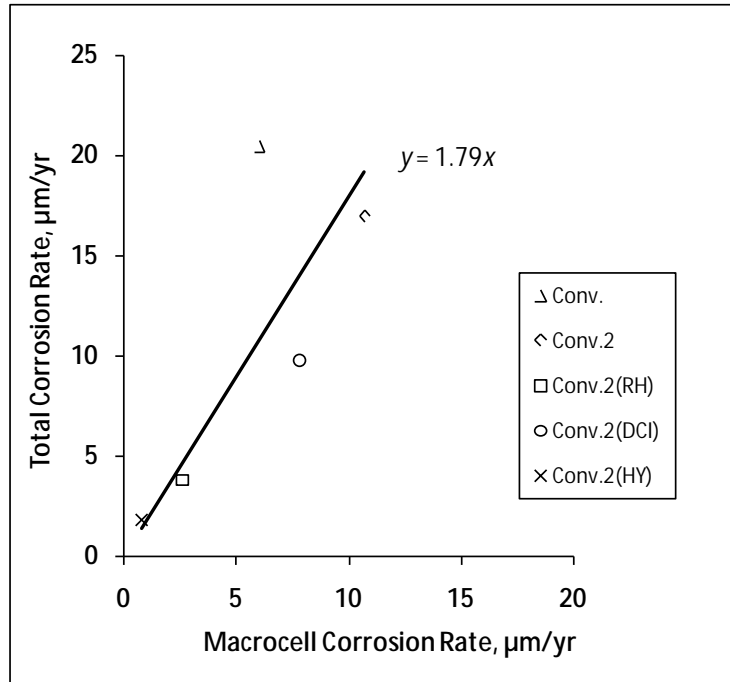
1 µm = 0.0394 mil

Figure 167. Graph. Total versus macrocell corrosion rate after corrosion initiation for southern exposure specimens with conventional reinforcement.
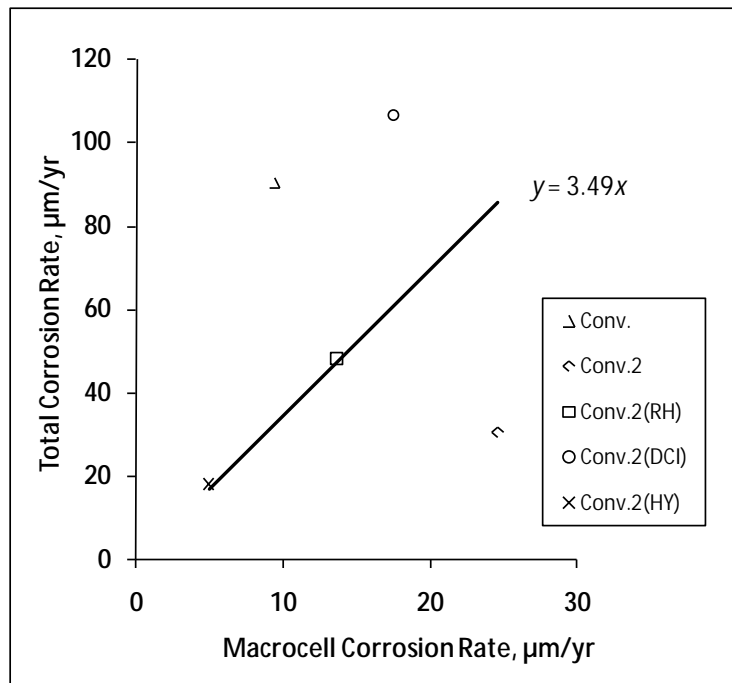
1 µm = 0.0394 mil

Figure 168. Graph. Total versus macrocell corrosion rate after corrosion initiation for cracked beam specimens with conventional reinforcement.

161
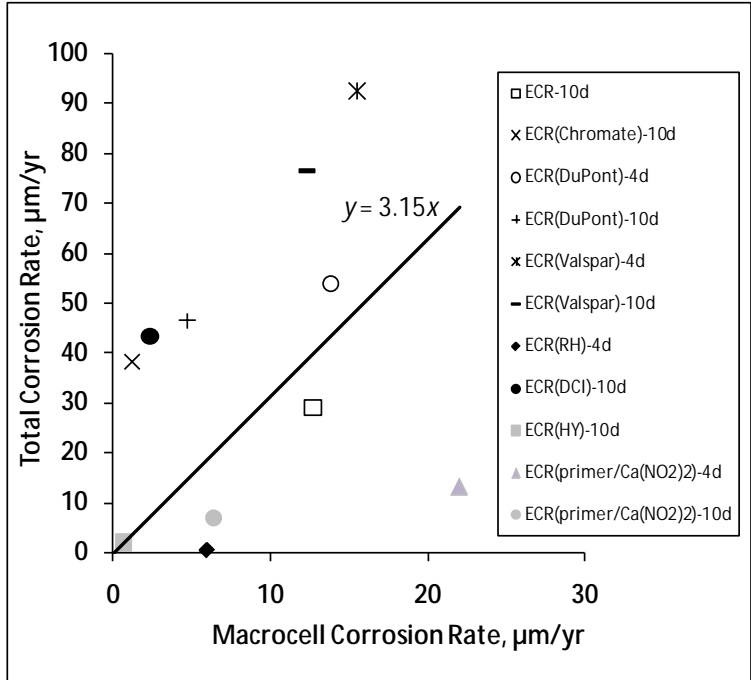
1 µm = 0.0394 mil

Figure 169. Graph. Total versus macrocell corrosion rate after corrosion initiation for southern exposure specimens with ECR.
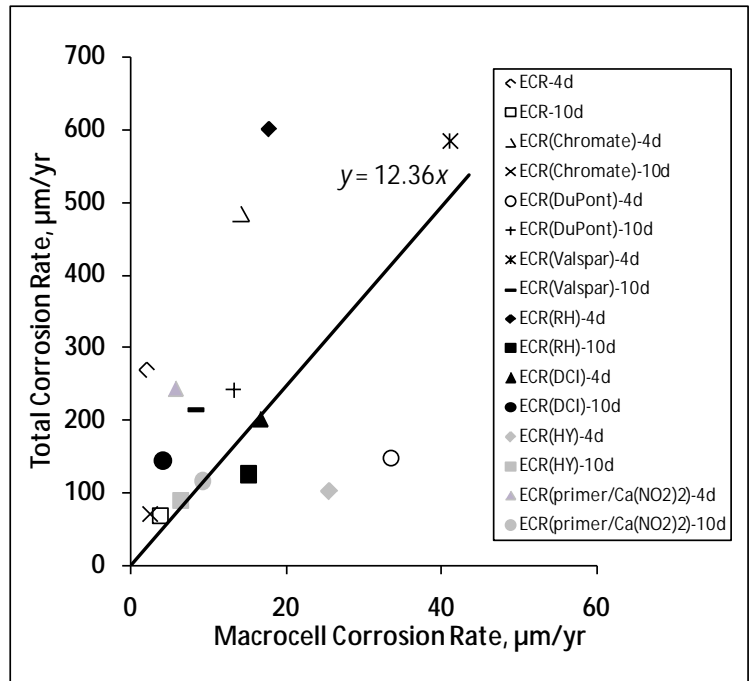
1 µm = 0.0394 mil

Figure 170. Graph. Total versus macrocell corrosion rate after corrosion initiation for cracked beam specimens with ECR.

162
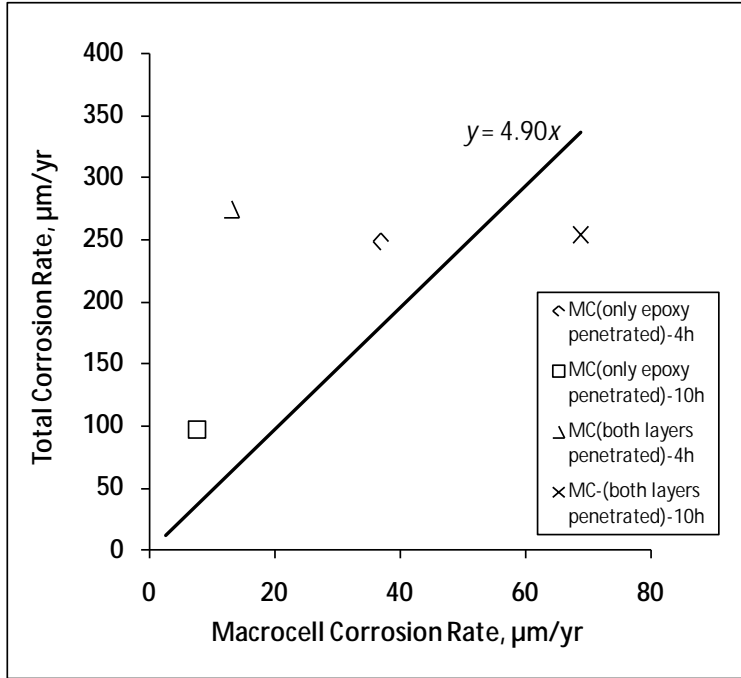
1 µm = 0.0394 mil

Figure 171. Graph. Total versus macrocell corrosion rate after corrosion initiation for southern exposure specimens with MC reinforcement.
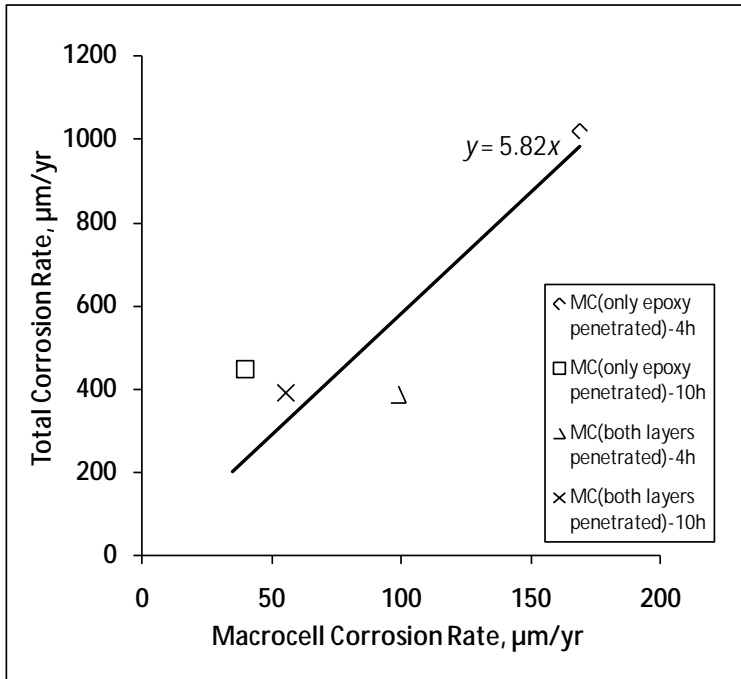
1 µm = 0.0394 mil

Figure 172. Graph. Total versus macrocell corrosion rate after corrosion initiation for cracked beam specimens with MC reinforcement.

As demonstrated in chapter 3, figure 167 through figure 172 show that corrosion rates are significantly higher for cracked concrete (cracks directly above and parallel to the reinforcement) than for uncracked concrete. The figures also show that the total corrosion rate is a higher multiple of the macrocell corrosion rate for coated bars than for uncoated bars and that the multiple is consistently higher for cracked concrete than for uncracked concrete. The multiples are closest between uncracked and cracked concrete for the MC bars, in all likelihood due to the combined effects of the amphoteric nature (corrodes in alkaline as well an acidic conditions) of zinc and the galvanic protection provided by the zinc.

The multiples developed in figure 167 through figure 172 are applied to the field test macrocell corrosion rates, including the equivalent rates for conventional bars cast in concrete containing corrosion inhibitors, to develop estimates of total corrosion rates in bridge decks. The macrocell corrosion rates used for the coated bars are based on the statistical analyses presented earlier in the chapter. Because the differences in corrosion rate are not statistically significant, an average macrocell rate based on exposed area of 5.66 µm/year (0.223 mil/year) is used for all but one system in uncracked concrete; the corrosion rate for that system, ECR(HY), (2.89 µm/year (0.114 mil/year)) does exhibit a statistically significant difference. Based on the results of the analysis for bars in cracked concrete, an average macrocell corrosion rate of 7.95 µm/year (0.313 mil/year) on an exposed area equal to that provided by a 3.2-mm (0.125-inch)-diameter penetration is used for conventional ECR, ECR with increased adhesion, ECR with corrosion inhibitor Rheocrete® in the concrete, and MC bars. Rates of 5.79, 4.32, and 4.65 µm/year (0.228, 0.170, and 0.183 mil/year) are used, respectively, for ECR in concrete with the corrosion inhibitors calcium nitrite and Hycrete™ and ECR with primer containing microencapsulated calcium nitrite. In the latter case, it is unlikely the calcium nitrite provided by the primer would be adequate for the full time to first repair. Thus, for purposes of the analysis, a corrosion rate equal to that used for conventional ECR is assumed beginning 10 years after corrosion initiation. The estimated total corrosion rates in bridge decks are shown in table 44.

Table 44. Estimated total corrosion rates in bridge decks (µm/year) for corrosion-protection systems.

Steel Designation[a]	Concrete[b]	Macrocell Corrosion Rate[c]	Estimated Total Corrosion Rate[d]
Corrosion rate (total area)			
Conv.	U	2.65	4.74
	C	2.35	8.19
Conv.*(RH)	U	0.765	1.37
	C	2.35	8.19
Conv.*(DCI)	U	1.75	3.14
	C	2.35	8.19
Conv.*(HY)	U	0.328	0.588
	C	0.602	2.10
Corrosion rate (exposed area)			
ECR	U	5.66	17.8
	C	7.95	98.3
ECR(Chromate)	U	5.66	17.8
	C	7.95	98.3
ECR(DuPont)	U	5.66	17.8
	C	7.95	98.3
ECR(Valspar)	U	5.66	17.8
	C	7.95	98.3
ECR(RH)	U	5.66	17.8
	C	7.95	98.3
ECR(DCI)	U	5.66	17.8
	C	5.79	71.6
ECR(HY)	U	2.89	9.1
	C	4.32	53.4
ECR(primer/Ca(NO$_2$)$_2$)	U	5.66	17.8
	C	4.65	57.5[e]
MC	U	5.66	27.7
	C	7.95	46.3[f]

1 µm = 0.0394 mil
[a] See table 1 for abbreviation definitions.
[b] U = uncracked concrete, C = cracked concrete.
[c] Macrocell corrosion rates for field test specimens.
[d] Macrocell corrosion rates multiplied by a ratio of 1.79, 3.15, and 4.90 for bare, coated, and MC bars in uncracked concrete and by 3.49, 12.36, and 5.82 for bare, coated, and MC bars in cracked concrete.
[e] Rate converts to value for ECR 10 years after corrosion initiation.
[f] Rate converts to value for ECR after 50-µm (1.9-mil) zinc layer is consumed.

For systems with bare bars in uncracked concrete, Conv. has the highest total corrosion rate, 4.74 µm/year (0.187 mil/year), while Conv.*(HY) has the lowest estimated total corrosion rate, 0.588 µm/year (0.0231 mil/year). For systems with bare bars in cracked concrete, Conv. has the greatest total corrosion rate, 8.19 µm/year (0.322 mil/year), and Conv.*(HY) again has the lowest estimated total corrosion rate, 0.0827 mil/year (2.10 µm/year).

For systems with coated bars in uncracked concrete, conventional ECR, ECR with increased adhesion, and ECR with Rheocrete® are assigned total corrosion rates of 17.8 and 98.3 µm/year (0.701 and 3.87 mil/year) in uncracked and cracked concrete, respectively. ECR with calcium nitrite is assigned total corrosion rates of 17.8 and 71.6 µm/year (0.701 and 2.82 mil/year) in uncracked and cracked concrete, and ECR with primer containing microencapsulated calcium nitrite is assigned total corrosion rates of 17.8 and 57.5 µm/year (0.701 and 2.26 mil/year) in uncracked and cracked concrete (the latter for the first 10 years, at which point it changes to 98.3 µm/year (3.87 mil/year), the value for conventional ECR). MC has a higher corrosion rate than ECR in uncracked concrete, 27.7 µm/year (1.09 mil/year), but a lower corrosion rate than ECR in cracked concrete, 46.2 µm/year (1.82 mil/year); this is due to the difference in multipliers compared to bars without the zinc coating under the epoxy. This behavior will govern until the 50-µm (2-mil) zinc layer is consumed, after which the bar is treated as corroding as conventional ECR. ECR with Hycrete™ has estimated total corrosion rates in both uncracked and cracked concrete of 9.1 and 53.4 µm/year (0.36 and 2.10 mil/year), respectively.

Corrosion Loss to Cause Concrete Cracking

A number of experimental studies have been performed to determine the corrosion loss on steel reinforcing bars required to crack (or delaminate) concrete. (See references 44 and 67–71.) All included corrosion of bare bars, and two included bars on which only a portion of the bar surface could corrode.[44,71] One of those efforts was conducted in concert with this study and included finite element analyses to supplement the experimental data.[44] Based on this work, which is summarized in appendix B, the corrosion loss in µm or mil required to crack concrete can be expressed as shown in figure 173 and figure 174.

$$x_{crit} = 45 \left(\frac{[C/25.4]^{2-A_f}}{D^{0.38} L_f^{0.1} A_f^{0.6}} + 0.2 \right) 3^{A_f-1}$$

Figure 173. Equation. Corrosion loss to crack concrete in SI units.

$$x_{crit} = 0.53 \left(\frac{C^{2-A_f}}{D^{0.38} L_f^{0.1} A_f^{0.6}} + 0.6 \right) 3^{A_f-1}$$

Figure 174. Equation. Corrosion loss to crack concrete in English units.

Where:

x_{crit} = Corrosion loss at crack initiation, µm or mil.

C = Cover, mm or inches.

D = Bar diameter, mm or inches.

L_f = Fractional length of bar corroding, $L_{corroding}/L_{bar}$.

A_f = Fractional area of bar corroding, $A_{corroding}/A_{bar}$.

For a conventional steel No. 16 (No. 5) bar with a concrete cover of 76.2 mm (3.0 inches), $L_f = A_f = 1.0$, and the value of x_{crit} is 56 µm (2.2 mil). For a No. 16 (No. 5) epoxy-coated bar with a damage pattern equal to that used for the field test specimens (3-mm (0.125-inch)-diameter holes

spaced at 0.124 m (4.9 inches) on each side of the bar), the fractional length of exposed bar L_f is 0.024, the fractional area of exposed bar A_f is 0.0023, and the value of x_{crit} is 2,430 μm (95.7 mil). For the purposes of the analysis, the bars in bridge decks are assumed to have the same damage pattern as the bars in the field tests.

Propagation Time

The time from corrosion initiation to initial delamination of the concrete cover due to the formation of stress-induced cracks caused by expansive corrosion products (propagation time) for each system is found by dividing the corrosion losses required to crack concrete, calculated above, by the estimated total corrosion rates listed in table 44. Because bridge decks inevitably develop cracks over and parallel to the reinforcement due to settlement of plastic concrete and shrinkage of the hardened concrete, the comparisons using the corrosion rates in cracked concrete should provide a more accurate representation of corrosion in bridge decks and are used for the balance of the analysis.

The estimated times to first cracking after corrosion initiation are presented in table 45. Based on the corrosion rate in cracked concrete, ECR with Hycrete™ has the longest propagation time, about 46 years, while the other coated bar systems have propagation times ranging from 25 to 34 years. Conventional reinforcement cast in concrete with Hycrete™ has a propagation time of about 27 years. The other systems involving conventional reinforcement cast in concrete without and with a corrosion inhibitor have propagation times of 6.8 years.

Table 45. Estimated times to formation of initial delamination cracks after corrosion initiation (propagation times) (years).

Steel Designation[a]	Cracked Concrete
Conv.	6.8
Conv.*(RH)	6.8
Conv.*(DCI)	6.8
Conv.*(HY)	26.6
ECR	24.8
ECR(Chromate)	24.8
ECR(DuPont)	24.8
ECR(Valspar)	24.8
ECR(RH)	24.8
ECR(DCI)	34.0
ECR(HY)	45.6
ECR(primer/Ca(NO$_2$)$_2$)	28.9
MC	33.6

[a] See table 1 for abbreviation definitions.

Time to First Repair

The time to first repair for each corrosion- protection system is found by combining the time to corrosion initiation, the time to initial delamination cracking of the concrete after corrosion

initiation, and the time between first cracking to the time when the deck is repaired. The latter period is based on the observation that a bridge deck is not fully repaired when the first crack forms. Rather, the bridge typically undergoes a series of short-term temporary repairs. To account for the period of temporary repairs, a 10-year delay between first cracking and repair is assumed based on the experience of the KDOT.

Table 46 compares expected times to first repair for all corrosion-protection systems based on the corrosion rate in cracked concrete. As shown in the table, conventional reinforcement has an expected time to first repair of 19 years, which is within the range of 10 to 25 years predicted by KDOT and SDDOT maintenance engineers.[23] Among systems with conventional reinforcement with inhibitors, conventional reinforcement used in conjunction with concrete containing Rheocrete® and calcium nitrite have expected times to first repair of 21 and 23 years, slightly greater than those observed for conventional reinforcement without inhibitors. At 38 years, conventional reinforcement used in conjunction with concrete containing Hycrete™ has more than twice the age to first repair as conventional reinforcement with no inhibitor. ECR and ECR with increased adhesion have expected times to first repair of 55 years compared to the 35 to 40 years estimated by KDOT and SDDOT.[23] Most bridges containing ECR have not yet reached this age. Systems containing ECR used in concrete containing corrosion inhibitors have times to first repair ranging from 55 to 69 years, with ECR with calcium nitrite and ECR with primer containing microencapsulated calcium nitrite giving the longest times at 64 and 69 years, respectively. Systems with MC reinforcement have an expected time to first repair of 56 years. Thus, based in the assumption that cracked concrete will dominate corrosion behavior, all systems will require at least one repair during the assumed 75-year design life of the deck.

Table 46. Time to first repair based on corrosion rate in cracked concrete (years).

Steel Designation[a]	Time to Initiation[b]	Time from Initiation to Cracking[c]	Time from Cracking to Repair[d]	Expected Time to First Repair
Conv.	2.2	6.8	10	19
Conv.*(RH)	4.0	6.8	10	21
Conv.*(DCI)	6.0	6.8	10	23
Conv.*(HY)	1.0	26.6	10	38
ECR	20.0	24.8	10	55
ECR(Chromate)	20.0	24.8	10	55
ECR(DuPont)	20.0	24.8	10	55
ECR(Valspar)	20.0	24.8	10	55
ECR(RH)	20.0	24.8	10	55
ECR(DCI)	20.0	34.0	10	64
ECR(HY)	2.8	45.6	10	58
ECR(primer/Ca(NO$_2$)$_2$)	29.7	28.9	10	69
MC	20.0	25.5	10	56

[a] See table 1 for abbreviation definitions.
[b] See table 41.
[c] See table 45 for cracked concrete.

COST EFFECTIVENESS

A 75-year economic life is used to compare the costs associated with the various corrosion-protection systems for a typical bridge deck. A 46-m (150-ft)-long, 11-m (36-ft)-wide, 216-mm (8.5-inch)-thick bridge deck is used in the analysis. Costs include those for initial construction and repair over the 75-year period. With the exception of steel and admixture prices, costs are based on experience in Kansas and South Dakota for the years 2004 through 2008. Prices during this period are considered to be more indicative of the long term than prices between 2008 and 2011, which are representative of a depressed construction market. User costs are not included in the analysis.

Initial Cost

The material costs for reinforcement and inhibitors used in this analysis are provided by the material suppliers. For conventional reinforcement, the base cost is $0.77/kg ($0.35/lb). ECR and ECR with increased adhesion from DuPont™ and Valspar® have a base cost of $0.99/kg ($0.45/lb). ECR with chromate pretreatment and ECR with the calcium nitrite primer have a base cost of $1.10/kg ($0.50/lb). MC reinforcement has a base cost of $1.65/kg ($0.75/lb). A placement cost of $1.14/kg ($0.52/lb) is used for all reinforcement. A steel reinforcement density of 163 kg/m^3 (275 lb/yd^3) is used, based on the average quantity of steel used in 12 bridge decks constructed in Kansas between 2004 and 2007.[58] A 216-mm (8.5-inch)-thick bridge deck requires 35.2 kg/m^2 (64.9 lb/yd^2) of steel based on the surface area of deck, as shown in figure 175.

$$\frac{163\,\text{kg}}{\text{m}^3} \cdot \frac{0.216\,\text{m}}{\text{typical deck}} = 35.2\,\text{kg/m}^2$$

Figure 175. Equation. Typical quantity of reinforcement.

Using the required reinforcement per unit surface area determined using the equation in figure 175, the reinforcement costs for each system are calculated, as shown in the equations in figure 176 through figure 179 and listed in table 47.

$$\frac{\$1.91}{\text{kg}} \cdot \frac{35.2\,\text{kg}}{\text{m}^2} = \$67.23/\text{m}^2$$

Figure 176. Equation. Reinforcement cost for conventional steel.

$$\frac{\$2.13}{\text{kg}} \cdot \frac{35.2\,\text{kg}}{\text{m}^2} = \$74.98/\text{m}^2$$

Figure 177. Equation. Reinforcement cost for ECR, ECR(Dupont), and ECR(Valspar).

$$\frac{\$2.24}{\text{kg}} \cdot \frac{35.2\,\text{kg}}{\text{m}^2} = \$78.85/\text{m}^2$$

Figure 178. Equation. Reinforcement cost for ECR(Chromate) and ECR(primer/Ca(NO$_2$)$_2$).

$$\frac{\$2.79}{kg} \times \frac{35.2\,kg}{m^2} = \$98.21/m^2$$

Figure 179. Equation. Reinforcement cost for MC reinforcement.

Table 47. Total in-place cost for reinforcement per unit area of bridge deck.

Steel Designation[a]	Reinforcement Cost		Reinforcement Used		Total Cost	
	$/kg	$/lb	kg/m^2	lb/yd^2	$/m^2	$/yd^2
Conv.	1.91	0.87	35.2	64.9	67.23	56.35
ECR	2.13	0.97	35.2	64.9	74.98	62.84
ECR(Chromate)	2.24	1.02	35.2	64.9	78.85	66.08
ECR(DuPont)	2.13	0.97	35.2	64.9	74.98	62.84
ECR(Valspar)	2.13	0.97	35.2	64.9	74.98	62.84
ECR(primer/Ca(NO$_2$)$_2$)	2.24	1.02	35.2	64.9	78.85	66.08
MC	2.79	1.27	35.2	64.9	98.21	82.31

[a] See table 1 for abbreviation definitions.

The base in-place cost of concrete with no inhibitors used in this study is $735.75/m^3 ($562.51/yd^3) based on costs between 2004 and 2007, updated to July 2008.[58,72] For corrosion inhibitors, the dosage rates are the rates used in this study and are based on manufacturer recommendations. Rheocrete® costs $6.08/L ($23.00/gal) and has dosage rate of 5 L/m^3 (1 gal/yd^3), equal to $30.40/m^3 ($23.00/yd^3) over the base cost of the concrete. DCI® S costs $1.32/L ($5.00/gal) and has a dosage rate of 15 L/m^3 (3 gal/yd^3), equal to $19.80/m^3 ($15/yd^3). Hycrete™ costs $4.95/L ($18.75/gal) and has a dosage rate of 7.6 L/m^3 (1.54 gal/yd^3). To counteract the reduction in strength and low freeze-thaw resistance observed in concrete containing Hycrete™, an additional 35.6 kg/m^3 (60 lb/yd^3) of portland cement at $0.138/kg ($0.0625/lb) is added, for a cost of $42.53/m^3 ($32.63/yd^3) for Hycrete™ over the in-place cost of conventional concrete.[1]

Assuming a 216-mm (8.5-inch)-thick bridge deck, 0.216 m^3 of concrete are required per 1-m^2 (0.236 yd^3 per 1-yd^2) surface area of deck. Concrete costs for all corrosion-protection systems per unit surface area are calculated using the equations in figure 180 through figure 183 and are shown in table 48.

$$\frac{\$735.74}{m^3} \times \frac{0.216\,m}{typical\,deck} = \$158.92/m^2$$

Figure 180. Equation. Costs for concrete placed with conventional reinforcement.

$$\left(\frac{\$735.75}{m^3} + \frac{\$30.40}{m^3}\right) \times \frac{0.216\,m}{typical\,deck} = \$165.49/m^2$$

Figure 181. Equation. Costs for concrete placed with Rheocrete® inhibitor.

---

[1] The addition of 60 lb/yd^3 (35.6 kg/m^3) is an estimate and is not based on laboratory or field observations.

$$\left(\frac{\$735.75}{m^3} + \frac{\$19.80}{m^3}\right) \div \frac{0.216\,m}{typical\,deck} = \$163.20\,/\,m^2$$

Figure 182. Equation. Costs for concrete placed with calcium nitrite inhibitor.

$$\frac{35.9\,kg\,of\,cement}{m^3} \cdot \frac{\$0.137}{kg} = \$4.91\,cement\,/\,m^3$$

$$\$4.91\,cement\,/\,m^3 + \$735.75\,concrete/\,m^3 = \$740.66\,/\,m^3$$

$$\left(\frac{\$740.66}{m^3} + \frac{\$37.62}{m^3}\right) \div \frac{0.216\,m}{typical\,deck} = \$168.11\,/\,m^2$$

Figure 183. Equation. Costs for concrete placed with Hycrete™ inhibitor.

Table 48. Total in-place cost for concrete per unit area of bridge deck.

Steel Designation[a]	Concrete Cost		Inhibitor Cost		Concrete Use		Total Cost	
	$/m³	$/yd³	$/m³	$/yd³	m³/m²	yd³/yd²	$/m²	$/yd²
Conv.	735.75	562.51	–	–	0.216	0.236	158.92	132.75
RH	735.75	562.51	30.40	23.00	0.216	0.236	165.49	138.18
DCI	735.75	562.51	19.80	15.00	0.216	0.236	163.20	136.29
HY[a]	740.66	566.29	37.62	28.88	0.216	0.236	168.11	140.46

– Indicates no inhibitor used.
[a] Additional 35.9 kg/m³ (60 lb/yd³) cement added to counteract strength reduction.

The total initial cost, equal to the sum of reinforcement and concrete costs, for each system is shown in figure 184 through figure 194 and table 49.

$$216\text{-mm Concrete Deck} + \text{Conventional Steel} = \$158.92/m^2 + \$67.23/yd^2 = \$226.15/m^2$$
Figure 184. Equation. Total initial cost for decks with conventional steel.

216-mm Concrete Deck with Rheocrete + Conventional Steel
$$= \$165.49/m^2 + \$67.23/m^2 = \$232.72/m^2$$
Figure 185. Equation. Total initial cost for decks with conventional steel and Rheocrete® inhibitor.

216-mm Concrete Deck with DCI + Conventional Steel
$$= \$168.11/m^2 + \$67.23/m^2 = \$230.43/m^2$$
Figure 186. Equation. Total initial cost for decks with conventional steel and calcium nitrite inhibitor (DCI).

216-mm Concrete Deck with Hycrete + Conventional Steel
$$= \$163.20/m^2 + \$67.23/m^2 = \$235.34/m^2$$
Figure 187. Equation. Total initial cost for decks with conventional steel and Hycrete™ inhibitor.

216-mm Concrete Deck + Epoxy-Coated Reinforcement

$$= \$158.92/m^2 + \$74.98/m^2 = \$233.90/m^2$$

Figure 188. Equation. Total initial cost for decks with ECR, ECR(Dupont), and ECR(Valspar).

216-mm Concrete Deck + Epoxy-Coated Reinforcement with Chromate

$$= \$158.92/m^2 + \$78.85/m^2 = \$233.90/m^2$$

Figure 189. Equation. Total initial cost for decks with ECR(Chromate).

216-mm Concrete Deck with Rheocrete + Epoxy-Coated Reinforcement

$$= \$165.49/m^2 + \$74.98/m^2 = \$240.46/m^2$$

Figure 190. Equation. Total initial cost for decks with ECR and Rheocrete® inhibitor.

216-mm Concrete Deck with DCI + Epoxy-Coated Reinforcement

$$= \$163.20/m^2 + \$74.98/m^2 = \$238.17/m^2$$

Figure 191. Equation. Total initial cost for decks with ECR and calcium nitrite inhibitor (DCI).

216-mm Concrete Deck with Hycrete and extra cement + Epoxy-Coated Reinforcement

$$= \$168.11/m^2 + \$74.98/m^2 = \$243.08/m^2$$

Figure 192. Equation. Total initial cost for decks with ECR and Hycrete™ inhibitor.

216-mm Concrete Deck + Epoxy-Coated Reinforcement with primer

$$= \$158.92/m^2 + \$78.85/m^2 = \$237.77/m^2$$

Figure 193. Equation. Total initial cost for decks with ECR with primer.

216-mm Concrete Deck + Multiple-coated reinforcement

$$= \$158.92/m^2 + \$98.21/m^2 = \$257.13/m^2$$

Figure 194. Equation. Total initial cost for decks with MC reinforcement.

Table 49. Total in-place cost for corrosion protection systems.

Steel Designation[a]	Reinforcement Cost		Concrete Cost		Total Cost	
	$/m²	$/yd²	$/m²	$/yd²	$/m²	$/yd²
Conv.	67.23	56.35	158.92	132.75	226.15	189.10
Conv.(DCI)	67.23	56.35	163.20	136.29	230.43	192.64
Conv.(RH)	67.23	56.35	165.49	138.18	232.72	194.53
Conv.(HY)	67.23	56.35	168.11	140.46	235.34	196.81
ECR	74.98	62.84	158.92	132.75	233.90	195.59
ECR(Chromate)	78.85	66.08	158.92	132.75	237.77	198.83
ECR(DuPont)	74.98	62.84	158.92	132.75	233.90	195.59
ECR(Valspar)	74.98	62.84	158.92	132.75	233.90	195.59
ECR(DCI)	74.98	62.84	163.20	136.29	238.17	199.13
ECR(RH)	74.98	62.84	165.49	138.18	240.46	201.02
ECR(HY)	74.98	62.84	168.11	140.46	243.08	203.30
ECR(primer/Ca(NO$_2$)$_2$)	78.85	66.08	158.92	132.75	237.77	198.83
MC	98.21	82.31	158.92	132.75	257.13	215.06

[a] See table 1 for abbreviation definitions.

A deck with conventional reinforcement has the lowest initial in-place cost, $226.15/m² ($189.10/yd²). This increases to $233.90/m² ($195.59/yd²) for ECR, which exceeds the cost of a deck with conventional steel and calcium nitrite or Rheocrete® at $230.43/m² ($192.64/yd²) or $232.72/m² ($194.53/yd²) but is less than the cost of a deck with conventional steel and Hycrete™ at $235.34/m² ($196.81/yd²). At $257.13/m² ($215.06/yd²), a deck with MC reinforcement has the highest in-place cost of all systems with an epoxy coating.

Repair Costs

Repair costs for a typical 216-mm (8.5-inch) bridge deck were obtained from KDOT. Current data include repair of bridge decks with conventional reinforcement only because bridge decks constructed since the late 1970s have been constructed using ECR and have not needed repair as of the date of this report. It is estimated that repair costs of bridge decks with ECR will be similar to those for decks with conventional reinforcement. Based on experience in Kansas and South Dakota, repairs are assumed to last for 25 years.[23]

In Kansas, repair consists of applying either a silica fume or polymer overlay to the deck. Repair costs include a unit cost for the overlay and machine preparation, costs for mobilization and traffic control, and patching costs based on the percentage of decks that received partial or full depth repairs, 5 and 17 percent, respectively. Based on an analysis of bid costs from 2008 through 2010, total repair costs are given in figure 195 and figure 196.

Total repair costs (silica fume overlay)

$$= \text{Total overlay deck} + \text{machine preparation} + \text{mobilization \& traffic control} + \text{partial-depth repair} + \text{full-depth repair}$$

$$= \$47/m^2 + \$30/m^2 + \$89/m^2 + (17\% \times \$247/m^2) + (5\% \times \$335/m^2)$$
$$(\$39/yd^2 + \$25/yd^2 + \$75/yd^2 + (17\% \times \$207/yd^2) + (5\% \times \$281/yd^2))$$

$$= \$224/m^2 \ (\$188/yd^2)$$

Figure 195. Equation. Total repair costs with silica fume overlay.

Total repair costs (polymer overlay)

$$= \text{Total overlay deck} + \text{machine preparation} + \text{mobilization \& traffic control} + \text{partial-depth repair} + \text{full-depth repair}$$

$$= \$52/m^2 + \$0/m^2 + \$89/m^2 + (2\% \times \$247/m^2) + (1\% \times \$335/m^2)$$
$$((\$44/yd^2 + \$0/yd^2 + \$75/yd^2 + (2\% \times \$207/yd^2) + (1\% \times \$281/yd^2))$$

$$= \$175/m^2 \ (\$147/yd^2)$$

Figure 196. Equation. Total repair costs with polymer overlay.

The current KDOT repair costs are compared with a previous analysis based on costs obtained from SDDOT, which are based on an average of costs for bridge deck repair projects for the year 2006.[72] A typical repair project includes costs for removing deleterious concrete and replacing with a low-slump dense concrete overlay, bridge rail modifications, approach guard rail replacement, approach pavement work, mobilization, traffic control, and other miscellaneous costs. Costs were determined per square yard for the 46-m (150-ft)-long deck described at the beginning of this section. A summary of the repair costs is shown in table 50 and described in figure 197 through figure 202.

Table 50. Repair costs for bridge decks in South Dakota.[75]

Item	Unit	Cost	Cost/yd²	Unit	Cost	Cost/m²
Low slump dense concrete overlay	Per yd²	$130.00	$130	Per m²	$155.00	$155
Bridge rail modification	Per linear ft	$62.00	$31	Per linear m	$814.00	$37
Approach guard rail	Lump sum	$16,500.00	$28	Lump sum	$16,500.00	$34
Approach pavement work	Lump sum	$17,000.00	$28	Lump sum	$17,000.00	$34
Mobilization	Lump sum	$25,000.00	$42	Lump sum	$25,000.00	$50
Traffic control and misc.	Lump sum	$20,000.00	$33	Lump sum	$20,000.00	$39
Total repair costs			$292			$349

1 m = 1.09 yd = 3.28 ft

$$\frac{\$814}{m} \cdot \frac{2 \text{ sides}}{\text{bridge}} \cdot \frac{1}{11 - m \text{ deck width}} = \$37/m^2$$

Figure 197. Equation. Bridge rail modification cost.

$$\frac{\$16,500}{\text{project}} \cdot \frac{\text{typical bridge}}{506 \, m^2} = \$34/m^2$$

Figure 198. Equation. Approach guard rail cost.

174

$$\frac{\$17,000}{\text{project}} \cdot \frac{\text{typical bridge}}{506\,\text{m}^2} = \$34/\text{m}^2$$

Figure 199. Equation. Approach pavement work cost.

$$\frac{\$25,000}{\text{project}} \cdot \frac{\text{typical bridge}}{506\,\text{m}^2} = \$50/\text{m}^2$$

Figure 200. Equation. Mobilization cost.

$$\frac{\$20,000}{\text{project}} \cdot \frac{\text{typical bridge}}{506\,\text{m}^2} = \$39/\text{m}^2$$

Figure 201. Equation. Traffic control and miscellaneous costs.

Total repair costs = Total overlay deck + bridge rail modification + approach guard rail + mobilization + traffic control and misc.

= $\$155/\text{m}^2 + \$37/\text{m}^2 + \$34/\text{m}^2 + \$34/\text{m}^2 + \$50/\text{m}^2 + \$39/\text{m}^2$
($\$130/\text{yd}^2 + \$31/\text{yd}^2 + \$28/\text{yd}^2 + \$28/\text{yd}^2 + \$42/\text{yd}^2 + \$33/\text{yd}^2$)

= $\$349/\text{m}^2$ ($\$292/\text{yd}^2$)

Figure 202. Equation. Total repair costs.

A comparison of the repair costs provided by KDOT for 2008 through 2010 ($\$224/\text{m}^2$ or $\$175/\text{m}^2$ ($\$188/\text{yd}^2$ or $\$147/\text{yd}^2$)) and those provided by SDDOT for 2006 ($\$349/\text{m}^2$ ($\$292/\text{yd}^2$)) shows that costs have significantly decreased in the current economic climate. Because the current highly competitive environment in the construction industry is not expected to be long term, the higher costs for 2006 analysis are used in this study.

Present Value

The total life cycle cost of each corrosion-protection system is calculated using the times to first repair for systems in cracked concrete listed in table 46. Cost effectiveness is based on the initial cost of the deck and the present value of future repair costs. The present value is calculated as shown in figure 203, where P is the present value, F is the future cost of a repair ($\$349/\text{m}^2$ ($\$292/\text{yd}^2$)), i is the discount rate, and n is the time to repair.

$$P = F(1+i)^{-n}$$

Figure 203. Equation. Present value.

For this study, discount rates of 2, 4, and 6 percent are assumed. As the most realistic, the value 2 percent is used for most of the discussion that follows.

Table 51 and table 52 list the estimated costs over a 75-year design life using the time to first repair based on the corrosion rate in cracked concrete. Under this scenario, all of the corrosion-protection systems must be repaired at least once during the 75-year design life. Conventional reinforcement in concrete without a corrosion inhibitor and conventional reinforcement in concrete with the inhibitors calcium nitrite (DCI) and Rheocrete® must be repaired three times, and conventional reinforcement in concrete with the inhibitor Hycrete™ must be repaired twice. All of the coated-bar systems must be repaired once during the 75-year design life of the deck.

Table 51. Total costs ($/m^2) over 75-year design life for corrosion-protection systems using time to first repair based on corrosion rates in cracked concrete.

Steel Designation[a]	Initial Cost, $/m^2	Time to Repair, years			Repair Cost, $/m^2	Present Cost, $/m^2		
		1	2	3		i=2%	i=4%	i=6%
Conv.	226	19	44	69	349	700	477	374
Conv.*(DCI)	230	23	48	73	349	670	446	349
Conv.*(RH)	233	21	46	71	349	690	466	366
Conv.*(HY)	235	38	63	–	349	502	345	283
ECR	234	55	–	–	349	351	274	248
ECR(Chromate)	238	55	–	–	349	355	278	252
ECR(DuPont)	234	55	–	–	349	351	274	248
ECR(Valspar)	234	55	–	–	349	351	274	248
ECR(DCI)	238	64	–	–	349	336	266	246
ECR(RH)	240	55	–	–	349	358	281	255
ECR(HY)	243	58	–	–	349	353	278	255
ECR(primer/Ca(NO$_2$)$_2$)	238	69	–	–	349	327	261	244
MC	257	56	–	–	349	373	296	271

– No repair required.
[a] See table 1 for abbreviation definitions.

Table 52. Total costs ($/yd^2) over 75-year design life for corrosion protection systems using time to first repair based on corrosion rates in cracked concrete.

Steel Designation[a]	Initial Cost, $/yd^2	Time to Repair, years			Repair Cost, $/yd^2	Present Cost, $/yd^2		
		1	2	3		i=2%	i=4%	i=6%
Conv.	189	19	44	69	292	586	399	313
Conv.*(DCI)	193	23	48	73	292	560	373	291
Conv.*(RH)	195	21	46	71	292	577	390	306
Conv.*(HY)	197	38	63	–	292	420	288	237
ECR	196	55	–	–	292	294	229	207
ECR(Chromate)	199	55	–	–	292	297	232	211
ECR(DuPont)	196	55	–	–	292	294	229	207
ECR(Valspar)	196	55	–	–	292	294	229	207
ECR(DCI)	199	64	–	–	292	281	223	206
ECR(RH)	201	55	–	–	292	299	235	213
ECR(HY)	203	58	–	–	292	295	233	213
ECR(primer/Ca(NO$_2$)$_2$)	199	64	–	–	292	274	219	204
MC	215	56	–	–	292	312	248	226

– No repair required.
[a] See table 1 for abbreviation definitions.

Because it requires three repairs and has the lowest time to first repair, conventional reinforcement without corrosion inhibitors in the concrete has the highest present cost, $700/m^2 ($586/yd^2) at a 2 percent discount rate. Conventional reinforcement used in conjunction with

concrete containing calcium nitrite and Rheocrete® has present costs of $670/m^2 and $690/m^2 ($560/yd^2 and $577/yd^2), respectively. Conventional reinforcement used in conjunction with concrete containing Hycrete has the lowest present cost among systems with conventional reinforcement, $502/m^2 ($420/yd^2), but is less cost effective than any of the coated bar systems.

ECR in concrete with the calcium nitrite primer is the most cost-effective protection system, with a present cost of $327/m^2 ($274/yd^2) at a discount rate of 2 percent. ECR with calcium nitrite is the next most efficient system with a present cost of $336 m^2 ($281/yd^2) at a discount rate of 2 percent. Conventional ECR, as well as increased adhesion epoxies from DuPont™ and Valspar®, have present costs of $351/m^2 ($294/yd^2) at a discount rate of 2 percent. ECR(HY) and ECR(Chromate) have present costs of $353/m^2 and $355/m^2 ($295/yd^2 and $297/yd^2) at a discount rate of 2 percent; however, at a discount rate of 6 percent, ECR(Chromate) is more cost effective than ECR(HY). MC reinforcement has a present cost of $373/m^2 ($312/yd^2) at a 2 percent discount rate. The total spread in cost for the coated bar systems is $46/m^2 ($38/yd^2), or about 12 percent of the highest price. Considering the level of uncertainty inherent in the analysis, the differences in present costs for coated bar systems are not significant. However, the differences in the number of projected repairs and the differences in present costs between uncoated and coated bars systems are significant.

CHAPTER 5. CONCLUSIONS

The following conclusions are based on the results and analyses presented in this report:

- Conventional fusion-bonded epoxy coatings significantly improve the corrosion resistance, life expectancy, and cost effectiveness of reinforcing steel in severe climates such as bridge decks requiring application of deicing chemicals.

- Coated bars with damaged coatings initiate corrosion at chloride contents within concrete that are several times greater and corrode at rates that are typically two orders of magnitude below those exhibited by conventional reinforcement.

- Limited additional protection and extension of the time to first repair are achieved using bars with a primer coating containing microencapsulated calcium nitrite underneath a conventional epoxy coating, multiple coated (MC) bars with a 50-µm (2-mil) coating of 98 percent zinc and 2 percent aluminum underneath a conventional epoxy coating, and concrete containing corrosion inhibitors calcium nitrite and Hycrete™. The differences in the costs over a 75-year design life are relatively small for coated bars. Concrete containing Hycrete™ may exhibit lower compressive strength and reduced resistance to surface scaling compared to concretes with other inhibitors or without an inhibitor unless modified, such as through an increase in cement content. As a result, additional research is required to establish criteria that will preclude a loss of durability when Hycrete™ is used.

- Conventional reinforcement in concrete containing a corrosion inhibitor has a longer service life and is more cost effective than conventional reinforcement in concrete without a corrosion inhibitor but has a shorter service life and is less cost effective than any of the coated bar systems evaluated.

- Cracks in concrete directly over and parallel to the reinforcement, such as found in bridge decks, result in earlier corrosion initiation and higher corrosion rates than obtained with intact concrete for all systems.

- Epoxies that provide initially high adhesion to the underlying steel provide no advantage in terms of improved corrosion performance or improved adhesion when used in concrete.

- Using concrete with a reduced water-cement (w/c) ratio lowers the corrosion rate for both conventional reinforcement and epoxy-coated reinforcement (ECR) under all conditions in intact concrete but provides only limited corrosion protection when cracks allow direct access of chlorides to reinforcing bars.

- Corrosion inhibitors consistently provide improved corrosion protection when used in conjunction with conventional reinforcement and ECR in intact concrete but to a lesser degree in cracked concrete.

- Corrosion inhibitors have a greater relative effect on uncoated than on coated reinforcement.

- Reinforcement with a multiple coating consisting of 98 percent zinc and 2 percent aluminum and conventional epoxy exhibits high corrosion rates in cases when the concrete is often wet but exhibits corrosion rates similar to those exhibited by conventional ECR under conditions similar to those in bridge decks; the metallic coating corrodes in preference to the underlying steel, providing some additional protection.

- All coated bars that were evaluated exhibit corrosion losses at openings through the coating. A reduction in adhesion between an epoxy coating and the reinforcing steel occurs after a period of exposure to corrosive conditions. This reduction increases with increasing chloride content in the concrete and in the presence of cracks and decreases with the use of corrosion inhibitors, with the use of MC reinforcement, and with electrical isolation of the epoxy-coated bars from each other. Corrosion products form under the coating where adhesion has been reduced.

- For periods up to 5 years under exposure conditions representative of those in bridge decks, the reduction in adhesion between an epoxy coating and the reinforcing steel did not affect the rate at which coated bars corrode.

APPENDIX A. DISBONDMENT OF CONVENTIONAL EPOXY-COATED AND MC BARS IN RAPID MACROCELL TEST

In addition to the rapid macrocell tests described in the body of the report, 24 ECR and 24 MC rapid macrocell tests using 6.04 molal ion (15 percent) concentration sodium chloride solution were used to compare the disbondment characteristics of conventional ECR and MC bars under the severe exposure conditions produced in the test as a function of corrosion loss and time. The specimens consisted of a single ECR or MC bar as the anode and two bare steel bars as the cathode. Every 5 weeks, three specimens were pulled from testing and a disbondment test was performed on the anode. The schedule of testing is shown in table 53. In addition, five control specimens of each type were placed in simulated pore solution with no chlorides to track disbondment in the absence of chlorides. Disbondment was performed using the procedures described in chapter 2 for the cathodic disbondment test. Measurements are expressed in terms of the total area of disbonded material at each test point.

Table 53. Rapid macrocell test program.

ECR		MC	
Specimen Designation	Weeks Tested	Specimen Designation	Weeks Tested
M-ECR-1	5	M-MC-1	5
M-ECR-2	5	M-MC-2	5
M-ECR-3	5	M-MC-3	5
M-ECR-4	10	M-MC-4	10
M-ECR-5	10	M-MC-5	10
M-ECR-6	10	M-MC-6	10
M-ECR-7[a]	15	M-MC-7	15
M-ECR-8	15	M-MC-8	15
M-ECR-9	15	M-MC-9	15
M-ECR-10	20	M-MC-10	20
M-ECR-11	20	M-MC-11	20
M-ECR-12	20	M-MC-12	20
M-ECR-13[a]	40	M-MC-13	25
M-ECR-14	25	M-MC-14	25
M-ECR-15	25	M-MC-15	25
M-ECR-16	25	M-MC-16	30
M-ECR-17	30	M-MC-17	30
M-ECR-18	30	M-MC-18	30
M-ECR-19[a]	40	M-MC-19	35
M-ECR-20	30	M-MC-20	35
M-ECR-21	35	M-MC-21	35
M-ECR-22	35	M-MC-22[a]	40
M-ECR-23	35	M-MC-23[a]	40
M-ECR-24	40	M-MC-24[a]	40
Control specimens in simulated pore solution (no salt)			
M-ECR-A	10	M-MC-A	10
M-ECR-B	20	M-MC-B	20
M-ECR-C	25	M-MC-C	30
M-ECR-D	30	M-MC-D	35
M-ECR-E	35	M-MC-E	40

[a] Linear polarization resistance tests performed on this specimen.

TEST RESULTS

The duration of the test ranged from 5 to 40 weeks. The purpose of the test program was to establish a relationship between corrosion loss, time, and disbondment of the epoxy coating for conventional ECR and MC reinforcement.

Corrosion Rate, Loss, and Potentials

The average macrocell corrosion rates based on total area for macrocell specimens with ECR and MC reinforcement are shown in figure 204. During the first five weeks of testing, the specimens with MC reinforcement exhibited significantly higher corrosion rates than the specimens with conventional ECR. A slight increase in corrosion rate was observed for the MC specimens between weeks 15 and 20. The corrosion rates were otherwise comparable to those observed in conventional ECR.
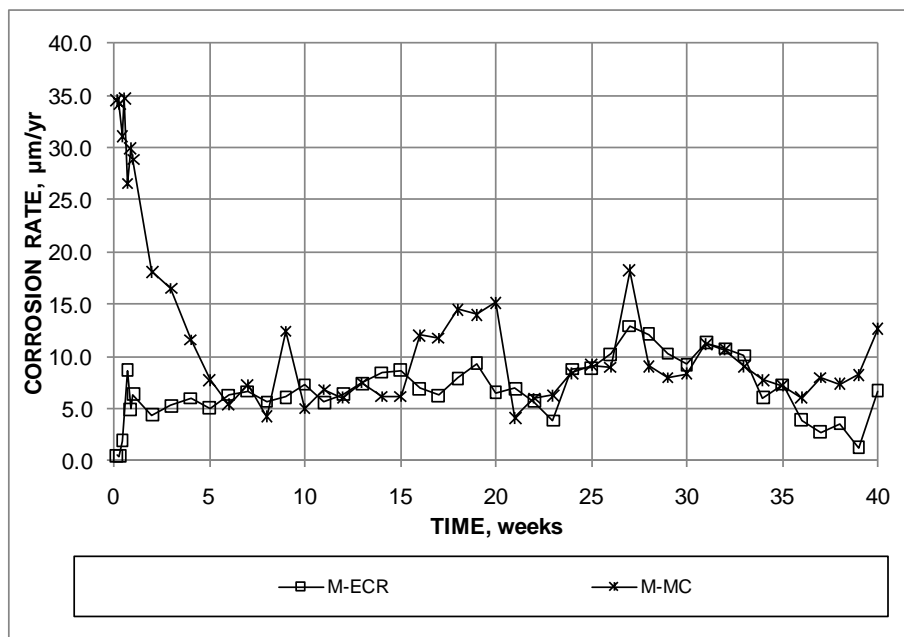
1 μm = 0.0394 mil

Figure 204. Graph. Rapid macrocell test, average corrosion rate based on total area of ECR and MC reinforcement.

The average corrosion losses based on average corrosion rates for the macrocell specimens with ECR and MC reinforcement are shown in figure 205. The increased corrosion rate observed for MC reinforcement from weeks 0 to 5 and weeks 15 to 20 resulted in a greater overall corrosion loss at 40 weeks (7.55 μm (0.297 mil) compared to 5.43 μm (0.214 mil) for ECR) as well as greater losses throughout the test.
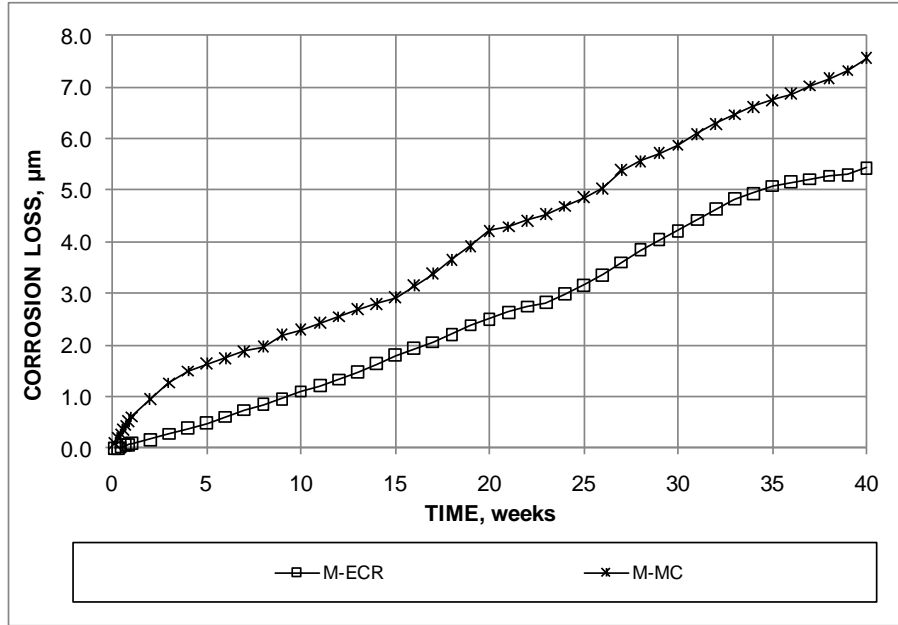
1 µm = 0.0394 mil

Figure 205. Graph. Rapid macrocell test, average corrosion loss based on total area of ECR and MC reinforcement.

The average anode and cathode potentials with respect to an SCE are shown in figure 206 and figure 207, respectively, for specimens with conventional ECR and MC reinforcement. At the anode, the corrosion potentials of both ECR and MC were more negative than -0.500 V for most of the test. The MC specimens showed a more negative anode potential than the ECR specimens for the first 27 weeks of testing. After 27 weeks, the corrosion potentials of the specimens with MC and ECR were comparable.
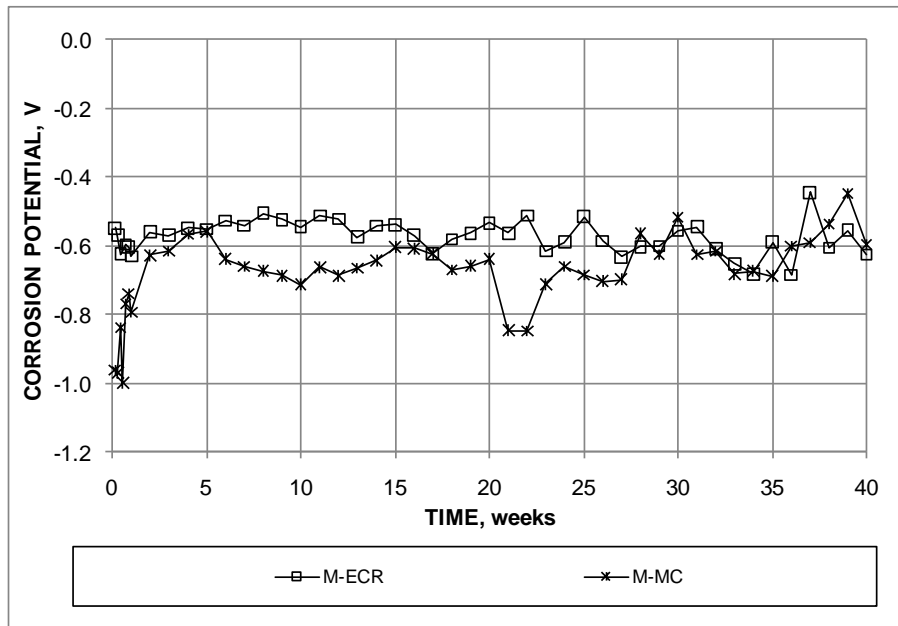
Figure 206. Graph. Rapid macrocell test, average anode potential of ECR and MC reinforcement.

183
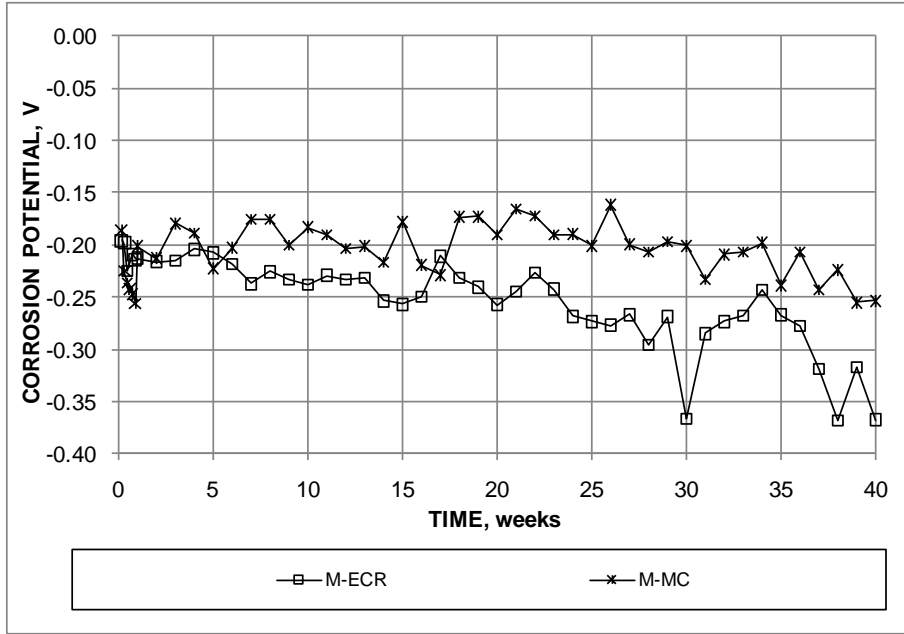
Figure 207. Graph. Rapid macrocell test, average cathode potential of ECR and MC reinforcement.

At the cathode, the corrosion potentials of the specimens with both ECR and MC reinforcement were approximately -0.200 V at the start of the test. For the ECR specimens, the corrosion potential gradually decreased to approximately -0.350 V by week 40, whereas the corrosion potential of the MC specimens remained at approximately -0.200 V until week 36, when it decreased to -0.300 V over a four-week period.

Linear polarization resistance measurements were performed on selected specimens on a monthly basis. The total corrosion losses calculated from the linear polarization readings are compared to the macrocell corrosion losses in table 54. On average, the total corrosion losses were 4.0 times greater than macrocell corrosion losses, with the ratio of total to macrocell corrosion loss ranging from 1.45 (M-ECR-7) to 8.41 (M-ECR-13).

Table 54. Total and macrocell corrosion loss for selected rapid macrocell specimens.

Specimen	Age (weeks)	Corrosion Loss (µm)	
		Microcell	Total
M-ECR-7	15	2.83	1.95
M-ECR-13	40	55.2	6.56
M-ECR-19	40	19.1	4.95
M-MC-22	40	18.2	7.64
M-MC-23	40	35.4	7.83
M-MC-24	40	31.0	9.04

1 µm = 0.0394 mil

184

Visual Observations

For the ECR specimens, corrosion products were visible at some damage sites after 5 weeks of testing (see figure 208), with moderate amounts of disbondment observed at some damage sites (see figure 209). Other damage sites on the ECR bars tested at 5 weeks showed no disbondment. The ECR bars tested for 10 weeks or longer showed disbondment at all damage sites. For the ECR specimens tested for 30 weeks or longer, corrosion products were observed at all damage sites (see figure 210), with the disbonded region covering much of the area of the bar (see figure 211). The ECR bars removed after 30 to 40 weeks of testing showed severe disbondment at all damage sites (see figure 211).

Figure 208. Photo. Rapid macrocell test, M-ECR-1, 5 weeks, before disbondment test.

Figure 209. Photo. Rapid macrocell test, M-ECR-1, 5 weeks, after disbondment test.

Figure 210. Photo. Rapid macrocell test, M-ECR-13, 40 weeks, before disbondment test.

Figure 211. Photo. Rapid macrocell test, M-ECR-21, 35 weeks, after disbondment test.

For the MC specimens, those removed after 5 or 10 weeks of testing showed no signs of iron corrosion products (see figure 212) in contrast to specimens with ECR, which showed visible

corrosion products after 5 weeks. Disbondment tests on the MC bars revealed minimal disbondment on specimens removed from testing after 5 or 10 weeks (see figure 213). Regions where disbondment did occur on the MC bars showed a ring of darkened metal around the damage site, indicating the zinc in this region has been consumed (see figure 214). The MC specimens began to show dark orange iron corrosion products by week 15, with all three of the MC specimens removed at week 40 showing dark iron corrosion products (see figure 215). The disbondment tests performed at 40 weeks on the MC bars showed moderate disbondment at all damage sites (see figure 216). The corrosion products in the disbonded regions of the MC bars consist of a central circle of dark iron corrosion products around the damage site surrounded by a larger region of light gray corrosion products, most likely from corroding zinc.

Figure 212. Photo. Rapid macrocell test, M-MC-4, 10 weeks, before disbondment test.

Figure 213. Photo. Rapid macrocell test, M-MC-4, 10 weeks, after disbondment test.
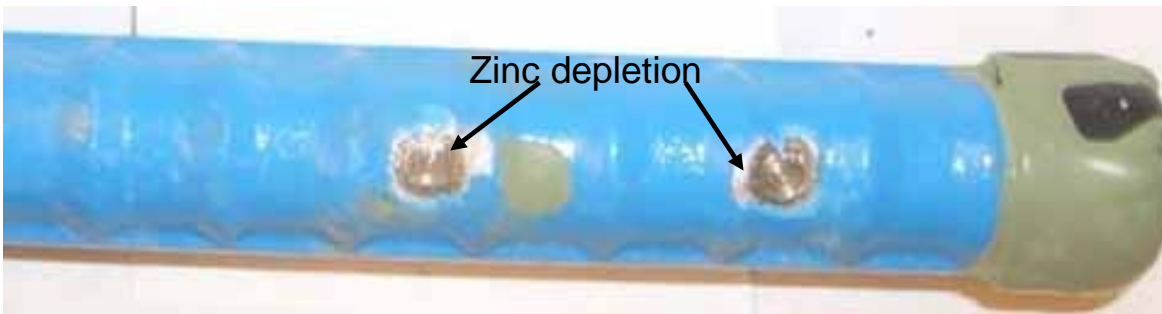
Figure 214. Photo. Rapid macrocell test, M-MC-5, 10 weeks (zinc depletion in regions surrounding damage sites).

Figure 215. Photo. Rapid macrocell test, M-MC-23, 40 weeks, before disbondment test.

Figure 216. Photo. Rapid macrocell test, M-MC-23, 40 weeks, after disbondment test.

In general, damage sites with visible corrosion products tended to exhibit greater disbondment than damage sites with no visible corrosion products for both ECR (figure 209) and MC (figure 216). Both the disbonded area and visible corrosion increased with time. The corrosion products at the damage sites were dark orange or brown in color. Corrosion products underneath disbonded epoxy were initially black (figure 209), but turned dark orange with exposure to air as the corrosion products oxidized.

Disbondment Results

Disbonded area and corrosion loss for the ECR and MC bars are summarized in table 55 and table 56, respectively. Figure 217 and figure 218 show average disbonded area at a damage site as a function of time for ECR and MC reinforcement, respectively. A best fit line is plotted for each set of data. Based on the best fit lines, disbondment of ECR progressed at about twice the rate of disbondment of MC reinforcement, with ECR showing increases in disbonded area averaging 10.8 mm^2/week (0.0167 in^2/week) compared to 5.32 mm^2/week (0.0082 in^2/week) for MC reinforcement. It should be noted that disbondment at a given age varies widely for individual specimens of both types, especially at later ages.

Table 55. Disbonded area and corrosion loss for rapid macrocell specimens with ECR.

Specimen	Week	Average Disbonded Area, mm^2	Corrosion Loss, μm	Disbondment Rate, mm^2/week	Disbondment Rate, mm^2/μm
M-ECR-1	5	35.5	0.359	7.10	98.8
M-ECR-2	5	16.1	0.318	3.23	50.7
M-ECR-3	5	37.1	0.233	7.42	159.2
M-ECR-4	10	74.2	0.638	7.42	116.3
M-ECR-5	10	158.1	0.513	15.8	308.1
M-ECR-6	10	133.9	1.29	13.4	103.8
M-ECR-7	15	116.1	1.92	7.74	60.5
M-ECR-8	15	154.8	0.428	10.3	361.8
M-ECR-9	15	187.1	3.35	12.5	55.8
M-ECR-10	20	175.8	4.99	8.79	35.2
M-ECR-11	20	338.7	4.59	16.9	73.8
M-ECR-12	20	140.3	4.71	7.02	29.8
M-ECR-13	40	456.5	4.94	11.4	92.4
M-ECR-14	25	567.7	3.73	22.7	152.2
M-ECR-15	25	187.1	1.04	7.48	179.9
M-ECR-16	25	408.1	2.16	16.3	188.9
M-ECR-17	30	232.3	3.35	7.74	69.3
M-ECR-18	30	162.9	2.37	5.43	68.7
M-ECR-19	40	261.3	4.64	6.53	56.3
M-ECR-20	30	198.4	5.75	6.61	34.5
M-ECR-21	35	874.2	6.24	25.0	140.1
M-ECR-22	35	222.6	5.41	6.36	41.1
M-ECR-23	35	598.4	3.27	17.1	183.0
M-ECR-24	40	241.9	5.38	6.05	45.0

1 mm^2 = 0.00155 in^2
1 μm = 0.0394 mil

Table 56. Disbonded area and corrosion loss for rapid macrocell specimens with MC reinforcement.

Specimen	Week	Average Disbonded Area, mm^2	Corrosion Loss, μm	Disbondment Rate, mm^2/week	Disbondment Rate, mm^2/μm
M-MC-1	5	9.7	1.11	1.94	8.7
M-MC-2	5	4.8	1.73	0.968	2.8
M-MC-3	5	21.0	1.3	4.19	16.1
M-MC-4	10	41.9	1.97	4.19	21.3
M-MC-5	10	43.5	3.42	4.35	12.7
M-MC-6	10	50.0	3.17	5.00	15.8
M-MC-7	15	77.4	4.97	5.16	15.6
M-MC-8	15	54.8	1.99	3.66	27.6
M-MC-9	15	74.2	2.98	4.95	24.9
M-MC-10	20	133.9	6.12	6.69	21.9
M-MC-11	20	125.8	4.19	6.29	30.0
M-MC-12	20	69.4	3.03	3.47	22.9
M-MC-13	25	162.9	3.58	6.52	45.5
M-MC-14	25	137.1	2.86	5.48	47.9
M-MC-15	25	146.8	6.61	5.87	22.2
M-MC-16	30	116.1	5.48	3.87	21.2
M-MC-17	30	98.4	3.13	3.28	31.4
M-MC-18	30	156.5	3.93	5.22	39.8
M-MC-19	35	117.7	6.89	3.36	17.1
M-MC-20	35	129.0	6.73	3.69	19.2
M-MC-21	35	308.1	8.64	8.80	35.7
M-MC-22	40	127.4	7.64	3.19	16.7
M-MC-23	40	177.4	7.83	4.44	22.7
M-MC-24	40	301.6	9.04	7.54	33.4

1 mm^2 = 0.00155 in^2
1 μm = 0.0394 mil
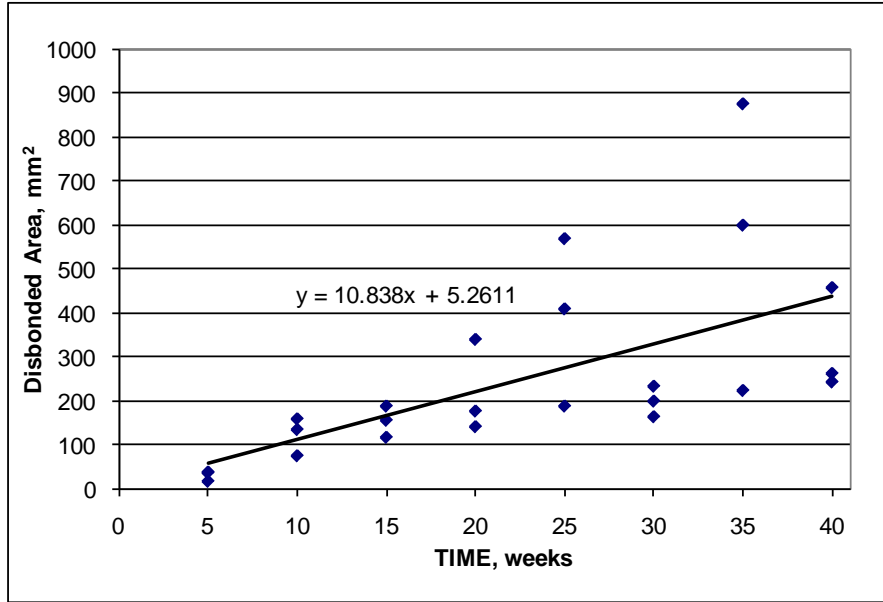
1 mm^2 = 0.00155 in^2

Figure 217. Graph. Rapid macrocell test, disbonded area versus time for specimens with ECR.
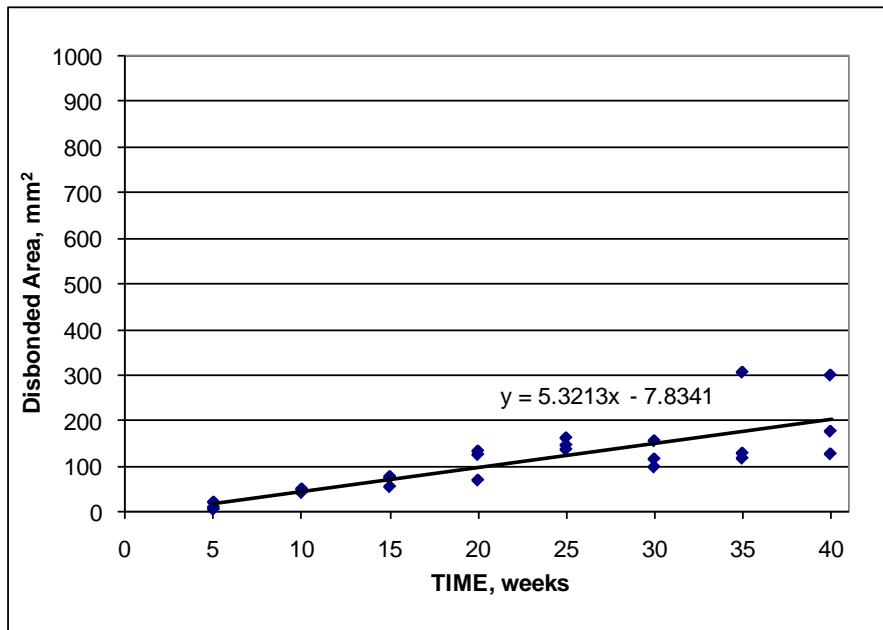
1 mm^2 = 0.00155 in^2

Figure 218. Graph. Rapid macrocell test, disbonded area versus time for specimens with MC reinforcement.

Figure 219 and figure 220 show disbonded area versus macrocell corrosion loss for ECR and MC reinforcement, respectively. The ECR showed greater disbondment at a given corrosion loss than the MC reinforcement. On average, the disbondment of the ECR increased by 56.3 mm^2 (2.21 in^2) for every 1 µm (1 mil) of corrosion loss, compared to an average increase of 26.5 mm^2 (1.04 in^2) for every 1 µm (1 mil) of corrosion loss for the MC bars. The difference in disbondment rate between ECR and MC reinforcement was more pronounced in specimens with low corrosion

190

losses. For epoxy-coated bars with less than 2.0 µm (0.079 mil) of corrosion loss, the disbondment rate ranged from 50.7 to 308.1 mm^2/µm (2.00 to 12.1 in^2/mil) of loss, with an average rate of 159.9 mm^2/µm (6.30 in^2/mil). For the MC bars with less than 2.0 µm (0.078 mil) of corrosion loss, the disbondment rate ranged from 2.80 to 27.6 mm^2/µm (0.11 to 1.09 in^2/mil) of loss, with an average rate of 15.3 mm^2/µm (0.60 in^2/mil).
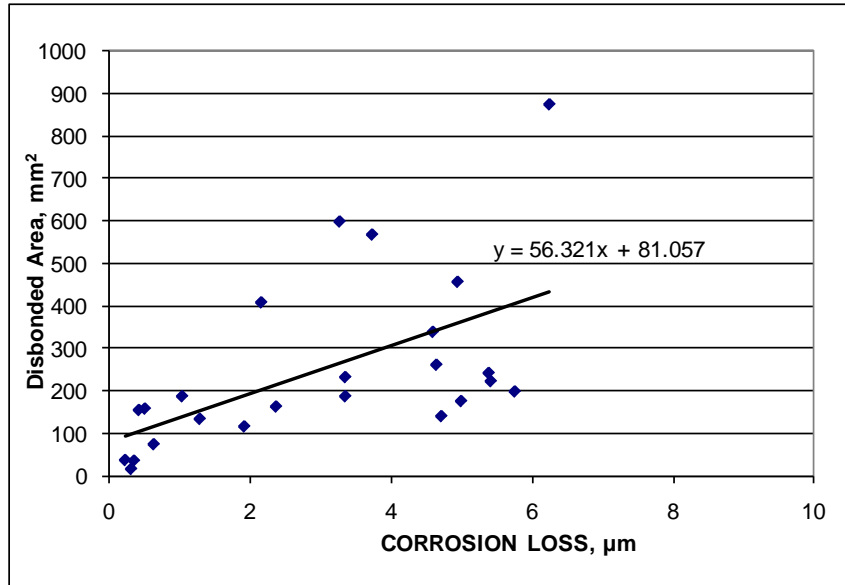
1 mm^2 = 0.00155 in^2
1 µm = 0.0394 mil

Figure 219. Graph. Rapid macrocell test, disbonded area versus corrosion loss for specimens with ECR.
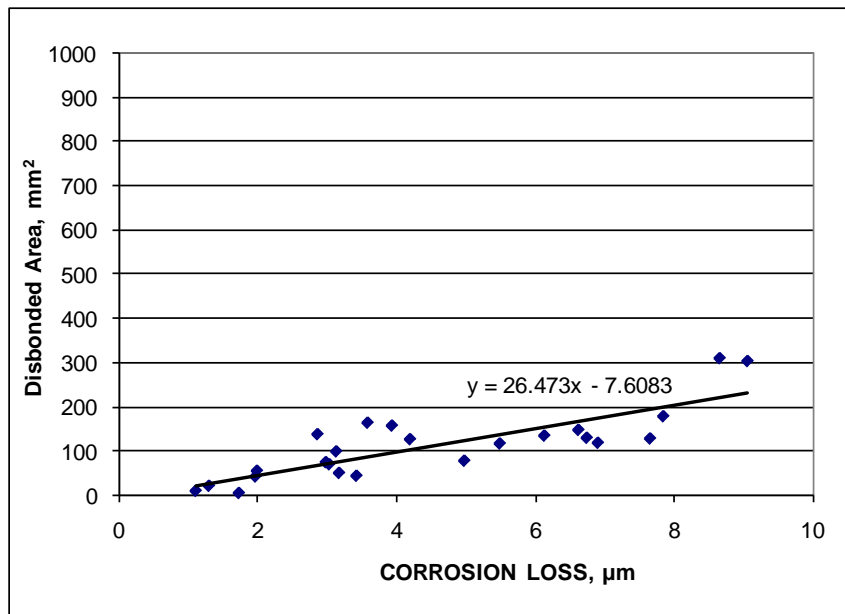
1 mm^2 = 0.00155 in^2
1 µm = 0.0394 mil

Figure 220. Graph. Rapid macrocell test, disbonded area versus corrosion loss for specimens with MC reinforcement.

In addition to the rapid macrocell specimens, five epoxy-coated bars and five MC bars with damaged regions identical to those used in the rapid macrocell test were exposed to a simulated pore solution without salt to determine the disbondment of the coatings with time in the absence of chlorides and chloride-induced corrosion. The results are shown in figure 221. At 10 weeks, the MC bars had a disbonded area of 25.8 mm^2 (0.0394 in^2), whereas ECR exhibited no disbondment. However, at 20 weeks, the ECR and MC reinforcement exhibited the same degree of disbondment in the absence of corrosion, and at later ages, specimens with ECR exhibited greater disbonded areas than specimens with MC reinforcement. For both ECR and MC bars, disbondment at 40 weeks in the absence of chlorides was 20–25 percent of the values observed at 40 weeks in bars subjected to chloride-induced corrosion.
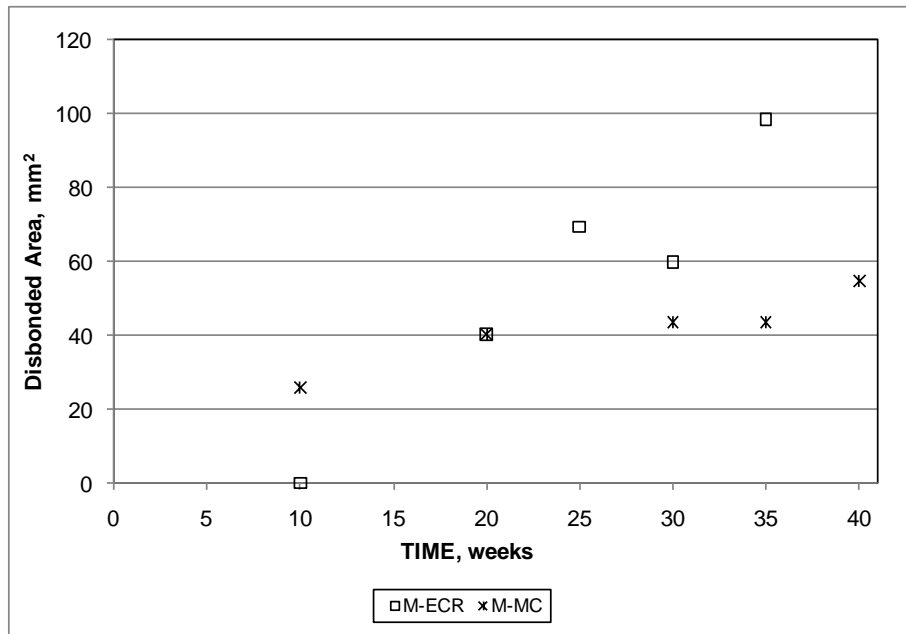
$1 \text{ mm}^2 = 0.00155 \text{ in}^2$

Figure 221. Graph. Disbonded area versus time for ECR and MC reinforcement in simulated pore solution without salt.

Summary

For the rapid macrocell test, the specimens with MC reinforcement showed greater corrosion losses than the specimens with conventional ECR. However, MC reinforcement showed significantly less disbondment than ECR, both as a function of corrosion loss and as a function of time.

APPENDIX B. CORROSION LOSS REQUIRED TO CRACK CONCRETE CONTAINING CONVENTIONAL, EPOXY-COATED, AND GALVANIZED REINFORCEMENT

INTRODUCTION

The corrosion of steel reinforcement in concrete is a destructive process for both the steel and the concrete. The corrosion products of steel occupy several times the volume of solid steel, resulting in cracking and spalling of the concrete cover once a sufficient amount of corrosion loss has occurred. Several prior studies have worked to establish a relationship between corrosion loss and cracking of concrete cover for uncoated conventional reinforcement.[68–71] In addition, Torres-Acosta and Sagues examined the effects of localized corrosion, although the corroding areas were much larger than the area typically exposed due to damage to ECR.[71]

Limited research has been performed on the amount of corrosion loss required to crack concrete for galvanized reinforcement. Sergi, Short, and Page found that the corrosion product of zinc is often zinc oxide.[73] The volume of zinc oxide is only 1.5 times that of solid zinc, whereas the volume of ferric oxide is 3 times that of solid steel, indicating that the corrosion loss required to crack concrete for specimens with galvanized reinforcement should be greater than the corrosion loss required to crack concrete with conventional reinforcement.[74,75] However, under certain conditions, zinc can also form zinc hydroxychloride II, which has 3.6 times the volume of solid zinc.[73,74] The formation of zinc hydroxychloride II will result in corrosion losses for galvanized reinforcement at the onset of cracking similar to those observed for conventional reinforcement. Rasheeduzzafar et al. studied conventional and galvanized reinforcement cast in concrete with chloride contents at casting ranging from 2.4 to 19.2 kg/m^3 (4 to 32 lb/yd^3).[76] Rasheeduzzafar et al. found specimens containing galvanized reinforcement took longer to crack concrete than specimens containing conventional reinforcement; however, the corrosion loss at crack initiation was not determined.

The research described in this appendix examines the corrosion losses required to crack concrete cover for conventional, galvanized, and damaged epoxy-coated reinforcement. Specimens with conventional and galvanized reinforcement were tested at varying covers to establish a relationship between corrosion loss and cracking for conventional and galvanized reinforcement. ECR was tested at 25-mm (1-inch) cover with varying damage patterns to determine the effect of the damaged area on corrosion loss required to crack concrete. Two- and three-dimensional finite element models were created to test the corrosion loss to crack concrete for multiple combinations of cover and damaged area. The results from the finite element models are compared with experimental results from this and other studies, and an expression is developed relating damaged area, concrete cover, and corrosion loss to cause cracking.

EXPERIMENTAL PROCEDURE

Mixture Proportions

The mixture proportions used in the concrete for all specimens are shown in table 57. The materials used are as follows:

- **Cement:** Type I/II portland cement.

- **Water:** Municipal tap water.

- **Fine aggregate:** Kansas River sand. Bulk specific gravity (SSD) = 2.62, absorption = 0.8 percent, fineness modulus = 2.51.

- **Coarse aggregate:** Crushed limestone with a nominal maximum size of 19 mm (0.75 inches), bulk specific gravity (SSD) = 2.58, absorption = 2.3 percent, unit weight = 95.9 lb/ft^3 (1,536 kg/m^3).

- **Salt:** Sodium chloride, added to mix water as specified in table 57.

- **Air entraining agent:** Daravair® 1400, manufactured by W.R. Grace.

The mixture includes salt equivalent to 2 percent chlorides by weight of cement to destabilize the passive layer of the reinforcement and increase the ionic conductivity of the concrete. The salt is dissolved in the mix water prior to casting.

Table 57. Mix proportions for cracking specimens.

Cement, kg/m^3 (lb/yd^3)	Water, kg/m^3 lb/yd^3	Fine Aggregate, kg/m^3 (lb/yd^3)	Coarse Aggregate, kg/m^3 (lb/yd^3)	Sodium Chloride, kg/m^3 (lb/yd^3)	Air Entraining Agent, L/m^3 (oz/yd^3)
356 (598)	160 (269)	854 (1,435)	883 (1,484)	11.7 (19.8)	2.66 (68.9)

Materials

The following materials are used in the cracking tests described in this appendix:

- **Wire:** External specimen connections from the reinforcing steel to the terminal box are made with 16-gauge multistrand copper wire.

- **Multimeter:** A multimeter is used to measure current flow to each specimen.

- **Power supply:** A power supply is used to drive the corrosion of the test bar. A galvanostat is used for conventional and galvanized reinforcement. A 30-V power supply is used for ECR. The change in equipment is necessitated by the higher resistance of specimens with ECR.

- **Stainless steel screws/washers:** Screws and washers are used to hold reinforcement in place in formwork and to connect wires to specimens during testing.

Specimens

A schematic of the cracking specimens is shown in figure 222. Cracking specimens are beam specimens, 152 mm (6 inches) wide by 305 mm (12 inches) long. Specimen height is dependent on the concrete cover. The top bar is the test bar and consists of conventional, galvanized, or epoxy-coated reinforcement. The bottom bars are pickled 2205 duplex stainless steel. All bars are No. 16 (No. 5) reinforcing steel. Specimens are connected to a power supply to drive corrosion on the test bar and are kept ponded with deionized water.
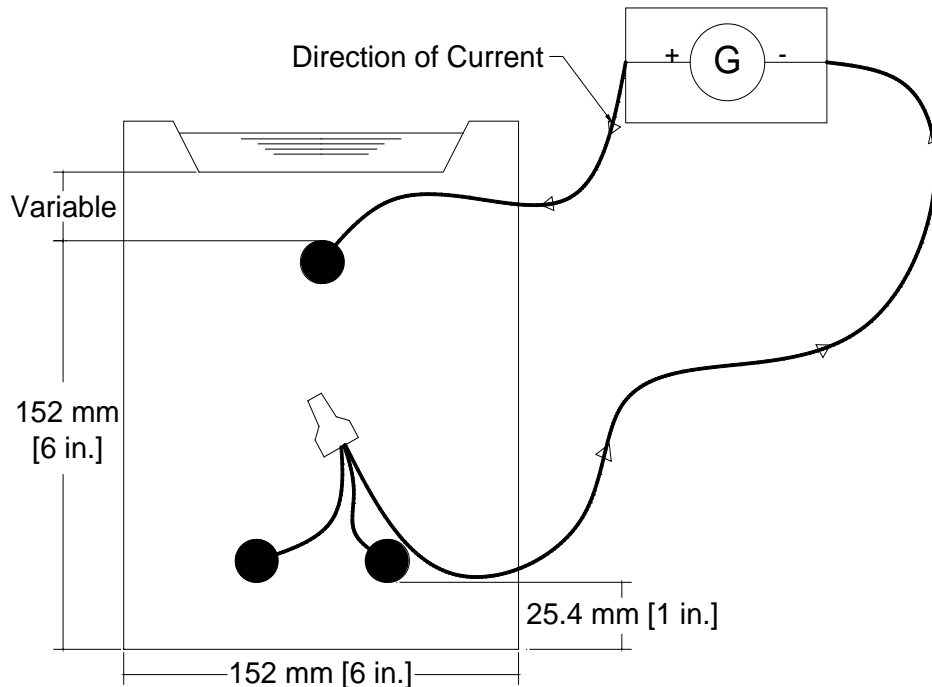
Figure 222. Illustration. Cracking specimen.

A total of 34 specimens were tested in five series. Series 1 consisted of beams with conventional and galvanized reinforcement with 25-mm (1-inch) concrete cover. Series 2 consisted of beams with conventional and galvanized reinforcement with 13-mm (0.5-inch) concrete cover. Series 3 tested conventional and galvanized reinforcement with 51-mm (2-inch) cover. Series 4 tested damaged ECR with 25-mm (1-inch) concrete cover. Series 5 tested two specimens with galvanized reinforcement and 25-mm (1-inch) cover, with specimens removed from testing at crack initiation. Testing continued on series 1, 2, and 3 until the crack reached a width of 0.508 mm (0.02 inches). Testing continued on series 4 until the crack spanned the full length of the specimen because the lower corrosion rate of specimens containing ECR made it impractical to continue the test until the crack reached a width of 0.508 mm (0.02 inches).

Test Procedure

The test begins 14 days after the specimens are cast. During the test, the current to each specimen is measured daily. Dividing the measured current by the surface area of the test bar (or the damaged area for ECR) gives the corrosion current density, which is used to determine corrosion rate using Faraday's equation (see chapter 2). Specimens are monitored daily for staining and cracking. The corrosion loss at staining, crack initiation, and propagation of the crack to the full specimen length are recorded. In addition, the crack width as a function of corrosion loss is tracked for specimens with conventional and galvanized reinforcement.

Fabrication

Specimen fabrication for cracking specimens follows the preparation procedure for bench-scale specimens outlined in chapter 2, with two exceptions. ECR is damaged in either a two-hole or

two half-ring pattern, as shown in figure 223 and figure 224. Specimens are also cured in molds for 14 days as opposed to the curing procedure used for bench-scale specimens.
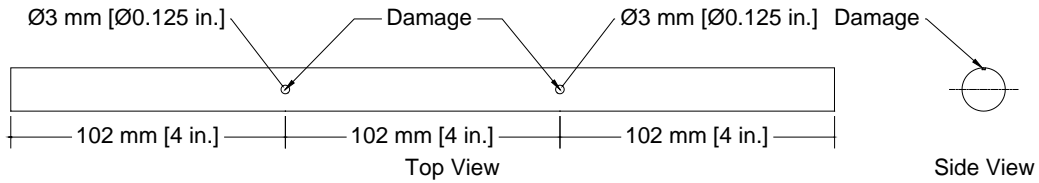
Figure 223. Illustration. Damage patterns for ECR with two holes.
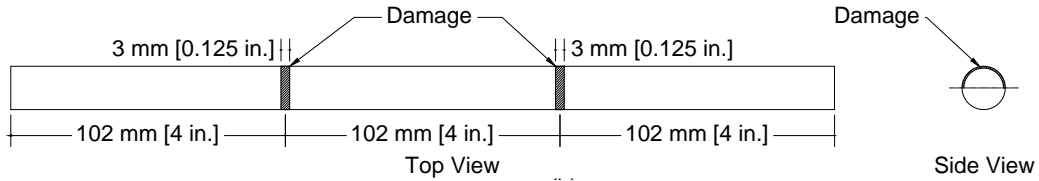
Figure 224. Illustration. Damage patterns for ECR with two half-rings.

Test Program

The test program is summarized in table 58. The conventional and galvanized reinforcement were tested with 13-mm (0.5-inch), 25-mm (1-inch), and 51-mm (2-inch) concrete covers. The galvanized reinforcement had a nominal coating thickness of 0.15 mm (6 mil). The ECR, with coating thickness ranging from 0.20 to 0.27 mm (8 to 10.5 mil) and an average of 0.25 mm (9.7 mil), was tested using a 25-mm (1-inch) cover with two damage patterns, as previously described.

Table 58. Corrosion loss to cause cracking, number of specimens in test program.

	Cover		
System	**13 mm (0.5 inches)**	**25 mm (1 inch)**	**51 mm (2 inches)**
Uncoated bars (Conv.)	4	4	4
Galvanized bars (Zn)	4	6[a]	4
ECR-2 hole damage pattern			
Horizontal alignment (ECR-2h-H)	–	2	–
Vertical alignment (ECR-2h-V)	–	2	–
ECR-2 ring damage pattern			
Horizontal alignment (ECR-2r-H)	–	2	–
Vertical alignment (ECR-2r-V)	–	2	–

– No data.
[a] Two specimens removed from testing at crack initiation.

Finite Element Modeling of Corrosion Loss and Cracking

To further study the relationship between corrosion loss and cracking, two- and three-dimensional finite element models were created using ABAQUS 6.9.[77] The two-dimensional models were used to model uniform corrosion of a reinforcing bar. The three-dimensional models were tested

with uniform corrosion over the entire bar, as well as with areas of localized corrosion. The model represents a slab with mirror symmetry about the axis of the reinforcement (see figure 225). The crack is assumed to propagate along the vertical boundary of the model centered on the reinforcing bar. A series of nonlinear springs were used to provide horizontal restraint along the plane of the crack to represent the nonlinear behavior of the concrete as it cracks.
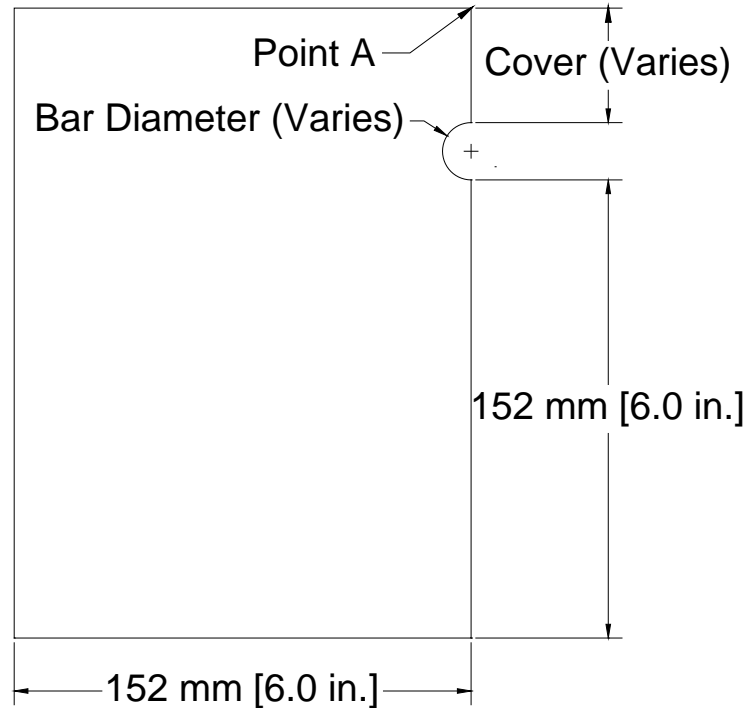
Figure 225. Illustration. Two-dimensional finite element model of concrete to measure cracking behavior.

The properties of the springs were based on measurements of fracture energy of concrete. Darwin et al. tested notched beams in center-point loading.[78] Fracture energy was calculated by determining the area under the load-deflection curves for each specimen. Darwin et al. found that for concretes older than 5 days, fracture energy is governed by coarse aggregate properties and is independent of w/c ratio, compressive strength, and age of concrete. The spring properties were adjusted to provide a fracture energy of 61 N/m (0.35 lb/in), comparable to the value reported by Darwin et al.[78] The initial stiffness of the springs provided an elastic modulus of 27.6 GPa (4,000 ksi) and a peak tensile stress of 2.76 MPa (400 psi). The spring behavior for a spring density of 6,200 springs/m^2 (4 springs/in^2) is shown in figure 226.
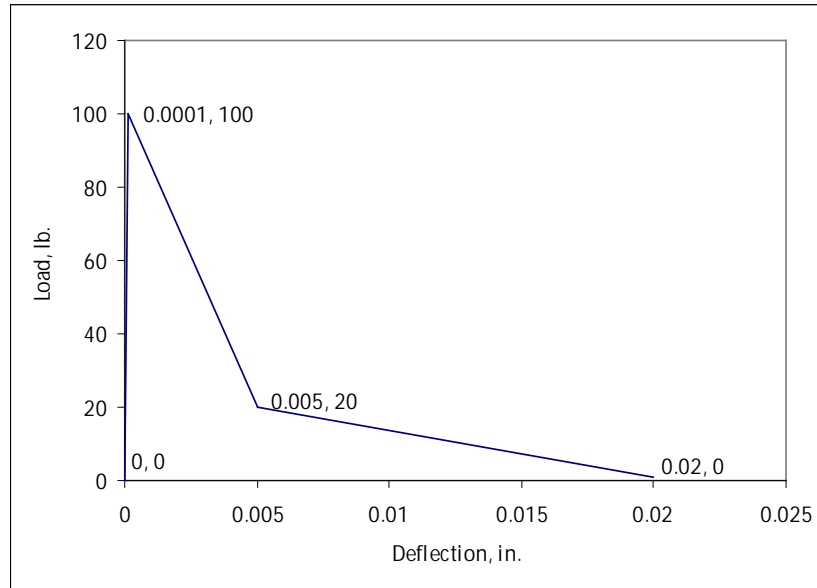
1 lb = 2.228 N
1 inch = 25.4 mm

Figure 226. Graph. Load-deflection behavior for nonlinear spring model, spring density of 6,200 springs/m^2 (4 springs/in^2).

Material away from the plane of the crack was assumed to be linear and elastic, with an elastic modulus of 27.6 GPa (4,000 ksi) and a Poisson's ratio of 0.2. Corrosion was assumed to occur uniformly over the entire surface of the conventional and galvanized bars and over the localized damaged regions of the epoxy-coated bars. The buildup of corrosion products was represented by applying a uniform deflection normal to the reinforcing bar surface. The volume ratio of corrosion products to corrosion loss n was assumed to be 3.0 based on work by Suda et al.[75] A visible crack was assumed to have formed when the horizontal deflection at the top surface of the model (point A in figure 225) reached 25 µm (1.0 mil). With the model symmetry, this corresponds to a 50-µm (2.0-mil)-wide crack. The displacement at the surface of the concrete at the location of the reinforcing bar required to cause the formation of the crack (Δ_{crit}) was converted to a corrosion loss (x_{crit}) using the equation in figure 227. The term in the denominator (n-1) accounts for the volume of the reinforcing bar that is converted to corrosion product.

$$x_{crit} = \frac{D_{crit}}{n-1}$$

Figure 227. Equation. Corrosion loss conversion.

Figure 228 and figure 229 show typical finite element model meshes used for the two- and three-dimensional models. The model dimensions are shown in figure 225. For the two-dimensional finite element models, concrete covers of 6.4, 13, 19, 25, 38, 51, 76, and 102 mm (0.25, 0.5, 0.75, 1, 1.5, 2, 3, and 4 inches) and bar diameters of 13, 19, and 25 mm (0.5, 0.75, and 1 inches) were evaluated. For the three-dimensional finite element models, concrete covers of 51 and 76 mm (2 and 3 inches) and bar diameters of 13, 19, and 25 mm (0.5, 0.75, and 1 inches) were used. The two-dimensional model had a unit length, and the three-dimensional model had a length of 508 mm (20 inches).
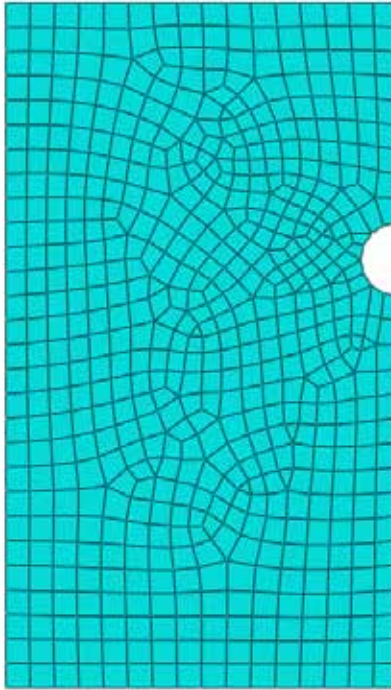
Figure 228. Illustration. Two-dimensional finite element analysis model.
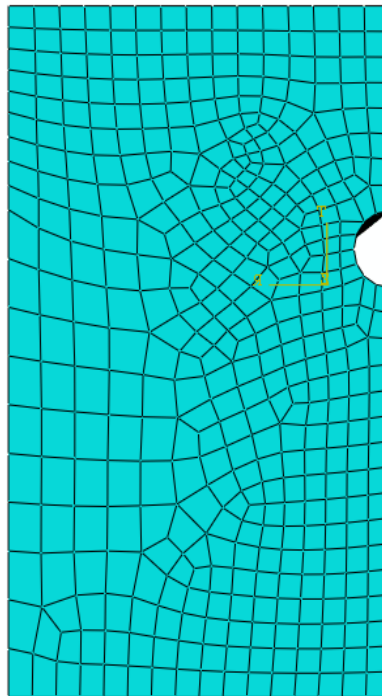
Figure 229. Illustration. Three-dimensional finite element analysis model (end view).

Trial models were run for both the two- and three- dimensional models to determine the effect of mesh type on model performance (see table 59 and table 60). In both cases, the mesh type had no significant effect on the model performance, so the default meshes for the two- and three-dimensional models (quad-dominated and hex, respectively) were used.

Table 59. Effect of two-dimensional element type on corrosion loss.

Mesh Type	Corrosion Loss to Produce a 50-μm Crack, μm
Quad	38.99
Quad-dominated	38.48
Tri	38.74

1 μm = 0.0394 mil

Table 60. Effect of three-dimensional element type on corrosion loss.

Mesh Type	Corrosion Loss to Produce a 50-μm Crack, μm
Hex	64.5
Hex-dominated	64.2
Wedge	64.8
Tet	65.4

1 μm = 0.0394 mil

Trial models were also run to determine the effect of mesh seed size on model performance. The mesh seed size was increased until the finite element model results were affected (see figure 230). A 6.4 mm (0.25-inch) mesh was chosen, as it was the largest mesh size for which the finite element model results were not affected.
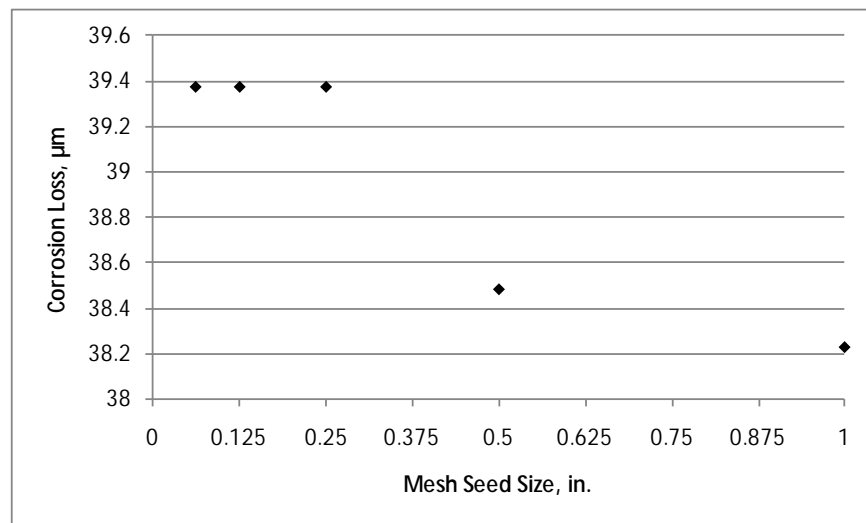
1 μm = 0.0394 mil

Figure 230. Graph. Effect of mesh seed size on corrosion loss required to produce a 50-μm (2-mil) crack.

The two-dimensional model was used to analyze uniform corrosion over the entire bar surface. For the three-dimensional model, three damage patterns were analyzed for each combination of cover and bar diameter, as shown in figure 231. The first damage pattern simulates corrosion along the entire circumference of the bar. Models with this damage pattern are designated FR (full ring corrosion pattern). The second damage pattern simulates corrosion along half the bar

circumference and is designated HR. The third damage pattern simulates corrosion along one-quarter of the bar circumference and is designated QR. The length of the FR damage pattern along the bar ranged from 3.2 to 508 mm (0.125 to 20 inches). The length of the HR damage pattern along the bar ranged from 3.2 to 203 mm (0.125 to 8 inches), and the length of the QR damage pattern along the bar ranged from 1.6 to 203 mm (0.0625 to 8 inches).
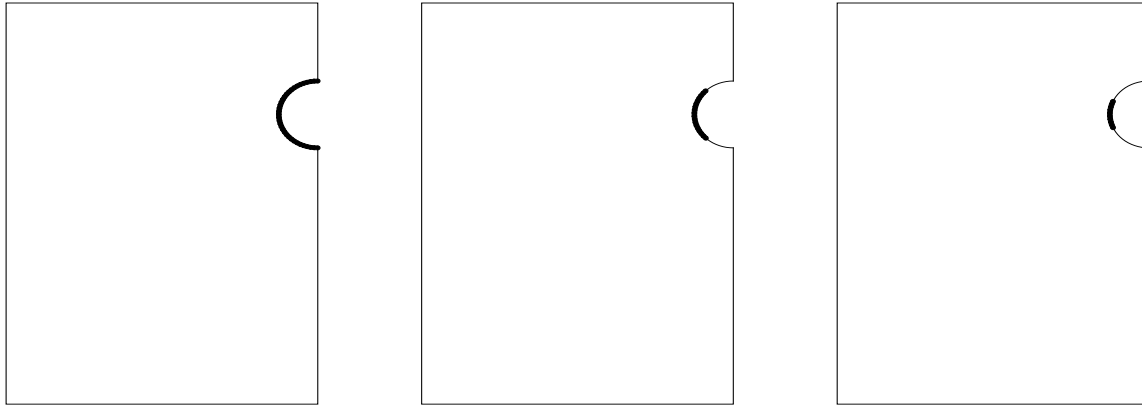
Figure 231. Illustration. Cross section of bar damage patterns for three-dimensional finite element models: full ring, half ring, and quarter ring.

EXPERIMENTAL RESULTS

Conventional and Galvanized Reinforcement

The values of corrosion loss to initiate cracking for conventional and galvanized reinforcement are shown in figure 232, with the standard deviation represented by error bars. For all concrete covers, galvanized reinforcement required significantly greater corrosion losses to crack the concrete cover than did conventional reinforcement. For 13-mm (0.5-inch) cover, conventional reinforcement required an average corrosion loss of 10.6 μm (0.417 mil) to crack the concrete cover, compared to 45.9 μm (1.81 mil) for galvanized reinforcement. For 25-mm (1-inch) cover, conventional reinforcement required an average corrosion loss of 22.4 μm (0.882 mil) to crack the concrete cover, compared to 49.7 μm (1.91 mil) for galvanized reinforcement, and for 51-mm (2-inch) cover, conventional reinforcement required an average corrosion loss of 29.7 μm (1.17 mil) to crack the concrete cover, compared to 68.0 μm (2.68 mil) for galvanized reinforcement. For conventional reinforcement, increasing the cover from 13 to 51 mm (0.5 to 2 inches) nearly tripled the corrosion loss required to crack concrete from 10.6 to 29.7 μm (0.417 to 1.17 mil), an increase of 19.1 μm (0.752 mil). For galvanized reinforcement, the loss increased by 48 percent from 45.9 to 68.0 μm (1.81 to 2.68 mil), an increase of 22.1 μm (0.870 mil).
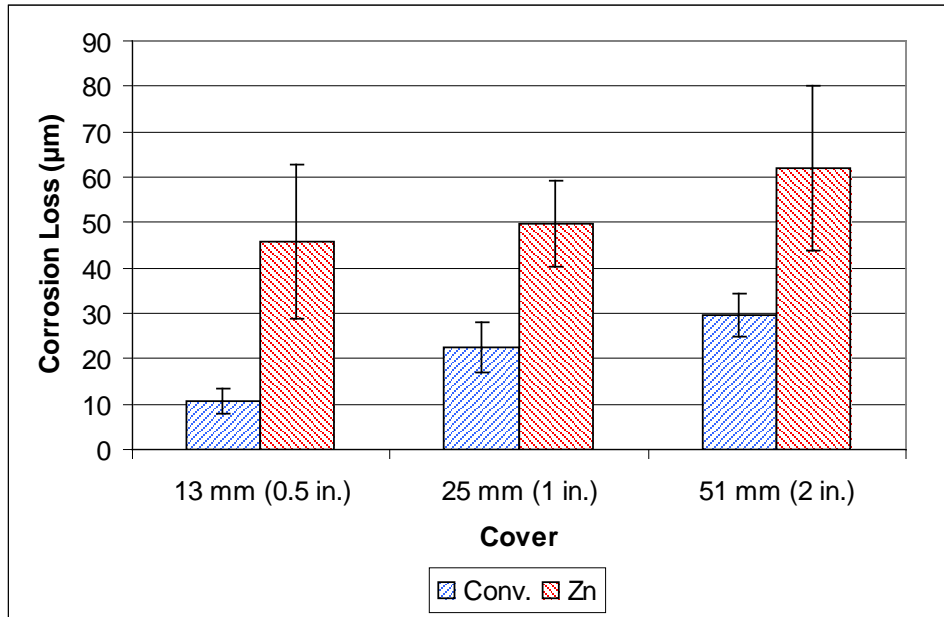
1 µm = 0.0394 mil

Figure 232. Graph. Average corrosion loss required to crack concrete for specimens with conventional and galvanized reinforcement.

Autopsy results from all specimens with conventional reinforcement showed heavy corrosion losses over the entire bar surface (see figure 233 and figure 234). Staining was apparent in the concrete surrounding the reinforcement. Figure 235 shows a side view of the concrete around the reinforcement split along the plane of the crack. Orange corrosion products are visible in regions where the staining reached the surface. In figure 236, greenish-black corrosion products are visible in regions isolated from the atmosphere. All photos were taken immediately after autopsy.

Figure 233. Photo. Top side of bar in specimen Conv.-3, 51-mm (2-inch) cover, after autopsy.

Figure 234. Photo. Bottom side of bar in specimen Conv.-3, 51-mm (2-inch) cover, after autopsy.
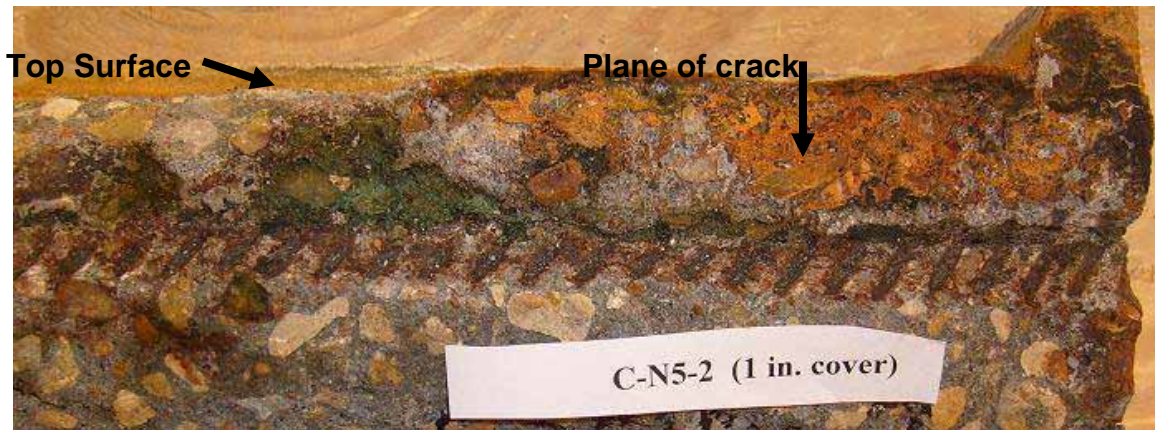
Figure 235. Photo. Side view of specimen Conv.-2, 25-mm (1-inch) cover, after autopsy (plane of crack visible above reinforcement).

Figure 236. Photo. Top view of specimen Conv.-2, 25-mm (1-inch) cover, after autopsy.

The autopsy found that galvanized reinforcement exhibited signs of pitting corrosion. Some regions of the test bar exhibited heavy corrosion products, while in other sections, the galvanized coating was unaffected (see figure 237 and figure 238). Most of the uncorroded regions were located on the top face of the bar, a result of the bottom side of the bar having more even exposure to the ions migrating from the bottom bars. Measurements with a coating thickness gauge showed no significant loss in the areas that appear uncorroded. Visual estimations of uncorroded surface areas were performed on all bars after autopsy, and results appear in table 61. The bars with 13-mm (0.5-inch) cover showed the greatest average uncorroded area, 29 percent, likely due to the decreased cover interfering with ion transport to the top side of the bar. The bars with 25- and 51-mm (1- and 2-inch) cover showed average uncorroded areas of 6 and 13 percent, respectively. The corrosion products on the concrete surrounding the galvanized reinforcement resembled those seen in specimens with conventional reinforcement, indicating that the bulk of corrosion products applying pressure to the surrounding concrete are corrosion products of iron and not those of zinc (see figure 239 and figure 240).

Figure 237. Photo. Top side of bar in specimen Zn-2, 25-mm (1-inch) cover, after autopsy.

Figure 238. Photo. Bottom side of bar in specimen Zn-2, 25-mm (1-inch) cover, after autopsy.

Table 61. Estimated uncorroded surface area of galvanized reinforcement.

Specimen	Estimated Uncorroded Area, percent		
	Cover		
	13 mm (0.5 inch)	25 mm (1 inch)	51 mm (2 inch)
Zn-1	30	8	5
Zn-2	30	5	10
Zn-3	40	5	50
Zn-4	15	5	30
Average	29	6	13

Figure 239. Photo. Side view of specimen Zn-4, 25-mm (1-inch) cover, after autopsy.

Figure 240. Photo. Top view of specimen Zn-4, 25-mm (1-inch) cover, after autopsy.

To determine if the pitting observed on galvanized reinforcement was also present at crack initiation, two additional specimens with galvanized reinforcement and 25-mm (1-inch) cover were cast and autopsied at the onset of cracking. Greenish-black corrosion products were visible along the crack at the upper surface of the specimens (see figure 241). The corrosion products turned orange about 2 h after exposure to air. The autopsy revealed pitting and localized corrosion on the bars similar to that observed in the specimens autopsied after the crack had propagated and widened (see figure 242 and figure 243). As previously discussed, uncorroded regions were more common on the top than the bottom side of the test bar (see figure 244). These results suggest that cracking of the concrete due to corrosion of the galvanized reinforcement did not result due to the buildup of zinc corrosion products but rather due to the formation of corrosion products from the intermetallic steel-zinc layers or from the underlying steel.

Figure 241. Photo. Staining on surface at crack initiation in galvanized reinforcement specimen, 25-mm (1-inch) cover.

Figure 242. Photo. Top side of galvanized reinforcement, 25-mm (1-inch) cover, after autopsy at crack initiation.

Figure 243. Photo. Detail of top side of galvanized reinforcement, 25-mm (1-inch) cover, after autopsy at crack initiation.

Figure 244. Photo. Bottom side of galvanized reinforcement, 25-mm (1-inch) cover, after autopsy at crack initiation.

ECR

The corrosion losses required to crack concrete cover for specimens containing damaged ECR are shown in table 62. The losses are presented based on both the total area of the bar and the damaged (exposed) area in the epoxy. The bars with two half-rings had a nominal exposed area ten times greater than the bars with two holes in the epoxy; however, autopsy results revealed significant blistering on bars with holes in the epoxy (see figure 245). Blistering was also present on the bars with the half-rings but was less severe and exposed less than the area exposed by the rings. Table 62 reflects an estimate of the increased exposed area from the blistered regions for all specimens. Ignoring the blistered regions, specimens with two half-rings had an exposed area of 150.8 mm^2 (0.234 in^2) and specimens with two holes had an exposed area of 15.8 mm^2 (0.024 in^2).

Table 62. Average corrosion loss to crack concrete cover for specimens with ECR.

Specimen	Exposed Area (Including Blisters), mm²	Corrosion Loss Based on Total Area, μm	Corrosion Loss Based on Exposed Area, μm
ECR-2 hole damage pattern			
ECR-2h-H-1	188.3	10.14	730
ECR-2h-H-2	233.5	10.10	587
ECR-2h-H Average		**10.12**	**659**
ECR-2h-V-1	181.8	11.67	874
ECR-2h-V-2	201.1	7.58	510
ECR-2h-V Average		**9.70**	**692**
ECR-2 ring damage pattern			
ECR-2r-H-1	208.9	6.07	421
ECR-2r-H-2	234	5.87	363
ECR-2r-H Average		**5.97**	**392**
ECR-2r-V-1	254	6.22	354
ECR-2r-V-2	208.9	6.15	426
ECR-2r-V Average		**6.18**	**390**

1 mm² = 0.00155 in²
1 μm = 0.0394 mil

Figure 245. Photo. Test bar from specimen ECR-2h-V-2.

Table 62 shows no significant difference in the corrosion loss required to crack the concrete cover between the specimens with the damage pattern oriented horizontally or vertically. The corrosion losses on both the total and exposed areas indicate that the corrosion loss required to crack the concrete cover increases as exposed area decreases. Based on total and exposed area including blisters, the specimens with two holes in the epoxy required somewhat less than twice the corrosion loss to crack the concrete cover as the specimens with two half-rings in the epoxy.

Figure 246 shows a specimen at crack initiation. Figure 247 shows a specimen with the crack spanning the length of the specimen. No specimens containing ECR showed signs of surface staining during the test. After testing, however, staining was observed on the concrete surrounding the damaged regions in the epoxy when the specimens were autopsied (see figure 248 and figure 249).
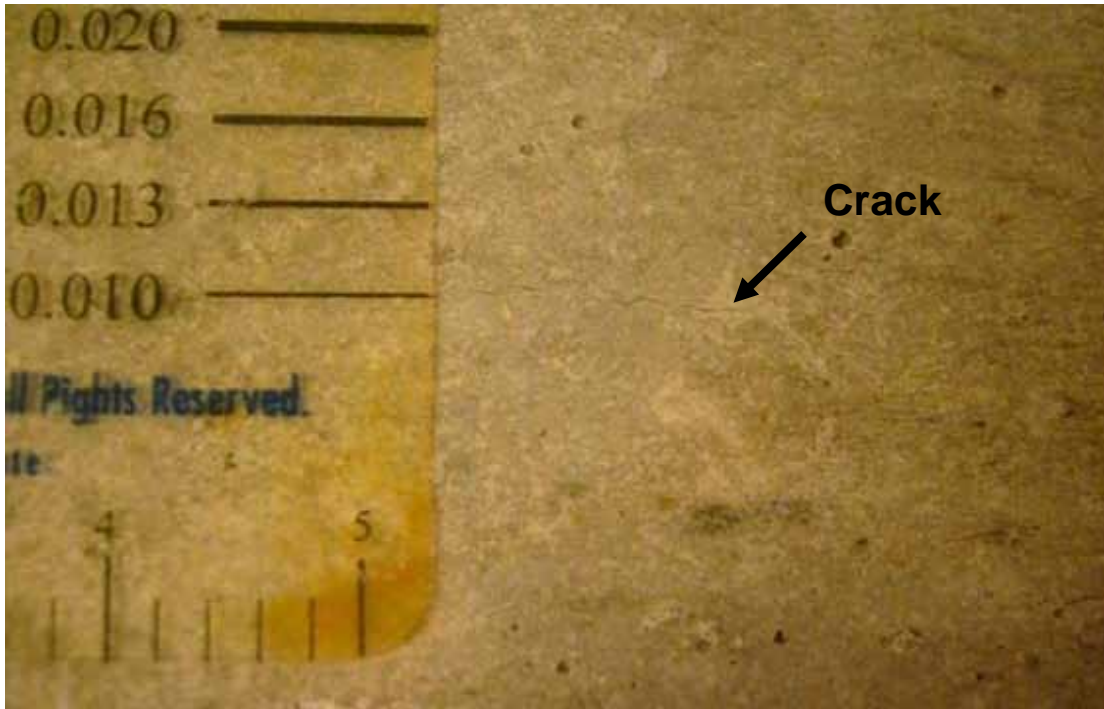
Figure 246. Photo. Crack initiation in specimen ECR-2r-H-2.
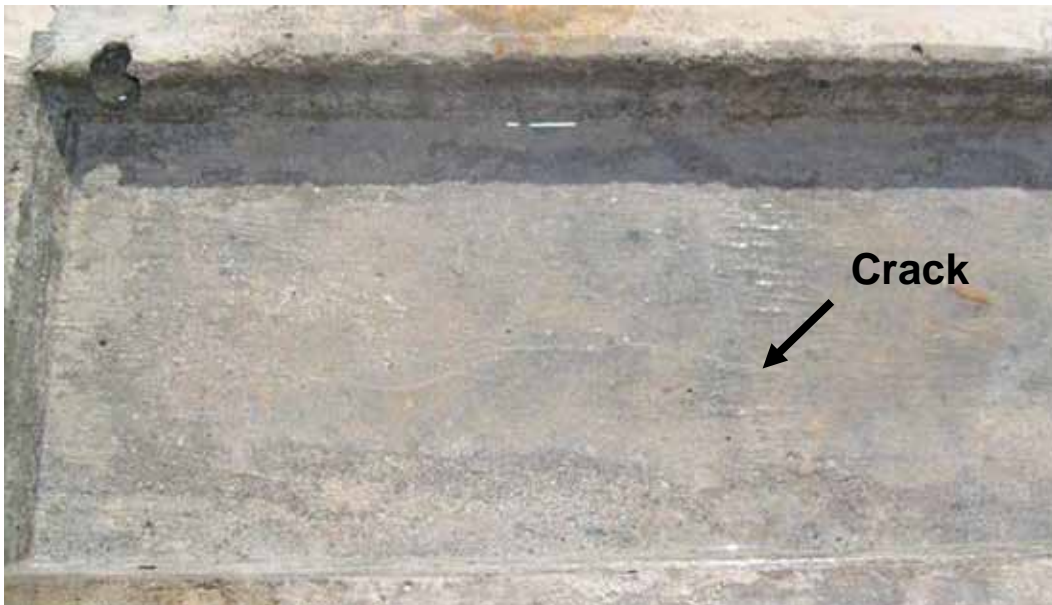
Figure 247. Photo. Crack propagation in specimen ECR-2h-V-1.

Figure 248. Photo. Concrete surrounding test bar from specimen ECR-2h-V-1.
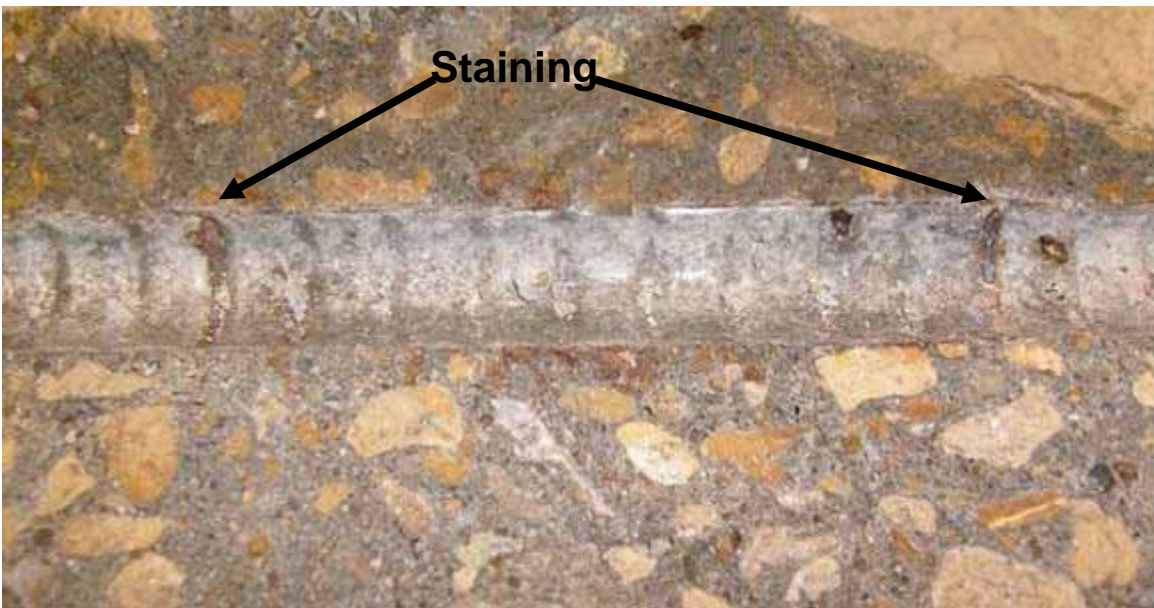
Figure 249. Photo. Concrete surrounding test bar from specimen ECR-2r-H-2.

FINITE ELEMENT RESULTS

The corrosion losses that cause a 50-μm (2-mil)-wide crack to form at the surface of the specimen based on the two-dimensional finite element analyses are shown in table 63. The corrosion losses are plotted as a function of concrete cover in figure 250. The results suggest a linear relationship (for covers between 6 and 102 mm (0.25 and 4 inches)) between concrete cover and corrosion loss required to cause cracking. A slight dependence on bar diameter is also noted; figure 251 shows best-fit lines for each of the three bar diameters over the range of covers from 19 to 76 mm (0.75 to 3 inches).

Table 63. Finite element results for two-dimensional model.

Cover, mm	Bar Diameter, mm	Corrosion Loss to Crack Concrete[a], μm
6.4	12.7	19.7
13	12.7	20.3
25	12.7	26.0
38	12.7	35.6
51	12.7	45.1
76	12.7	59.5
9.5	19	19.7
19	19	25.4
38	19	33.7
57	19	45.1
76	19	56.5
13	25.4	20.3
25	25.4	26.7
51	25.4	40.6
76	25.4	51.1
102	25.4	76.2

1 mm = 0.039 inches

1 μm = 0.0394 mil

[a] 50-μm (0.002-inch) crack width.
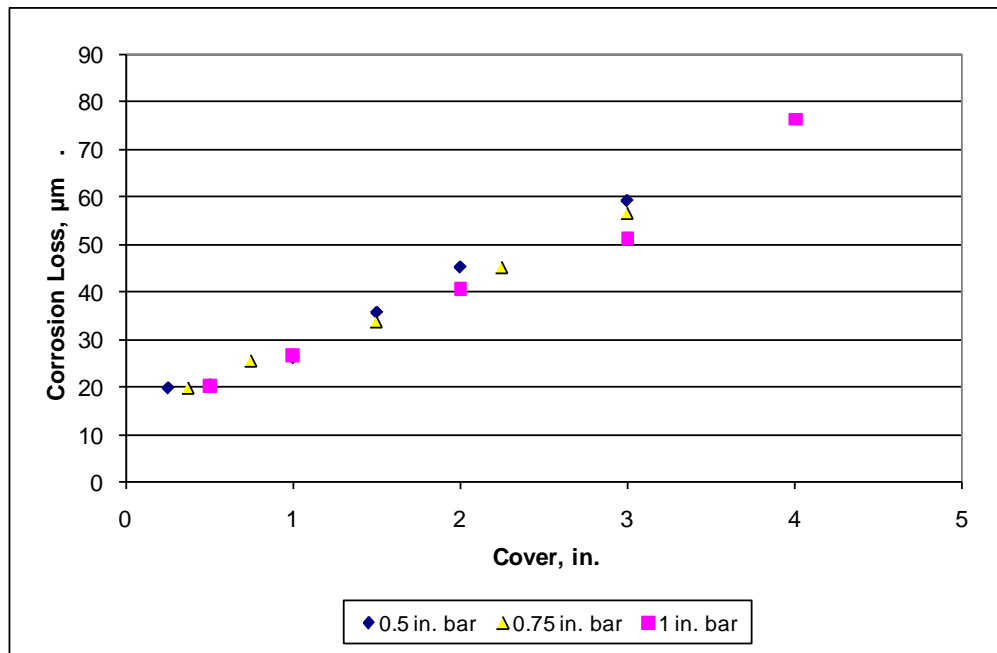
1 μm = 0.0394 mil

1 inch = 25.4 mm

Figure 250. Graph. Corrosion loss to crack concrete versus cover for two-dimensional finite element model.

210
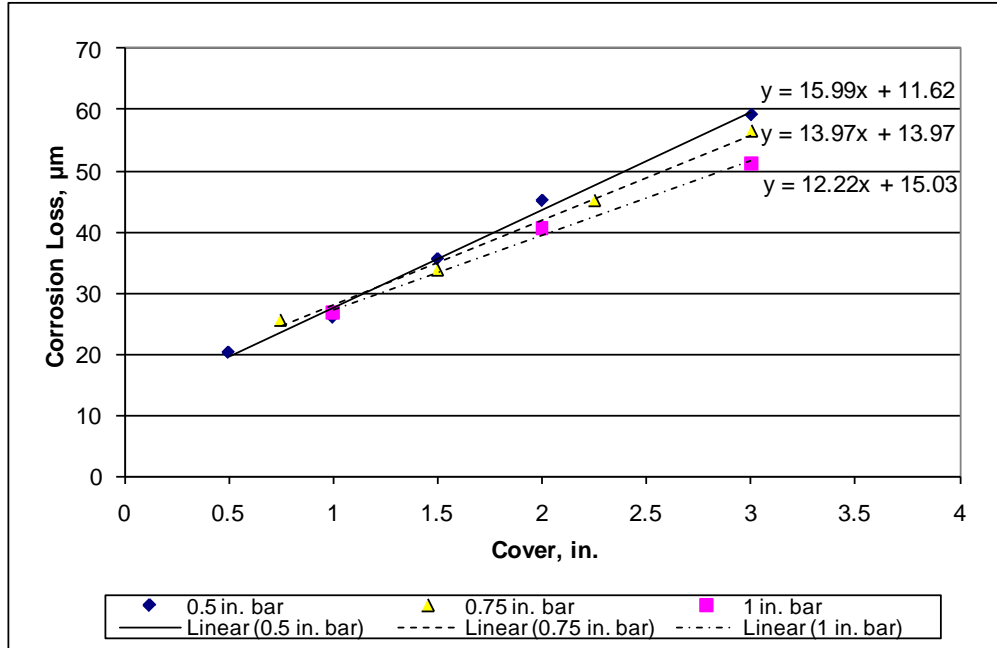
$$1 \ \mu m = 0.0394 \ mil$$
$$1 \ inch = 25.4 \ mm$$

Figure 251. Graph. Corrosion loss to crack concrete versus cover showing effect of bar diameter for two-dimensional finite element model.

Table 63 and figure 251 show that as cover increases, bars with smaller diameters require somewhat greater corrosion losses to crack concrete than bars with larger diameters for covers between 25 and 76 mm (1 and 3 inches). An analysis of the data suggests the equation in figure 252 as a best-fit expression. The English equivalent is presented in figure 253.

$$x_{crit} = 1.8 \left(\frac{C}{D^{0.38}} + 7.5 \right)$$

Figure 252. Equation. Suggested best-fit in SI units.

$$x_{crit} = 0.53 \left(\frac{C}{D^{0.38}} + 1 \right)$$

Figure 253. Equation. Suggested best-fit in English units.

Where:

x_{crit} = Corrosion loss at crack initiation, μm or mil.

C = Cover, mm or inches.

D = Bar diameter, mm or inches.

To verify the accuracy of the two-dimensional finite element model, the results obtained from the model are compared with experimental results presented in this appendix along with experimental results obtained by Saeki et al., Rasheeduzzafar et al., Alonso et al., and Torres-Acosta and Sagues for corrosion along the full length of conventional reinforcement. (See references 68, 69,

71, and 79.) The data from these sources are shown in table 64. The experimental data are plotted along with the finite element results in figure 254. Data presented in this appendix are labeled "KU." Other data are identified by the first author. A best-fit line for the results from the finite element model is also shown. While there is much scatter in the experimental data, the corrosion loss required to crack concrete, as predicted by the finite element model, provides an excellent representation of the bulk of the experimental data.

Table 64. Corrosion loss to crack concrete (corrosion along entire bar length).

Study	Cover, mm	Diameter, mm	Corrosion Loss, μm
Torres-Acosta and Sagues[71]	39	13	35.9
	39	13	31.1
Alonso et al.[69]	20	16	15
	15	8	20
	30	16	25
	30	16	28
	30	16	30
	50	16	31
	50	12	51
	70	16	55
	70	10	68
	20	16	25
	20	16	18
Rasheeduzzafar et al.[68]	19	13	33
	19	13	26
	19	13	34
	38	13	32
	38	13	30
	38	13	47
	38	13	38
	38	13	27
	38	13	27
	50	13	70
	50	13	71
	50	13	74
	50	13	61
	60	13	67
Saeki et al.[79]	31.75	9.5	42
	31.75	12.7	34
	31.75	19	23
	31.75	25	13

1 mm = 0.039 inches
1 μm = 0.0394 mil

Figure 254. Graph. Corrosion loss to crack concrete versus cover in two-dimensional finite element model with experimental data.
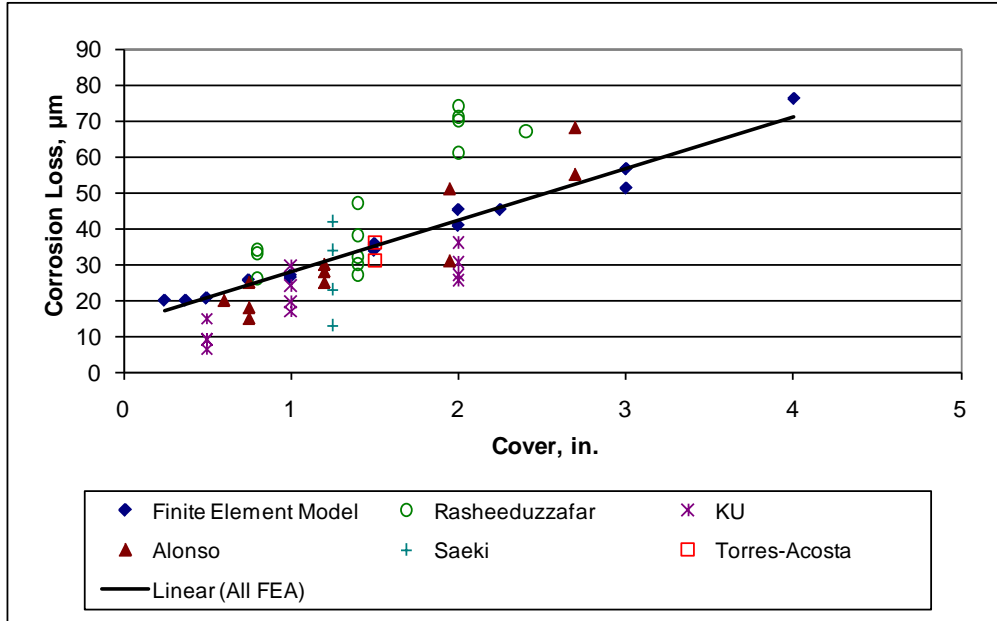
1 μm = 0.0394 mil
1 inch = 25.4 mm

Figure 254. Graph. Corrosion loss to crack concrete versus cover in two-dimensional finite element model with experimental data.

To determine its accuracy, the results predicted by the equation in figure 252 are compared with experimental results and finite element model results in figure 255.
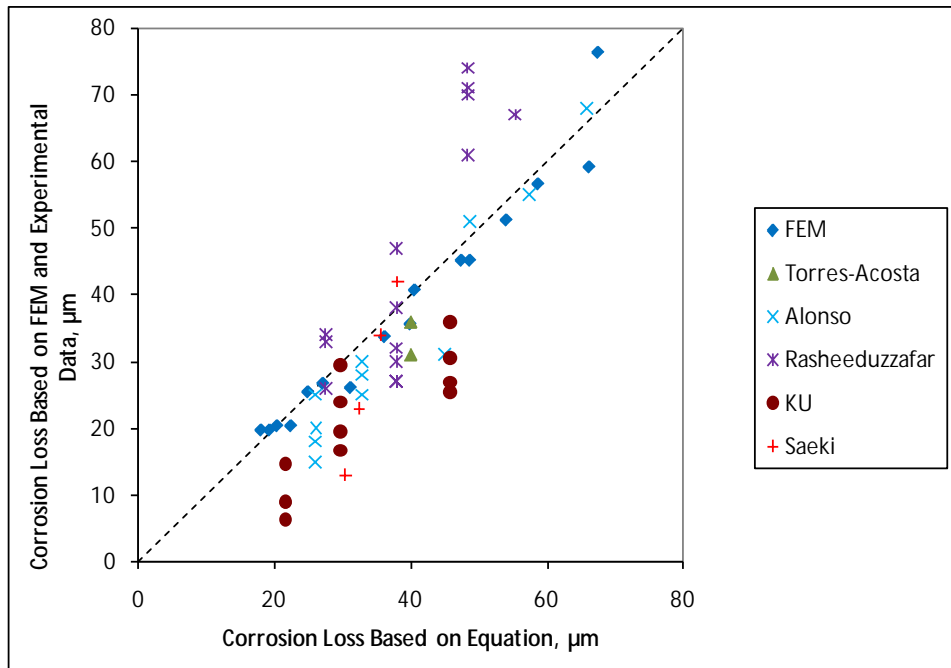
1 μm = 0.0394 mil

Figure 255. Graph. Corrosion loss to crack concrete for uniform general corrosion based on experimental and finite element results versus predicted corrosion losses using figure 252.

The proposed equation overestimates the corrosion loss required to crack concrete for most cases in which the actual corrosion loss required to crack the concrete is less than 45 µm (1.78 mil). An alternate equation is proposed in figure 256 and figure 257 that provides a somewhat more conservative estimate of the corrosion loss required to crack concrete (see figure 258).

$$x_{crit} = 1.8 \left(\frac{C}{D^{0.38}} + 4.5 \right)$$

Figure 256. Equation. Alternate best-fit in SI units.

$$x_{crit} = 0.53 \left(\frac{C}{D^{0.38}} + 0.6 \right)$$

Figure 257. Equation. Alternate best-fit in English units.

Where:

x_{crit} = Corrosion loss at crack initiation, µm or mil.

C = Cover, mm or inches.

D = Bar diameter, mm or inches.
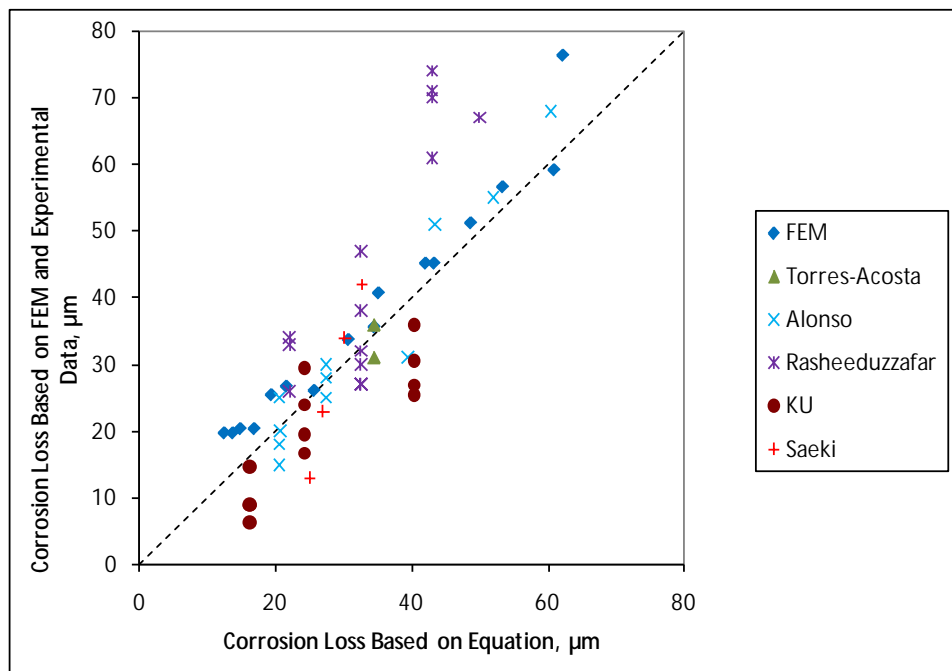
1 µm = 0.0394 mil

Figure 258. Graph. Corrosion loss to crack concrete for uniform general corrosion based on experimental and finite element results versus predicting corrosion losses using figure 256.

The corrosion losses to cause cracking based on the three-dimensional finite element model are shown in table 65 and table 66. The models with a 51-mm (2-inch) cover and a 203-mm (8-inch) and 508-mm (20-inch) length of bar corroding show similar corrosion losses at crack initiation. The behavior of the three-dimensional finite element model under full-bar-length (508 mm

(20 inches)) corrosion is compared to that of the two-dimensional finite element model in figure 259. The corrosion losses to cause cracking obtained from these models are similar. The differences in corrosion loss to crack concrete between two- and three-dimensional models is less than 1 µm (0.039 mil), with the exception of models with a 25-mm (1-inch)-diameter bar and 76-mm (3-inch) cover, which show a 2.9-µm (0.11-mil) or 5.7 percent difference in corrosion loss to cause cracking.

Table 65. Finite element results for three-dimensional model, 51-mm (2-inch) cover.

Corrosion Pattern	13-mm (0.5-in.) Bar Diameter		19-mm (0.75-in.) Bar Diameter		25-mm (1-in.) Bar Diameter	
	Exposed Area, mm² (in²)	Corrosion Loss at Cracking, µm	Exposed Area, mm² (in²)	Corrosion Loss at Cracking, µm	Exposed Area, mm² (in²)	Corrosion Loss at Cracking, µm
Full Ring						
508 mm (20 in.) length	10,134 (15.7)	46	15,201 (23.6)	43	20,268 (31.4)	40
203 mm (8 in.) length	4,054 (6.28)	57	6,080 (9.42)	44	8,107 (12.6)	41
102 mm (4 in.) length	2,027 (3.14)	79	3,040 (4.71)	57	4,054 (6.28)	56
51 mm (2 in.) length	1,013 (1.57)	159	1,520 (2.36)	133	2,027 (3.14)	80
25 mm (1 in.) length	507 (0.785)	330	760 (1.18)	254	1,013 (1.57)	144
13 mm (0.5 in.) length	253 (0.392)	483	380 (0.589)	381	507 (0.785)	281
6.4 mm (0.25 in.) length	127 (0.196)	659	190 (0.295)	508	253 (0.392)	361
3.2 mm (0.125 in.) length	63.3 (0.098)	851	95 (0.147)	658	127 (0.196)	502
Half Ring						
102 mm (4 in.) length	1,013 (1.57)	178	1,520 (2.36)	152	2,027 (3.14)	88
51 mm (2 in.) length	507 (0.785)	273	760 (1.18)	229	1,013 (1.57)	150
25 mm (1 in.) length	253 (0.392)	425	380 (0.589)	347	507 (0.785)	279
13 mm (0.5 in.) length	127 (0.196)	635	190 (0.295)	502	253 (0.392)	418
6.4 mm (0.25 in.) length	63.3 (0.098)	904	95.0 (0.147)	704	127 (0.196)	572
3.2 mm (0.125 in.) length	31.7 (0.049)	1,228	47.5 (0.074)	973	63.3 (0.098)	784
Quarter Ring						
102 mm (4 in.) length	507 (0.785)	216	760 (1.18)	191	1,013 (1.57)	170
51 mm (2 in.) length	253 (0.392)	337	380 (0.589)	292	507 (0.785)	259
25 mm (1 in.) length	127 (0.196)	546	190 (0.295)	470	253 (0.392)	404
13 mm (0.5 in.) length	63.3 (0.098)	861	95.0 (0.147)	737	127 (0.196)	622
6.4 mm (0.25 in.) length	31.7 (0.049)	1,293	47.5 (0.074)	1,090	63.3 (0.098)	890
3.2 mm (0.125 in.) length	15.8 (0.025)	1,969	23.8 (0.037)	1,562	31.7 (0.049)	1,226
1.6 mm (0.0625 in.) length	7.9 (0.012)	2654	11.8 (0.018)	2,223	15.8 (0.025)	1,930

1 µm = 0.0394 mil

Table 66. Finite element results for three-dimensional model, 76-`mm (3-inch) cover.

Corrosion Pattern	13-mm (0.5-in.) Bar Diameter		19-mm (0.75-in.) Bar Diameter		25-mm (1-in.) Bar Diameter	
	Exposed Area, mm² (in²)	Corrosion Loss at Cracking, μm	Exposed Area, mm² (in²)	Corrosion Loss at Cracking, μm	Exposed Area, mm² (in²)	Corrosion Loss at Cracking, μm
Full Ring						
508 mm (20 in.) length	10,134 (15.7)	57	15,201 (23.6)	56	20,268 (31.4)	54
203 mm (8 in.) length	4,054 (6.28)	102	6,080 (9.42)	152	8,107 (12.6)	83
102 mm (4 in.) length	2,027 (3.14)	216	3,040 (4.71)	267	4,054 (6.28)	108
51 mm (2 in.) length	1,013 (1.57)	445	1,520 (2.36)	406	2,027 (3.14)	267
25 mm (1 in.) length	507 (0.785)	660	760 (1.18)	584	1,013 (1.57)	446
13 mm (0.5 in.) length	253 (0.392)	927	380 (0.589)	813	507 (0.785)	611
6.4 mm (0.25 in.) length	127 (0.196)	1,295	190 (0.295)	1,067	253 (0.392)	853
3.2 mm (0.125 in.) length	63.3 (0.098)	1,689	95 (0.147)	1,321	127 (0.196)	1,116
Half Ring						
102 mm (4 in.) length	1,013 (1.57)	368	1,520 (2.36)	356	2,027 (3.14)	328
51 mm (2 in.) length	507 (0.785)	559	760 (1.18)	521	1,013 (1.57)	483
25 mm (1 in.) length	253 (0.392)	838	380 (0.589)	762	507 (0.785)	693
13 mm (0.5 in.) length	127 (0.196)	1,219	190 (0.295)	1,118	253 (0.392)	968
6.4 mm (0.25 in.) length	63.3 (0.098)	1,676	95.0 (0.147)	1,461	127 (0.196)	1,283
3.2 mm (0.125 in.) length	31.7 (0.049)	2,261	47.5 (0.074)	1,842	63.3 (0.098)	1,689
Quarter Ring						
102 mm (4 in.) length	507 (0.785)	508	760 (1.18)	445	1,013 (1.57)	394
51 mm (2 in.) length	253 (0.392)	737	380 (0.589)	622	507 (0.785)	610
25 mm (1 in.) length	127 (0.196)	1,067	190 (0.295)	927	253 (0.392)	902
13 mm (0.5 in.) length	63.3 (0.098)	1,626	95.0 (0.147)	1,308	127 (0.196)	1,270
6.4 mm (0.25 in.) length	31.7 (0.049)	2,350	47.5 (0.074)	1,791	63.3 (0.098)	1,702
3.2 mm (0.125 in.) length	15.8 (0.025)	3,226	23.8 (0.037)	2,502	31.7 (0.049)	2,273
1.6 mm (0.0625 in.) length	7.9 (0.012)	4,343	11.8 (0.018)	3,543	15.8 (0.025)	3,226

1 μm = 0.0394 mil
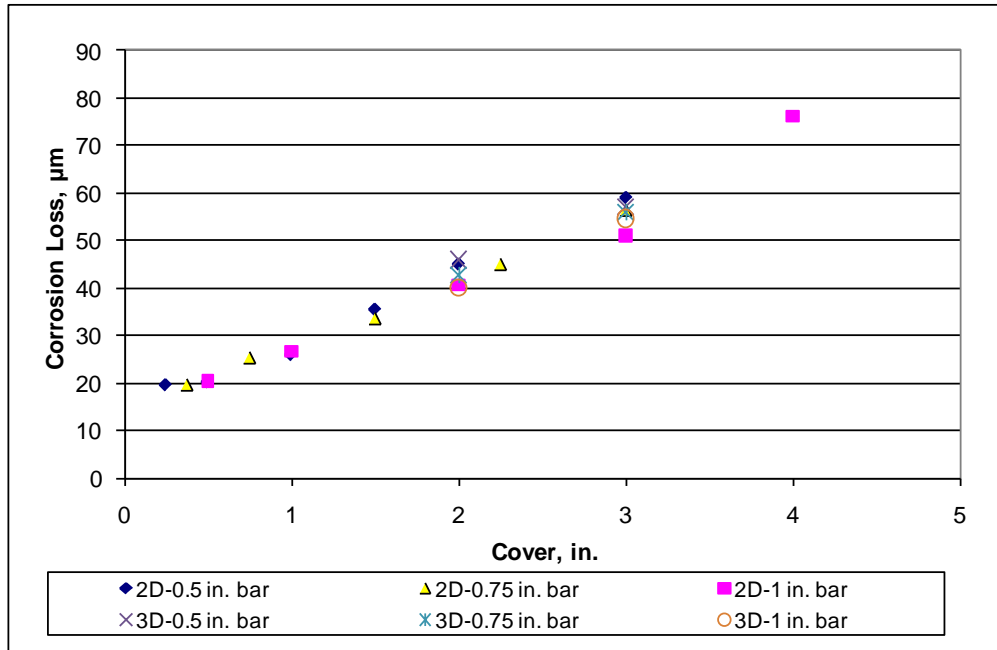
Figure 259. Graph. Corrosion loss to crack concrete for uniform general corrosion versus cover for two-and three-dimensional finite element model.

The number of variables studied in the three-dimensional finite element model makes plotting all data points on a single plot impractical. Instead, data subsets holding as many variables constant as possible are analyzed to determine the effect of a variable on the corrosion loss required to crack concrete. Furthermore, corroding area, bar diameter, length of corroding region, and damage pattern are not independent variables—specifying any three variables restricts the fourth to a single value. For this analysis, the effect of cover, bar diameter, corroding area, and corroding length are analyzed with the goal of creating an equation that reduces to figure 256 in the case of general corrosion. Corroding area is expressed as a fraction of the total area of the bar, A_f ($A_f = A_{corroding}/A_{bar}$). Corroding length is expressed as a fraction of the total length of the bar, L_f ($L_f = L_{corroding}/L_{bar}$).

The corrosion loss to crack concrete is plotted versus exposed area for a 13-mm (0.5-inch)-diameter bar with 51-mm (2-inch) cover in figure 260. A curve of the form $x_{crit} = m(A_f)^b$ is fit to the data. Table 67 summarizes the values of m and b for all three-dimensional finite element models. Based on table 67, it may be reasonably assumed the constant b is equal to -0.6, while the constant A is dependent on other variables.
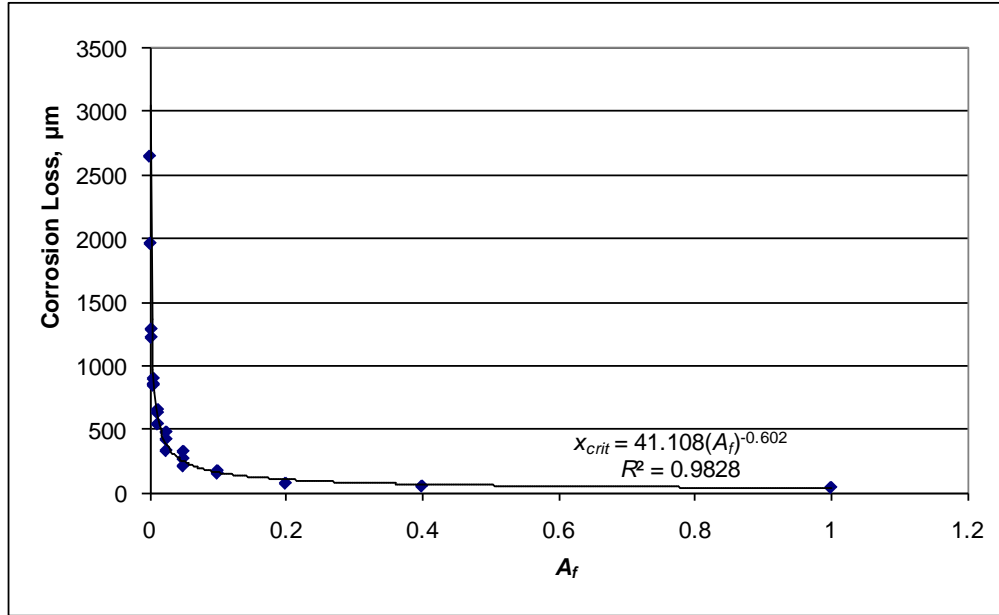
1 µm = 0.0394 mil

Figure 260. Graph. Corrosion loss to crack concrete versus fraction of exposed area with best-fit line for 13-mm (0.5-inch)-diameter bar and 51-mm (2-inch) cover.

Table 67. Constants *m* and *b* for best-fit curve $x_{crit} = m(A_f)b$ to corrosion loss versus A_f plots.

Bar Diameter, mm (inches)	Cover, mm (inches)	*m*	*b*
13 (0.5)	51 (2)	41.11	-0.602
19 (0.75)	51 (2)	34.20	-0.597
25 (1)	51 (2)	26.60	-0.600
13 (0.5)	76 (3)	85.11	-0.587
19 (0.75)	76 (3)	78.97	-0.592
25 (1)	76 (3)	60.65	-0.589

Figure 261 shows the relationship between corrosion loss and cover for all bars with a corroding area of 1,013 mm^2 (1.57 in^2). Similar plots were analyzed for other exposed areas. For bars with a fixed damage pattern and diameter, increasing the cover from 51 to 76 mm (2 to 3 inches) approximately doubles the corrosion loss required to crack concrete. This suggests that for localized corrosion, the corrosion loss required to crack concrete is proportional to cover squared. For larger corroding areas, the relationship between corrosion loss and cover becomes linear, as shown in figure 252 and figure 256.

218

$x_{crit} = 100.96C^{1.7095}$

$x_{crit} = 77.44C^{1.8511}$

$x_{crit} = 50.00C^{2.1103}$

| ✕FR, D = 0.5 in. | ⊿FR, D = 1 in. | ✳HR, D = 0.5 in. |
| □HR, D = 1 in. | ○QR, D = 0.5 in. | ⌒QR, D = 1 in. |
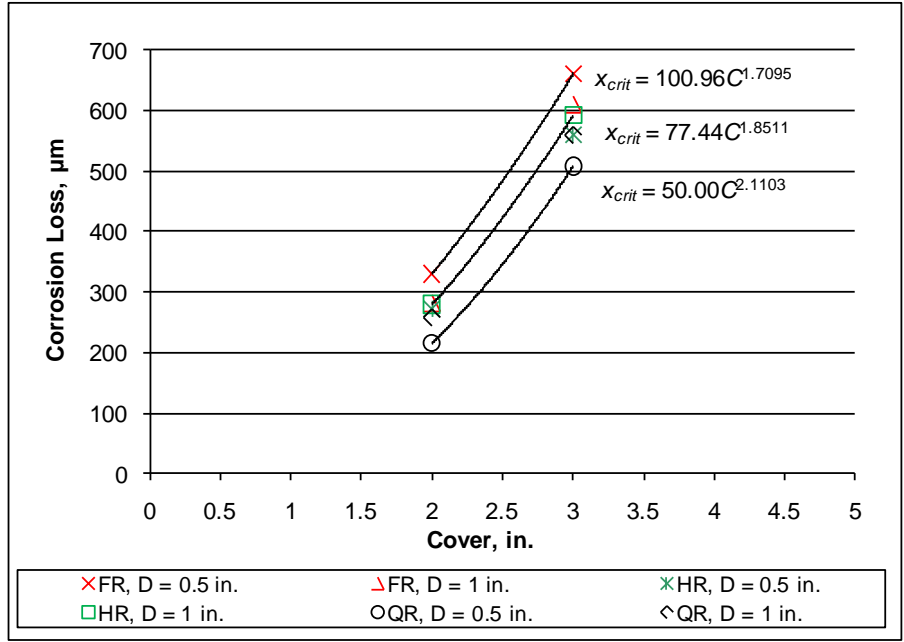
1 μm = 0.0394 mil
1 inch = 25.4 mm

Figure 261. Graph. Corrosion loss to crack concrete x_{crit} versus cover C for 1,013-mm^2 (1.57-in^2) corroding area.

Figure 262 shows the relationship between corrosion loss and fractional corroding length L_f ($L_f = L_{corroding}/L_{bar}$) for all bars with a corroding area of 1013 mm^2 (1.57 in^2). Similar plots are analyzed for other lengths. A best-fit power line to the data suggests a relationship between corrosion loss and fractional corroding length to the -0.1 power.

$x_{crit} = 451.95(L_f)^{-0.086}$
$R^2 = 0.9672$
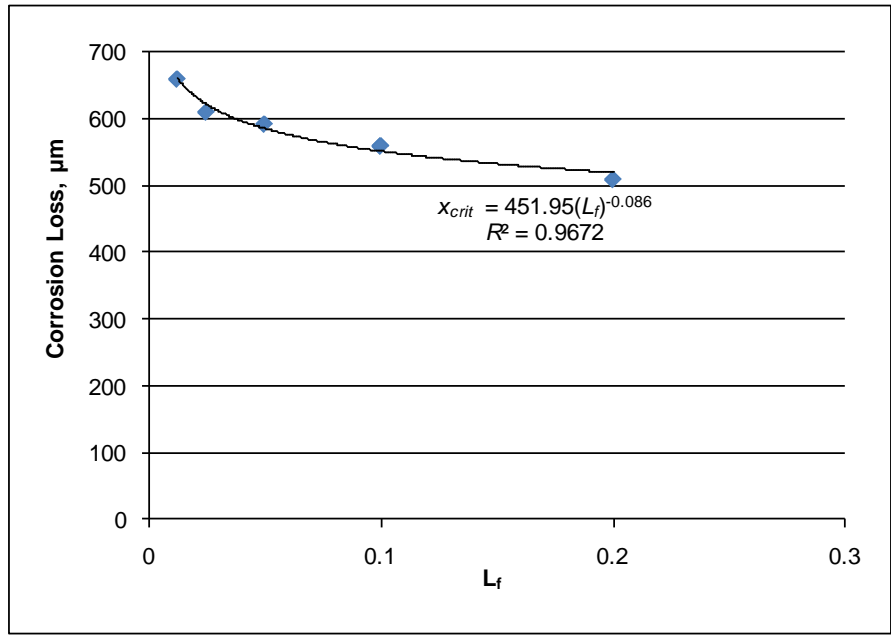
1 μm = 0.0394 mil

Figure 262. Graph. Corrosion loss to crack concrete x_{crit} versus L_f with best fit line for 1,013-mm^2 (1.57-in^2) corroding area.

219

Based on the data presented, the equations in figure 263 and figure 264 represent a potential relationship between corrosion loss and the variables in this study. The term 3^{A_f-1} is required for localized corrosion and reduces to 1 for general corrosion.

$$x_{crit} = 0.53 \left(\frac{C^{2-A_f}}{D^{0.38} L_f^{0.1} A_f^{0.6}} + 0.6 \right) 3^{A_f-1}$$

Figure 263. Equation. Potential relationship between corrosion loss and variables in English units.

$$x_{crit} = 45 \left(\frac{\left[C/25.4 \right]^{2-A_f}}{D^{0.38} L_f^{0.1} A_f^{0.6}} + 0.2 \right) 3^{A_f-1}$$

Figure 264. Equation. Potential relationship between corrosion loss and variables in SI units.

Where:

x_{crit} = Corrosion loss at crack initiation, mil or μm.

C = Cover, inches or mm.

D = Bar diameter, inches or mm.

L_f = Fractional length of bar corroding, $L_{corroding}/L_{bar}$.

A_f = Fractional area of bar corroding, $A_{corroding}/A_{bar}$.

Figure 265 compares the corrosion losses for the finite element models with the corrosion losses predicted by the equation. There is some scatter, but the equations in figure 263 and figure 264 provide a reasonable match with the results obtained from the finite element model.
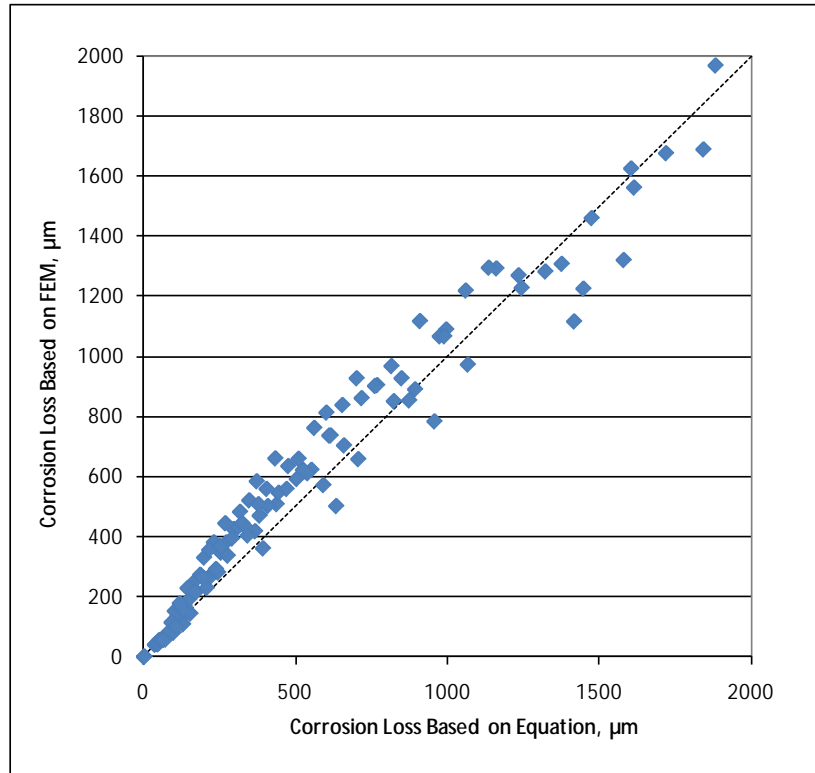
1 µm = 0.0394 mil

Figure 265. Graph. Corrosion loss to crack concrete for localized corrosion based on the finite element model results versus corrosion losses calculated by the equations in figure 263 and figure 264.

To further verify the accuracy of the equations in figure 263 and figure 264, the corrosion loss predicted by the equation is compared to the experimental data for localized corrosion of ECR, as well as experimental results presented by Rasheeduzzafar et al., Alonso et al., and Torres-Acosta and Sagues, which are summarized in table 68.[68,69,71] Data for generalized corrosion of steel are also included in the analysis to check the accuracy of the equation for bars with large corroding areas. The comparison is presented in figure 266 and figure 267 along with the comparison for the three-dimensional finite element model results shown in figure 265.

Table 68. Results from other research: corrosion loss to crack concrete (localized corrosion).

	Cover, mm	Diameter, mm	Exposed Area, mm²	Bar Area, mm²	Exposed Length, mm	Bar Length, mm	Corrosion Loss, µm
Torres-Acosta and Sagues[72]	27.6	21	2,105	16,757	32	254	48.3
	27.6	21	2,105	16,757	32	254	66.4
	40.3	21	2,738	20,122	42	305	88.2
	40.3	21	2,738	20,122	42	305	69.6
	65.7	21	4,486	26,785	68	406	76.5
	65.7	21	4,486	26,785	68	406	121.8
	40.3	21	2,764	20,122	42	305	55.2
	40.3	21	2,764	20,122	42	305	68.9
	40.3	21	1,260	13,393	19	203	141.2
	40.3	21	1,260	13,393	19	203	70.6
	40.3	21	2,738	20,122	42	305	60.3
	40.3	21	2,738	20,122	42	305	65.0
	40.3	21	22,827	26,785	346	406	28.4
	40.3	21	22,827	26,785	346	406	7.2
	27.5	21	1,649	26,785	25	406	30.8
	40.3	21	1,649	26,785	25	406	61.6
	45	13	4,084	16,581	100	406	84.0
	45	13	1,021	16,581	25	406	336.0
	38	13	4,084	16,581	100	406	49.8
	38	13	4,084	16,581	100	406	49.8
	13	13	4,084	16,581	100	406	31.1
	13	13	1,021	16,581	25	406	37.3
	13	13	1,021	16,581	25	406	49.8
	13	13	4,084	16,581	100	406	3B2
	28.8	13	796	16,581	20	406	207.4
	30.3	13	796	16,581	20	406	111.7
	39	13	15,928	16,581	390	406	35.9
	39	13	15,928	16,581	390	406	31.1
	39	13	1,593	16,581	39	406	151.6
	39	13	1,593	16,581	39	406	159.6
	39	13	327	16,581	8	406	233.3
	39	13	327	16,581	8	406	272.2
	27.5	6.4	603	8,163	30	406	63.2
	26.5	6.4	603	8,163	30	406	8B3
	39	13	1,593	16,581	39	406	271.2
	39	13	1,593	16,581	39	406	191.5
	39	13	1,593	16,581	39	406	159.6
	39	13	1,593	16,581	39	406	151.6

Table 68. Results from other research: corrosion loss to crack concrete (localized corrosion)—Continued.

	Cover, mm	Diameter, mm	Exposed Area, mm²	Bar Area, mm²	Exposed Length, mm	Bar Length, mm	Corrosion Loss, µm
Alonso et al.[70]	19	1B6	17,448	17,448	381	381	15
	15.2	8.0	9,550	9,550	381	381	20
	30.4	16.0	19,101	19,101	381	381	25
	30.4	16.0	19,101	19,101	381	381	28
	30.4	16.0	19,101	19,101	381	381	30
	49.4	15.9	19,024	19,024	381	381	31
	49.4	11.8	14,041	14,041	381	381	51
	68.4	15.5	18,558	18,558	381	381	55
	68.4	9.8	11,665	11,665	381	381	68
	19	1B6	17,448	17,448	381	381	25
	19	1B6	17,448	17,448	381	381	18
	29	38.1	91,207	91,207	381	381	3
Rasheeduzzafar et al.[69]	20	13	22,462	22,462	550	550	33
	20	13	22,462	22,462	550	550	26
	20	13	22,462	22,462	550	550	34
	35	13	22,462	22,462	550	550	32
	35	13	22,462	22,462	550	550	30
	35	13	22,462	22,462	550	550	47
	35	13	22,462	22,462	550	550	38
	35	13	22,462	22,462	550	550	27
	35	13	22,462	22,462	550	550	27
	50	13	22,462	22,462	550	550	70
	50	13	22,462	22,462	550	550	71
	50	13	22,462	22,462	550	550	74
	50	13	22,462	22,462	550	550	61
	60	13	22,462	22,462	550	550	67

1 mm = 0.039 inches
1 mm² = 0.00155 in²
1 µm = 0.0394 mil
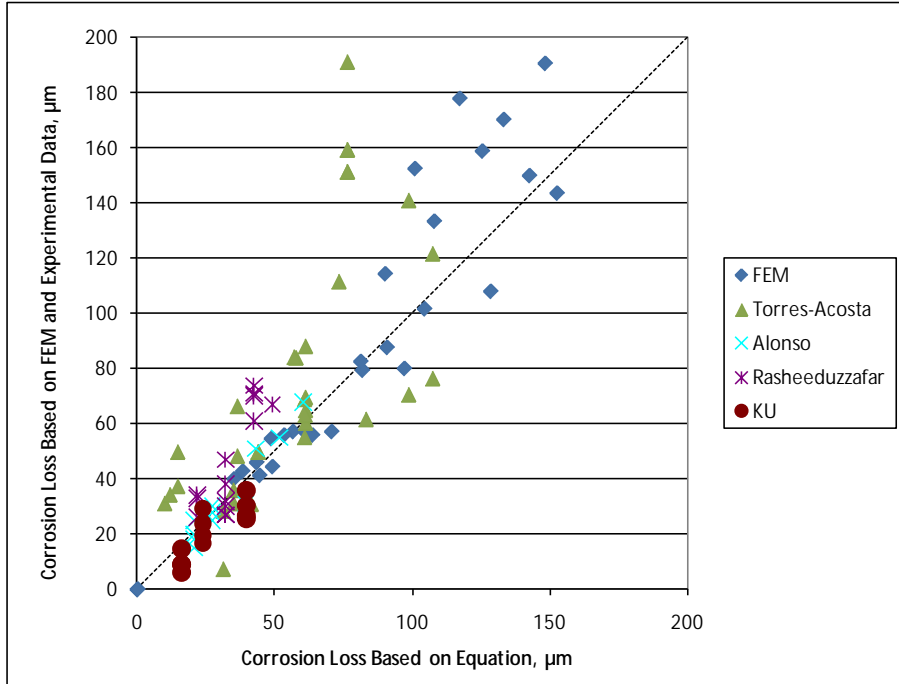
Figure 266. Graph. Corrosion loss in localized corrosion specimens versus corrosion loss predicted by the equation in figure 263 and figure 264 for three-dimensional finite element model and experimental data.

1 µm = 0.0394 mil
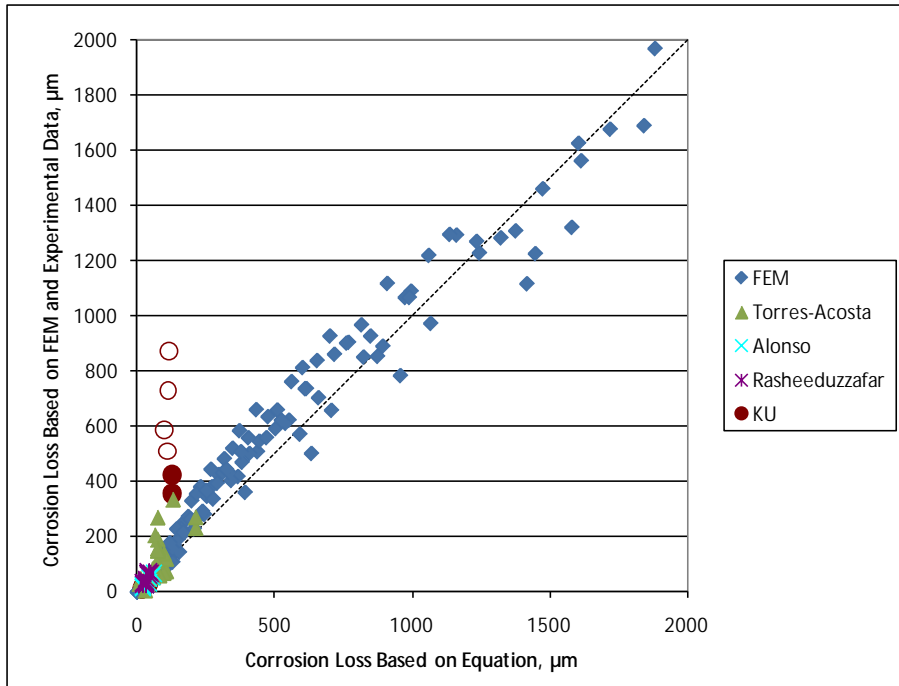
Figure 267. Graph. Corrosion loss in localized corrosion specimens versus corrosion loss predicted by the equation in figure 263 and figure 264 for three-dimensional finite element model and experimental data (revised scale).

224

Figure 266 covers the range of the experimental data in table 68. There is a moderate degree of scatter for both the finite element model and experimental results, but the finite element model generally agrees with the experimental data. The equations in figure 263 and figure 264 provide a generally conservative estimate of the corrosion loss required to crack concrete based on both the experimental and finite element results; that is, in most cases, the equations in figure 263 and figure 264 underestimate the loss required to cause a crack to form.

The finite element models extend well beyond the range of experimental data (see figure 267); additional testing will be needed to verify the accuracy of the finite element model in this range. The KU specimens with actual corrosion losses between 350 and 900 µm (14 and 35 mil) represent the epoxy-coated bars with half-rings and holes in the epoxy. Figure 263 and figure 264 are very conservative for these specimens, predicting losses of approximately 200 µm (7.8 mil), compared to the 350 and 900 µm (14 and 35 mil) range in actual losses. The equation is most conservative for the epoxy-coated specimens with two holes in the epoxy; these specimens are shown as open circles in figure 267, as the uncertainty in the exposed area due to blistering of the epoxy calls the accuracy of these data points into question.

DISCUSSION

Torres-Acosta and Sagues derived an expression, shown in figure 268, relating bar cover, bar diameter, and localized corrosion length with the corrosion loss required for crack initiation based on experimental results.[71]

$$x_{crit} = 11.0 \frac{C}{D} \left(\frac{C}{L} + 1 \right)^2$$

Figure 268. Equation. Torres-Acosta and Sagues' corrosion loss to crack initiation.

Where:

x_{crit} = Corrosion loss at crack initiation, µm.

C = Cover, mm.

D = Bar diameter, mm.

L = Length of exposed steel, mm.

Figure 269 and figure 270 compare the corrosion losses predicted by the equation with the experimental data for localized corrosion of ECR presented in table 62, as well as the finite element results and the experimental results presented by Rasheeduzzafar et al., Alonso et al., and Torres-Acosta and Sagues, as done for the equations in figure 263 and figure 264 in figure 266 and figure 267.[68,69,71]
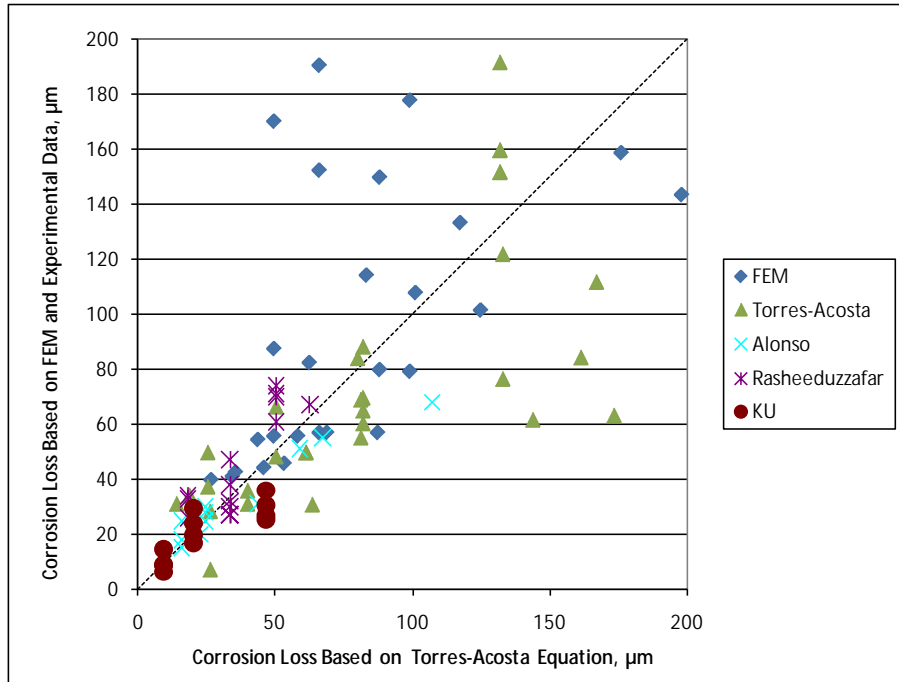
Figure 269. Graph. Corrosion loss in localized corrosion specimens versus corrosion loss predicted by the equation in figure 268 with three-dimensional finite element model and experimental data.
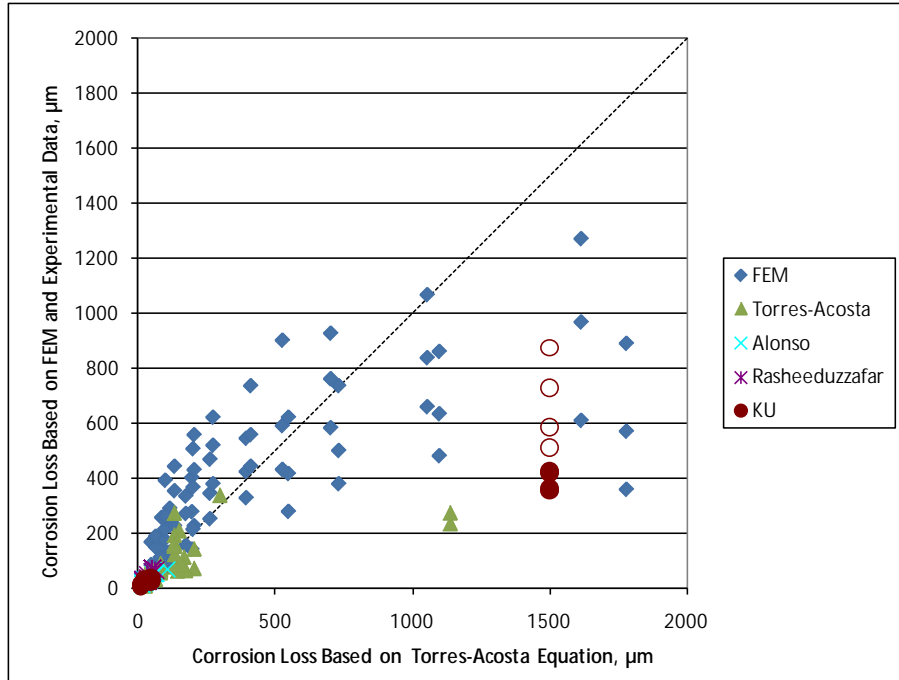
Figure 270. Graph. Corrosion loss in localized corrosion specimens versus corrosion loss predicted by the equation in figure 268 with three-dimensional finite element model and experimental data (revised scale).

Comparing figure 266 and figure 269 shows that for bars that require less than 50 µm (2 mil) of loss to crack concrete, the equations in figure 263 and figure 264 and the equation in figure 268 perform comparably. However, the equation developed by Torres-Acosta is less conservative based on both experimental and finite element model results for bars that require greater than 50 µm (2 mil) of loss to crack concrete; that is, the corrosion loss required to crack concrete predicted by the equation in figure 268 is greater than the corrosion loss required to crack concrete in the test specimens and for many of the finite element results. The equations in figure 263 and figure 264, in contrast, are more conservative with respect to many of the experimental specimens. The equation in figure 268 overestimates a significant portion of the experimental results obtained by Torres-Acosta and Sagues, in one case predicting a corrosion loss of 173 µm (6.81 mil) for a specimen that only required 63 µm (2.48 mil) of loss to crack concrete. For all experimental specimens with actual losses greater than 60 µm (2.4 mil), the equation in figure 268 overestimates the corrosion loss requited to crack concrete for over 75 percent of the specimens. In comparison, the equation in figure 263 and figure 264 overestimates the corrosion loss to crack concrete for only 14 percent of the specimens with actual losses greater than 60 µm (2.4 mil).

Comparing the two expressions based on results from the finite element model suggests that the equation in figure 268 becomes increasingly inaccurate and unconservative for bars that require very large corrosion losses to crack concrete (see figure 270). Furthermore, results from the finite element models where greater than 1,200 µm (47 mil) of loss is required to crack concrete do not appear in figure 270, as the equation in figure 268 predicts that greater than 2,000 µm (79 mil) of loss is required to crack the concrete.

The ratio of experimentally obtained corrosion losses required to crack concrete to the corrosion losses obtained by the two equations is also used to judge the degree of conservatism in each equation. A ratio less than 1.0 indicates an unconservative estimate for that specimen. Figure 271 and figure 272 compare this ratio for each equation based on corrosion losses obtained from experimental and finite element model results, respectively. Over the range of available experimental data, the two equations perform comparably, with the equations in figure 263 and figure 264 being more conservative for systems where actual losses exceeded 50 µm (2 mil). As previously discussed, the available experimental data involves exposed areas far larger than those typically observed on damaged ECR. The specimens with damaged ECR tested as part of this study developed blisters that greatly increased the exposed area; therefore, only finite element model results are available for small exposed areas. Over the range of finite element model data, the equation in figure 268 rapidly becomes unconservative, as noted by the large percentage of ratios of finite element model-predicted corrosion losses to figure 268-predicted losses that are much less than 1.0 for models with expected corrosion losses greater than 500 µm (20 mil). In contrast, the equations in figure 263 and figure 264 do not exhibit this behavior. Therefore, the equations in figure 263 and figure 264 are used to determine the corrosion loss required to crack concrete for damaged ECR.

1 µm = 0.0394 mil
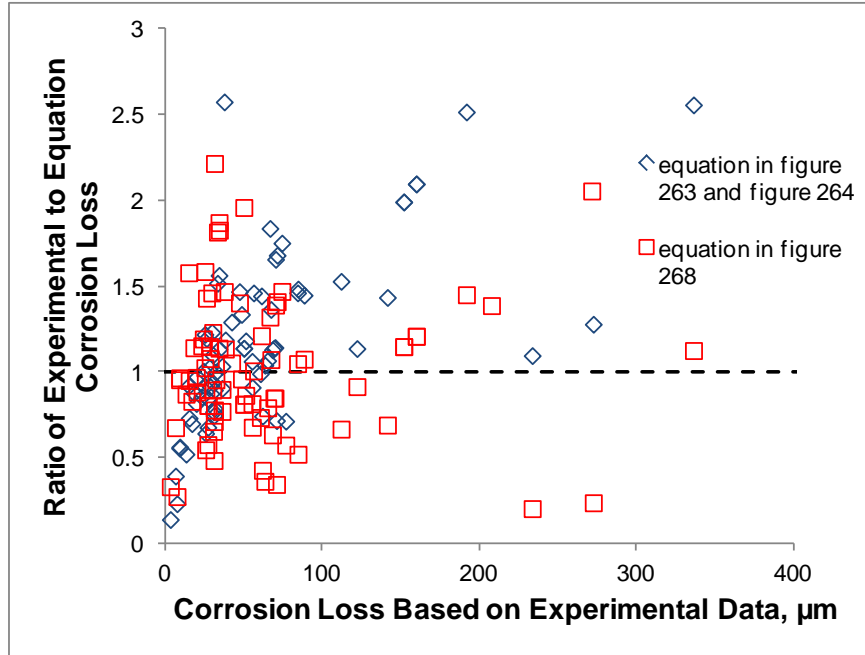
Figure 271. Graph. Ratio of experimentally derived corrosion loss to predicted corrosion loss versus corrosion loss to crack concrete based on experimental data.

1 µm = 0.0394 mil
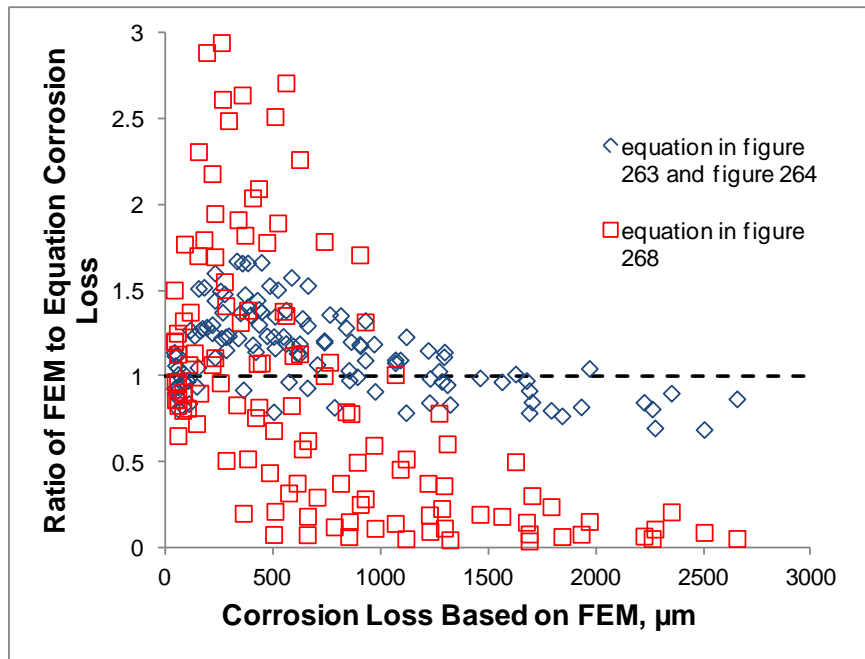
Figure 272. Graph. Ratio of finite element model-derived corrosion loss to predicted corrosion loss versus corrosion loss to crack concrete based on finite element model.

ACKNOWLEDGMENTS

REFERENCES

1. Federal Highway Administration (2007). "Deficient Bridges by State and Highway Systems." McLean, VA. Accessed online: September 23, 2011. (http://www.fhwa.dot.gov/bridge/defbr07.cfm)

2. Koch, G., Broongers, H., Thompson, N., Virmani, Y., and Payer, J. (2002). *Corrosion Cost and Preventive Strategies in the United States*, Report No. FHWA-RD-01-156, Federal Highway Administration, Washington, DC.

3. Lindquist, W.D., Darwin, D., Browning, J., and Miller, G.G. (2006). "Effect of Cracking on Chloride Content in Concrete Bridge Decks," *ACI Materials Journal*, Vol. 103, No. 6, pp. 467–473, American Concrete Institute, Farmington Hills, MI.

4. Smith, J.L. and Virmani, Y.P. (1996). *Performance of Epoxy-Coated Rebars in Bridge Decks*, Report No. FHWA-RD-96-092, Federal Highway Administration, Washington, DC.

5. Virmani, Y.P. and Clemeña, G.G. (1998). *Corrosion Protection—Concrete Bridges*, Report No. FHWA-RD-98-099, Federal Highway Administration, Washington, DC.

6. Clear, K.C. (1992). "Effectiveness of Epoxy-Coated Reinforcing Steel," *Concrete International,* Vol. 14, No. 5, pp. 58–64, American Concrete Institute, Farmington Hills, MI.

7. Sagues, A.A., Powers, R.G., and Kessler, R. (1994). "Corrosion Processes and Field Performance of Epoxy-Coated Reinforcing Steel in Marine Structures," *Corrosion 94,* Paper No. 299, National Association of Corrosion Engineers, Houston, TX.

8. Sprinkel, M.M., Weyers, R., Blevins, C., Ramniceanu, A., and Weyers, S. (2010). "Failure and Repair of Deck Closure Pour on Interstate 81," *Transportation Research Record No. 2150*, pp. 119–128, Transportation Research Board, Washington, DC.

9. Schiessl, P. (1992). *Review of the KC, Inc., Reports on Effectiveness of Epoxy-Coated Reinforcing Steel*, Canadian Strategic Highway Research Program, Ottawa, Ontario.

10. Concrete Reinforcing Steel Institute (1995*). Adhesion Loss Mechanisms of Epoxy Coatings on Rebar Surfaces,* Surface Science Western, Schaumberg, IL.

11. Weyers, R.E., Zemajtis, J., and Drumm, R.O. (1995). "Service Lives of Concrete Sealers," *Transportation Research Record No. 1490*, pp. 54–59, Transportation Research Board, Washington, DC.

12. ASTM A615/A615M-01b (2001). "Standard Specification for Deformed and Plain Carbon-Steel Bars for Concrete Reinforcement," ASTM International, West Conshohocken, PA.

13. ASTM A775/A775M-04a (2004). "Standard Specification for Epoxy-Coated Steel Reinforcing Bars," ASTM International, West Conshohocken, PA.

14. ASTM G8-96(2003) (1996). "Standard Test Methods for Cathodic Disbonding of Pipeline Coatings," ASTM International, West Conshohocken, PA.

15. ASTM A775/A775M-07a (2007). "Standard Specification for Epoxy-Coated Steel Reinforcing Bars," ASTM International, West Conshohocken, PA.

16. McDonald, D.B., Pfeifer, D.W., and Sherman, M.R. (1998). *Corrosion Evaluation of Epoxy-Coated, Metallic Clad and Solid Metallic Reinforcing Bars in Concrete*, Report No. FHWA-RD-98-153, Federal Highway Administration, Washington, DC.

17. Martinez, S.L., Darwin, D., McCabe, S.L., and Locke, C.E. (1991). *Rapid Test for Corrosion Effects of Deicing Chemicals in Reinforced Concrete*, SL Report 90-4, University of Kansas Center for Research, Lawrence, KS.

18. Chappelow, C.C., McElroy, A.D., Blackburn, R.R., Darwin, D., deNoyelles, F.G., and Locke, C.E. (1992). *Handbook of Test Methods for Evaluating Chemical Deicers*, Strategic Highway Research Program, National Research Council, Washington, DC.

19. Smith, J.L., Darwin, D., and Locke, C.E., Jr. (1995). *Corrosion-Resistant Steel Reinforcing Bars Initial Tests*, SL Report 95-1, University of Kansas Center for Research, Lawrence, KS.

20. Senecal, M.R., Darwin, D., and Locke, C.E., Jr. (1995). *Evaluation of Corrosion-Resistant Steel Reinforcing Bars*, SM Report Number 40, University of Kansas Center for Research, Lawrence, KS.

21. Schwensen, S.M., Darwin, D., and Locke, C.E., Jr. (1995). *Rapid Evaluation of Corrosion Resistant Concrete Reinforcing Steel in the Presence of Deicers*, SL Report 95-6, University of Kansas Center for Research, Lawrence, KS.

22. Darwin, D., Locke, C.E., Senecal, M.R., Schwensen, S.M., and Smith, J.L. (1996). "Corrosion Resistant Steel Reinforcing Bars," *Materials for the New Millennium*, K.P. Chong (Ed.), American Society of Civil Engineers, Reston, VA.

23. Darwin, D., Browning, J., Nguyen, T.V., and Locke, C.E. (2002) *Mechanical and Corrosion Properties of a High-Strength, High Chromium Reinforcing Steel for Concrete*, Report No. SD2001-05-F, South Dakota Department of Transportation, SM Report No. 66, University of Kansas Center for Research. Accessed online: Sept. 23, 2011. (http://www.iri.ku.edu/projects/corrosion/SM66.pdf)

24. Gong, L., Darwin, D., Browning, J.P., and Locke, C.E. (2002). *Evaluation of Mechanical and Corrosion Properties of MMFX Reinforcing Steel for Concrete*, SM Report No. 70, University of Kansas Center for Research. Lawrence, KS. Accessed online: September. 23, 2011. (http://www.iri.ku.edu/projects/corrosion/SM70.pdf)

25. Balma, J., Darwin, D., Browning, J.P., and Locke, C.E. (2002). *Evaluation of Corrosion Resistance of Microalloyed Reinforcing Steel*, SM Report No. 71, University of Kansas Center for Research, Lawrence, KS. Accessed online: September 23, 2011. (http://www.iri.ku.edu/projects/corrosion/SM71.pdf)

26. Ji, J., Darwin, D., and Browning, J.P. (2005). *Corrosion Resistance of Duplex Stainless Steels and MMFX Microcomposite Steel for Reinforced Concrete Bridge Decks*, SM Report No. 80, University of Kansas Center for Research, Lawrence, KS. Accessed online: September 23, 2011. (http://www.iri.ku.edu/projects/corrosion/SM80.pdf)

27. ASTM A955/A955M-10a (2010). "Standard Specification for Deformed and Plain Stainless-Steel Bars for Concrete Reinforcement" ASTM International, West Conshohocken, PA.

28. Farzammehr, H. (1985). Pore Solution Analysis of Sodium Chloride and Calcium Chloride Containing Cement Pastes, master's thesis, University of Oklahoma, Norman, OK.

29. Farzammehr, H., Dehghanian, C., and Locke, C.E. (1987). "Study of the Effects of Cations on Chloride Caused Corrosion of Steel in Concrete," *Revista Técnica de la Facultad de Ingeniería*, Vol. 10, No. 1, University of Zulia, Venezuela.

30. Jones, D.A. (1992). *Principles and Prevention of Corrosion*, Macmillan Publishing Company, New York, NY.

31. Balma, J., Darwin, D., Browning, J.P., and Locke, C. E. (2005). *Evaluation of Corrosion Protection Systems and Corrosion Testing Methods for Reinforcing Steel in Concrete*, SM Report No. 76, University of Kansas Center for Research, Lawrence, KS. Accessed online: September 23, 2011. (http://www.iri.ku.edu/projects/corrosion/SM76.PDF)

32. ASTM C 150-05 (2005). "Standard Specification for Portland Cement," ASTM International, West Conshohocken, PA.

33. ASTM C778-02 (2002). "Standard Specification for Standard Sand," ASTM International, West Conshohocken, PA.

34. ASTM C305-99e1 (1999). "Standard Practice for Mechanical Mixing of Hydraulic Cement Pastes and Mortars of Plastic Consistency," ASTM International, West Conshohocken.

35. ASTM G109-99a (1999). "Standard Test Method for Determining the Effects of Chemical Admixtures on the Corrosion of Embedded Steel Reinforcement in Concrete Exposed to Chloride Environments," ASTM International, West Conshohocken, PA.

36. Kepler, J.L., Darwin, D., and Locke, C.E. (2000). *Evaluation of Corrosion Protection Methods for Reinforced Concrete Highway Structures*, SM Report No. 58, University of Kansas Center for Research, Lawrence, KS. Accessed online: September 23, 2011. (http://www.iri.ku.edu/projects/corrosion/SM58.PDF)

37. Pfeifer, D.W. and Scali, M.J. (1981). *Concrete Sealers for Protection of Bridge Structures*, NCHRP Report No. 244, National Cooperative Highway Research Program, Transportation Research Board, Washington, DC.

38. Perenchio, W.F. (1992). "Corrosion of Reinforcing Bars in Concrete," Annual Seminar, Master Builders Technology, Cleveland, OH.

39. ASTM C 192/C 192M-05 (2005). "Standard Practice for Making and Curing Concrete Test Specimens in the Laboratory," ASTM International, West Conshohocken, PA.

40. Guo, G., Darwin, D., Browning, J., and Locke, C.E. (2006). Laboratory and Field Tests of Multiple Corrosion Protection Systems for Reinforced Concrete Bridge Components and 2205 Pickled Stainless Steel, SM Report No. 85, University of Kansas Center for Research, Lawrence, KS. Accessed online: September 23, 2011. (http://www.iri.ku.edu/projects/corrosion/SM85.pdf)

41. Gong, L., Darwin, D., Browning, J., and Locke, C.E. (2006). *Evaluation of Multiple Corrosion Protection Systems and Stainless Steel Clad Reinforcement for Reinforced Concrete*, SM Report No. 82, University of Kansas Center for Research, Lawrence, KS. Accessed online: September 23, 2011. (http://www.iri.ku.edu/projects/corrosion/SM82.pdf)

42. Roberge, P. (2008). *Corrosion Engineering: Principles and Practice*, McGraw Hill, Chicago, IL.

43. Lindquist, W.D., Darwin, D., and Browning, J. (2005). *Cracking and Chloride Contents in Reinforced Concrete Bridge Decks*, SM Report No. 78, University of Kansas Center for Research, Lawrence, KS. Accessed online: September 23, 2011. (http://www.iri.ku.edu/projects/concrete/SM78.PDF)

44. O'Reilly, M., Darwin, D., and Browning, J. (2011). *Performance of Multiple Corrosion Protection Systems for Reinforced Concrete Bridge Decks*, SM Report No. 100, University of Kansas Center for Research, Lawrence, KS. Accessed online: September 23, 2011. (http://www.iri.ku.edu/projects/corrosion/SM100.pdf)

45. Kansas Department of Transportation (2007). Kansas Standard Specifications for State Road and Bridge Construction, Topeka, KS.

46. AASHTO T 260-94 (1997). "Standard Method of Test for Sampling and Testing for Chloride Ion in concrete and Concrete Raw Materials," *Standard Specifications for Transportation Materials and Methods of Sampling and Testing*, pp. 925–931, American Association of State Highway and Transportation Officials, Washington, DC.

47. Berke, N.S. (1991). "Corrosion Inhibitors in Concrete," *Concrete International*, Vol. 13, No. 7, pp. 24–27, American Concrete Institute, Farmington Hills, MI.

48. Darwin, D., Browning, J., Nguyen, T.V., and Locke, C E. (2007). *Multiple Corrosion Protection Systems for Reinforced Concrete Bridge Components*, Report No. FHWA-HRT-07-043, Federal Highway Administration, Washington, DC, and SM Report No. 84, University of Kansas Center for Research, Lawrence, KS. Accessed online: September 23, 2011. (http://www.iri.ku.edu/projects/corrosion/07043dd.pdf)

49. Draper, J., Darwin, D., Browning, J., and Locke, C.E. (2009). *Evaluation of Multiple Corrosion Protection Systems for Reinforced Concrete Bridge Decks*, SM Report No. 96, University of Kansas Center for Research, Lawrence, KS. Accessed online: September 23, 2011. (http://www.iri.ku.edu/projects/corrosion/SM96.pdf)

50. Darwin, D., Browning, J., O'Reilly, M., Xing, L., and Ji, J. (2009). "Critical Chloride Corrosion Threshold of Galvanized Reinforcing Bars," *ACI Materials Journal*, Vol. 106, No. 2, pp. 176–183, American Concrete Institute, Farmington Hills, MI.

51. Hope, B. and Ip, A. (1989). "Corrosion Inhibitors for Use in Concrete," *ACI Materials Journal,* Vol. 86, No. 6, pp. 602–608, American Concrete Institute, Farmington Hills, MI.

52. Pyc, W., Zemajtis, J., Weyers, R., and Sprinkel, M. (1999). "Evaluating Corrosion-Inhibiting Admixtures," *Concrete International*, Vol. 21, No. 4, pp. 39–44, American Concrete Institute, Farmington Hills, MI.

53. Nmai, C., Farrington, S., and Bobrowski, G. (1992). "Organic-Based Corrosion-Inhibiting Admixture for Reinforced Concrete," *Concrete International,* Vol. 14, No. 4, pp. 45–51, American Concrete Institute, Farmington Hills, MI.

54. Goodwin, P., Frantz, G., and Stephens, J. (2000). *Protection of Reinforcement with Corrosion Inhibitors, Phase II*, CDOT Report No. JHR 00-279, Connecticut Department of Transportation, Newington, CT.

55. Civjan, S., LaFave, J., Lovett, D., Sund, D., and Trybulski, J. (2003). Performance Evaluation and Economic Analysis of Combinations of durability Enhancing Admixtures (Mineral and Chemical) in Structural Concrete for the Northeast U.S.A., Report NETCR-36, New England Transportation Consortium, Fall River, MA.

56. Soylev, T.A. and Richardson, M.G. (2008). "Corrosion Inhibitors for Steel in Concrete: State-of-the-Art Report," *Construction and Building Materials*, Vol. 22, No. 4, pp.609–622, Elsevier, Amsterdam.

57. Somuah, S., Boah, J., Leblanc, P., Al-Tayyib, A., and Al-Mana, A. (1991), "Effect of Sulfate and Carbonate Ions on Reinforcing Steel Corrosion as Evaluated Using AC Impedance Spectroscopy," *ACI Materials Journal*, Vol. 88, No. 1, pp. 49–55, American Concrete Institute, Farmington Hills, MI.

58. Xing, L., Darwin, D., and Browning, J. (2010). *Evaluation of Multiple Corrosion Protection Systems and Corrosion Inhibitors for Reinforced Concrete Bridge Decks*, SM Report No. 99, University of Kansas Center for Research, Lawrence, KS. Accessed online: September 23, 2011. (http://www.iri.ku.edu/publications/SM99Xing.pdf)

59. Tuutti, K. (1982). *Corrosion of Steel in Concrete*, Swedish Cement and Concrete Research Institute, Stockholm, Sweden.

60. Maage, M., Helland, S., Poulsen, E., Vennesland, O., and Carl. J.E. (1996). "Service Life Prediction of Existing Concrete Structures Exposed to Marine Environment," *ACI Materials Journal*, Vol. 93, No. 6, pp. 602–608, American Concrete Institute, Farmington Hills, MI.

61. Williamson, G.S., Weyers, R.E., Brown, M.C., Ramniceanu, A., and Sprinkel, M.M. (2008). "Validation of Probability-Based Chloride-Induced Corrosion Service-Life Model," *ACI*

Materials Journal, Vol. 105, No. 4, pp. 375–380, American Concrete Institute, Farmington Hills, MI.

62. Ehlen, M.A., Thomas, M.D.A., and Bentz, E.C. (2009). "Life-365 Service Life Prediction Model™ Version 2.0," *Concrete International*, Vol. 31, No. 5, pp. 41–46, American Concrete Institute, Farmington Hills, MI.

63. Darwin, D., Browning, J., and Lindquist, W.D. (2004). "Control of Cracking in Bridge Decks: Observations from the Field," *Cement, Concrete and Aggregates*, Vol. 26, No. 2, pp. 148–154, ASTM International, West Conshohocken, PA.

64. Lindquist, W.D., Darwin, D., and Browning, J. (2008). Development and Construction of Low-Cracking High-Performance Concrete (LC-HPC) Bridge Decks: Free Shrinkage, Mixture Optimization, and Concrete Production, SM Report No. 92, University of Kansas Center for Research, Lawrence, KS. Accessed online: September 23, 2011. (http://www.iri.ku.edu/projects/concrete/SM92r.pdf)

65. McLeod, H.A.K. , Darwin, D., and Browning, J. (2009). Development and Construction of Low-Cracking High-Performance Concrete (LC-HPC) Bridge Decks: Construction Methods, Specifications, and Resistance to Chloride Ion Penetration, SM Report No. 94, University of Kansas Center for Research, Lawrence, KS. Accessed online: September 23, 2011. (http://www.iri.ku.edu/projects/concrete/SM94.pdf)

66. Darwin, D., Browning, J., Lindquist, W., McLeod, H.A.K., Yuan, J., Toledo, M., and Reynolds, D. (2010). "Low-Cracking, High-Performance Concrete Bridge Decks—Case Studies Over the First 6 Years," *Transportation Research Record No. 2202*, pp. 61–69, Transportation Research Board, Washington, DC.

67. Miller, G.G. and Darwin, D. (2000). *Performance and Constructability of Silica Fume Bridge Deck Overlays*, SM Report No 57, University of Kansas Center for Research, Lawrence, KS.

68. Rasheeduzzafar, A.S. and Al-Gahtani, A. (1992). "Corrosion Cracking in Relation to Bar Diameter, Cover, and Concrete Quality," *Journal of Materials in Civil Engineering*, Vol. 4, No. 4, pp. 327–342, American Society of Civil Engineers, Reston, VA.

69. Alonso, C., Andrade, C., Rodriguez, J., and Diaz, J.M. (1998). "Factors Controlling Cracking of Concrete Affected by Reinforcement Corrosion," *Materials and Structures*, Vol. 31, No. 211, pp. 435–441, Journal Citation Reports, Thomson Reuters, Philadelphia, PA.

70. Maaddawy, T. and Soudki, K. (2003). "Effectiveness of Impressed Current Technique to Simulate Corrosion of Steel Reinforcement in Concrete," *Journal of Materials in Civil Engineering*, Vol. 15, No. 1, pp. 41–47, American Society of Civil Engineers, Reston, VA.

71. Torres-Acosta, A.A. and Sagues, A.A. (2004). "Concrete Cracking by Localized Steel Corrosion—Geometric Effects," *ACI Materials Journal*, Vol. 101, No. 6, pp. 501–507, American Concrete Institute, Farmington Hills, MI.

72. Darwin, D., Browning, J., Nguyen, T.V., and Locke, C.E. (2007). *Evaluation of Metallized Stainless Steel Clad Reinforcement*, South Dakota Department of Transportation Report, SD2002-16-F, and SM Report No. 90, University of Kansas Center for Research, Lawrence, KS. Accessed online: September 23, 2011. (http://www.iri.ku.edu/projects/corrosion/SD200216Fa.pdf)

73. Sergi, G., Short, N., and Page, C. (1985). "Corrosion of Galvanized and Galvanannealed Steel in Solutions of pH 9.0-14.0," *Corrosion/85: International Corrosion Forum Devoted Exclusively to the Protection and Performance of Materials*, Boston, MA.

74. Hime, W. and Machin, M. (1993). "Performance Variations of Galvanized Steel in Mortar and Concrete," *Corrosion,* Vol. 49, No. 10, pp. 858–860, NACE International, Houston, TX.

75. Suda, K., Misra, S., and Motohashi, K. (1993). "Corrosion Products of Reinforcing Bars Embedded in Concrete," *Corrosion Science*, Vol. 35, No. 7, pp. 1543–1549, Elsevier, Amsterdam.

76. Rasheeduzzafar, A.S., Dakhil, F., Bader, M., and Khan, M. (1992). "Performance of Corrosion Resisting Steels in Chloride-Bearing Concrete," *ACI Materials Journal,* Vol. 89, No. 5, pp. 439–448, American Concrete Institute, Farmington Hills, MI.

77. ABAQUS FEA 6.9, Dassault Systèmes. Accessed online: September 23, 2011. (http://www.3ds.com/)

78. Darwin, D., Barham, S., Kozul, R., and Luan, S. (2001). "Fracture Energy of High-Strength Concrete," *ACI Materials Journal*, Vol. 98, No. 5, pp. 410–417, American Concrete Institute, Farmington Hills, MI.

79. Saeki, N., Fujita, Y., Takada, N., and Ohta, T. (1988). "Control of Rust Damage of Reinforced Concrete in a Corrosive Environment," *Concrete in Marine Environment*, Proceedings of the Second International Conference, SP-109, pp. 163–177, American Concrete Institute, Farmington Hills, MI.